

# **THE EFFECT OF BEDDING ERRORS ON THE ACCURACY OF PLATE LOAD TESTS**

**H. F. T. BARNARD**

**UNIVERSITY OF PRETORIA**  
**DEPARTMENT OF CIVIL ENGINEERING**

**THE EFFECT OF BEDDING ERRORS ON THE ACCURACY  
OF PLATE LOAD TESTS**

**BY**

**H. F. T. BARNARD**

**2013**

**THE EFFECT OF BEDDING ERRORS ON THE ACCURACY  
OF PLATE LOAD TESTS**

**HENDRIK FRANCOIS TALJAARD BARNARD**

**A dissertation submitted in partial fulfilment of the requirements for the  
degree of**

**MASTER OF ENGINEERING (GEOTECHNICAL ENGINEERING)**

**In the**

**FACULTY OF ENGINEERING**

**UNIVERSITY OF PRETORIA**

**AUGUST 2013**

**DIE UITWERKING VAN BEDDING FOUTE OP DIE  
AKKURAAKTHEID VAN PLAAT BELASTING TOETSE**

**HENDRIK FRANCOIS TALJAARD BARNARD**

**‘n Verhandeling voorgelê ter gedeeltelike vervulling van die vereistes  
vir die graad**

**MAGISTER IN INGENIEURSWESE (GEOTEGNIESE INGENIEURSWESE)**

**In die**

**FAKULTEIT INGENIEURSWESE**

**UNIVERSITEIT VAN PRETORIA**

**AUGUSTUS 2013**

## DISSERTATION SUMMARY

### THE EFFECT OF BEDDING ERRORS ON THE ACCURACY OF PLATE LOAD TESTS

**H. F. T. BARNARD**

**Supervisor:** Professor Gerhard Heymann

**Department:** Civil Engineering

**University:** University of Pretoria

**Degree:** Master of Engineering (Geotechnical Engineering)

## SUMMARY

This dissertation addresses the effect of bedding errors on the accuracy of plate load tests on soil. For this research project the bedding errors were quantified by measuring the surface roughness by means of a high precision laser measuring system. The test area was scanned before and after each test in order to evaluate the change in surface roughness during each test. In addition, a modified plate load test was designed to eliminate the effect of bedding errors that occur during these tests. Telescopic probes were used to measure the relative displacement at two points below the centre of the plate.

A series of plate load tests was conducted at the experimental farm of the University of Pretoria. In total six precise plate load tests were performed. The test areas were levelled by means of three surface preparation methods namely, i) a thin layer of plaster of Paris; ii) a thin layer of well-graded sand and iii) by using only hand tools.

The stiffness values, determined from the vertical displacement of the plate, were compared with the internal stiffness values determined by means of the telescopic probes. All stiffness values were compared with continuous surface wave (CSW) measurements performed on the same material.

The main objectives of this research project were, firstly, to quantify the bedding errors that occurs during plate load tests. Secondly, to study and evaluate three different surface preparation methods used in plate load tests to achieve a levelled and smooth test surface and lastly to evaluate the effectiveness of using telescopic probes in routine plate load tests to eliminate the effects of bedding errors.

The results of this dissertation have demonstrated that bedding errors could have a significant effect on soil stiffness values, which have been determined by the 'conventional' method of conducting plate load tests. Plaster of Paris resulted in the most accurate stiffness values determined by conventional plate load tests. The results have further demonstrated that telescopic probes are necessary to determine soil stiffness values with a high level of accuracy and bedding errors cannot be eliminated on a poorly prepared surface by applying initial load cycles.

## **SAMEVATTING VAN VERHANDELING**

### **DIE UITWERKING VAN BEDDING FOUTE OP DIE AKKURAAKTHEID VAN PLAAT BELASTING TOETSE**

**H. F. T. BARNARD**

**Promotor:**        Profesor Gerhard Heymann

**Departement:**    Siviele Ingenieurswese

**Universiteit:**    Universiteit van Pretoria

**Graad:**            Magister in Ingenieurswese (Geotegniese Ingenieurswese)

## SAMEVATTING

Hierdie verhandeling fokus op die uitwerking van bedding foute op die akkuraatheid van die plaat belasting toetse op grond. Die bedding foute is gekwantifiseer vir hierdie navorsingsprojek deur die oppervlak grofheid te meet deur middel van 'n hoë presisie laser meet stelsel. Die toets area is geskandeer voor en na elke toets ten einde die verandering in oppervlak grofheid te evalueer tydens elke toets. Daarbenewens is 'n aangepaste plaat belasting toets ontwerp om die uitwerking van bedding foute wat tydens plaat toetse bestaan uit te skakel. Teleskopiese sondes is gebruik om die relatiewe verplasing te meet tussen twee punte onder die plaat.

'n Reeks van plaat belasting toetse is uitgevoer op die proefplaas van die Universiteit van Pretoria. Ses plaat belasting toetse is uitgevoer in totaal. Die toets gebiede is gelyk gemaak deur middel van drie oppervlak voorbereiding metodes, naamlik i) 'n dun laag gips; ii) 'n dun laag goed-gegradeerde sand en iii) deur die gebruik van slegs hand gereedskap.

Die styfheid waardes, wat van die vertikale verplasing van die plaat bepaal was, is vergelyk met die interne styfheid waardes wat bepaal was deur middel van die teleskopiese sondes. Alle styfheid waardes is vergelyk met kontinue oppervlak golf metings geneem op dieselfde materiaal.

Die belangrikste doelwitte van hierdie navorsingsprojek was om eerste die bedding foute te kwantifiseer wat tydens plaat belasting toetse bestaan. Tweedens, om die drie verskillende oppervlak voorbereiding metodes wat gebruik word in plaat belasting toetse te bestudeer en te evalueer en laastens om die doeltreffendheid van die gebruik van teleskopiese sondes in roetine plaat belasting toetse om bedding foute uit te skakel, te evalueer.

Die resultate van hierdie verhandeling bewys dat bedding foute 'n beduidende uitwerking kan hê op die grond styfheid waardes wat deur die konvensionele metode van plaat belasting toetse uitgevoer word. Gips lewer die mees akkurate styfheid waardes wat bepaal word deur konvensionele plaat belasting toetse. Die resultate bewys verder dat teleskopiese sondes nodig is om grond styfheid waardes te bepaal met 'n hoë vlak van akkuraatheid en bedding foute kan nie uitgeskakel word op 'n swak voorbereide oppervlak deur slegs die toepassing van 'n aanvanklike belasting siklus nie.

## ABSTRACT

**Title:** The Effect of Bedding Errors on the Accuracy of Plate Load Tests

**Author:** H. F. T. Barnard

**Supervisor:** Professor Gerhard Heymann

**Department:** Civil Engineering

**University:** University of Pretoria

**Degree:** Master of Engineering (Geotechnical Engineering)

A series of plate load tests were conducted at the experimental farm of the University of Pretoria. The test areas were levelled by means of three surface preparation methods namely, i) a thin layer of plaster of Paris; ii) a thin layer of well-graded sand and iii) by using only hand tools. In addition, a modified plate load test was designed to eliminate the effect of bedding errors that occur during these tests. Telescopic probes were used to measure the relative displacement at two points below the centre of the plate. The main objective of this research project was to first quantify the bedding errors that occur during plate load tests. Secondly, to evaluate the three different surface preparation methods used in plate load tests to achieve a levelled and smooth test surface, and lastly to evaluate the effectiveness of using telescopic probes in routine plate load tests to eliminate the effects of bedding errors. The stiffness values, determined from the vertical displacement of the plate, were compared with the internal stiffness values determined by means of the telescopic probes. All stiffness values were compared with continuous surface wave (CSW) measurements performed on the same material. The test apparatus, methods and results are discussed in this dissertation.

**To my wife**

## ACKNOWLEDGEMENT

This research project could not be possible without the support, assistance and guidance of certain people and organisations. Therefore, I wish to express my appreciation to the following organisations and persons who made this dissertation possible:

- a) First, I would like to thank my Heavenly Father for giving me the opportunity and ability to expand my knowledge and horizons in Geotechnical engineering. I am also grateful to God for His empowering grace and Godly wisdom that I received to complete this dissertation for my Master's degree.
- b) I want to thank my beloved wife, Deloryse, for all her love and support. This research project could not be possible without her in my life.
- c) Professor Gerhard Heymann, my supervisor, for his professional guidance, support and commitment.
- d) My parents for their on-going support and motivation during this research project. I also want to thank my parents for financial support in completing my undergraduate studies.
- e) The University of Pretoria for financial support and the use of the geotechnical laboratory facilities during the course of the study.
- f) Aurecon for the financial support and career development opportunities, invested in me during the last few years.
- g) The following persons are gratefully acknowledged for their assistance during the course of the study:
  - Mr J. van Staden for his helpful assistance in the geotechnical laboratory;
  - Mr D. Mostert, Mr J. Peens, Johan and Rikus for their technical assistance in the Civil engineering laboratory;
  - Mr N. Smit for his technical assistance and life lessons learned in the mechanical laboratory;

- Professor Schalk Els and Mr C. Becker for assistance in the mechanical laboratory especially with the laser measuring system;
  - Colin, Arn and Thabo from Geostrada for their assistance during the experimental work;
  - Christiaan Ungerer for his assistance during the experiment design phase.
- h) Mrs Marion Pfeiffer for professionally editing this dissertation.

## **TABLE OF CONTENT**

	<b><u>PAGE</u></b>
<b>1. INTRODUCTION</b>	
1.1. Background	1-1
1.2. Objectives of Study	1-2
1.3. Scope of Study	1-2
1.4. Methodology	1-2
1.5. Hypothesis	1-3
1.6. Organisation of the Report	1-4
<b>2. LITERATURE REVIEW</b>	
2.1. Introduction to soil stiffness	2-1
2.2. Factors affecting soil stiffness	2-3
2.2.1. Soil state factors	2-3
2.2.2. Factors affecting plate load tests measurements	2-5
2.3. Determination of soil stiffness	2-7
2.3.1. Direct laboratory tests	2-9
2.3.2. Direct field ( <i>In-situ</i> ) tests	2-10
2.4. Plate Load Tests (PLT)	2-12
2.4.1. History on plate loading tests	2-12
2.4.2. PLT apparatus	2-16
2.4.3. Calibration for plate load test systems	2-18
2.4.4. Test standards and procedures	2-20
2.4.5. Data analyses and interpretation techniques	2-21
2.5. Multi-depth displacement measurements	2-23
2.6. Conclusions from Literature Review	2-25
<b>3. INDUSTRY RESEARCH</b>	
3.1. Introduction	3-1
3.2. Questionnaire	3-1
3.3. Results	3-3
3.3.1. Plate sizes	3-3
3.3.2. Reaction force	3-3
3.3.3. Applied load measurements	3-3
3.3.4. Plate settlement measurements	3-4
3.3.5. Number of displacement instruments	3-4
3.3.6. Surface preparation method	3-4
3.3.7. Type and length of reference beam	3-5
3.3.8. Standard test procedures	3-5
3.4. Conclusions from Industry Research	3-5
<b>4. EXPERIMENTAL WORK</b>	
4.1. Introduction	4-1
4.2. Experiment strategy	4-1

	<b><u>PAGE</u></b>
4.3. Components of the Experiment	4-2
4.3.1. Laser Measuring System	4-2
4.3.2. Conventional plate load test Apparatus	4-4
4.3.3. Development of Telescopic Probes	4-5
4.4. Calibration of plate load Test system	4-6
4.4.1. Calibration methodology	4-6
4.4.2. Laser measuring system calibration	4-7
4.4.3. Load cell calibration	4-8
4.4.4. Transducer calibration	4-9
4.5. Test Surface Preparation	4-11
4.6. Plate Load Test Procedure	4-12
4.7. Data Analyses	4-15
4.7.1. Quantification of Surface Roughness	4-15
4.7.2. Determination of External Stiffness	4-19
4.7.3. Determination of Internal Stiffness	4-20
<b>5. DISCUSSION</b>	
5.1. Introduction	5-1
5.2. Quantification of surface roughness	5-2
5.2.1. Comparison of initial surface roughness	5-2
5.2.2. Change in surface roughness	5-6
5.3. Pressure-displacement Relationships	5-9
5.3.1. External measurements	5-9
5.3.2. Internal measurements	5-10
5.3.3. $E_{50}$ stiffness values	5-11
5.4. Performance of a conventional plate load test	5-12
5.4.1. External stiffness comparison	5-12
5.5. Performance of a modified plate load test	5-13
5.5.1. Internal stiffness comparison	5-14
5.5.2. Comparison between external and internal Stiffness	5-15
5.6. Limitations of data	5-17
5.6.1. Cycle 1	5-17
5.6.2. Cycle 2	5-17
5.6.3. Cycle 3	5-18
<b>6. CONCLUSIONS AND RECOMMENDATIONS</b>	
6.1. Conclusions	6-1
6.2. Recommendations	6-2
<b>7. REFERENCES AND STANDARDS</b>	
7.1. References	7-1
7.2. Standards	7-13

## **APPENDIX A – Plate load test questionnaire**

## **APPENDIX B – Publications by the author**

### **LIST OF TABLES**

Table 2-1: Effect of soil state factors on soil stiffness.

Table 3-1: Technical detail for plate load test apparatus from standards.

Table 4-1: Manufacturers' specifications for the laser distance gage (AR700-8).

Table 4-2: Manufacturers' specifications for the cable-extension transducers (PT1A-30).

Table 4-3: Manufacturers' specifications for the 5 mm (WI) LVDT.

Table 4-4: Manufacturers' specifications for the Budenberg 283/500 series tester.

Table 4-5: Manufacturers' specifications for the Mitutoyo 543-558A digital indicator.

Table 4-6: Instrument behaviour.

Table 4-7: Surface roughness parameters.

Table 4-8: Clayton-Heymann stiffness degradation envelope.

Table 5-1: Surface preparation methods.

Table 5-2: Surface roughness parameters for all tests.

Table 5-3: Surface roughness parameters for 'Sand' tests.

Table 5-4: Surface roughness parameters for 'Plaster of Paris' tests.

Table 5-5: Initial bedding errors for different surface preparation methods.

Table 5-6: Comparison of bedding errors for 'No interface material' tests.

Table 5-7: Comparison of bedding errors for 'Sand' tests.

Table 5-8: Comparison of bedding errors for 'Plaster of Paris' tests.

Table 5-9: External displacement for all tests.

Table 5-10: Internal displacement for all tests.

Table 5-11: E50 stiffness values for all tests (Cycle 3).

Table 5-12: External stiffness values.

Table 5-13: Internal stiffness values.

Table 5-14: Comparison between external and internal stiffness values.

## LIST OF FIGURES

Figure 2-1: Typical stress-strain curve.

Figure 2-2: Definition of soil stiffness.

Figure 2-3: Characteristic shear stiffness-strain behavior of soil with typical strain ranges for laboratory tests and structures.

Figure 2-4: Stiffness of Calcarenite.

Figure 2-5: Conventional triaxial set-up.

Figure 2-6: Local strain transducers.

Figure 2-7: Typical configuration of a conventional oedometer.

Figure 2-8: Basic components of the pressure meter.

Figure 2-9: Marchetti dilatometer.

Figure 2-10: Screw-plate load test apparatus.

Figure 2-11: Correlation between plate bearing tests and settlement of foundations.

Figure 2-12: London clay (Hendon) stiffness from triaxial and plate load tests.

Figure 2-13: Comparison of plate tests and laboratory test results in London clay.

Figure 2-14: Different layouts of conventional plate loading tests.

Figure 2-15: Conventional plate load test layout and results.

Figure 2-16: System for load application.

Figure 2-17: Accuracy versus precision: the target analogy.

Figure 2-18: Single-point measuring system below 865 mm diameter loading plate.

Figure 2-19: Multi-point measuring system below 865 mm diameter loading plate.

Figure 2-20: Details of the instrumentation system of the METU plate-loading apparatus.

Figure 3-1: Preferred method to provide reaction load.

Figure 3-2: Preferred method to measure applied loads.

Figure 3-3: Preferred method to measure plate settlement.

Figure 3-4: Number of displacement measuring devices.

Figure 3-5: Preferred surface preparation methods.

Figure 3-6: Length of reference beams.

Figure 3-7: Preferred standard test procedures.

Figure 4-1: Schematic illustration of the modified plate load test set-up.

Figure 4-2: Laser measuring system.

- Figure 4-3: Configuration of the 12 consecutive scan lines.
- Figure 4-4: Laser data acquisition system.
- Figure 4-5: Modified plate load test set-up.
- Figure 4-6: Anchor installation.
- Figure 4-7: DCDTs, load cell and hydraulic jack set-up.
- Figure 4-8: Plate load test data acquisition system.
- Figure 4-9: Telescopic probes set-up.
- Figure 4-10: LVDT set-up.
- Figure 4-11: Components of the modified plate load test.
- Figure 4-12: Typical laser distance gauge calibration result.
- Figure 4-13: Typical Cable-Extension Position Transducer calibration result.
- Figure 4-14: Typical load cell calibration result.
- Figure 4-15: Budenberg 283/500 Series set-up.
- Figure 4-16: Amsler 2000 kN Compression testing machine.
- Figure 4-17: Mitutoyo 543-553-1 digital indicator set-up.
- Figure 4-18: Typical displacement transducer calibration result.
- Figure 4-19: Plaster of Paris surface preparation.
- Figure 4-20: Preparation methods: a) 'No interface material' b) Well-graded Silica sand c) Plaster of Paris.
- Figure 4-21: Test procedure: Steps 1 to 15.
- Figure 4-22: Test procedure: Steps 16 to 30.
- Figure 4-23: Same Ra values for different profiles.
- Figure 4-24: Calculation of the average roughness parameter, Ra.
- Figure 4-25: Raw data plot for different surface preparation methods.
- Figure 4-26: Calculation of perpendicular height ( $y_i$ ).
- Figure 4-27: Pressure bulbs beneath a uniformly loaded circular area.
- Figure 4-28: Variation of stiffness with choice of origin.
- Figure 4-29: Stiffness degradation curves.
- Figure 5-1: Bearing area curves for different surface preparation methods before tests.
- Figure 5-2: Comparison between before and after bearing area curves ('No interface material' test).
- Figure 5-3: Comparison between before and after laser scans for 'No interface material' test.
- Figure 5-4: Comparison between before and after bearing area curves ('Sand' test).

- Figure 5-5: Comparison between before and after laser scans for ‘Sand’ test.
- Figure 5-6: Comparison between before and after bearing area curves (‘Plaster of Paris’ test).
- Figure 5-7: Comparison between before and after laser scans for ‘Plaster of Paris’ test.
- Figure 5-8: Typical external pressure-displacement curve (All cycles).
- Figure 5-9: Typical internal pressure-displacement curve (All cycles).
- Figure 5-10: Comparison between E50 values from external measurements (Cycle 3).
- Figure 5-11: Comparison between E50 values from internal measurements (Cycle 3).
- Figure 5-12: Comparison between external stiffness for different preparation methods (Cycle 1).
- Figure 5-13: Comparison between external stiffness for different preparation methods (Cycle 2).
- Figure 5-14: Comparison between external stiffness for different preparation methods (Cycle 3).
- Figure 5-15: Comparison between internal stiffness for different preparation methods (Cycle 1).
- Figure 5-16: Comparison between internal stiffness for different preparation methods (Cycle 2).
- Figure 5-17: Comparison between internal stiffness for different preparation methods (Cycle 3).
- Figure 5-18: Comparison between external stiffness and internal stiffness for ‘No interface material’ test (Cycle 3).
- Figure 5-19: Comparison between external stiffness and internal stiffness for ‘Sand’ test (Cycle 3).
- Figure 5-20: Comparison between external stiffness and internal stiffness for ‘Plaster of Paris’ test (Cycle 3).
- Figure 5-21: Comparison between external stiffness and internal stiffness.

## DECLARATION OF ORIGINALITY

### UNIVERSITY OF PRETORIA

The Department of CIVIL ENGINEERING places great emphasis upon integrity and ethical conduct in the preparation of all written work submitted for academic evaluation.

While academic staff teach you about referencing techniques and how to avoid plagiarism, you too have a responsibility in this regard. If you are at any stage uncertain as to what is required, you should speak to your lecturer before any written work is submitted.

You are guilty of plagiarism if you copy something from another author's work (eg a book, an article or a website) without acknowledging the source and pass it off as your own. In effect you are stealing something that belongs to someone else. This is not only the case when you copy work word-for-word (verbatim), but also when you submit someone else's work in a slightly altered form (paraphrase) or use a line of argument without acknowledging it. You are not allowed to use work previously produced by another student. You are also not allowed to let anybody copy your work with the intention of passing it off as his/her work.

Students who commit plagiarism will not be given any credit for plagiarised work. The matter may also be referred to the Disciplinary Committee (Students) for a ruling. Plagiarism is regarded as a serious contravention of the University's rules and can lead to expulsion from the University.

The declaration which follows must accompany all written work submitted while you are a student of the Department of CIVIL ENGINEERING. No written work will be accepted unless the declaration has been completed and attached.

Full names of student: HENDRIK FRANCOIS TALJAARD BARNARD

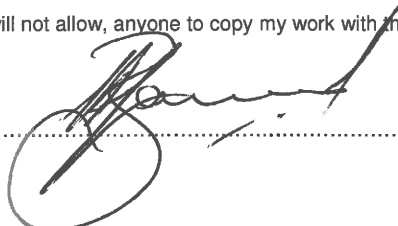
Student number: 2500 4817

Topic of work: THE EFFECT OF BEDDING ERRORS ON THE ACCURACY OF PLATE LOAD TESTS

#### Declaration

1. I understand what plagiarism is and am aware of the University's policy in this regard.
2. I declare that this dissertation (eg essay, report, project, assignment, dissertation, thesis, etc) is my own original work. Where other people's work has been used (either from a printed source, Internet or any other source), this has been properly acknowledged and referenced in accordance with departmental requirements.
3. I have not used work previously produced by another student or any other person to hand in as my own.
4. I have not allowed, and will not allow, anyone to copy my work with the intention of passing it off as his or her own work.

SIGNATURE



## CHAPTER 1: INTRODUCTION

### 1.1. BACKGROUND

Plate load tests have been used extensively in the past as a means of determining the bearing capacity and the stiffness of soil. Most geotechnical problems are governed by allowable settlement requirements, and therefore, geotechnical engineers are continuously searching for improved test methods and new devices to determine soil stiffness, which are more accurate and cost-effective. Two of the main advantages of plate load tests are their cost-effectiveness and the relatively straightforward test procedure.

However, there are bedding errors which affect soil stiffness measurements during conventional plate load tests and these should be eliminated or kept to a minimum. The limitations of conventional plate load tests create room for improvements on current instrumentation and test apparatus for the measurements of soil displacements and applied loads during these tests.

For this research project, the bedding errors were quantified by measuring the surface roughness by means of a high precision laser measuring system. The test area was scanned before and after each test in order to evaluate the change in surface roughness during each assessment. Three different surface preparation methods were used to achieve a smooth bedding surface before each test, and in addition, a modified plate load test was designed to eliminate the effect of bedding errors that may occur during these tests. Telescopic probes were used to measure the relative displacement at two points below the centre of the plate. A series of plate tests were performed: 1) to determine which surface preparation method would give the most accurate stiffness values when performing conventional plate load tests and, 2) to evaluate the effectiveness of installing telescopic probes to eliminate the effect of bedding errors.

The stiffness values determined from the vertical displacement of the plate were compared with the internal stiffness values that were determined by means of the telescopic probes. All stiffness values were compared with continuous surface wave (CSW) measurements, which were performed on the same material.

## **1.2. OBJECTIVES OF STUDY**

The purpose of the study was to evaluate the effect of bedding errors on the accuracy of plate load tests; to investigate a modified plate load test method, and to assess its measurement performance. This research project has the following objectives:

- a) To quantify the bedding errors that occur during plate load tests.
- b) To evaluate three different surface preparation methods used in plate load tests to achieve a levelled and smooth test surface.
- c) To evaluate the effectiveness of using telescopic probes in routine plate load tests to eliminate the effects of bedding errors.

## **1.3. SCOPE OF STUDY**

For the purpose of this research project, a series of 450 mm plate load tests were carried out at the experimental farm of the University of Pretoria on residual Andersite, which is described as firm, reddish brown, clayey silt. Three different surface preparation methods were used to achieve a smooth bedding surface before each test. In total, six plate load tests were performed (two tests on each preparation method). In addition, telescopic probes were used to measure the relative displacement of the soil, at two positions below the centre of the plate, in order to eliminate the effects of bedding errors on the determination of soil stiffness values.

## **1.4. METHODOLOGY**

A series of plate load tests were conducted at the experimental farm of the University of Pretoria. In total six precise plate load tests were performed. The test areas were levelled by the use of three surface preparation methods namely, i) a thin layer plaster of Paris; ii) a thin layer of well-graded sand, and iii) by using only hand tools, respectively.

It was important to first describe the surface roughness before each test was conducted and this was measured by means of a well-designed laser measuring system.

To describe the surface roughness, a seven-step process was performed for each set of data. The surface roughness was again measured after each test, to determine any change in surface roughness during the tests.

In addition to the six conventional plate load tests, telescopic probes were developed and installed to measure the relative displacement of two points below the centre of the plate during each test. From these measurements, internal stiffness values could be determined and compared with the external stiffness values calculated from the average plate settlement.

External stiffness was determined by measuring the plate settlement with three calibrated Direct Current Differential Transformers (DCDTs) which were placed 120 degrees apart and combined with the applied load assessed with a calibrated 10 ton load cell. The applied load was supplied with a hydraulic pump and jack system.

Internal stiffness for each test was determined simultaneously by using a calibrated 5 mm Linear Variable Differential Transducer (LVDT), attached to the telescopic probes placed at specific distances below the plate to measure relative displacements. All four measuring devices and load cell readings were recorded at the same time during each plate load test with an electronic data acquisition system.

## **1.5. HYPOTHESIS**

It is believed that:

- i. Bedding errors have a significant effect on the accuracy of plate load tests;
- ii. Plaster of Paris will prove to be the surface preparation method that measures the most accurate stiffness values in conventional plate load tests; and
- iii. The use of telescopic probes to determine soil stiffness during plate load tests will provide a satisfactory level of performance.

## 1.6. ORGANISATION OF THE REPORT

This dissertation consists of the following chapters:

A review of the current background and technical knowledge of soil stiffness and plate load testing is discussed in Chapter 2. This includes a brief introduction to soil modulus and the factors that affect soil stiffness measurements. Emphasis is placed on the factors associated with plate load tests and the main components of conventional plate load tests are reviewed, and in addition, some other field and laboratory tests to determine soil stiffness are presented.

Results from the industry research conducted for this dissertation are presented in Chapter 3. A nine-question “Plate load test questionnaire” was set-up to understand in what way and where plate load tests are currently being performed in South Africa. The questions asked in the survey are discussed and followed by the results. The chapter concludes with a few lessons learned from the industry research and sets the platform for the experiment design.

The test apparatus, preparation and procedure designed for this dissertation is described in Chapter 4. The experimental strategy is discussed, followed by the various components of the experiment. Furthermore, the statistical methods and interpretation techniques that have been used to analyse all data are presented.

The surface roughness observed for the three different surface preparation methods and the performance of the modified plate load tests designed for this dissertation are described in Chapter 5. The quantification of bedding errors is discussed followed by the load-settlement relationships observed, as well as comparisons made between external and internal stiffness values determined during the experimental study.

Chapter 6 presents the main conclusions and recommendations of this dissertation. The list of all references used for this dissertation is presented in Chapter 7. Appendix A shows an example of the plate load test questionnaire. Appendix B contains the publications written to date from work carried out as part of this dissertation.

## CHAPTER 2: LITERATURE REVIEW

This chapter presents a review of the background and current knowledge of soil stiffness and plate load testing. A brief introduction to soil modulus is discussed followed by a description of the factors, which affect soil stiffness measurements with emphasis placed on those associated with plate load tests (PLT). In addition, some other field and laboratory tests to determine soil stiffness are briefly presented.

### 2.1. INTRODUCTION TO SOIL STIFFNESS

Soil stiffness is one of the most difficult soil parameters to estimate because it can be affected by many factors (Briaud, 2001). Where geotechnical problems are governed by allowable settlement requirements, soil stiffness determination is an important part of the foundation investigation (Wrench, 1984) and geotechnical engineers are continuously searching for more accurate and cost effective tests to determine the stress-strain behaviour of soil. It is well known that the stress-strain behaviour of soil is highly non-linear and soil stiffness may decay with strain by order of magnitude (Atkinson, 2000). Figure 2-1 shows a typical stress-strain relationship of soil.

Many moduli can be defined from triaxial tests results for example, see Figure 2-2 the secant slope  $S_s$  is obtained by drawing a line from the origin to point A and the secant stiffness  $E_s$  is calculated from this slope. The secant stiffness is typically used to predict the foundation settlements due to the first loading in the case of a spread footing (Briaud, 2001). If it is necessary to calculate the incremental settlement due to an incremental load, the tangent stiffness  $E_t$  will be the most suitable modulus to determine this (refer to  $S_t$  on Figure 2-2).

The unloading slope  $S_u$  is obtained by drawing a line between points A and B on Figure 2-2 and this is used to calculate the unloading stiffness  $E_u$  of the soil. This stiffness is referred to as the resilient modulus and for example, would be used to calculate the heave at the bottom of an excavation. If the slope is drawn from point B to point D, then the reloading slope  $S_r$  is obtained and the reloading stiffness  $E_r$  is calculated from this.

The reloading stiffness  $E_r$  can be used to calculate the settlements of an excavation if the excavated soil or a building of equal weight was placed back in the excavation and it must be

noted that the reloading stiffness is lower than the unloading stiffness. Lastly, the cyclic slope  $S_c$  is obtained with a line from point B to point C. The cyclic stiffness  $E_c$  will be used, together with its development as a function of the number of cycles, to calculate the settlement of a pile foundation which has been subjected to repeated wave loading. Therefore, it is important to know the state of the soil at any given time in order to define and consider the correct soil stiffness (Briaud, 2001).

Another important factor is to know in which strain range a geotechnical problem will occur and Figure 2-3 illustrates a typical relationship between shear stiffness and strain of soil. Non-linear soil behaviour means that at small strains the stiffness is relatively large and at strains close to failure, the stiffness is small (Atkinson, 2000). Figure 2-3 also indicates typical ranges of strain for different geotechnical structures (Mair, 1993) and techniques (Atkinson & Salfors, 1991). It is important to understand how sensitive the instrumentation and test equipment should be for the measurement of effective soil stiffness.

Wrench (1984) reported that the nature of shallow horizons in Southern African is often granular and this is one reason why these materials are often the most suitable horizons to be used as a founding layer for structures that will impose light and medium loads. Gravels are difficult to sample and therefore it is practically impossible to determine soil stiffness in laboratory tests, however, in-situ testing does provide the opportunity to obtain reasonable design parameters for settlement designs (Wrench, 1984).

Plate load tests have been used extensively in the past four decades to determine soil stiffness for foundations and earthworks designs, as well as to check the compaction of road and airfield earthworks (Pantelidis, 2008). One of the major concerns in plate load testing are the bedding errors (Kay, 1986) that can occur between the plate and in-situ material, if sufficient surface preparation has not been performed before the plate load tests. This raises the question as to whether plate load tests can still be used as a practical and effective test method in routine field testing.

## 2.2. FACTORS AFFECTING SOIL STIFFNESS

This section will give an overview of the important factors that affect soil stiffness in general with emphasis placed on the factors affecting soil stiffness during plate load test measurements.

### 2.2.1. Soil state factors

Prior to discussing the specific factors that affect stiffness during plate load tests a few state factors that affect stiffness in general must be deliberated. This summary of the most important state factors that influence soil stiffness is taken largely from Heymann (1998) and Briaud (2001).

All natural soils can be represented by a three-phase system, which consists of solid particles, water, and air and the content of any soil can change depending on the current moisture condition of the soil. A soil can either be perfectly dry (no water content) or be fully saturated (no air content) or be partly saturated, with both air and water present (Davison, 2002). Low water content will lead to higher soil stiffness (especially for fine grained soils) which is caused by suction forces between the particles that result in an increase of mean effective stress. On the other hand, for coarse grained soils at very low water content, the compaction is not as effective as it would be at higher or optimum moisture content, because the lubrication effect of water is not present. Therefore, this phenomenon will lead to lower soil stiffness (Briaud, 2001).

The basic characteristics of a soil include particle size, particle shape, composition of the particles, and the structure of the soil. The average particle size ( $D_{50}$ ) and coefficient of uniformity ( $D_{60}/D_{10}$ ) enables understanding the overall grading of the soil. More particles per unit volume results in more contacts per unit volume and causes greater inter-particle sliding. Furthermore, well-graded soils have lower void ratios than uniform soils. Soil stiffness decreases with decreasing average particle size and coefficient of uniformity (Heymann, 1998). Uniform soils tend to be more loosely compacted in comparison to well-graded soils, which will normally be denser in their natural state. Dense soils with low void ratio, are deformed by particle deformation and loose soils with higher void ratio, deform by inter-particle sliding, therefore soil stiffness decreases with increasing void ratio.

The volume of soil includes both the volume of the solid particles and volume of voids (water and air), but the weight of soil only takes account of the mass of the solid particles and the mass of water, since the mass of air is negligible. The relationship between mass and volume is called the soil density and can be expressed as either dry density or in-situ density. Note that two soil samples may have the same dry density, but different structures and as a result have different soil stiffness. Caution should be taken here, because this may lead to laboratory and field moduli which are different, although the soil has been reconstituted to the same dry density and water content (Briaud, 2001).

In general soil stiffness is dependent on the mean effective stress (Heymann, 1998) and will increase with increasing mean effective stress. However, it has been proved in numerous studies that the effect of mean effective stress on soil stiffness becomes less critical as the bonding and cementation in soils increases to a significant level (Stokoe et al., 1995; Cuccovillo and Coop, 1997b). In cemented soil, sliding is prevented by interparticle bonds formed between particles (Acar and El-Tahir, 1986; Bressani, 1990) and therefore the soil stiffness will increase with increasing level of bonding and cementation. Figure 2-4 illustrates the findings from Cuccovillo and Coop (1997b) who investigated the effect of mean effective stress on the stiffness of intact and reconstituted calcarenite in a high pressure triaxial apparatus. The results show the effect of the breaking of the soil structure and bonding in the reconstituted samples. Table 2-1 summarizes the effects of different soil state factors on soil stiffness.

**Table 2-1: Effect of soil state factors on soil stiffness**

Soil State Factor	Factor	Soil Stiffness	Reference*
In-situ Density/ In-situ Unit weight	↑	↑	8
Void ratio	↓	↑	1 & 3
Plasticity	↑	↓	2
Average Particle size ( $D_{50}$ )	↑	↑	1
Coefficient of uniformity ( $D_{60}/D_{10}$ )	↑	↑	1
Particle angularity	↓	↑	5
Particle roughness	↓	↓	1
Water content (Coarse grained soils)	↓	↓	8
Water content (Fine grained soils)	↓	↑	8
Cementation	↑	↑	1
Ageing and bonding	↑	↑	6 & 7
Degree of saturation (cohesive soil)	↑	↓	4
Mean effective stress	↑	↑	1 & 3
Over-consolidation ratio (OCR)	↑	↑	1
1. Heymann (1998) 2. Jardine (1995) 3. Clayton et al. (1984) 4. Hardin & Drnevich (1972) 5. Park & Tatsuoka (1994) 6. Leonards & Ramiah (1959) 7. Bjerrum (1973) 8. Briaud (2001)			

Note: ↑Increase; ↓Decrease

### 2.2.2. Factors affecting plate load test measurements

Many researchers have published their solutions for calculation of the settlement of a uniform loaded rigid plate which rests on a semi-infinite elastic isotropic medium. The most commonly used equation for determination of Young's Modulus,  $E$ , from plate load test data is:

$$E = \frac{\pi Dq}{4\rho} (1 - \nu^2) \quad (2-1)$$

Where:

$D$  = Plate diameter

$\nu$  = Poisson's ratio

$q$  = Average plate stress

$\rho$  = Plate settlement

From Equation 2-1 the importance of determining the average plate stress and plate settlement correctly during plate load tests is clearly evident. The Poisson's ratio is dependent on the drainage conditions of the soil (Briaud, 2001) and for undrained soils during loading, Poisson's ratio can be taken as 0.5. For drained tests on soil, Poisson's ratio is normally between 0.2 and 0.3 (Wrench, 1984) and in the case where no excess pore pressure is present during loading, Briaud (2001) has suggested that a value of 0.35 may be acceptable. However, with the Poisson's ratio being squared in Equation 2-1, it means that a variation in Poisson's ratio will result in a relatively insignificant effect on the soil stiffness (Wrench, 1994).

In assessing the applicability of the simplified model described in Equation 2-1 it is necessary to consider how the requirements of the theory are justified in practice and the requirements that must be considered are homogeneity, isotropy and boundary conditions. Significant stress changes during plate load tests are only induced to about 1,5 times plate diameter below the plate. For most soils the stiffness and consistency vary with depth even over relatively small distances (Wrench, 1984).

The ratio between the plate diameter and the largest soil particle is also important, because large particles that occur in the loaded zone cause non-uniform stress distribution and therefore the elastic theory will not apply anymore. Typically, the plate diameter should not be less than six times the diameter of the maximum soil particle size (Wrench, 1994). Thus, although most soil horizons are not homogeneous, their effect on plate load tests can be minimized by carefully prepared and selected test locations. Wrench (1984) also suggested that a number of plate load tests should be performed in each horizon to establish average characteristics.

Real soil is generally anisotropic and unfortunately there is no simple analytical tool available that incorporates such an assumption of soil. Although a linear elastic stiffness parameter as normally determined during plate load tests, assuming the isotropic conditions will be incorrect from a fundamental standpoint, but the error should be relatively small due to

similar boundary conditions compared to the large scale structure (Kay, 1986). In addition, a study by Koning (1960), demonstrated that the response of plate tests and prototype footings on six anisotropic materials differed by less than seven per cent.

The elastic theory assumes that a rigid plate rests on the surface of a semi-infinite horizon. Therefore, vertical tests performed at ground surface will satisfy this condition, provided that the plate is not underlain by either a much stiffer or less stiff horizon. Tests performed in test pits or auger holes may not satisfy this requirement and may alter the stress distribution beneath the plate due to the boundary conditions and it must be ensured that the loaded soil is free from edge effects. Boyle (1992) suggested that the width of the test pit or height in the case of horizontal tests, should be at least 1,5 to 2,0 times greater than the plate diameter. Van Heerden and Maschek (1979) suggested that an acceptable ratio between the test area and plate diameter should not be less than 6 times. As a rule, horizontal tests should not be performed within 1 meter from the top or bottom of a test pit or trial hole. For vertical tests it is considered good practice by Wrench (1984) to limit the plate size to less than one third of the test pit or trial hole.

### **2.3. DETERMINATION OF SOIL STIFFNESS**

A number of methods have been developed and researched in the past to measure soil stiffness and in this section these methods will be discussed and briefly explained. In order to classify these methods, some important details should be taken into account, such as the theoretical basis of the test and the method of execution. In addition, the measurement principle of the tests may be used to differentiate between soil stiffness methods and based on these details, soil stiffness methods may be classified as direct, indirect or empirical measurement techniques. Furthermore, this classification system can be divided into two groups namely laboratory tests and field (in-situ) tests.

Direct techniques generally consist of tests where the stress increment is measured together with the corresponding strain increment and the soil stiffness can then be established by this relationship. Examples of direct field tests (in-situ) for measuring soil stiffness are the pressuremeter test (for example Gibson and Anderson, 1961), the screw plate test (for example Strout & Senneset, 1998), dilatometer tests (Marchetti, 1980; Totani et al., 2001), the German dynamic plate load test (German specification, 1992) and the plate load test (for

example Wrench, 1984; Marsland, 1971a). Direct measurement of soil stiffness in the laboratory includes the triaxial test (for example Jardine et al., 1984), the oedometer test (Terzaghi, 1925; Reznik, 1995) and hydraulic consolidation test (Rowe and Barden, 1966).

For indirect techniques, a theoretical foundation is required in which a relationship between soil stiffness and an additional material parameter is established. One example of such a relationship is between shear wave velocity ( $V_s$ ) and shear modulus ( $G_0$ ) of an elastic material as shown in Equation 2-2 (for example Heymann, 1998):

$$G_0 = \rho \cdot (V_s)^2 \quad (2-2)$$

Where:

$\rho$  = Mass density

Many techniques have been developed to measure shear wave velocity in both the field and the laboratory (for example Heymann, 1998). The two most frequently used laboratory tests which are based on shear wave velocity measurements are the resonant column test (Hardin and Richart, 1963) and bender element tests (Shirley and Hampton, 1977). In the field, shear waves are propagated either as surface waves or body waves. Examples of body wave techniques include down-hole (for example Lau, 1998) and cross-hole (for example Wong et al., 1983) techniques. Surface wave techniques include the continuous surface wave (CSW) test (for example Matthews and Clayton, 2004; Heymann, 2007) and the multi-channel analysis surface wave (MASW) method (for example Sanchez-Salinero et al., 1987; Park et al., 1996a).

Lastly, empirical techniques such as the standard penetration test (for example Stroud, 1989) and the cone penetration test (for example Meigh, 1987) are based on past experience where correlations have been made between soil stiffness and penetration resistance. It is important to use fair engineering judgment when these empirical techniques are employed, since they rely on the correlations made from the specific material conditions and soil type which may change from one site to another. This information may not be available and can result in inaccurate correlations (Heymann, 1998).

In the following sections, methods of measuring soil stiffness directly in the laboratory and the field will be discussed as well as the advantages and limitations of the techniques are briefly deliberated.

### 2.3.1. Direct laboratory tests

#### *The triaxial test*

The conventional triaxial test has been used widely in the past few decades to measure the stress-strain behaviour of soils (for example Jardine et al., 1986; Burland, 1989; Simpson, 1993; Hight and Higgins, 1995); however the reliability of the test results is influenced by numerous factors such as measurement methods and configuration of conventional triaxial apparatus. Figure 2-5 shows a typical set-up for a conventional triaxial test. The triaxial tests are one of the most popular methods for measuring soil behaviour in the laboratory, although it is suggested by several researchers (for example Atkinson, 1993) that results from conventional tests are only reliable for strains larger than 0.1 per cent (%). Strain levels may be categorized into three categories namely large, intermediate and small (Lo Presti, 1994), and during conventional triaxial testing these measurements are affected by errors such as bedding and tilting errors between the sample and porous stones. This may result in underestimating the soil stiffness values when compared to back calculations using measured settlements in the field (Ratananikom et al., 2007).

To measure strain levels smaller than 0.1% more accurately, local strain measurements have been used. Several types of local instrumentation have been developed in the past that can be used to directly measure the local soil deformation on the sample. Examples of local strain instruments include the Electrolytic Level Type Transducer (Burland and Symes, 1982), the Hall Effect Local Strain Transducer (Clayton and Khatrush, 1986), Local Deformation Transducer developed by Goto et al. (1991) and the Proximity Transducer (Kokusho, 1980). See Figure 2-6 which illustrates each small-strain instrument schematically. For more information on soil stiffness at very small strains see Heymann (1998). The main disadvantages of triaxial tests include disturbance of sampling due to reduction of external stresses, especially with granular material, jointed rock and fissured clays; and disturbance during the preparation and setting up of a sample, which can be avoided during field tests (Kung, 2007; Marsland, 1971).

### *The oedometer test*

The oedometer test is one of the most popular consolidation tests used in the laboratory. A sample is cut with a sharp edge steel ring that forms part of the testing apparatus and water drainage is allowed by either a top and/or bottom porous stones. A vertical load is applied to the top of the soil specimen through a rigid cap, while the settlement is measured with a dial gauge. Figure 2-7 shows the typical configuration of a conventional oedometer. The possible limitations of oedometer tests include sample disturbance, bedding errors, stress relief during excavation, time interval between sampling and testing, and the size of the tests may not be representative.

## 2.3.2. Direct Field (*In-situ*) tests

### *The pressuremeter test*

In the early 1950s, Ménard (1957) developed the pressuremeter in France. The pressuremeter is a simple, robust mechanical tool, which is well-adapted to use in routine investigations and Mair and Wood (1987) have recently completed a review of pressuremeter testing. Similar devices, designed for hard soils at higher pressure are sometimes referred to as ‘dilatometers’, and these will be discussed in the following subsection. Pressuremeter tests can be carried out in soils and rocks. The pressuremeter probe applies a uniform pressure on the ground by means of a flexible membrane and the usual practice is that the pressuremeter apparatus is installed vertically while the loading take place horizontally.

Figure 2-8 shows a typical pressure meter set-up in the field. The main aim of a pressuremeter test is to measure the relationship between radial applied pressure and the resulting deformation in order to obtain information on the stiffness. One disadvantage of the conventional self-boring pressure meters is that they are unable to penetrate very hard, cemented or stoney soils or rocks and in these materials, a borehole pressuremeter or Ménard pressuremeter is normally used.

### *The dilatometer tests*

In the 1980’s, the flat dilatometer test (DMT), with the test procedure and the original correlations was developed by Marchetti in Italy. The main advantages of DMT include simple equipment and operations, high reproducibility, cost effectiveness and the variety of

penetration equipment (Lutenegger, 1988). Figure 2-9 shows the basic components of the dilatometer.

The dilatometer consists of a steel blade that measures penetration resistance while it is being pushed or hammered into the soil. The most effective insert method is to push the blade in with a 20 ton penetrometer truck (up to 100m per day). Soil pressures are measured by expanding a 60mm diameter thin steel membrane about 1mm into the soil. Gas pressure is used for the inflation-deflation cycle of the steel membrane and is regulated by a control unit on the surface, which is connected by an electro-pneumatic tube running through the insertion rods. The main limitation of the dilatometer is that the required force for penetration should be preferably relatively low and in most areas of South Africa the soil is too hard to allow penetration, making it impractical to penetrate the blade to the required depth. For more design applications, recent findings and new developments in DMT see Marchetti's state-of-the-art report (1997).

#### *The screw plate load test*

The screw plate load test is an at depth plate load test for measuring deformation moduli which was originally developed in Norway at the Norwegian Institute of Technology, NTNU. The screw plate was first reported for use in sand by Kummeneje (1956) and in clay by Schwab and Broms (1977). A test method suggested for screw plate load tests was proposed by Schmertmann in 1970 based on his research experience from the University of Florida (Strout and Senneset, 1998) and Figure 2-10 illustrates a typical screw plate load test set-up.

Installation of the screw plate may cause pre-stressing effects on the soil and therefore it is recommended to apply a 50 kPa seating load after installation to remove such effects. The main limitation for this method is that with the initial applied load of 50 kPa, the soil has already been disturbed and stressed in the small strain range, which may be critical in the understanding and description of the soil behaviour. Another limitation for the screw plate load test is the installation complications that occur in more granular soil types.

## 2.4. PLATE LOAD TESTS (PLT)

In this section a brief history on how the plate load test was developed and evaluated over the last 65 years is discussed. The apparatus, standards and procedures, instrument calibration and data interpretation techniques are considered with the emphasis placed on the advantages and limitations of plate load tests.

### 2.4.1. History on plate loading tests

#### *Prior 1970s*

The most well-known plate load test used was by Terzaghi and Peck (1948) with the development of their settlement charts for footings on sand. One of their main observations concluded that settlement predictions on footings made on the basis of uniform compressibility with depth will result in over-estimating the settlement of structures. It is known that in most cases soil become less compressible with depth. However, Terzaghi and Peck (1948) proposed a relationship between settlement of a footing and a 1 ft plate, which leads to a maximum settlement ratio of 4 (See Figure 2-11), depending on the footing size (Clayton et al., 1995):

$$\rho_B = \rho_1 \left( \frac{2B}{B+1} \right)^2 \quad (2-3)$$

Where:

$\rho_B$  = settlement of a footing of width B;

$\rho_1$  = settlement of a 1 ft diameter plate ( $B_1$ ).

The first plate load test method was described by the British standard institute (CP 2001: 1957) in the code of practice for site investigations and was later re-approved in 1981 (BS 5930: 1981). Later when Terzaghi and Peck's relationship for settlement ratio, as shown in Equation 2-3, was investigated by Bjerrum and Eggestad (1963) a substantial scatter was found. In Figure 2-11 it can be seen that Terzaghi and Peck's relationship is similar to the lower bound of Bjerrum and Eggestad, while the upper bound is similar to results from D'Appolonia et al. (1970) for a breadth ratio of about 10 (Clayton et al., 1995).

Plate load tests are also useful in evaluating the properties of weak rocks (Ward et al., 1968; Marsland, 1972). Ward et al. (1968) have shown that the compressibility of weak rocks is governed by the discontinuities in the rock mass, and not in the intact rock. They have concluded that actual test values of weak rocks can only be obtained successfully from in situ loading tests.

*Year 1970-1990*

In 1970, Lake and Simons have proposed the following equation for calculating foundation settlements from plate load tests on chalk:

$$\frac{\rho_f}{\rho_p} = \left( \frac{B_f}{B_p} \right)^\alpha \quad (2-4)$$

Where:

$\rho_f$  = settlement of foundation;

$\rho_p$  = settlement of plate;

$B_f$  = width of foundation;

$B_p$  = width of plate.

Lake and Simons (1970) concluded that  $\alpha$  can be taken as unity when extrapolating from plate load tests at the foundation level and this conclusion was later supported by results reported by Hobbs (1975). In 1971, Marsland made a few very good comparisons between large diameter plate load tests (865 mm plate diameter) and triaxial tests (38 mm and 98 mm diameter specimens). These comparisons have shown that triaxial tests can overestimate the large-scale strength of stiff fissured clays (Marsland, 1971a, 1971b). The large diameter plate tests were performed at 25 m depths and installed in 900 mm boreholes on several types of stiff fissured clays.

Further research has shown that deformation moduli determined from load-settlement curves of these large diameter plate tests were several times higher than those measured in standard

triaxial tests (Marsland, 1971c). Figure 2-12 shows some of the results from these comparisons.

The following year (1972), Marsland achieved much better repeatability of ultimate bearing pressures with plate tests than those obtained with undrained triaxial tests in fissured over-consolidated London clay at Wraysbury (Marsland, 1972). Figure 2-13a shows the usual scatter of triaxial test results which is normally expected from tests on stiff fissured clays, while Figure 2-13b shows the individual plate test results achieved by testing the base of a bucket-augured borehole. Although great effort was made to reduce the time incurred while the clay was unloaded and to remove all disturbed material, some expansion of the clay had still occurred due to the rapid stress relief caused by the borehole excavation. This resulted in an under-estimation of soil moduli and the only way that the bedding disturbance and expansion of the clay could be investigated was to measure the movements of the fissured clay at a distance below the plates.

Multi-point measurement equipment was engineered by Wallace, Slebir and Anderson in 1969, but this equipment could not meet the rapid installation procedure required (Wallace et al., 1969) in deep borehole measurements. Marsland and Eason have developed improved measuring equipment in 1973 to meet these requirements (Marsland and Eason, 1973). This has proved to be a very reliable measuring system with a consistent pattern of settlement measurements at four positions below the plate.

Pells (1983) made a significant contribution when he summarised the analytical solutions that formed the basis of interpreting different plate load tests at that time. Figure 2-14 reflects different types of plate load test layouts, which were discussed by Pells (1983). Smaller plate loading tests were carried out by Wrench (1984) as routine tests on granular soils in South Africa. Over 170 plate load tests were performed and analysed on gravel, where the soil modulus had been determined. Wrench (1984) has presented relationships between measured modulus and observed consistencies which are very useful when dealing with preliminary designs governed by settlement requirements.

The ASTM standard D1196-64 for static plate load tests (March 1972) were re-approved and published by the ASTM committee D-18 in 1987. This standard test method is today still one of the most preferred standards by various laboratories and companies in South Africa.

*After 1990s*

In clause 4.1 of the BS 1377-9: 1990 the plate load test was described and this highlighted the preliminary information required before the apparatus and test procedure for plate load tests can be determined. These include:

- a) In order to judge the required loading and size of the apparatus, the expected strength and deformation characteristics of the soil need to be estimated;
- b) The position and elevation of the test plate with respect to the loading frame needs to be determined;
- c) The parameters to be determined and their required precision;
- d) The size of the loading plate needs to be selected;
- e) The range of loads to be measured, the maximum reaction load required and how the total load will be provided;
- f) An estimate of the expected plate settlement to be measured and the accuracy required.

Ervin and Kurzeme (1992) have used plate load tests to assess the deformation properties of gravelly soil. Renovation to an eight-storey building was planned and resulted in the increase of the initial design loads. Plate load tests were successfully used to determine if the allowable bearing capacity would be sufficient to accommodate the additional loading.

In 1994, Wrench described the principles and applications of plate load tests in South Africa and it is important to note that these principles still apply today. An important advantage of plate load tests is that they allow geotechnical engineers to successfully determine the compressibility of soils and rocks that cannot be easily sampled (Wrench, 1994). In 1997, a new generation plate load test was introduced by the Middle East Technical University (METU) that presented a hydraulic loaded rigid plate and a multi-borehole displacement measuring system (Unal, 1997). More details on this test method will be provided in Section 2.5.

A series of nine large diameter (1,8 m) plate load tests were performed by Matthews and Clayton (2004) on three different weathered chalks in order to support the empirical method proposed by Burland and Lord (1970). The results of these nine tests were interpreted in terms of Burland and Lord's model, and these were similar to the pattern of behaviour that

was observed by Ward et al. (1968) at Mundford. The results have revealed that the initial modulus of hard chinks could be lower than comparable values for soft chinks, because of block looseness. In most tests, the limit of linear load-settlement behaviour was reached at, or slightly above 200 kPa, which is similar to that suggested by Ward et al. (1968).

The last contribution towards this plate load test history, which should be mentioned here, is the numerical analyses of the plate load tests carried out by Teodoru and Toma (2009). A finite element method (FEM) was used and this was analysed with the Mohr-Coulomb soil model in order to highlight the plate size effect on settlements and coefficient of sub-grade reaction. The results have revealed that the coefficient of sub-grade reaction is mainly affected by the deformation characteristics of the soil and even more importantly, the size of the contact area between the plate and the soil.

#### 2.4.2. PLT apparatus

In this subsection the main components for the conventional plate load tests are discussed. Figure 2-15a, b and c shows all the components and the layout of the conventional plate load test as well as typical results.

Plate load tests have been used extensively in the past to determine the bearing capacity and the stiffness of soil and can either be performed vertically or horizontally. A typical plate load test consists of a rigid plate that typically varies between 300 mm and 762 mm (ASTM 1194-72), which is loaded using a hydraulic pump and jack system. Some means of reaction force is used to provide the required load applied to the plate. The displacement of the plate is typically measured with two or more calibrated displacement measuring devices attached to the plate.

##### *Loading plates*

In the past, plate sizes that varied in diameter between 100 mm and 1,8 m have been used for plate load tests (Wrench, 1984; Matthews and Clayton, 2004). The two main factors that affect the loading plate size include the available reaction force and the expected maximum particle size of the soil.

It is suggested that the loading plate diameter should be at least six times the diameter of the maximum particle size (Wrench, 1994; Clayton et al., 1995), but preferably ten times larger (ENV 1997-3:1999). It is suggested that a set of steel plates at least 25 mm in thickness be stacked in a pyramid fashion to ensure rigidity (ASTM 1195-64; ASTM 1196-64). Flexible or rigid plates may be used effectively in soil or rock (Pells, 1983), however it is more suitable to use a stiff contact plate when testing soil or soft rock (Vrkljan et al., 1995). The suggested practical range for loading plates is 0.4 to 1.0 m in diameter and therefore it is important to consider that if a larger plate is used, the loading capacity of the hydraulic system and reaction force should be adequate (Unal, 1997).

#### *Applied load measuring system*

Typically the loading is applied by means of a hydraulic pump and jack system. However, several methods have been suggested to measure the applied load. The most popular methods are either a calibrated load cell, or a pressure gauge which is connected to the hydraulic pump. The Euro Code 7 Part 3 (ENV 1997-3: 1999) suggests that the load measuring system shall be able to measure any applied load with 5% accuracy and that it shall be free from any hysteresis effects. It is further suggested that a hydraulic jack be used with sufficient load capacity for applying the maximum load required (ASTM 1196-64).

#### *Reaction force system*

The reaction force can be provided by either jacking against kentledge blocks (Wrench 1984), against tension piles, against grouted anchors (ENV 1997-3: 1999) or an existing abutment (Ervin and Kurzeme, 1992). It is suggested by ENV 1997-3: 1999 that the distance between the centre of the plate and the reaction system should be at least 3,5 times the plate diameter as shown in Figure 2-16. In the case of tension piles, a distance of 3 times the plate diameter between the pile centres and the centre of the plate is normally sufficient (BS 1377-9: 1990).

#### *Plate displacement measuring system*

Various plate load test standards suggest that at least three displacement measuring devices should be used to account for any tilt that occur during testing and to measure the average settlement of the plate. The most common devices to measure the plate settlement are either dial gauges or electrical displacement transducers such as LVDTs (ASTM 1196-64; Wrench, 1984; ENV 1997-3: 1999).

Preferably the displacement measuring devices should be placed 120 degrees apart from each other (Wrench, 1994; Clayton et al. 1995) and 25 mm from the perimeter of the plate (ASTM). It is suggested that the measuring devices should be able to measure up to at least 15% of the plate diameter with an accuracy of 2% of the measuring range or 100  $\mu\text{m}$  (ENV 1997-: 1999).

It is further suggested that the displacement measuring devices should be fixed to a reference beam which is anchored at least twice the plate diameter away from the plate perimeter (Clayton et al. 1995; Wrench, 1994). However, ASTM 1196-64 suggests a distance of 2,4 m should exist between reference beam anchor and plate perimeter. This appears to be overly conservative, at least for small plates, when compared to the guidelines suggested by Clayton et al. (1995) and Wrench (1994). The reference beam should be protected against temperature effects, wind and direct sunlight. In addition, a reference beam shall be designed to be adequately stiff to avoid creep and vibration effects in the beam (ENV 1997-: 1999).

#### *Boundary conditions*

It is important to consider the boundary conditions for conducting plate load tests during the experiment design phase. Wrench (1984) concluded that for tests conducted inside an auger hole the plate settlement may be underestimated, due to the confining pressures of the surrounding soil, and he suggested that the plate size be limited to less than a third of the auger hole diameter. In order to reduce these restraining effects and to be able to assume a half space model, Unal (1997) suggested that the perimeter of the plate should be a distance of 1,5 times the plate diameter from the sides of the test pit. If more than one test is required in a given area, the spacing between consecutive plates should not be less than six times the plate diameter (ENV 1997-3: 1999).

#### 2.4.3. Calibration for plate load test systems

This subsection describes the calibration of plate load test systems and instrumentation used for the experimental work. Emphasis is placed on the calibration parameters which are commonly used to define the behaviour of instrumentation.

Calibration refers to the operation that establishes the relationship between measured values with measurement uncertainties and the corresponding “true value” with associated

measurements uncertainties (JCGM/WG 2, 2008). There are different ways in which calibration may be expressed and these include a calibration diagram, a calibration curve, a calibration table, a calibration function, or it may simply consist of an additive or multiplicative correction of the “true value” indication with the associated measurement uncertainty (JCGM/WG 2, 2008).

It is important that the “true value” indicator or reference system should be at least 3 to 10 times more accurate than the measuring system being used during the experiment (for example Doebelin, 1990). Therefore, it is advisable to know the calibration hierarchy of the instrument being calibrated. The calibration hierarchy is the sequence of calibrations from a reference system to the final measuring system. The measurement uncertainty will increase along a sequence of calibrations and the outcome of each calibration will depend on the outcome of the previous calibration operation (JCGM/WG 2, 2008).

The two most commonly used terms to describe the calibration of a measuring instrument are those of accuracy and precision. The accuracy of a measuring instrument is defined by Working Group 2 of the Joint Committee for Guides in Metrology (2008) as the degree of closeness of measurements compared against the “true” values. Precision is defined as the closeness of the agreement between the measured values which are obtained by replicate measurements on the same object. Precision can also be described as the degree of repeatability (SANS 100099). Figure 2-17 illustrates the difference between accuracy and precision.

Another important part of the process is to establish the resolution and sensitivity of a measuring device. The resolution of a measuring device is defined by SANS 100099 as the smallest change in a quantity being measured that causes a visible change in the corresponding reference measuring device.

The sensitivity of a measuring device refers to the proportion of the change in the quantity of a reference measuring device and the corresponding change in a value of the quantity being measured. This change, when considered in a value of the quantity being measured, should preferably be large compared with the resolution (JCGM/WG 2, 2008).

It is further suggested that the load transducer system and the displacement measuring devices of plate load tests are calibrated at least every 6 months. One way of checking the calibration on site is to insert a measuring block of known size under the tip of the displacement transducer (ENV 1997-3: 1999).

#### 2.4.4. Test standards and procedures

Various standards for conducting plate loading tests have been developed and described by:

- CP 2001: 1957: Code of practice for Site Investigation.
- ASTM D1194-72: Standard test method for bearing capacity of soil for static load and spread footings;
- ASTM D1195-64: Repetitive static plate load method for soils;
- ASTM D1196-64: Non-repetitive static plate load method for soils;
- BS 5930:1981: Code of practice for Site Investigation (Formerly CP 2001: 1957);
- BS 1377-9:1990: In-situ vertical deformation and strength tests;
- Eurocode ENV 1997-3:1999: Plate load tests

A general test procedure will consist of the following steps:

- a) The test area should first be levelled to achieve a uniform bearing. All disturbed material should be removed (ENV 1997-3: 1999). ASTM 1195-64 and ASTM 1996-64 proposed the following surface preparation methods to achieve a smooth test area:
  - A thin bed of mixture of sand and plaster of Paris; or
  - Plaster of Paris alone; or
  - Fine sand.

A thin plaster of Paris layer of not more than 20 mm in thickness is the most preferred surface preparation method suggested by most test standards, especially if the tests are being conducted for research purposes and on cohesive soils (Wrench, 1994; ENV 1997-3: 1999). For tests on granular soils, any hollows should be filled with clean dry sand to produce a level surface on which to bed the plate (BS 1377-9: 1990). Other standards suggest that an initial load sufficient to produce a settlement of not less than 0.25 mm or more than 0.51 mm be applied to the ground in an attempt to reduce bedding errors present prior to the test (ASTM 1195-64). The disadvantage of such an approach is that

vital information about the soil behaviour qualities might be lost during this initial settlement.

- b) The next step involves the preparation and erection of the loading and measuring equipment (ENV 1997-3: 1999). The reaction force system, hydraulic jack, force measuring and displacement measuring systems should be carefully put in place without preloading the plate.
- c) Loading can be applied in two different ways, namely incremental loading or a constant rate of penetration. For the incremental loading test, about ten equal load increments (no more than 95 kPa) should be applied and these kept constant for a certain time (ASTM 1194-72). Normally each load is applied for 8 minutes, but preferably 16 minutes should be allowed, (ENV 1997-3: 1999) and are kept constant until the rate of displacement (creep) is less than 0.030 mm per minute for three consecutive minutes (ASTM 1195-64). Displacement readings should be recorded on a 'square of the integer' basis (1, 4, 9; 16, 25 minutes etc.) to ensure that sufficient reading are taken in the early stages of loading (Clayton et al., 1995). Load increments should be applied until shear failure of the soil occurs, or until the contact pressure reaches two or three times the design bearing pressure (Clayton et al., 1995).

The constant rate of penetration test is normally conducted when the undrained loading characteristics of cohesive soil are to be obtained (ENV 1997-3: 1999). The load should be applied to the soil to reach a constant rate of settlement and the test will be terminated once the average plate settlement reaches 15% of the plate diameter (BS 1377-9: 1990).

#### 2.4.5. Data analyses and interpretation techniques

This subsection describes the different data analyses and interpretation techniques used in the past to present plate load test results. Plate load tests are mainly performed to determine both the ultimate bearing pressure and the stiffness of the soil.

One method of presenting plate load test results is by plotting a pressure-settlement curve and the time-settlement curve as shown in Figure 2-15b and c. This will give an indication of the

maximum contact pressure (ENV 1997-3: 1999) being reached during the tests and the time allowed for the soil to creep after each load application (Clayton et al. 1995).

The ultimate contact pressure from plate load test results may be defined as:

- a) the largest possible pressure in dense sand or sensitive clays;
- b) the pressure that results in a settlement equal to 15% of the plate diameter; or
- c) the pressure where the creep has increased considerably (ENV 1997-3: 1999).

The most general equation used for plate load tests to provide elastic moduli values is derived from elastic theory for a uniformly loaded rigid plate on a semi-infinite elastic isotropic solid, (For example Timoshenko and Goodier, 1951) and can be presented as:

$$E = \frac{\pi D q (1 - \nu^2)}{4\rho} \quad (2-5)$$

Where:

- $D$  = Plate diameter  
 $\nu$  = Poisson's ratio  
 $q$  = Average plate stress  
 $\rho$  = Plate settlement

For granular soils and soft rocks Poisson's ratio will normally be between 0.1 and 0.3, and so the term  $(1 - \nu^2)$  has a relatively small effect.

More complicated analytical techniques are available which include solutions by Poulos and Davis (1974) for homogeneous single and two layer mediums; techniques by Kondner (1963) where plate load test results are presented by a rectangular hyperbola, and solutions presented by Carrier and Christian (1973) for cases where soil stiffness increases with depth. However, due to the complexity of these techniques and the difficulty of determining soil properties at each site, these solutions are not the preferred techniques for interpreting routine plate load test results (Wrench, 1984).

## 2.5. MULTI-DEPTH DISPLACEMENT MEASUREMENTS

Various methods and techniques have been developed to measure the displacement below the plate by means of a multi-point or multi-hole measuring system in soil and rock (Wallace et al., 1969; Burland, 1970; Marsland & Eason, 1973 and Unal, 1997). This section reviews some of these methods and techniques with the emphasis placed on their advantages and limitations.

Several studies were made on deep borehole plate load tests with plates up to 865 mm in diameters on stiff fissured London clay (Marsland, 1971a, 1971b, 1971c). One of the main objectives for these tests was to design the equipment and test procedure in such a way as to reduce the time between excavation and re-loading to a minimum (Marsland & Eason, 1973). This was required in order to keep the expansion of the clay below the base of the borehole as small as possible. However, it was found that some expansion of the clay was still unavoidable, due to the stress reduction during excavation that had caused the rapid opening of fissures. As a result this confirmed that the only way to investigate the effect of the expansion of the clay and the effect of bedding disturbance on the load-settlement behaviour was to measure the soil movements at positions below the plate (Marsland & Eason, 1973).

Multi-point measurement equipment was engineered by Wallace, Slebir and Anderson in 1969, but this could not meet the rapid installation procedure which was required in deep borehole measurements (Wallace et al., 1969). Marsland and Eason (1973) then developed improved measuring equipment with the aim of meeting these requirements and their main objective was to design a system that could be easily and quickly installed in the confined space of a 900 mm borehole.

Marsland and Eason (1973) successfully developed two measuring systems for both a single-point and a multi-point measuring set-up. Figure 2-18 shows the single-point measuring system. The relative displacement between the loading plate and an aluminium tube, installed at 400 mm below the plate, was measured with a displacement transducer. The results revealed that more than 50 per cent of the plate settlement occurred in the first 400 mm below the plate, compared to the theoretical value of 15 per cent for an isotropic homogeneous elastic material (Marsland & Eason, 1973).

A highly sophisticated system was designed by Marsland and Eason (1973) to measure the movements of the soil at four positions below a loading plate. Figure 2-19 illustrates the multi-point measuring system. This has proved to be a very reliable measuring system with a consistent pattern of settlement measurements at the four positions below the plate. For more detail on the equipment description and test procedure see Marsland and Eason (1973). The results from these tests have revealed that the modulus value calculated at 610 mm below the plate was about twice the stiffness value that was calculated with the plate settlement. Another advantage of this measuring system was that the settlements at points below the plate provided a more sensitive measure of the swelling pressure of the clay compared to the settlements of the plate (Marsland & Eason, 1973).

Although Marsland and Eason (1973) proved that these techniques do provide good results in stiff fissured clays, it is still uncertain whether similar results may be expected for other soil types. The use of this multi-point measuring system described by Marsland and Eason (1973) was considered by a few others (For example Matthews and Clayton, 2004) but was rejected due to a number of limitations. These limitations included the complex installation process; uncertainties about the ability of the system to anchor itself effectively, and the difficulty in determining the reduction in stress below the plate for the interpretation of the results (Matthews and Clayton, 2004). The settlements of points below the plate may be smaller than the plate settlement and can be caused by various factors which include bedding errors, plastic deformations concentrated in the soil near the plate and measurement errors (Pells, 1983).

Two examples of new generation plate load tests conducted in rock include those developed by the International Society of Rock Mechanics (ISRM, 1981) and the Middle East Technical University (METU) that use a hydraulic loaded rigid plate and a multi-borehole displacement measuring system (Unal, 1997). For more detail on the equipment description and test procedure see ISRM (1981) and Unal (1997). Figure 2-20 shows the details of the instrumentation system of the METU plate-loading apparatus.

Two of the disadvantages of the ISRM-suggested method are that: (i) it requires the estimation of Poisson's ratio and, (ii) it may estimate higher modulus values than the intact modulus values determined in the laboratory, which are not possible (Boyle, 1992).

An alternative numerical computation method was suggested by Boyle (1992) which took into account the disadvantages of the ISRM method. This method determines the Poisson's ratio and deformation modulus by using the least-squares technique; however it was pointed out by Unal (1997) that this alternative method suggested by Boyle (1992) contains a typographical error (Unal, 1997).

By utilizing the method suggested by METU, the stress-strain behaviour of the rock mass can be represented graphically and from these graphs, the loading, unloading and overall deformation modulus of the rock mass can be established. Unal (1997) concluded that in order to obtain accurate results from this new-generation plate load tests, the proper testing and accurate interpretation of the test data are essential.

## **2.6. CONCLUSIONS FROM LITERATURE REVIEW**

The following summarises the most important conclusions made in this chapter:

- a) The secant stiffness is typically used to predict the foundation settlements due to the first loading of a spread footing (Briaud, 2001).
- b) Bedding errors affect the soil stiffness measurements during plate load tests and they need to be eliminated or kept to a minimum.
- c) The main advantages of plate load tests are:
  - The cost-effectiveness of the test;
  - The relative straightforward test procedure;
  - That no soil sampling is required.
- d) The limitations of plate load tests are:
  - It has limited depth of influence and only provides the bearing capacity of soils with depth up to 1,5 times the diameter of the plate (Clayton et al. 1995);
  - It may not provide information on the potential for long term consolidation of foundation soils;
  - There is scale effect as the size of test plate is smaller than the actual foundation;
  - To gain access to a test position, excavation is sometimes carried out which causes significant ground disturbance. The change in ground stress itself may lead to the change of soil properties, which the test intended to measure.

- e) In order to obtain accurate results from the new-generation plate load tests, proper testing and accurate interpretation of the test data are essential.

From the discussion above, the following shortcomings that exist in technical knowledge on plate load tests can be identified:

- i. The effect of bedding errors on the accuracy of plate load tests has not yet been fully investigated;
- ii. The effectiveness of different surface preparation methods for plate load tests is not yet fully understood;
- iii. The use of a multi-point measuring system for plate load tests in soil is not used in routine tests.

From the shortcomings in the current background and technical knowledge on plate load tests, the objectives for this dissertation are as follows:

- i. To quantify the bedding errors that occur during plate load tests;
- ii. To evaluate the different surface preparation methods used in plate load tests;
- iii. To develop a modified plate load test capable of measuring displacements below the loading plate and to successfully eliminate the effects of bedding errors.

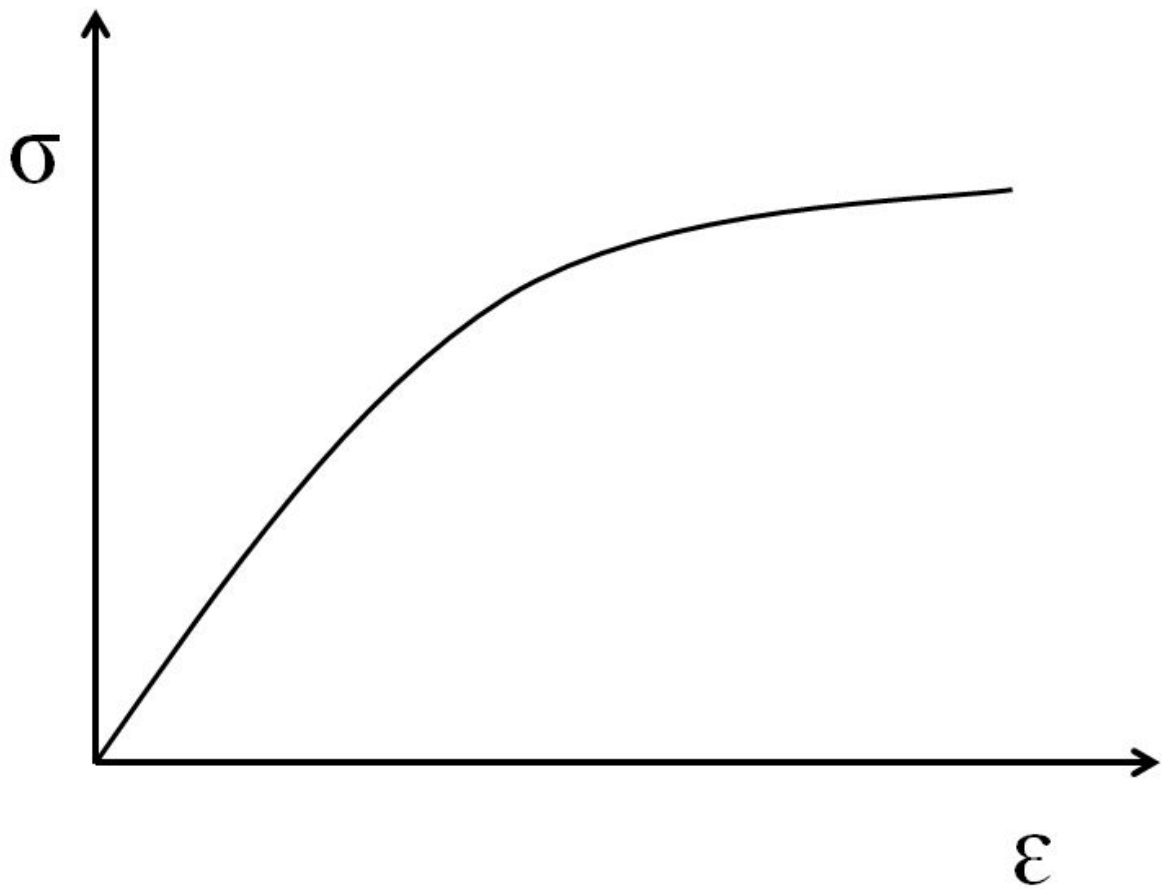


Figure 2-1: Typical Stress-Strain Curve.

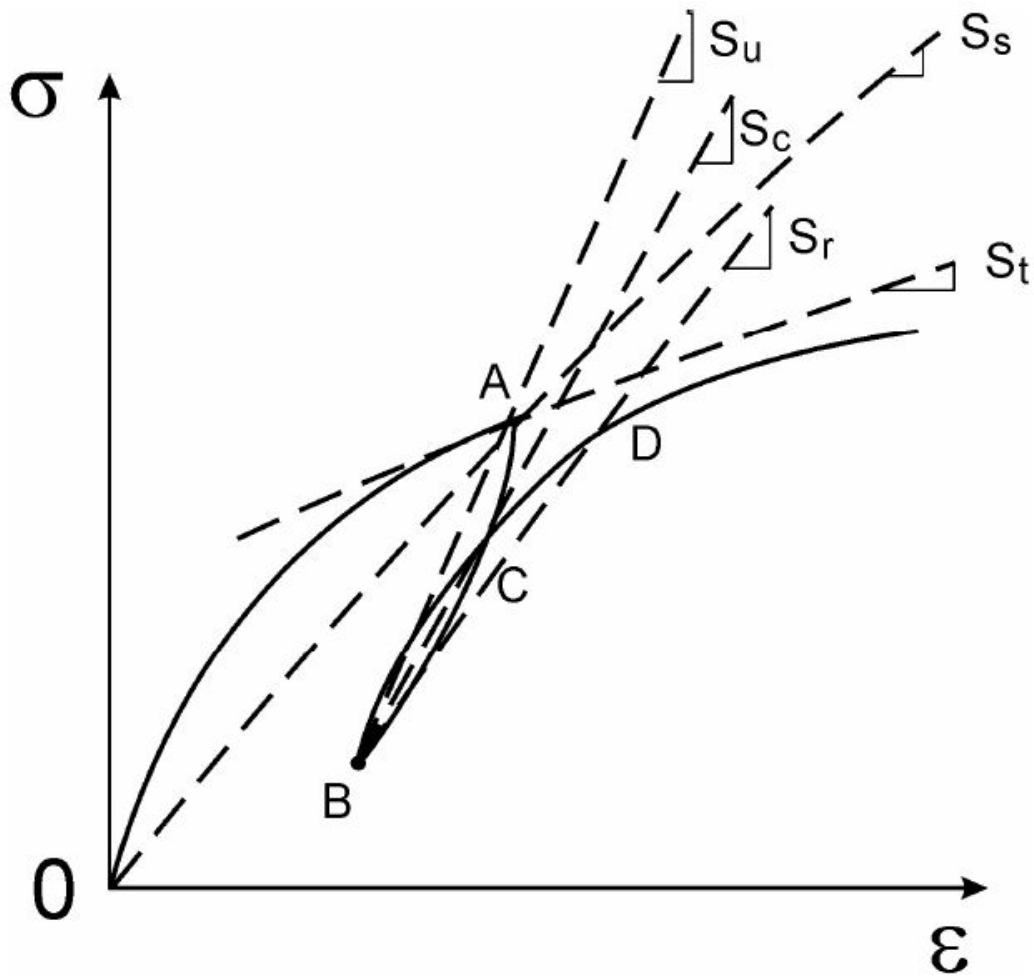


Figure 2-2: Definition of Soil Stiffness (After Jean-Louis Briaud, 2001).

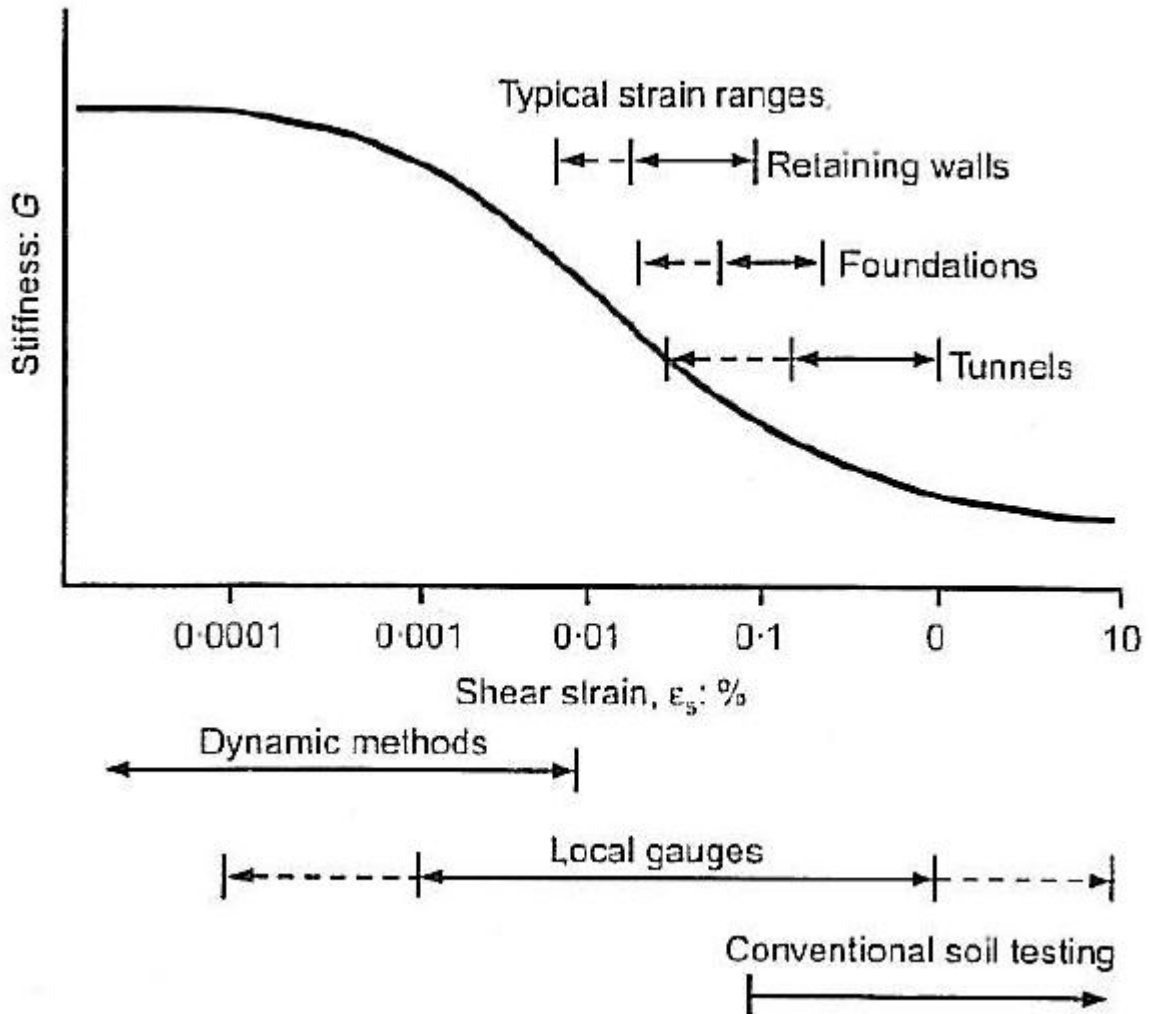


Figure 2-3: Characteristic shear stiffness-strain behaviour of soil with typical strain ranges for laboratory tests and structures (after Atkinson & Salfors, 1991 and Mair, 1993).

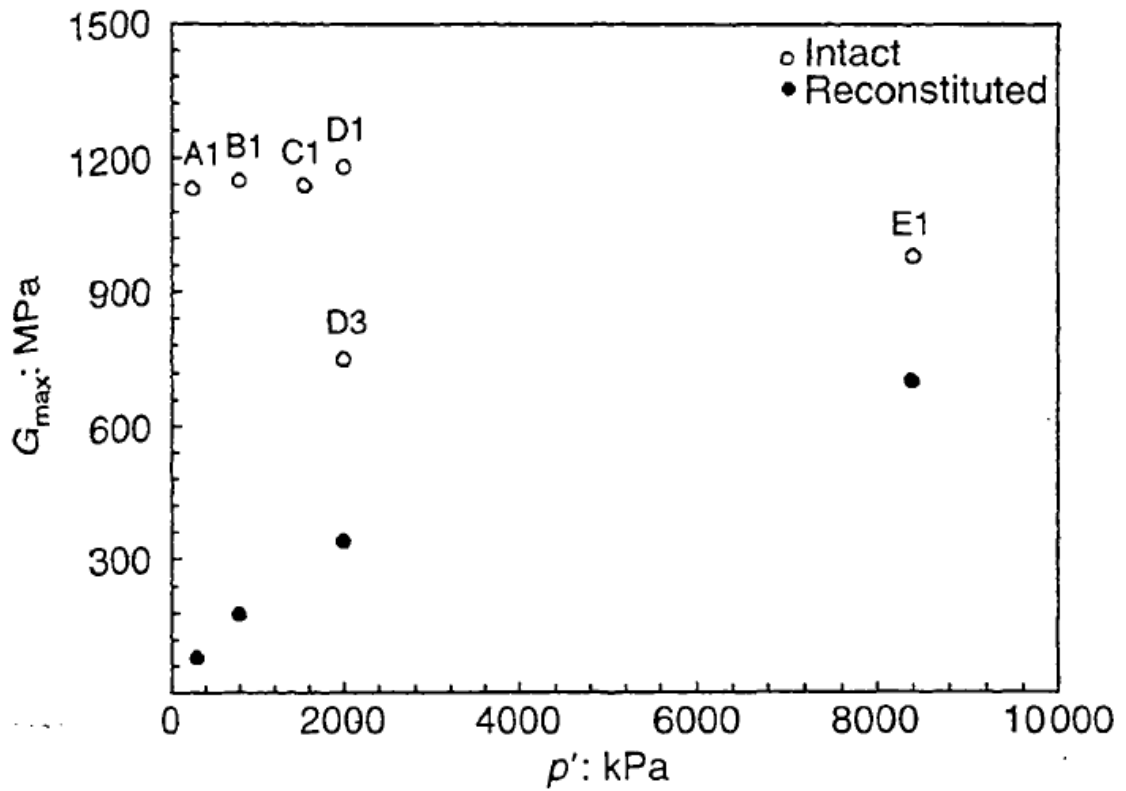


Figure 2-4: Stiffness of Calcarenite (After Cuccovillo and Coop, 1997b).

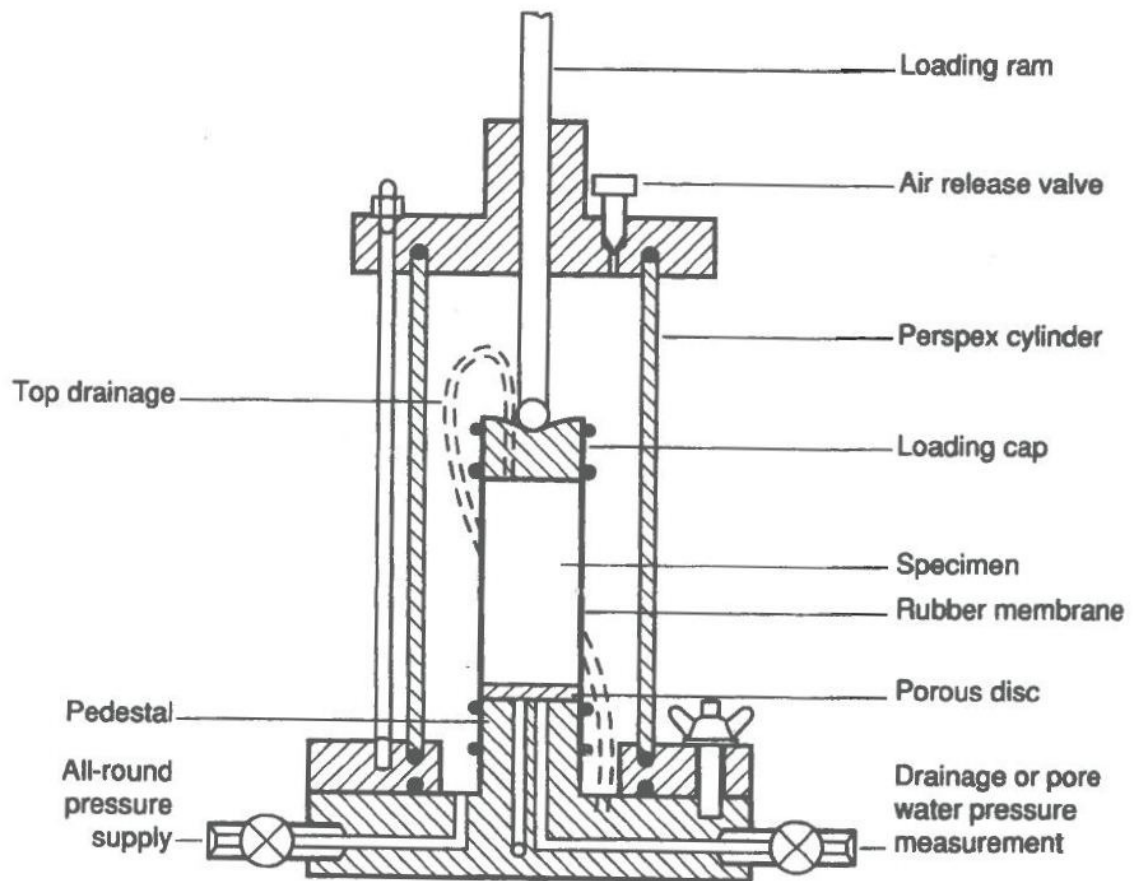
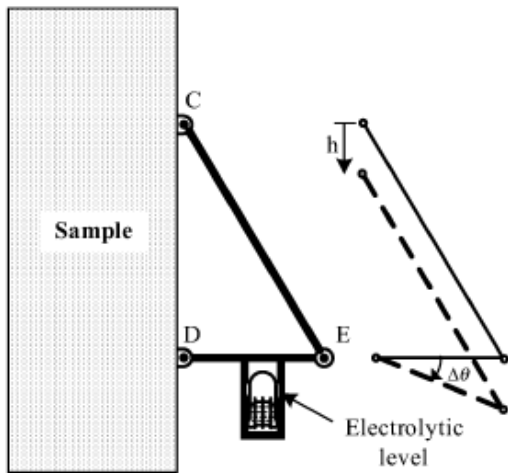
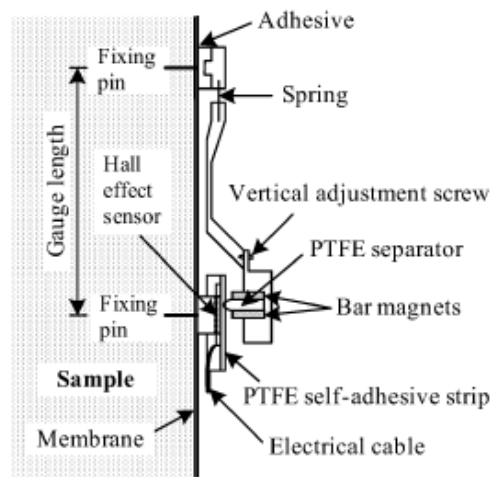


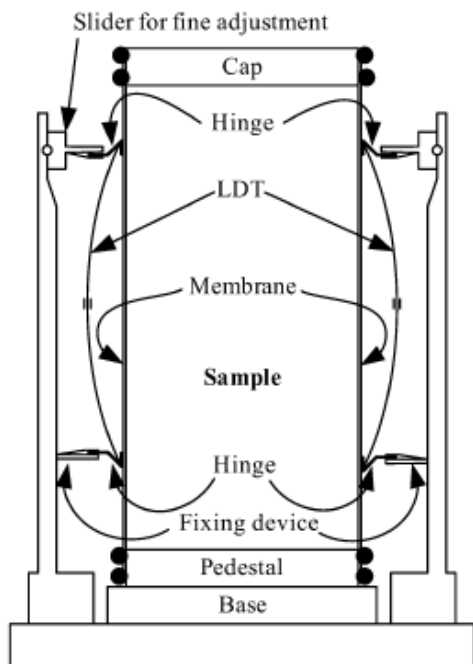
Figure 2-5: Conventional triaxial set-up (After Craig, 2004).



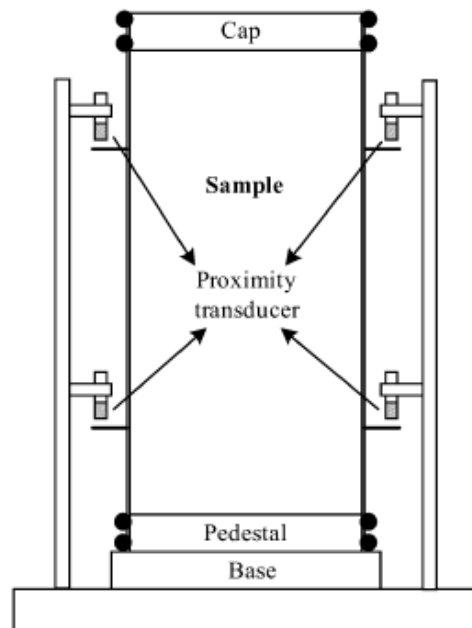
(a) Burland and Symes (1982)



(b) Clayton and Khatrush (1986)



(c) Goto et al. (1991)



(d) Kokusho (1980)

Figure 2-6: Local strain transducers (after Kung, 2007).

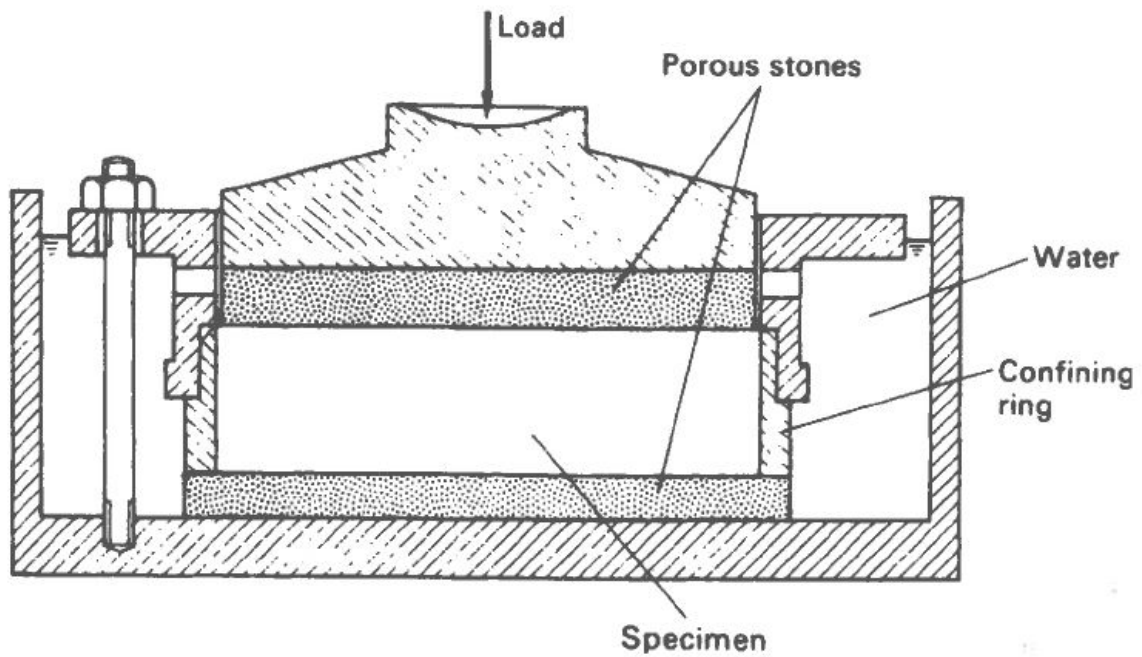


Figure 2-7: Typical configuration of a conventional oedometer (After Craig, 2004).

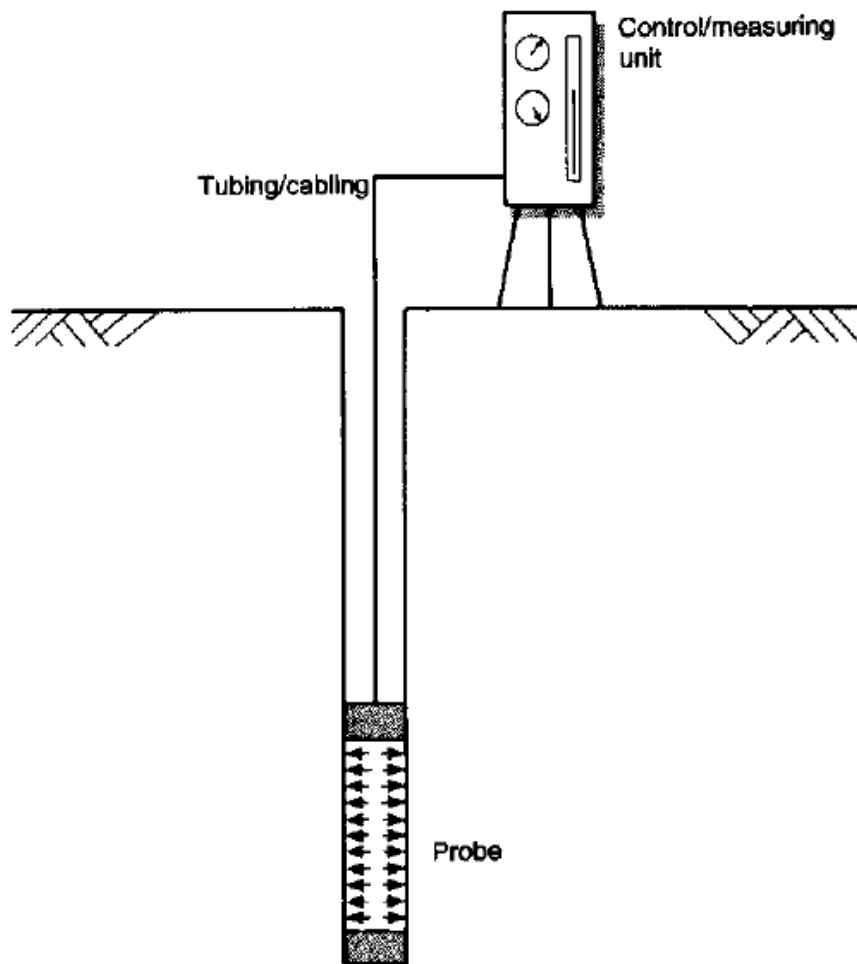
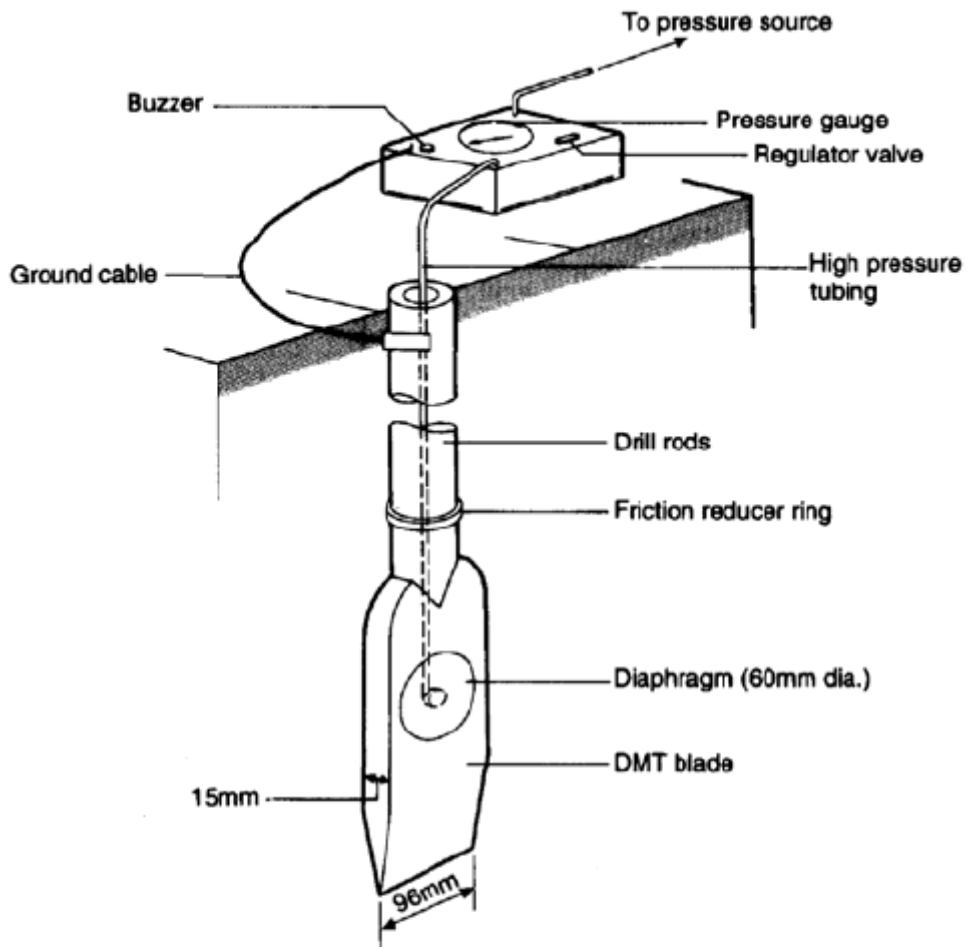


Figure 2-8: Basic components of the pressure meter (After Clayton et al. 1995).



Dilatometer test sequence

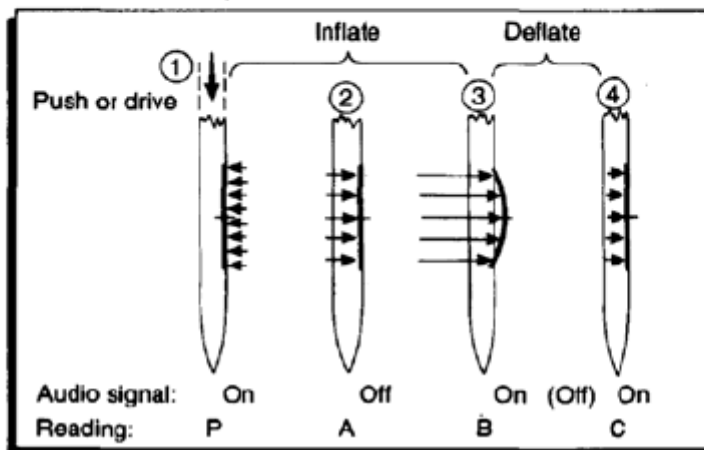


Figure 2-9: Marchetti dilatometer (After Marchetti, 1980).

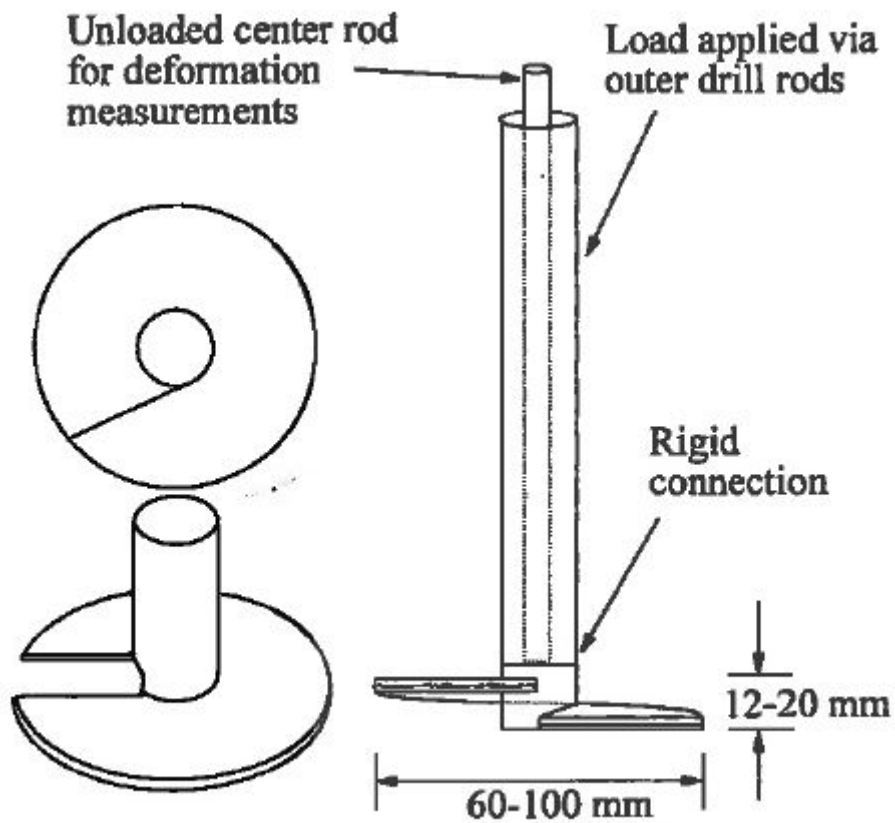


Figure 2-10: Screw-plate load test apparatus (Strout and Senneset, 1998).

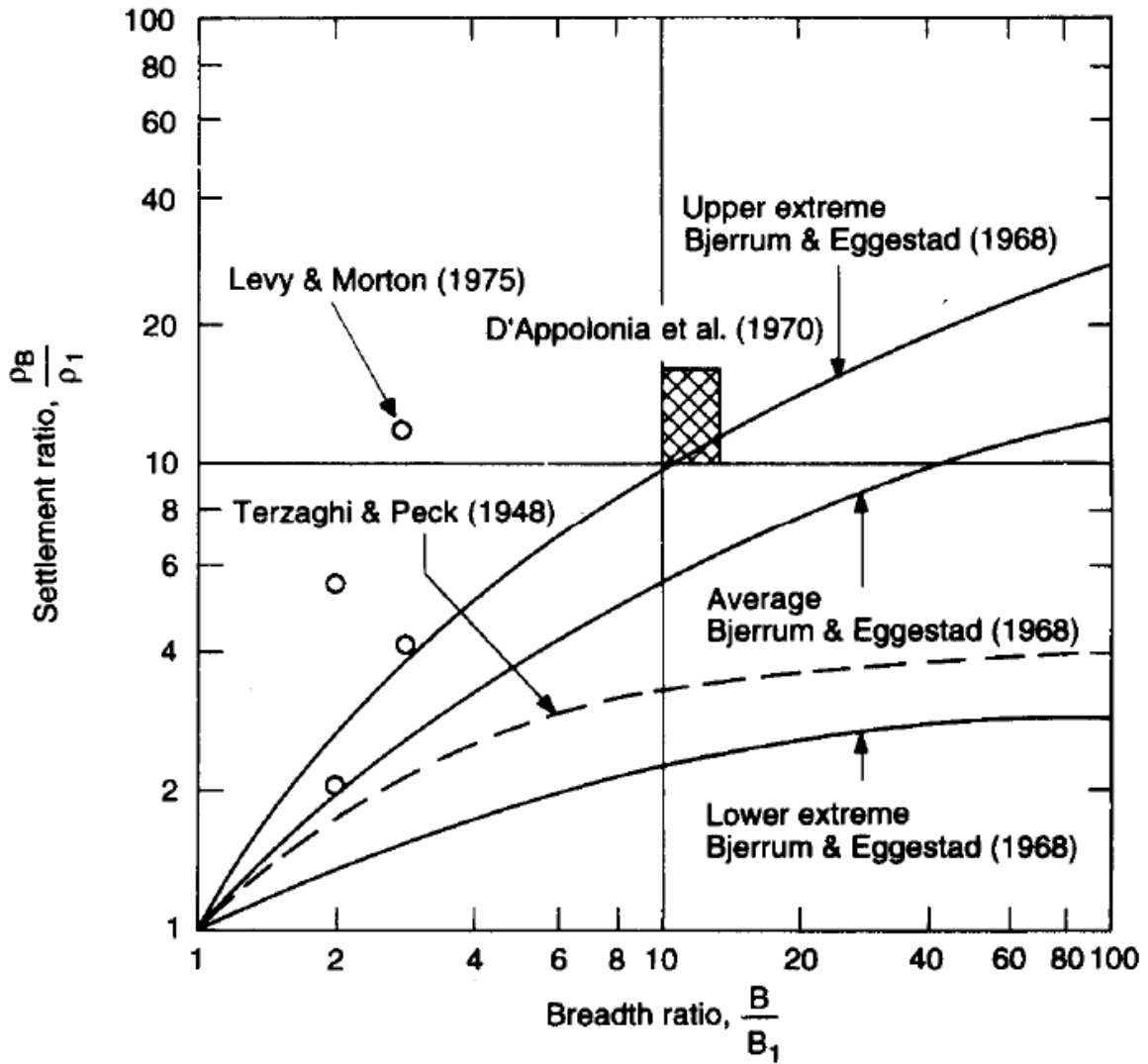


Figure 2-11: Correlation between plate bearing tests and settlement of foundations (After Sutherland, 1975).

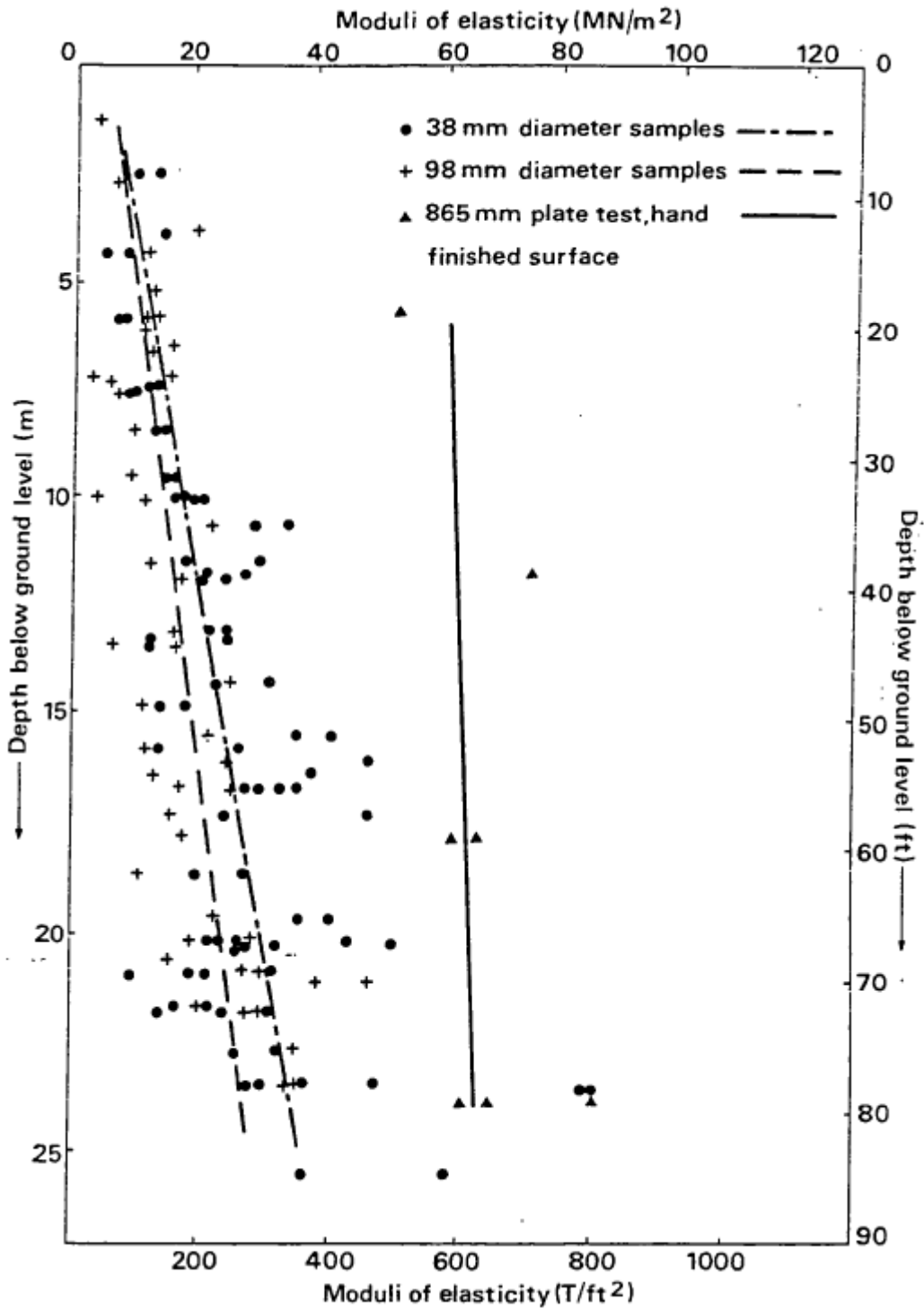


Figure 2-12: London clay (Hendon) stiffness from triaxial and plate load tests (After Marsland, 1971).

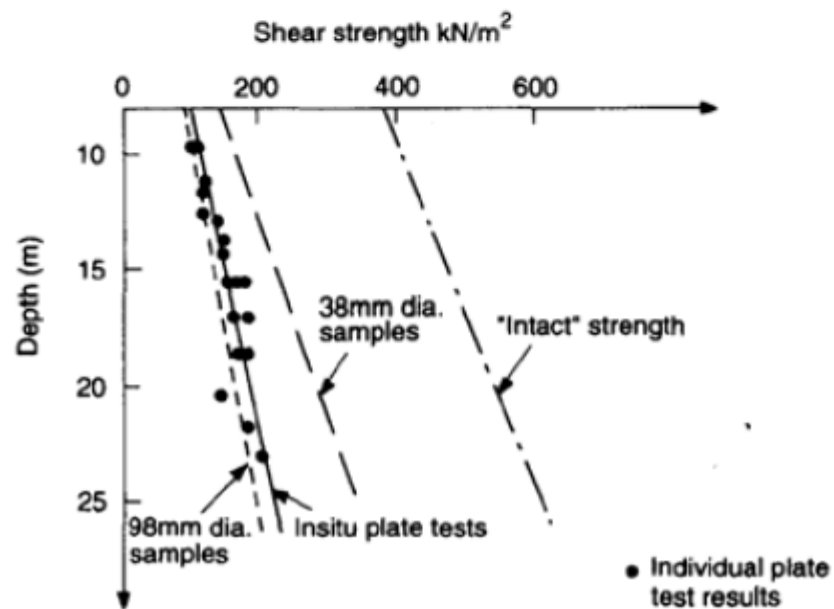
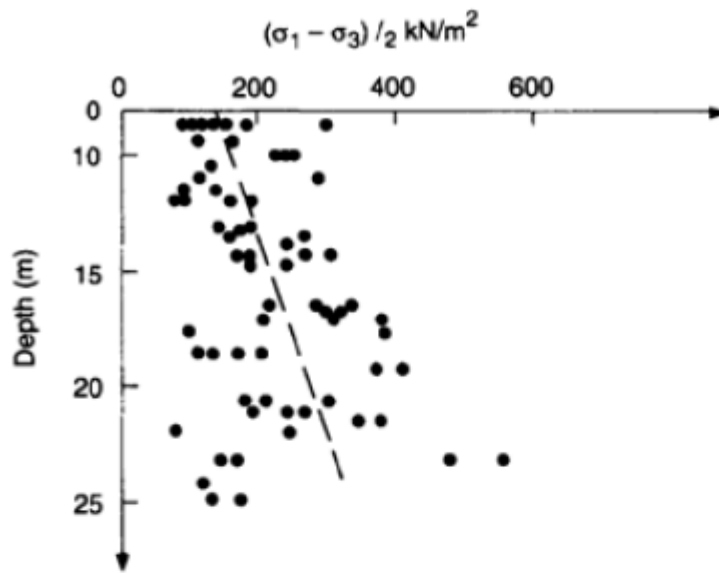


Figure 2-13: Comparison of plate tests and laboratory test results in London clay (Marsland 1972).

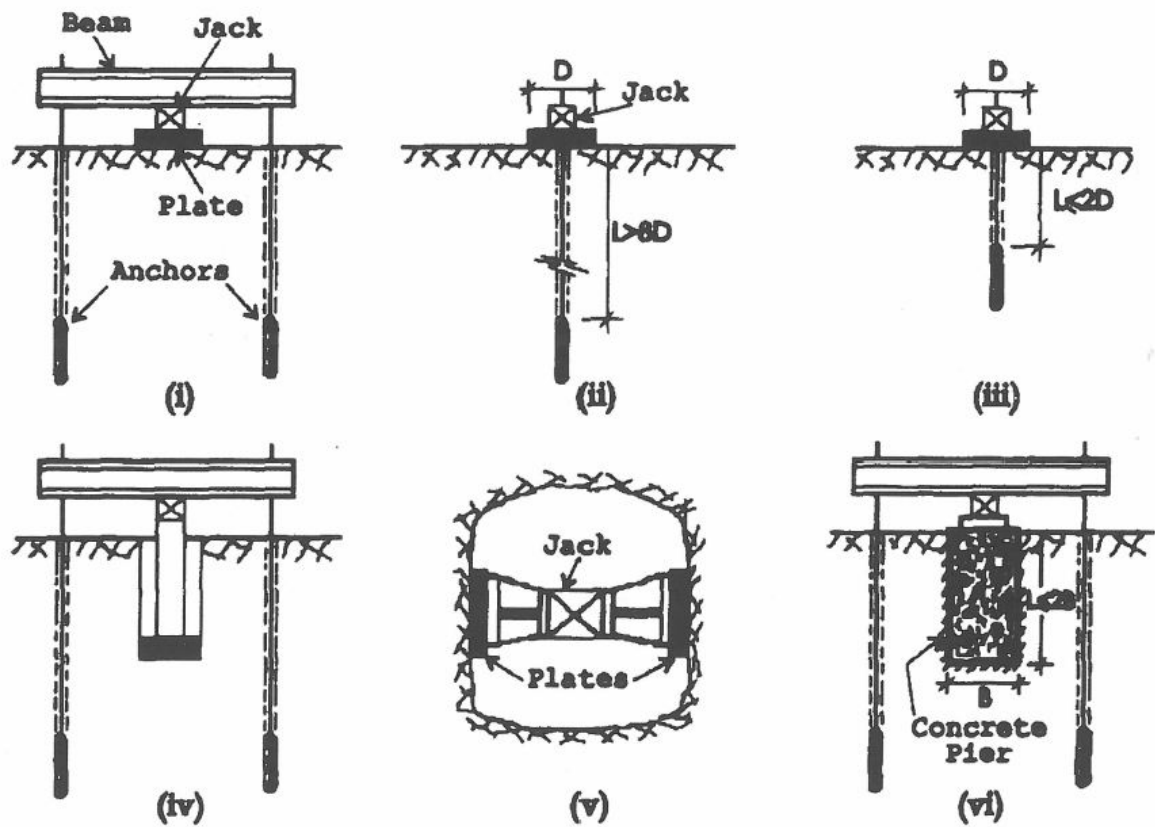
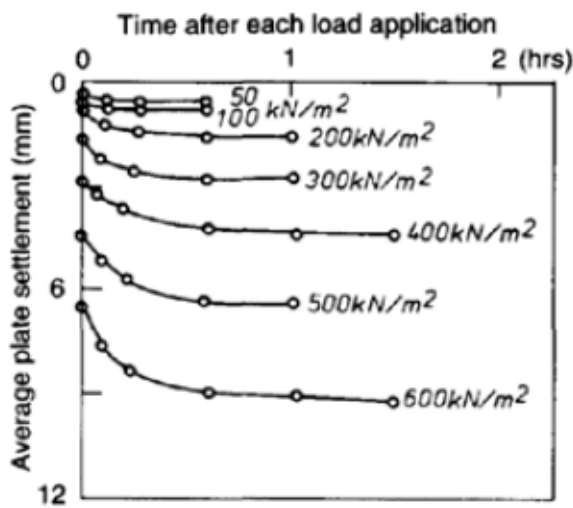
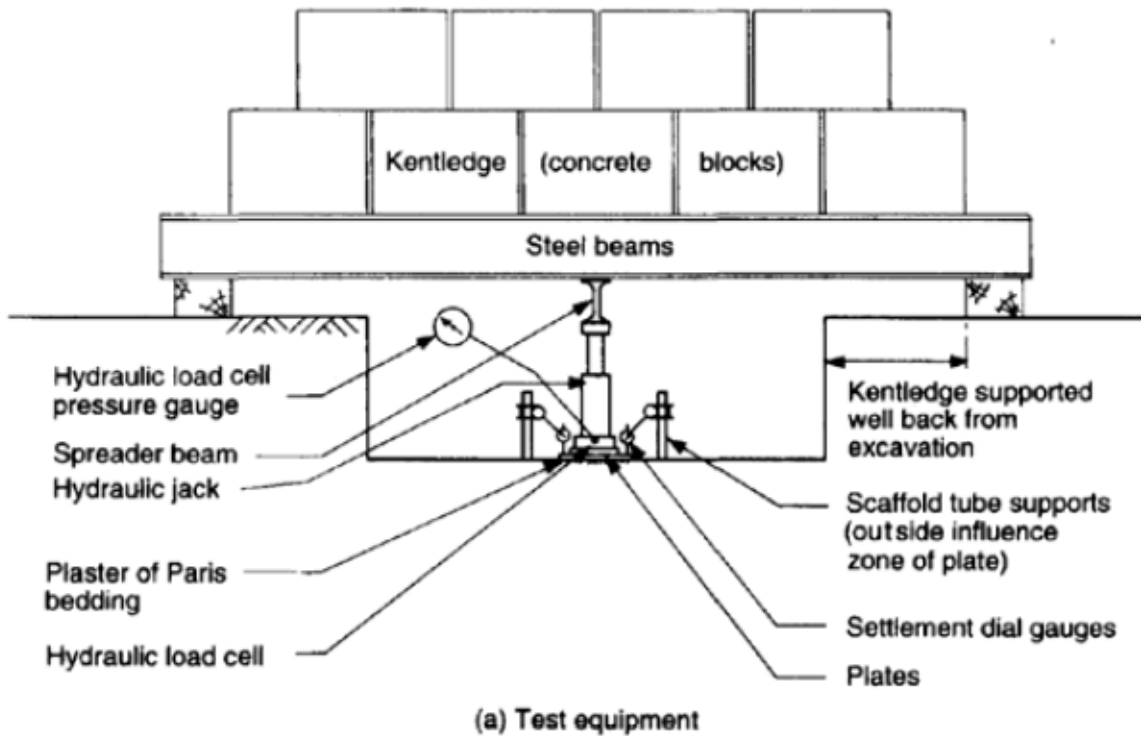
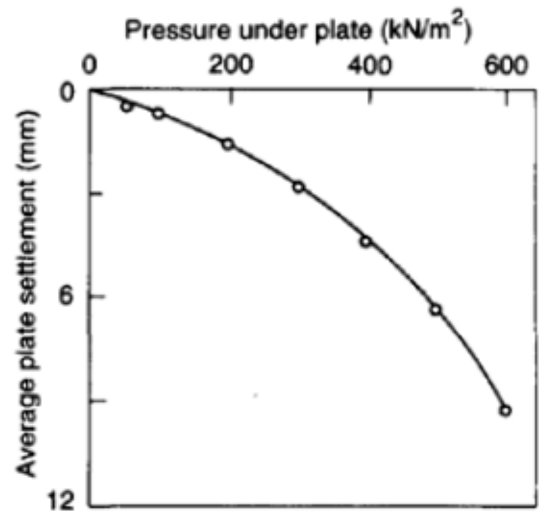


Figure 2-14: Different layouts of conventional plate loading tests (After Pells, 1983).



(b) Time - settlement records



(c) Load - settlement curve

Figure 2-15: Conventional plate load test layout and results (After Clayton et al., 1995).

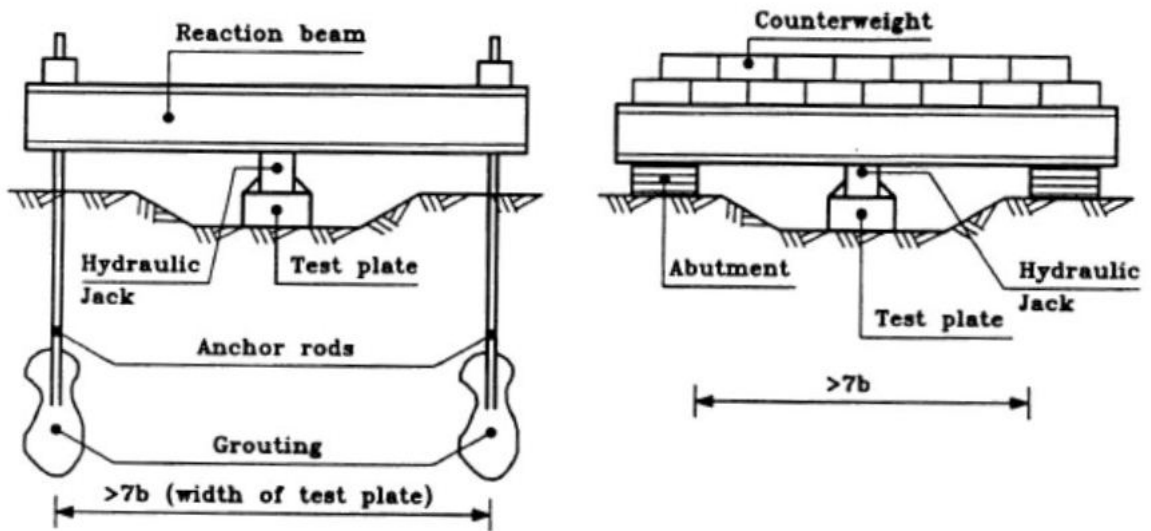
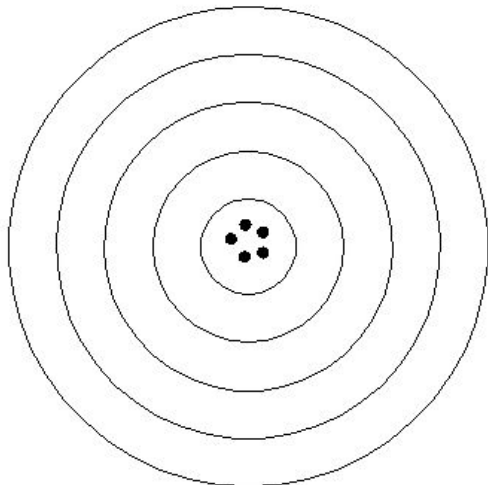
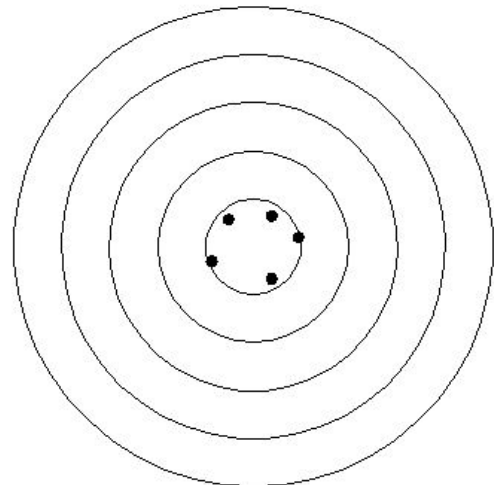


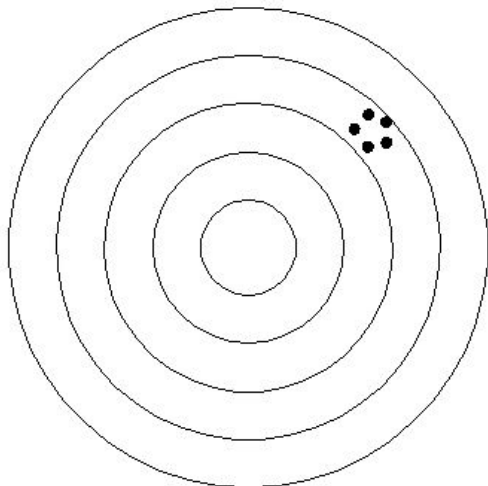
Figure 2-16: System for load application (After ENV 1997-3:1999).



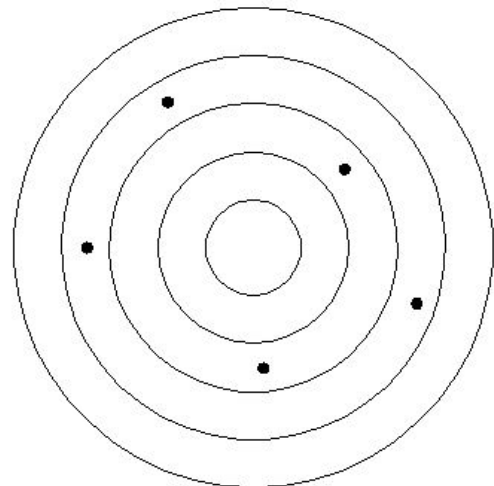
HIGH ACCURACY  
HIGH PRECISION



HIGH ACCURACY  
LOW PRECISION



LOW ACCURACY  
HIGH PRECISION



LOW ACCURACY  
LOW PRECISION

**Figure 2-17: Accuracy versus precision: the target analogy.**

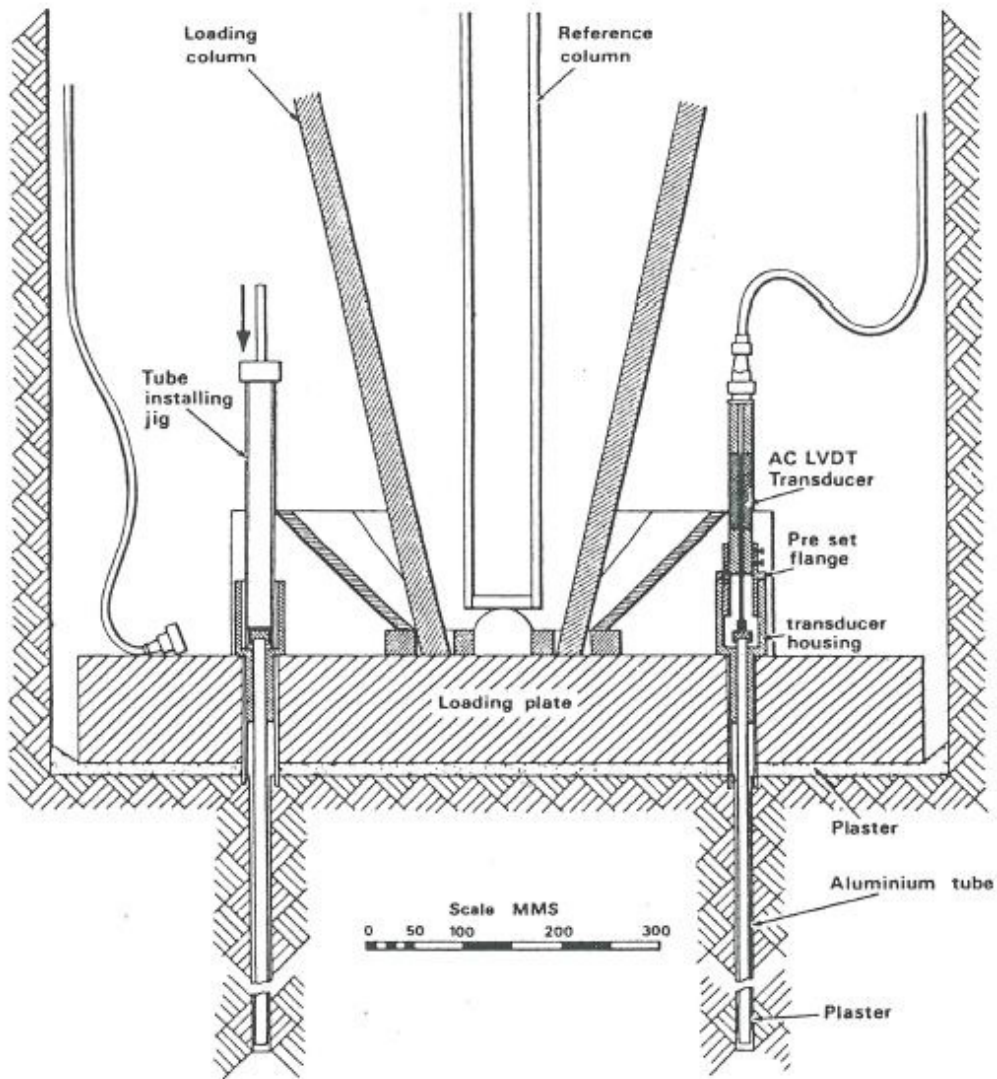


Figure 2-18: Single-point measuring system below 865 mm diameter loading plate (After Marsland & Eason, 1973).

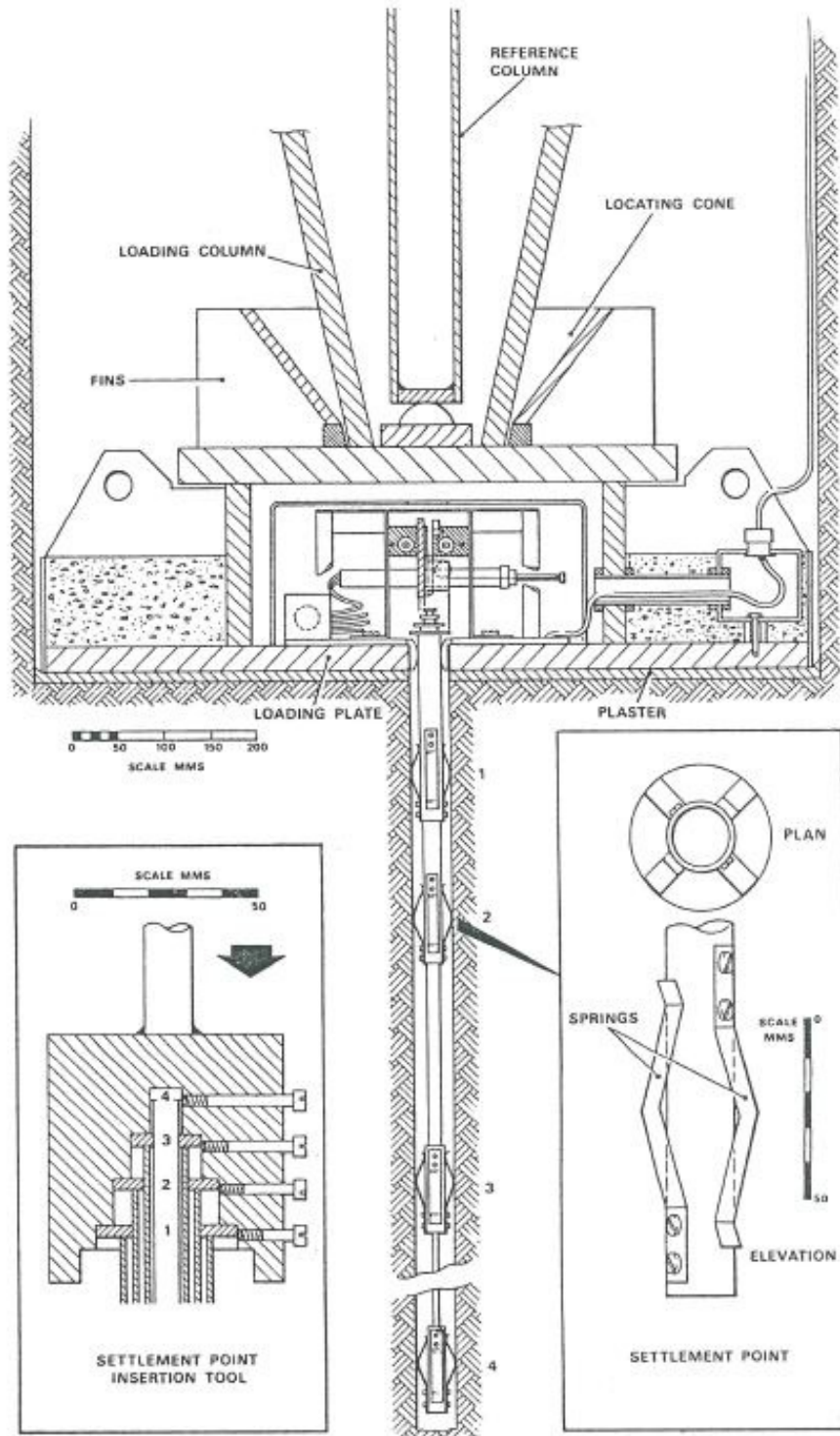


Figure 2-19: Multi-point measuring system below 865 mm diameter loading plate (After Marsland & Eason, 1973).

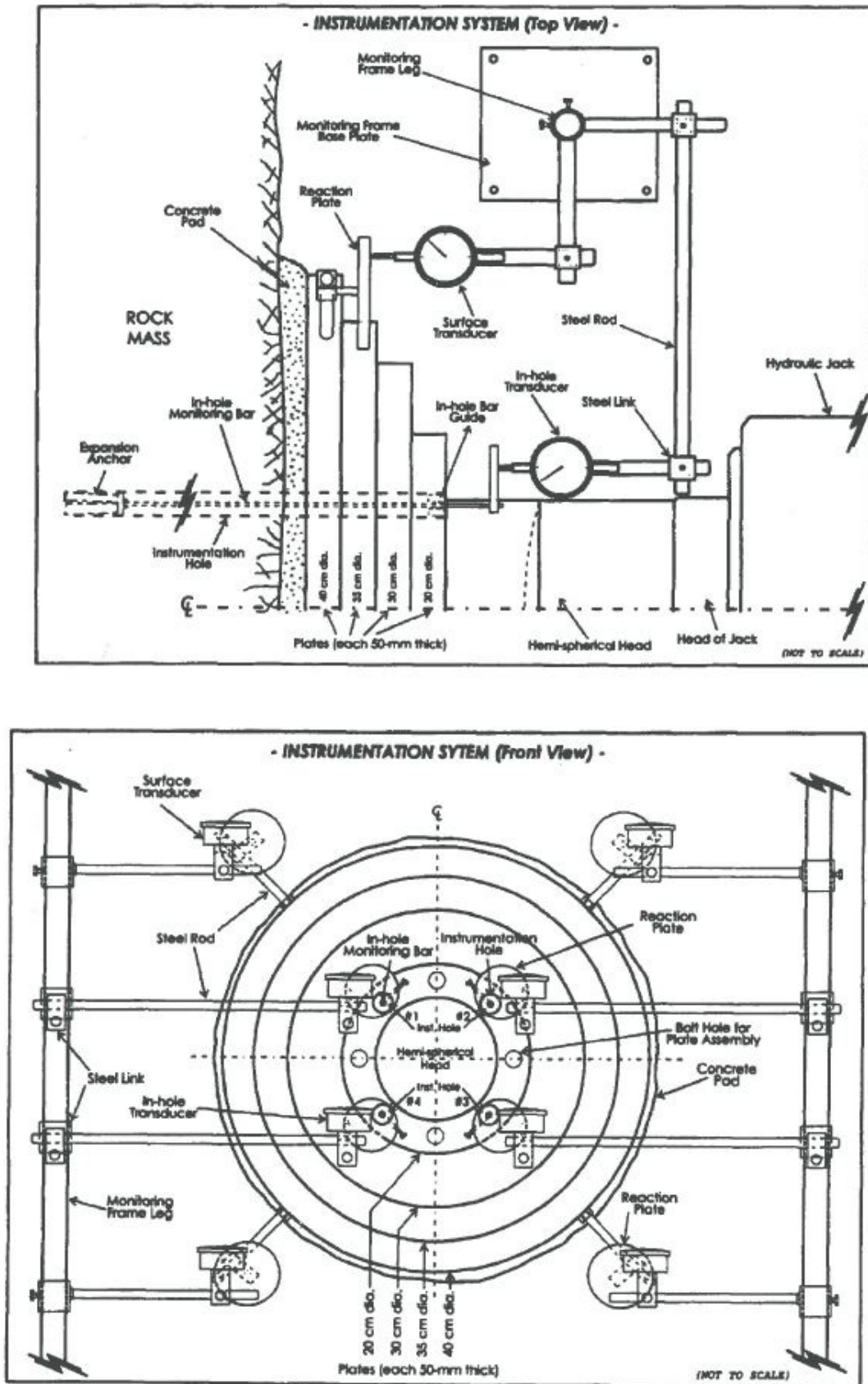


Figure 2-20: Details of the instrumentation system of the METU plate-loading apparatus (After Unal, 1997).

## CHAPTER 3: INDUSTRY RESEARCH

### 3.1. INTRODUCTION

The main objective of this chapter is to report the results of the industry research that has been conducted for this research project. A nine-question “Plate load test questionnaire” was set-up to understand how these plate load tests are currently being performed in South Africa. This questionnaire was sent to over 90 geotechnical laboratories and companies in South Africa with the aim of receiving completed questionnaires back from the companies that are performing plate load tests on a routine basis. The questions asked in the survey are discussed here followed by the results. The chapter concludes with a few lessons learned from the industrial research and sets the platform for the design of the experiment.

### 3.2. QUESTIONNAIRE

The purpose of the questionnaire was to obtain an understanding of the current status of plate load testing in South Africa. The questionnaire consisted of nine questions about these tests to investigate the following aspects:

- a) Typical plate sizes;
- b) Type of reaction force used to apply loads on the plate;
- c) Type of measuring system used to measure the applied loads;
- d) Type of displacement instruments used to measure plate settlement during loading;
- e) The amount and arrangement of displacement instruments to measure plate settlement and tilt;
- f) Surface preparation method used to achieve a level and smooth test area;
- g) Type of reference beam used to attach displacement instrumentation;
- h) Typical span of reference beam;
- i) Standard test procedure implemented to perform plate load tests.

It was important to first summarise what standards are expected for routine plate load tests. Table 3-1 summarises the technical details from the available standard test procedures for the difference aspects as mentioned above (a to h).

**Table 3- 1: Technical detail for plate load test apparatus from standards**

	ASTM Standards <sup>1</sup>	British Standard <sup>2</sup>	Eurocode <sup>3</sup>
a)	Plate diameter may vary between 152 mm to 762 mm and should be at least 25 mm in thickness.	Plate diameter should be at least 300 mm and at least five times the nominal size of the coarsest material.	Plate diameter should be at least 600 mm.
b)	Reaction force can include an anchored frame; loaded truck or trailer. The supporting points shall be at least 2,4 m from the plate perimeter.	Reaction force can include Kentledge block; tension piles; or existing structures. The supporting points shall be at least 3 times the plate diameter from the plate centre.	Reaction force can include counterweights; tension piles; anchors; or existing abutments. The supporting points shall be at least 3,5 times the plate diameter from the plate centre.
c)	Pressure gauge.	Pressure gauge.	Pressure gauge.
d)	Dial gauges.	Dial gauges and levelling directly on the plate.	Dial gauges or electrical displacement transducers.
e)	Two or more devices with minimum resolution equal to 0.03 mm and placed 25 mm from the plate perimeter.	The required number of measuring devices is not specified.	Three-point measuring system equally spaced around the plate.
f)	<ul style="list-style-type: none"> <li>- Thin bed of a mixture of sand and plaster of Paris;</li> <li>- Plaster of Paris alone; or</li> <li>- Fine sand alone.</li> </ul>	<ul style="list-style-type: none"> <li>- Cohesive soils: Quick setting gypsum plaster;</li> <li>- Granular soils: Clean dry sand.</li> </ul>	<ul style="list-style-type: none"> <li>- Cohesive soils: Quick setting plaster;</li> <li>- Granular soils: Clean dry sand.</li> </ul>
g)	The beam shall be a 63 mm standard black pipe or a 76 by 76 by 6-mm steel angle.	Any type of reference beam is acceptable.	The reference beam should be sufficiently stiff in order to avoid creep and vibration in the beam.
h)	It shall be at least 5,5 m long, rested on supports located at least 2,4 m from the plate perimeter.	The reference beam should span far enough not to be influence by the plate movements.	Two fixed reference points are to be chosen which are close enough but outside the area influence by the loading.

Notes: <sup>1</sup>ASTM 1194/94; 1195/64; 1196/64, <sup>2</sup>BS 5930 (1981), <sup>3</sup>ENV 1997-3:1999

Appendix A shows an example of the questionnaire used in this industry research. In total, twenty (20) completed questionnaires were received that revealed very interesting results.

This was believed to be an acceptable representative sample in light of the fact that there are most probably not many more institutes or companies that perform plate load tests in South Africa. The results are discussed in the next section.

### **3.3. RESULTS**

#### **3.3.1. Plate sizes**

A wide range of plate sizes are being used throughout the country from as small as 100 mm in diameter to a maximum of 1000 mm in diameter. The results revealed the most popular plate sizes are 450 mm and 600 mm in diameter. Given that the influence of the soil depth is about 1,5 times the plate diameter (Clayton et al. 1995), one can conclude that depths of between 675 mm and 900 mm soil thickness are typically being tested by plate load tests in South Africa.

#### **3.3.2. Reaction force**

The options provided for the type of reaction force included Kentledge blocks, anchors, excavator buckets and the chassis of a loaded truck. Figure 3-1 shows the results and reveals that for 40 per cent of all plate load tests, the reaction force has been provided by the chassis of loaded trucks. This raises the question as to whether the suggested distance of 2,4 m or 3,5 times the plate diameter has been allowed between the truck wheels and the loading plate.

Just over a third prefers using an excavator bucket to provide the reaction force on site. Excavator buckets are probably the most practical method since most plate load tests are performed during geotechnical investigations where excavators are commonly used to excavate test pits. The last quarter (25%) of the results has used other methods to provide the reaction force which includes anchors (1 out of 20), Crawler crane (1 out of 20), excavator chassis (1 out of 20) and Kentledge blocks (2 out of 20).

#### **3.3.3. Applied load measurements**

The options provided for the type of devices used to measure the applied load have included pressure gauges and load cells. The results have revealed that 17 out of 20 suppliers are using analogue pressure gauges and only 10 per cent are using load cells to measure the applied

loads. Another type of device that was recorded in one case was a digital pressure transducer linked to a laptop. These results are shown in Figure 3-2.

#### 3.3.4. Plate settlement measurements

The options provided for the type of displacement instruments used to measure the plate settlement included dial gauges and Linear Variable Differential Transducers (LVDTs). The results revealed that 19 out of 20 of suppliers are using mechanical dial gauges and one is using LVDTs to measure the settlement of the plate. These results are shown in Figure 3-3.

#### 3.3.5. Number of displacement instruments

The two options provided for the number of displacement instruments that were used to measure the plate settlement was either two or three. There was a choice of two options provided for this measurement; this was that either two or three displacement instruments could be used. The results revealed that approximately 85 per cent of suppliers are using three displacement instruments placed at 120 degrees apart and the other 15 per cent are using only two displacement instruments which are placed on opposing sides of the plate. The disadvantage of using only two instruments is that any tilt of the plate that occurs during the test cannot be adequately taken into account. These results are shown in Figure 3-4.

#### 3.3.6. Surface preparation method

Three surface preparations methods were provided as the possible options which would achieve a levelled and smooth test area. The results revealed that approximately 60 per cent of respondents use well-graded sand in their attempt to achieve a levelled test area and 20 per cent prefer plaster of Paris. Ten per cent of respondents believe that by the use of only hand tools, an acceptable levelled and smooth test area can be achieved. Other surface preparation methods recorded during the survey was the use of cement powder, fine fly-ash and quick set grout. These results are shown in Figure 3-5.

### 3.3.7. Type and length of reference beam

The two material types of reference beams that it was expected would be used were steel and wood, but surprisingly the results have revealed that all respondents are using steel reference beams. The reference beams varied in length from the shortest at 1,8 m to as long as 10 m in one case. One supplier is using a 600 mm diameter steel ring beam to keep the displacement instruments firmly in place. The average length was 3,0 m and was recorded in 55 per cent of all cases. These results are shown in Figure 3-6.

### 3.3.8. Standard test procedures

The options provided for the test procedures included BS 5930 (1981), ASTM D 1194/94, ASTM D 1195/64 and ASTM D 1196/64. The results have revealed that about 35 per cent are using the BS 5930 (1981) standard procedure and about 20 per cent prefer to use the ASTM D1196/64 as the standard test procedure for plate load tests. A third is using other test standards methods and client specific procedures which include the modified AASHTO T 222-78 and the method that is proposed by Wrench (1984). These results are shown in Figure 3-7.

## 3.4. CONCLUSIONS FROM INDUSTRY RESEARCH

The results from this industry research questionnaire demonstrate that:

- The typical plate sizes used for plate load tests conducted in South Africa varies between 300 mm and 600 mm;
- The two types of reaction force most frequently used during plate load tests include the chassis of a loaded truck and jacking against the bucket of an excavator;
- More than 80 per cent of suppliers are using pressure gauges to measure the applied loads;
- Approximately 95 per cent of respondents are using dial gauges to measure plate settlement during loading, of these about 85 per cent are using three dial gauges spaced 120 degrees apart, to measure any tilt of the plate;
- Approximately 60 per cent of suppliers are using well-graded sand as the preferred surface preparation method to achieve a level and smooth test area, where only 4 out of 20 suppliers prefer plaster of Paris;

- All suppliers are using steel reference beams to keep the displacement measuring devices firm on the plate and 11 out of the 20 reference beams were recorded as being 3 m long;
- The two most preferred standard test procedures adopted to perform plate load tests are BS 5930 (1980) and ASTM 1196/64.

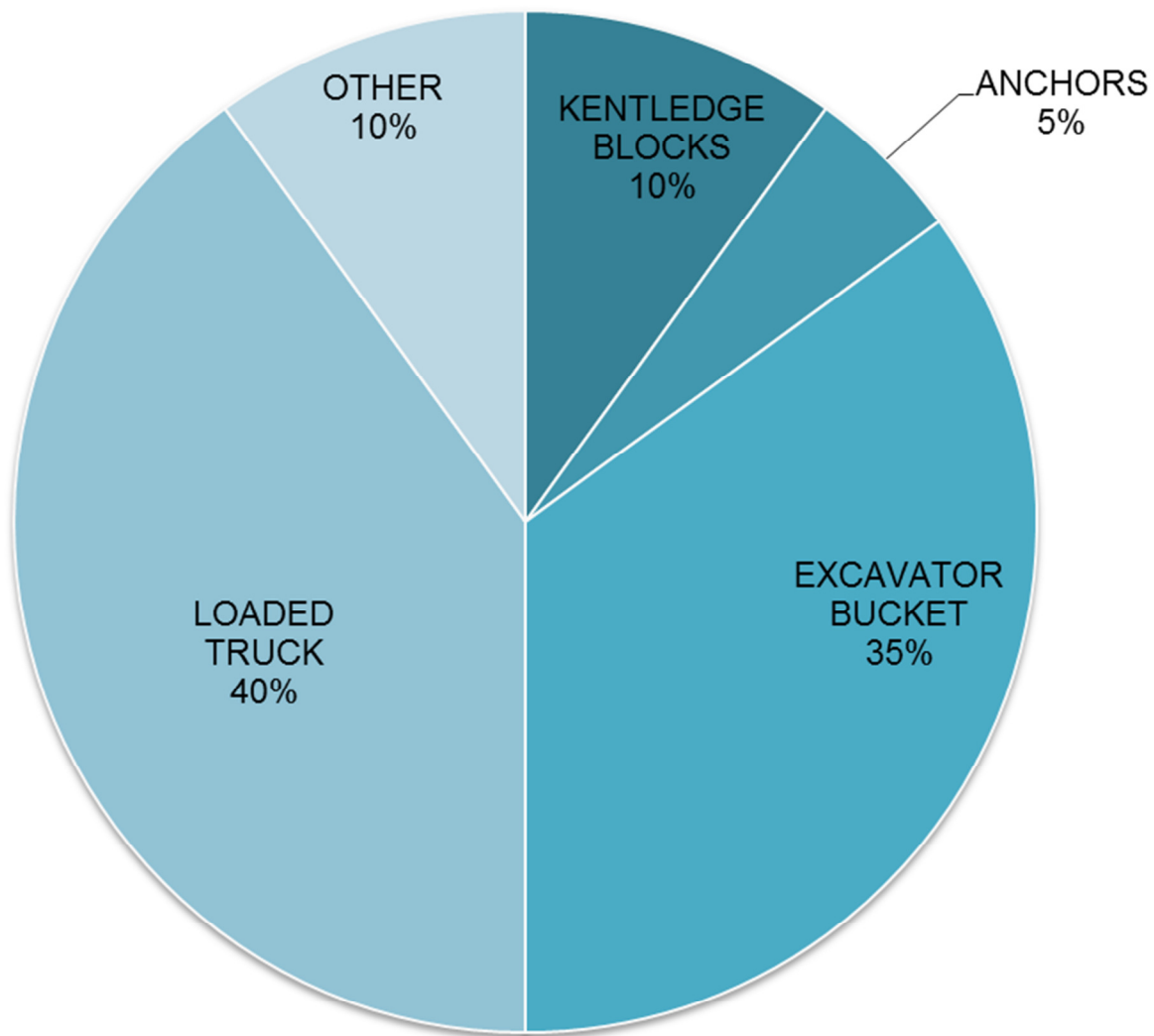


**Figure 3-1: Preferred method to provide reaction load.**

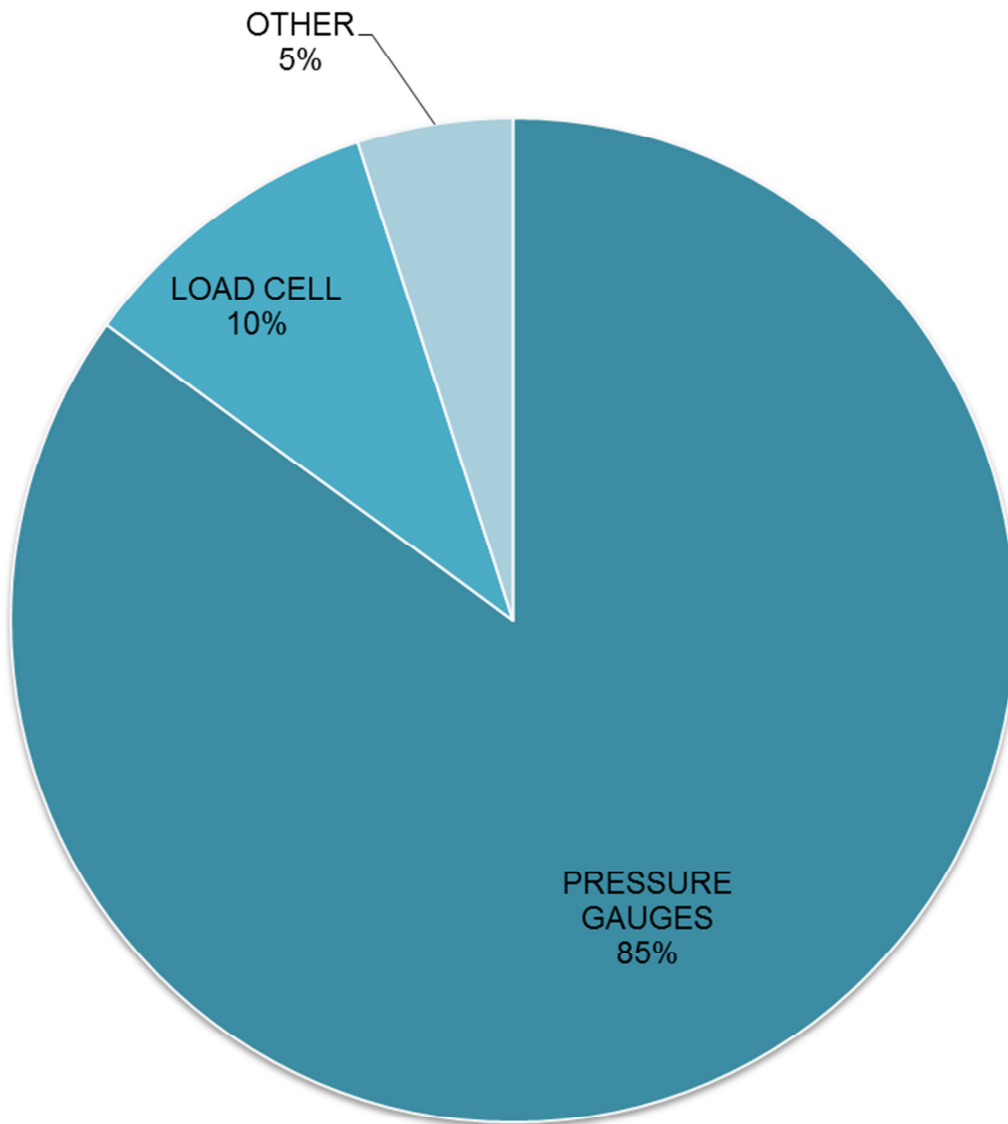


**Figure 3-2: Preferred method to measure applied loads.**

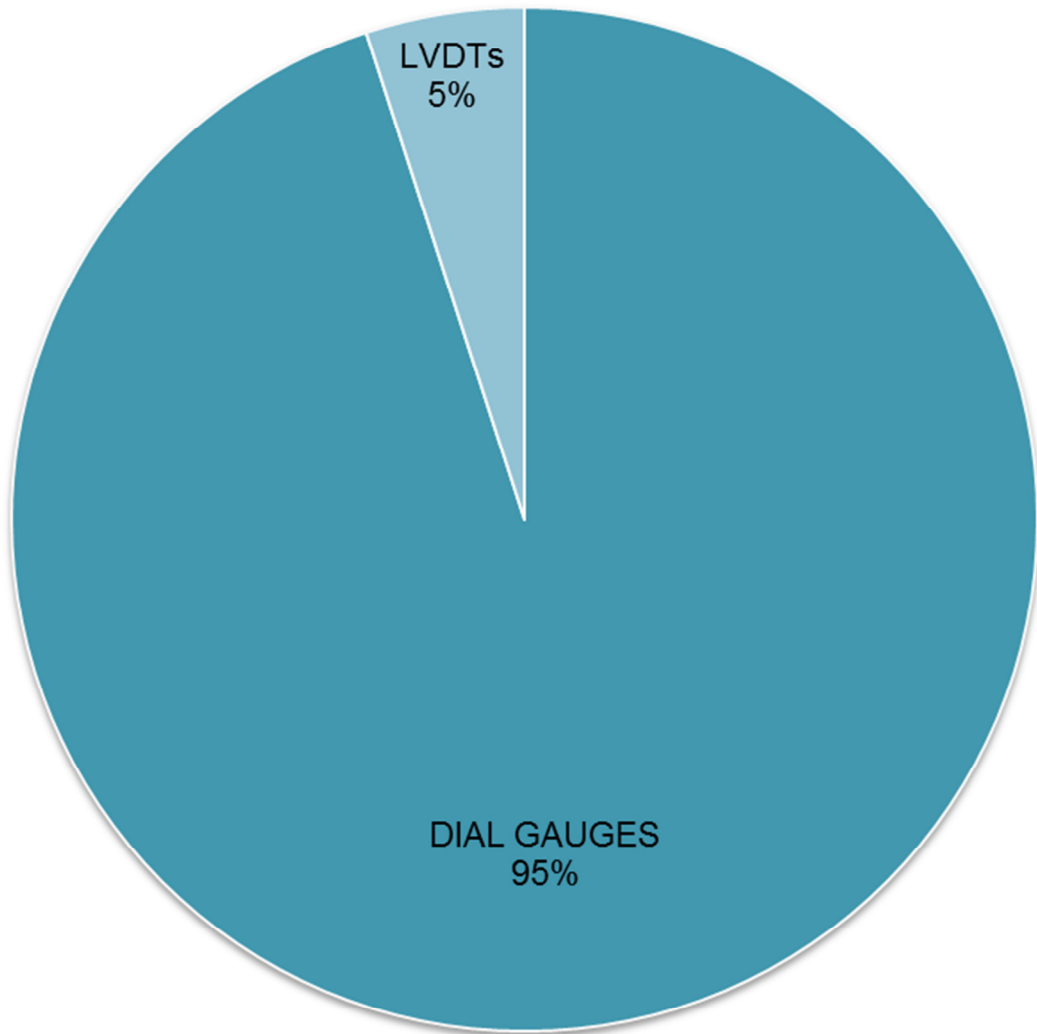


**Figure 3-3: Preferred method to measure plate settlement.**

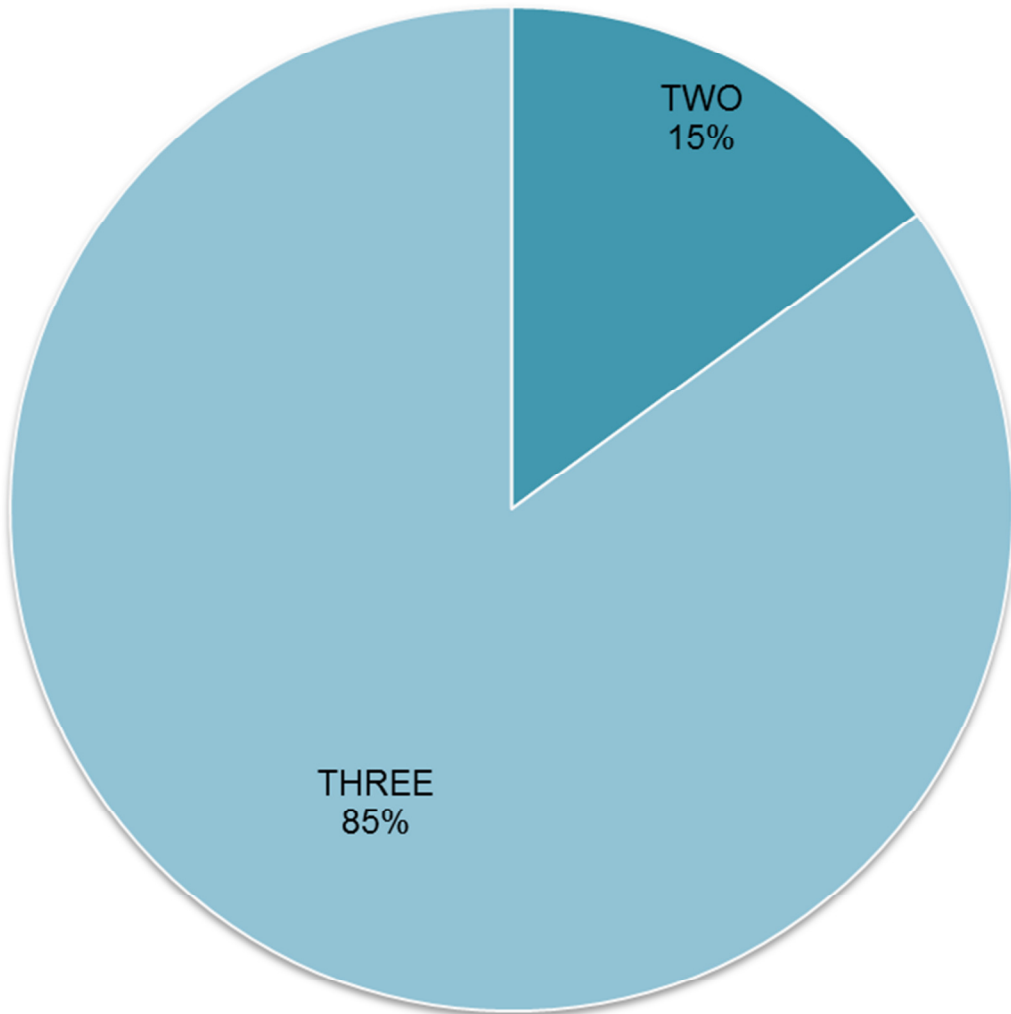


**Figure 3-4: Number of displacement measuring devices.**

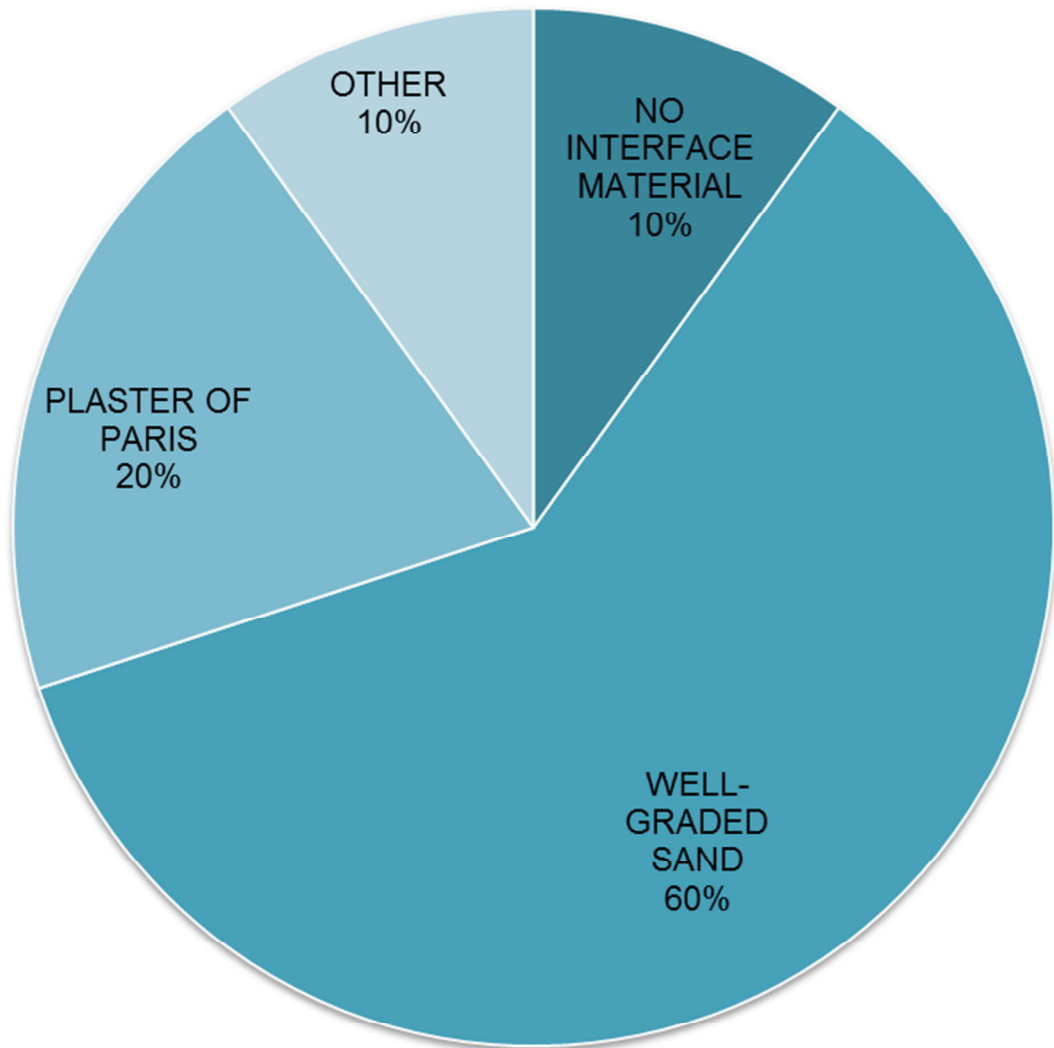


**Figure 3-5: Preferred surface preparation methods.**

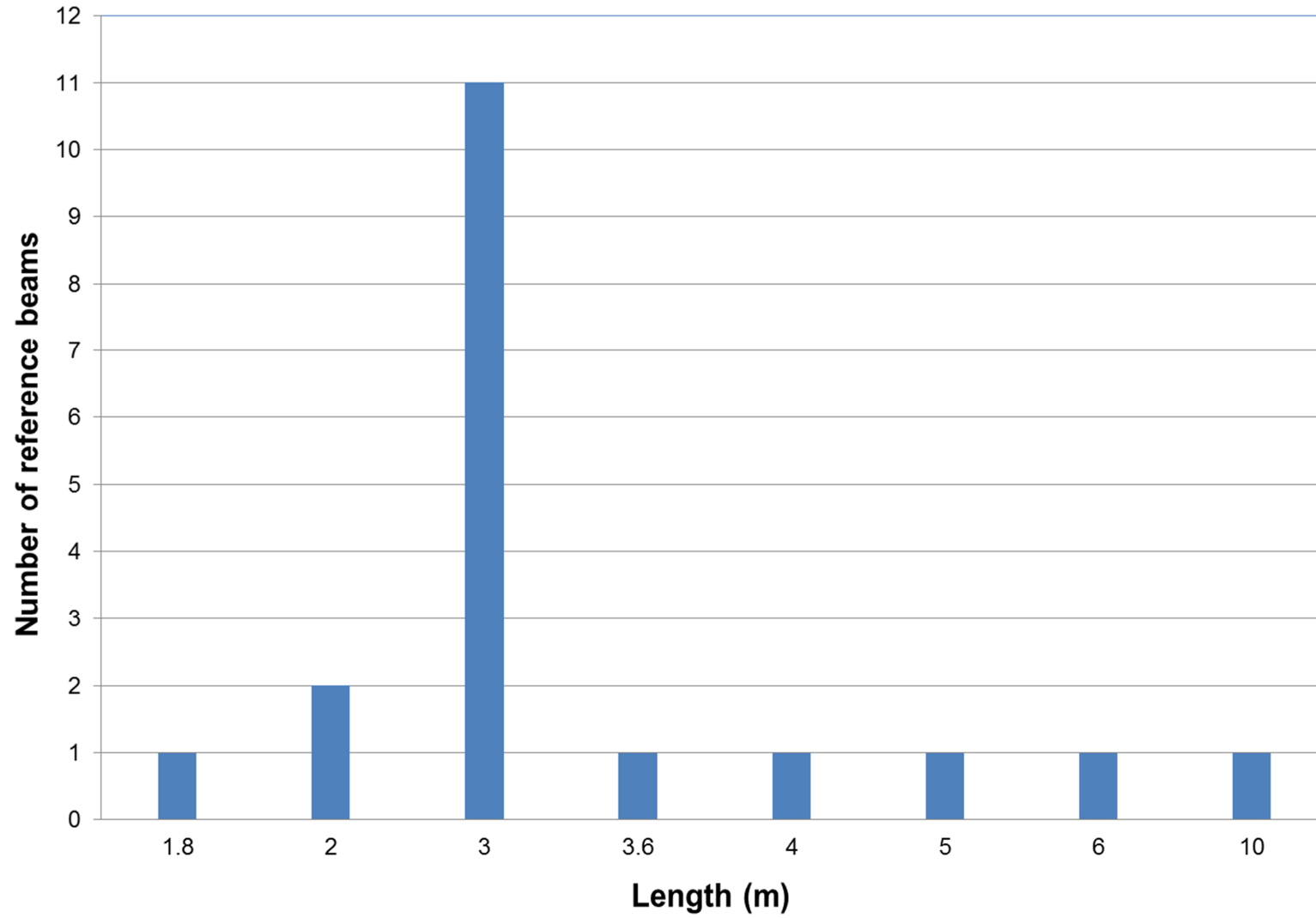
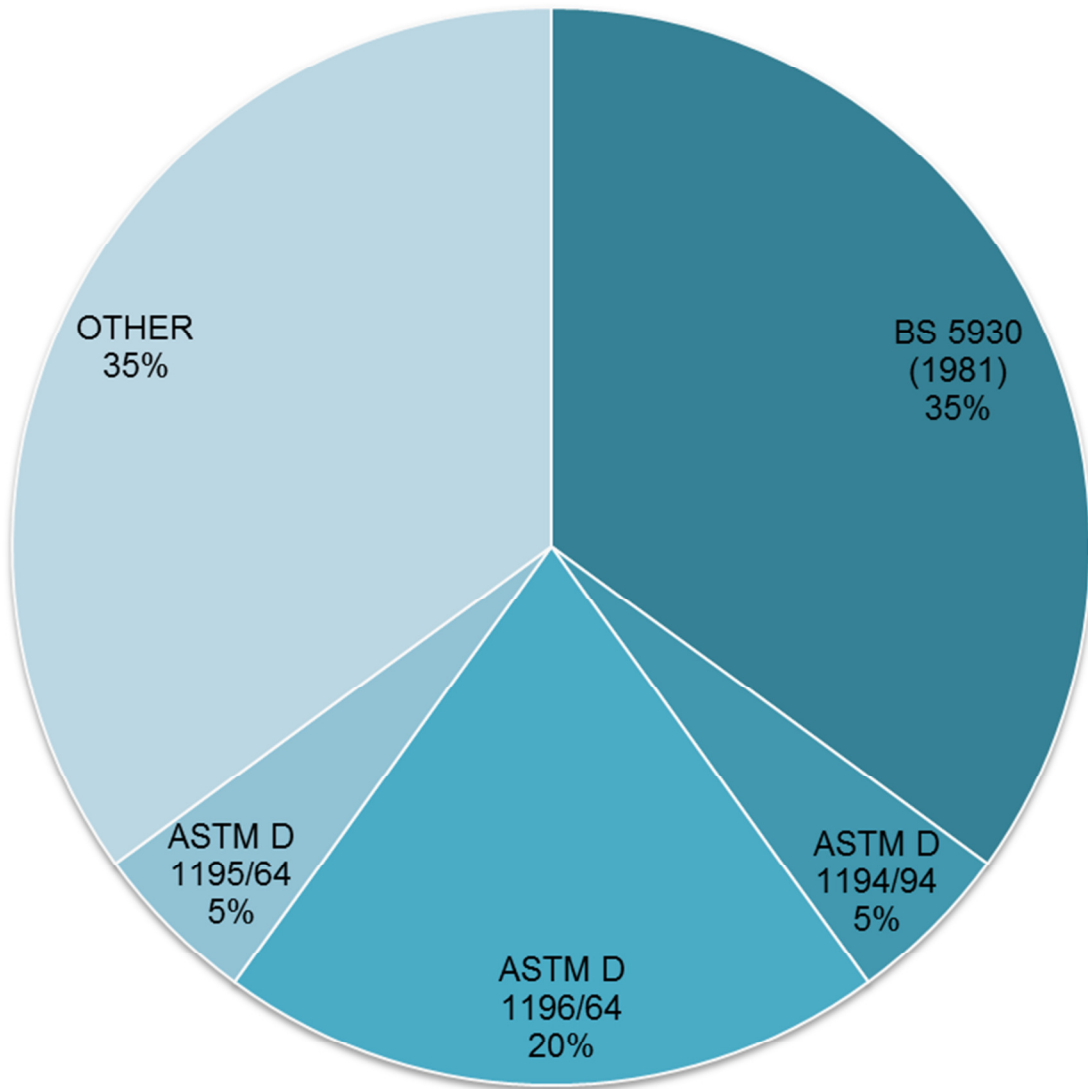


Figure 3-6: Length of reference beams.



**Figure 3-7: Preferred standard test procedures.**

## **CHAPTER 4: EXPERIMENTAL WORK**

### **4.1. INTRODUCTION**

The purpose of this chapter is to give an in-depth description of the experimental design used for this research project. The experimental strategy is discussed and this is followed by a review of the various components of the experimental study. The calibration methods and the behaviour of all measuring instruments are described, and followed by the experiment preparation and test procedure adopted for this experiment. Lastly, the statistical methods and interpretation techniques used to analyse all data are discussed.

### **4.2. EXPERIMENT STRATEGY**

To successfully determine the effect of bedding errors on the accuracy of plate load tests a three point strategy was applied. Figure 4-1 shows the modified plate load test set-up that has been designed for the experimental work.

A series of plate load tests was conducted at the experimental farm of the University of Pretoria. In total, six precise plate load tests were performed on residual Andersite, which is described as firm, reddish brown, clayey silt. The test areas were levelled by means of three surface preparation methods which included, i) a thin layer of plaster of Paris; ii) a thin layer of well-graded sand and iii) by using only hand tools.

It was important to first describe the surface roughness before each test was conducted and prior to each test this was measured by means of a laser measuring system. To describe the surface roughness, a seven-step process was performed for each set of data. The surface roughness was again measured after each test to determine any change in surface roughness during the test.

In addition to the conventional plate load tests, telescopic probes were developed and installed to measure the relative displacement of two points below the centre of the plate during each of the tests. From these measurements, internal stiffness values could be calculated and then compared to the external stiffness values which were calculated from the plate settlement.

### 4.3. COMPONENTS OF THE EXPERIMENT

#### 4.3.1. Laser measuring system

Various methods and devices have been developed to measure in situ soil surface roughness (Tay et al., 2003). Such devices include laser profilometer (Bertuzzi & Caussignac, 1988) and Digital photogrammetry (Rieke-Zapp et al., 2001).

The laser measuring system used for this research project was built to measure the surface roughness before and after each test. The main components of the laser measuring system included a steel frame with a tri-pod stand, a two-directional scan unit mounted on the steel frame, a Cable-Extension Position Transducer (CEPT) with a maximum range of 762 mm, a laser distance gauge with a resolution of 10.2  $\mu\text{m}$  and a data acquisition system to record the measurements electronically. Figure 4-2 shows a photo taken of the laser measuring system.

The steel frame was built with 40 mm x 40 mm angle bars that are welded together and had an outer dimension of 900 mm x 740 mm. The tripod stand could be adjusted in height between 0 mm and 400 mm and was used to level the frame. The mechanical scan unit could manually be moved on the steel frame in an X-Y plane. Both the laser distance gauge and the CEPT were attached to the movable scan unit to measure the distances in the Z and Y directions, respectively. The scan unit was fixed in the X direction at twelve (12) points while being manually moved in the Y direction to create twelve (12) scanning lines across the test area. The laser distance gauge attached to the scan unit measured the elevation in the Z direction and at the same time, the horizontal distance in the Y direction was recorded with the Cable-Extension Position Transducer (CEPT). Figure 4-3 shows the configuration of the twelve (12) consecutive lines on which the test area was scanned before and after each test.

The instrumentation belonging to the laser measuring system included a laser distance gauge and a CEPT. This laser distance gauge forms part of the AR700 series manufactured by Schmitt Measurement Systems, Inc. and the specifications for this gauge are shown in Table 4-1.

The standoff distance, where the laser spot size is the smallest and greater accuracy can be expected, is at 305 mm from the face of the sensor and this also represents the centre point of

the measuring range. Before the surface roughness could be measured, the laser distance gauge attached to the frame was adjusted to roughly 305 mm from the ground profile.

**Table 4-1: Manufacturers' specifications for the laser distance gauge (AR700-8).**

Measuring range	-101.5 to 0 to +101.5 mm (8 inches)
Linearity	$\pm 0.03\%$ of Span
Resolution	10.2 $\mu\text{m}$
Operating temperature	0° to 40°C
Laser type	670 nm, 5 mW visible RED
Laser spot size	120 $\mu\text{m}$
Output signal	0 - 10 V

The Cable-Extension Position Transducer (CEPT) is part of the PT1A series manufactured by Celesco Transducer Products, Inc. and the specifications are shown in Table 4-2. Both instruments were plugged into a data acquisition system to record the measurements at 10Hz (10 readings per second) simultaneously. The data acquisition system is shown in Figure 4-4. All data were saved on a flash drive immediately after all lines were scanned to ensure that no data was lost.

**Table 4-2: Manufacturers' specifications for the cable-extension transducers (PT1A-30)**

Full stroke range	0 to 762 mm (0-30 inches)
Sensor	Plastic-hybrid precision potentiometer
Operating temperature	-17° to 90°C
Output signal	0 - 10 mV/V
Electrical connection	6-Pin plastic connector with mating plug

### 4.3.2. Conventional plate load test apparatus

In this section, the conventional plate load test apparatus used for this research project is discussed. The main components of the conventional plate load test included:

- a 1,3 ton steel reaction beam together with four grouted anchors;
- a double action hydraulic pump;
- a hollow cylinder hydraulic jack with a 257 mm push-out piston;
- a hollow load cell with 100 kN load capacity;
- selection of plates with central holes;
- three Direct Current Differential Transformers (DCDTs);
- two 3,0 m long wooden reference beams;
- a data logging unit and acquisition system.

Figure 4-5 shows a photo of the plate load set-up. The steel beam with a total weight of 1,3 ton consisted of two 560 mm x 275 mm x 3000 mm steel frames bolted together with six M24 bolts and 70 mm x 70 mm x 50 mm spacer between these to create space for the telescopic probes which were to be set in position through the middle of the beam. The 3,0 m grouted anchors were installed into 150 mm diameter holes to a depth of 1,5 m with non-shrinkage grout. A K9-4 PRO dingo auger was used to excavate the anchor holes. The non-shrink grout which is manufactured by Aveng Group: Duraset was used to install the anchors and was cured for 7 days to reach 40 MPa strength. Figure 4-6 shows the anchor installation process.

A hydraulic jack cylinder and pump system was used to provide the required contact pressure by the process of jacking against a base plate that was welded to the anchored steel beam. The applied load was directly measured with a 100 kN load cell, which is placed on top of circular plates, and was logged with an automatic logging system. Both the hydraulic jack cylinder and load cell were designed to have 30 mm diameter holes through the centre to create space for the installation of the telescopic probes. This load cell forms part of the Universal Low Profile (ULP-10T) series which is manufactured by Transducer Developments Company (TDC).

The 300 mm steel plate was stacked on top of the 450 mm and placed on the prepared test surface. The vertical displacement of the bottom 450 mm plate was measured with three calibrated DCDT's placed 120 degrees apart and approximately 25 mm from the plate perimeter to accommodate any tilt that might occur during testing.

The three DCDTs were supported by two 3,0 m long wooden reference beams which were placed on both sides of the test area far enough away to avoid interfering with any of the test equipment. Aluminium brackets were built to hold the DCDTs firmly in place on top of the plate. Figure 4-7 illustrates this Plate load test set-up with the external DCDTs being attached to the plate. The applied load that was measured with the load cell, together with the displacement measured by the three DCDTs, as well as a 5 mm LVDT (discussed in the next section) were logged automatically with a data acquisition system. Figure 4-8 shows a photo of the data acquisition system used to log the data simultaneously at 10 Hz (10 reading per second).

#### 4.3.3. Development of telescopic probes

The components of the telescopic probes included a solid 8 mm inner aluminium rod, a 13 mm aluminium tube and a probe head that consisted of three bent spring steel strips. The solid 8 mm inner aluminium rod was designed to slide freely inside a 13 mm aluminium tube. The three bent spring steel strips were welded onto a 20 mm stainless steel nut and then screwed into the threaded 13 mm aluminium tube as shown in Figure 4-9.

A 25 mm central hole was drilled into the soil by means of a hand bore at the centre of the 2 m x 2 m test area to a depth of one plate diameter below ground surface. Poulos and Davis (1974) concluded that a central hole with a radius equal to 30% of the plate radius will only have a 5% effect on the measured stiffness. Therefore, the 25 mm hole with a radius of approximately 5% of the plate radius should not have a significant effect on the measured soil stiffness. The solid 8 mm aluminium rod was grouted at the bottom of the 25 mm hole, with quick-set grout and the spring steel probe head fixed at a depth of half a plate diameter below the ground surface.

The calibrated 5 mm LVDT (Linear Variable Differential Transducer) was attached to the top of the probes; the purpose of this was to measure the relative displacement of two positions

below the centre of the plate. Two aluminium brackets were constructed to hold the LVDT firmly in position. Figure 4-10 shows the LVDT set-up.

The LVDT is part of the WI-inductive miniature displacement transducer series, which are manufactured by Hottinger Baldwin Messtechnik GmbH (HBM) and the specifications are shown in Table 4-3. All the components of the modified plate load test that have been described in Sections 4.3.2 and 4.3.3 are shown together in Figure 4-11.

**Table 4-3: Manufacturers' specifications for the 5 mm (WI) LVDT**

Measuring range	0 mm to 5 mm
Linearity	$\pm 0,2\%$ of FS
Total weight	19,8 grams
Operating temperature	$-20^{\circ}$ to $80^{\circ}\text{C}$
Transducer type	WI/5mm-T
Dimensions (L x Diam.)	100 mm x 20 mm $\Phi$
Initial stroke	0,5 mm

#### 4.4. CALIBRATION OF PLATE LOAD TEST SYSTEM

The purpose of this section is to discuss the calibration methodology that was followed to calibrate all instrumentation used during the experimental study. The calibration of all three external DCDTs, internal LVDT, load cell, laser distance gauge and the Cable-extension Positional Transducer will be reviewed. Furthermore, the instrument behaviour will be presented.

##### 4.4.1. Calibration methodology

As noted in the literature study, calibration is a vital phase in any experiment as it is important to be able to compare results with a 'true value'. In other words the system must first be calibrated with values that are recognised as being precise and accurate. In fact, the accuracy of the reference system should be 3 to 10 times better than that of the instrument that is being calibrated (Doebelin, 1990). For this research project the accuracy of the (i) three external DCDTs, (ii) the internal LVDT, (iii) the 10 ton Load cell, (iv) the Laser

distance gauge and (v) the Cable-Extension Position Transducer described in Section 4.3 were determined by using a consistent methodology. This calibration methodology consisted of the following steps:

- i. A calibration range was selected for each instrument, for which digital output values were recorded for each ‘true value’ interval, measured with a suitably accurate reference system.
- ii. The relationship between the digital output (V or mV) and the ‘true value’ (engineering units) was described by a least squares linear transfer equation.
- iii. The error was calculated for each calibration point as the difference between the ‘true value’ (engineering units) and the measured value (digital output converted to engineering units using the least squares linear transfer equation).
- iv. The errors were plotted against the ‘true value’ so as to present the maximum error, hysteresis and non-linearity of each instrument. Figure 4-12 to Figure 4-14 shows examples of these plots.
- v. The standard deviation and mean of the errors was determined. The accuracy of each instrument was calculated as  $\pm 2$  times the standard deviation. By assuming a Normal distribution of the errors, this has resulted in a confidence level of 95% in that the difference between any measured value and the “true value” would be less than the specific accuracy.

#### 4.4.2. Laser measuring system calibration

The laser measuring system was calibrated with a 1000 mm precision stainless steel indicator for calibration range of 0 to 40 mm. The typical calibration results for the 40 mm calibration range are shown in Figure 4-12. Ten equally spaced distance increments were recorded during the calibration. The accuracy for the laser distance gauge for the full range was determined as  $\pm 0,199$  mm and less than  $\pm 0.50\%$  as a ratio of the full calibration range.

The calibration range for the Cable-Extension Position Transducer (CEPT) was 0 to 500 mm. The calibration procedure consisted of ten equally spaced distance increments which were measured with the precision steel indicator. A typical calibration result is shown in Figure 4-13 as the error of each calibration point plotted against the measured distance. The accuracy for the CEPT as a ratio of the full calibration range was found to be  $\pm 0.232\%$ .

#### 4.4.3. Load cell calibration

The 10-ton load cell was calibrated for two calibration ranges with two different dead-weight calibration systems. For the first calibration range of 0 to 25 kN a dead-weight system manufactured by Budenberg Gauge Co Ltd was used. A typical calibration results is shown in Figure 4-14. The Budenberg system operates on the principle of pressure balance between a piston loaded by calibrated dead weights and the pressure at the output port. The pistons are machined to high tolerance to minimise friction in the system and for this reason no seals are required and the slow leakage of the oil that passes the piston provides lubrication. Both pistons were continuously rotated during calibration to further reduce friction. The accuracy of the test procedure takes into account the effect of the buoyancy of the piston submersed in oil and the buoyancy of the calibrated weights in air. Table 4-4 shows the specifications and accuracy of the Budenberg tester and Figure 4-15 shows a photo taken of the Budenberg calibration tester used for this research project.

**Table 4-4: Manufacturers' specifications for the Budenberg 283/500 series tester**

Measuring range	0,1 kN to 50 kN
Accuracy of Full Stroke	0,02%

The total load capacity of the Budenberg 283/500 series dead-weight tester is only 50 kN and therefore another dead-weight system was required to calibrate the load cell for the 0 to 100 kN range. An Amsler Universal Testing Machine with a load capacity of 2000 kN was used to calibrate the load cell for this calibration range and this was controlled with an electromechanical beam that was able to move up and down on a two-legged frame as shown in Figure 4-16.

#### 4.4.4. Transducer calibration

A calibration programme was designed to evaluate the accuracy and resolution of the three external DCDTs and the internal LVDT. The three DCDTs and LVDT were calibrated with a Mitutoyo 543-553-1 digital indicator. Given the high accuracy of the Mitutoyo Digital Indicator it was decided that this would be ideally suited as a reference instrument for the calibration of all measuring devices. Figure 4-17 shows the measuring transducer calibration set-up. The Mitutoyo ID-F150 Digital Indicator is part of the 543-553-1 transducer series manufactured by Mitutoyo Corp. and the specifications are shown in Table 4-5.

**Table 4-5: Manufacturers' specifications for the Mitutoyo 543-558A digital indicator**

Measuring range	0 mm to 50,8 mm
Accuracy (At 20°C)	3,0 $\mu\text{m}$
Accuracy of Full Stroke	0.006%
LCD Resolution	1,0 $\mu\text{m}$
Total weight	19,8 grams
Power	DC 9 Volt 500mA

The DCDTs were calibrated over a typical range of 25 mm. The accuracy of the three DCDTs as a ratio of the calibration range was found to be  $\pm 0.09\%$ ,  $\pm 0.14\%$  and  $\pm 0.16\%$ , respectively. The resolution of the DCDTs ranged between 0,47  $\mu\text{m}$  and 0,48  $\mu\text{m}$  and the digital output signal was stable in all cases, which indicated that the noise level was less than the resolution. However, some hysteresis and non-linearity was evident. Figure 4-18 shows a typical calibration results.

The calibration range for the LVDT was chosen as 0 to 5 mm and the accuracy as a ratio of the calibration range was found to be  $\pm 0.16\%$ . The resolution of the LVDT is found to be 0.195  $\mu\text{m}$  and again the digital output signal was stable. The sensitivity of the LVDT for all cycles was found to be 2,0543 Volts/mm. All calibration results for all instruments which were used for this research project are summarised in Table 4-6.

**Table 4-6: Instrument behaviour**

Instrument	Measurement	Calibration range (FS)	Accuracy	Accuracy FS (%)	Precision	Resolution	Sensitivity
LDG*	Surface Roughness (Z-direction)	0,0 to 40,0 mm	± 0,199 mm	± 0,497	± 5,2 µm	10,2 µm	0,04909 V/mm
CEPT*	Displacement (Y-direction)	0,0 to 500,0 mm	± 1,16 mm	± 0,232	± 0,95 mm	0,03 mm	0,01328 mV/mm
LC*	Axial load (External)	0,0 to 25 kN	± 0,032 kN	± 0,128	± 0,030 kN	5,8 N	0,02083 mV/kN
LC*	Axial load (External)	0,0 to 100 kN	± 0,096 kN	± 0,096	± 0,030 kN	5,8 N	0,02013 mV/kN
DCDT* #1	Axial displacement (External)	0,0 to 25,0 mm	± 22,77 µm	± 0,091	± 16,65 µm	0,48 µm	0,25192 mV/mm
DCDT* #2	Axial displacement (External)	0,0 to 22,5 mm	± 32,17 µm	± 0,143	± 20,16 µm	0,47 µm	0,25305 mV/mm
DCDT* #3	Axial displacement (External)	0,0 to 25,0 mm	± 39,87 µm	± 0,159	± 18,19 µm	0,48 µm	0,25038 mV/mm
LVDT*	Axial displacement (Internal)	0,0 to 5,0 mm	± 8,15 µm	± 0,163	± 27,75 µm	0,195 µm	2,0543 V/mm

Note: \*DCDT – Direct Current Differential Transformer  
 \*LVDT – Linear Variable Differential Transducer  
 \*LC – Load Cell  
 \*LDG – Laser Distance Gauge  
 \*CEPT - Cable-Extension Position Transducer

#### 4.5. TEST SURFACE PREPARATION

This section described the method used to prepare the test surface before each plate load test. One of the main objectives of this research project is to evaluate the different surface preparation methods which are used in plate load tests to achieve a levelled and smooth test surface. The three most preferred surface preparation methods in South Africa were investigated which include; i) a thin layer of plaster of Paris; ii) a thin layer of well-graded sand and iii) the use of only hand tools to level the test area. Before the test surface could be levelled for each test, a 2 m x 2 m test pit was excavated between the four grouted anchors, to a depth of approximately 300 mm.

For the first method, the surface was only levelled as smoothly as possible using hand tools. The occasional gravel particles in some of the test holes made it difficult to level the test surface in this manner. This method is described as the ‘No interface material’ test for the remainder of this dissertation. For the second method a thin layer of well-graded Silica sand was used to level the test surface. The test surface was first levelled with hand tools and after that a thin layer of sand, less than 20 mm in thickness was spread across the testing area. This method is described as the ‘Sand’ test for the remainder of this dissertation.

The third method was to prepare the surface with a thin layer of plaster of Paris prior to testing. This method requires skilled personal due to the quick setting time of plaster of Paris. Figure 4-19 shows the steps followed for the plaster of Paris method. First a thin plastic film sheet was placed over the plate to prevent the plaster from sticking to the plate. The plaster of Paris was mixed with water until a soft to firm consistency was reached and it was then quickly applied to the test area and spread evenly using hand tools. The plate was placed on top of the wet plaster, and allowed to dry completely. This third method is described as the ‘Plaster of Paris’ test for the remainder of this dissertation.

In order to successfully evaluate the three surface preparation methods, six precise plate load tests were conducted. Two tests were performed for each test method and these included 2 times ‘No interface material’ tests, 2 times ‘Sand’ tests and 2 times ‘Plaster of Paris’ tests. Figure 4-20 shows the three surface preparation methods.

#### 4.6. MODIFIED PLATE LOAD TEST PROCEDURE

The purpose of this section is to describe the test procedure which has been adopted for this research project. The preparations carried out prior to the tests are discussed here followed by a description of the complete step-by-step test procedure that was used for all six plate load tests. Furthermore, the load and unload cycles which are used consistently throughout the study will be described.

It was necessary for a few preparations to be carried out before the actual plate load tests could commence. These preparations included:

- Identifying a large enough area on the experimental farm of the University of Pretoria to perform the required number of plate load tests;
- Preparing and installing the grouted anchors in a fashion that the paired-anchors could be used twice for consecutive tests. It was important to install the anchors at least a week before the first test so that they would reach the required concrete strength;
- Calibrating all measuring instruments as described in Section 4.4.;
- Servicing of the hydraulic pump, hydraulic jack and all pressure pipes in order to ensure that all seals and pipes are working properly;

A well-designed test procedure was adopted for the six plate load tests conducted during this research project. It was important to aim for a consistent test procedure that allowed a comparison between the results which were obtained from different tests. The test procedure is described by the following steps:

1. A 2 m x 2 m test pit was first excavated between the four grouted anchors, to a depth of approximately 300 mm;
2. The four anchors were inspected for any faults and bricks were placed next to the anchors to support the reaction frame.
3. The reaction frame was placed over the anchors to mark off the middle-point of the frame. The frame was then removed;
4. A 25 mm central hole was drilled at the middle-point with the hand bore to a depth of 450 mm. Figure 4-21a shows this step;

5. Pipe #1 (25 mm diameter steel pipe, 500 mm long) was placed inside the 25 mm hole to ensure the middle-point is maintain at all times and to prevent collapsing of the hole;
6. The test surface was prepared to achieve a levelled and smooth test surface. The three surface preparation methods described in Section 4.5 were used for consecutive tests;
7. The test surface was scanned with the laser measuring system before each test took place. All six tests were scanned after the test surface was levelled using only hand tools. In addition, scans of the sand and plaster of Paris tests were made again after the sand or plaster of Paris was applied to the test surface. This step is shown in Figure 4-21b;
8. The positions of the measuring frame's tri-pod stand were marked in order to scan the same area after the test;
9. All scan data were immediately saved on the laptop and additional flash disk to ensure that no data would be lost;
10. The 450 mm diameter loading plate was placed on the test area and was located to allow the middle-point and the central hole in the 450 mm plate to be lined up. Pipe #1 was removed once the 450 mm plate was in position;
11. The reaction frame was again placed on top of the bricks and fastened to the four grouted anchors. Figure 4-21c shows this step;
12. The 300 mm loading plate was stacked on top of the 450 mm plate followed by the hollow load cell and hydraulic jack cylinder. All these components were fitted well between the ground and reaction frame with a small gap available for the hydraulic jack piston. Figure 4-21d shows this step;
13. The hydraulic pump was connected to the hydraulic jack in order to extend the piston to a position just before it touched the reaction frame;
14. Pipe #2 (25 mm diameter steel pipe, 1,75 m long which had a washer welded to the end as shown in Figure 4-21e), was inserted through all components to the bottom of the 450 mm deep central hole below the loading plates. A marker was used to indicate the length from the bottom of the hole to the top of the reaction frame;
15. After pipe #2 was removed, the marker was moved down by 30 mm and then inserted back into the hole to create a gap at the bottom of the hole as shown in Figure 4-21f;
16. Once pipe #2 was in place, the ROCSET<sup>®</sup> quick-set grout was mixed to the right water/grout ratio to fill the bottom 20 mm of the hole (see Figure 4-22a). An extended injection tube was used to fill the bottom of the hole with the grout through the opening at the bottom of pipe #2 (see Figure 4-22b);

17. After the extended injection tube was removed from pipe #2, the 8 mm aluminium rod was inserted all the way to the bottom of the hole through the opening in pipe #2 to ensure it was located in the centre of the hole. The aluminium rod was allowed to dry completely for approximately one hour;
18. While the grout was being allowed to set, there was enough time was available to set-up the wooden reference beams and holding brackets for DCDTs. The external DCDTs were installed on the perimeter of the 450 mm plate as shown in Figure 4-7;
19. The data acquisition system was set up to plug in the load cell and the three DCDTs. The digital output signals were checked to ensure that all instruments were working properly as shown in Figure 4-8;
20. Once the grout was completely set, pipe #2 was removed;
21. The probe head attached to the 13 mm aluminium tube was inserted into the release pipe #3 (25 mm diameter steel pipe, 1,45 m long). Figure 4-22c and Figure 4-22d shows this step. Pipe #3 together with the aluminium tube was inserted over the 8 mm rod and sunk until 225 mm below the ground surface;
22. The aluminium tube was held firmly in place while pulling pipe #3 upwards and releasing the probe head 225 mm below the surface. Pipe #3 was removed as shown in Figure 4-22e;
23. The telescopic probe was rotated 45 degrees clockwise to ensure that it had an even better grip into the soil;
24. The brackets used to attach the LVDT were fixed onto the telescopic probes. The LVDT was then attached and fixed as close to the zero reading as possible as shown in Figure 4-10. The LVDT was also plugged into the data acquisition system;
25. All digital output signals were checked a final time to ensure that all instruments worked properly. The output signals are shown in Figure 4-22f;
26. A load sequence was applied which comprised three cycles (8 kN, 24 kN and 100 kN) and with the 450 mm plate diameter these loads resulted in 50 kPa, 150 kPa and 628 kPa contact pressures, respectively. Each load was kept constant until the rate of displacement (creep) was less than 0.03 mm per minute for three consecutive minutes. The applied loads were continuously recorded during the load and unload cycles at 10 readings per second (10Hz) throughout the tests together with the four displacement transducers;
27. After all load cycles were applied, the data was saved immediately on the laptop and the flash disk to ensure no data could be lost during power failures;

28. All equipment was removed carefully without disturbing the test area;
29. The test surface was again scanned with the laser measuring system on the same position as before the test. All scan data was saved immediately;
30. The reaction frame was moved with a fork lifter to the next test position.

## 4.7. DATA ANALYSES

The statistical methods and interpretation techniques used to analyse all data for this research project are discussed in this section. The seven-step process used to describe the surface roughness for each surface preparation method is presented, and this is followed by a brief discussion on the means used to determine the external stiffness values. Furthermore, the determination of the internal stiffness values is discussed.

### 4.7.1. Quantification of surface roughness

The surface roughness, before and after each test, was described by the calculation of the surface roughness parameters for each test. Surface roughness is a measure of the texture of a surface and is quantified by the perpendicular deviation ( $y_i$ ) of a real surface from its ideal form. Several standard parameters were used to describe the surface roughness for each surface preparation method and these included:

- a. Average roughness,  $R_a$  – Also known as arithmetic average (AA) or centre line average (CLA) is the average of absolute values of the individual asperities (heights) and valleys (depths) from the arithmetic mean elevation of the profile. It also represents the area between the roughness profile and its mean line. Figure 4-23 shows the calculation of the average roughness parameter.
- b. Root Mean Square (RMS) roughness,  $R_q$  – The root mean square roughness computes the standard deviation for the height distribution of the surface. It is the square root of the sum of the squares of the individual asperities and depths from the mean line.
- c. Maximum valley depth,  $R_v$  – The maximum valley depth is the depth between the mean line and the deepest valley of the profile.
- d. Maximum peak height,  $R_p$  – The maximum peak height is the height between the highest peak of the profile and the mean line.

- e. Maximum Height,  $R_t$  – The maximum height of the profile is the total height variation calculated between the deepest valley and the highest peak.
- f. Skewness,  $R_{sk}$  – Skewness qualifies the symmetry of the height distribution. For a Gaussian surface (Normal distribution) which has a symmetrical shape for the surface height distribution, the skewness is zero. In terms of surface roughness, a negative value of  $R_{sk}$  indicates that the surface is composed of mainly one plateau which has deep and shallow valleys. On the other hand, a surface with a positive  $R_{sk}$  value indicates a surface that mainly contains peaks and asperities.
- g. Kurtosis,  $R_{ku}$  – Kurtosis of the profile is calculated as the average of the fourth derivative of the surface. Kurtosis qualifies the sharpness of the surface height distribution and characterises the spread of the height distribution. The kurtosis value for a Gaussian surface (Normal distribution) is typically 3. A well spread distribution has a kurtosis value of smaller than 3 whereas a centrally distributed surface has a kurtosis value of larger than 3.

The average roughness,  $R_a$  is the most common parameter used to describe a surface, but unfortunately  $R_a$  does not fully describe a surface's shape (Sahoo, 2005). Figure 4-24 illustrates how different surface profiles can result in the same  $R_a$  value. As a result other parameters are required to completely understand a surface's shape and spacing. These parameters were calculated here for each data set with the equations presented in Table 4-7, to describe the surface roughness of the different surface preparation methods.

Another statistical method that was used to present each surface preparation method was to plot the bearing area curve (*BAC*) for each data set. The *BAC* or Abbott-Firestone curve was first proposed in 1933 and is still used by many engineering disciplines to specify and evaluate surface roughness (Abbott and Firestone, 1933). The bearing area curve (*BAC*) is a complete and concise means of describing a surface. In terms of statistics, the Cumulative Distribution Curve will present exactly the same curve (Stewart, 1990). The bearing area curve is by definition the integral of the probability distribution, which is also known as the Amplitude Distribution Function (*ADF*) (Stewart, 1990):

$$BAC = \int ADF = \int P(y) \cdot dy \quad (4-1)$$

Where:

$y$  = Height deviation from the mean line.

**Table 4-7: Surface roughness parameters.**

Parameter	Description	Formula*
$R_a$	Arithmetic Average	$R_a = \frac{1}{n} \sum_{i=1}^n  y_i $
$R_q$	Root Mean Squared	$R_q = \sqrt{\frac{1}{n} \sum_{i=1}^n y_i^2}$
$R_v$	Maximum Valley Depth	$R_v = \min_i y_i$
$R_p$	Maximum Peak Height	$R_p = \max_i y_i$
$R_t$	Maximum Height of the Profile	$R_t = R_p - R_v$
$R_{sk}$	Skewness	$R_{sk} = \frac{1}{nR_q^3} \sum_{i=1}^n y_i^3$
$R_{ku}$	Kurtosis	$R_{ku} = \frac{1}{nR_q^4} \sum_{i=1}^n y_i^4$

Note: \*After Degarmo et al., 2003; Sahoo, 2005.

One option available in the creation of the bearing area curves was to first generate and then to integrate the Amplitude Distribution Function (*ADF*) for each data set. However, for this research project another approach was used that is much faster and still produces the same curve. The bearing area curves were created for each data set by sorting all height deviations in descending order and plotting the sorted data, from 0 to 100%, where 100% =  $n$  (the total number of scanned points). All curves were then plotted together on one scale which allowed for comparisons between the different surface preparation methods.

All laser scan data, which was recorded before and after each test, was analysed by using a consistent seven-step process to ensure that the results could be compared between the

different surface preparation methods. For each before and after scan, twelve (12) consecutive lines were scanned across the test area as described in Section 4.3.1. The analysing process comprised of the following steps:

- Step 1. The digital output signals recorded during each scan were converted into engineering units (millimetres) with the least squares linear transfer equation being determined during the calibration. Figure 4-25 shows a typical plot of the raw data taken from the three surface preparation methods.
- Step 2. As indicated on Figure 4-3, for each scan line, a certain portion was scanned on the outside of the plate and another segment in the loaded area. For this reason it was important to determine and plot only the portions of those lines within the loaded area. A linear line was plotted through all the relevant data points to represent its ideal form and was described by a least squares linear transfer equation.
- Step 3. The vertical error was calculated for each data point as the difference between the least squares linear equation and the measured value (digital output was converted to engineering units using the calibration equation).
- Step 4. Surface roughness was quantified by the perpendicular deviation ( $y_i$ ) of the measured surface from the linear equation. The vertical errors which were calculated in the previous step were used together, with the slope of the least squares linear equation, to calculate the perpendicular height ( $y_i$ ) of each measured point. Figure 4-26 illustrates the calculation of the perpendicular height ( $y_i$ ).
- Step 5. The seven (7) surface roughness parameters,  $R_a$ ,  $R_q$ ,  $R_v$ ,  $R_p$ ,  $R_t$ ,  $R_{sk}$  and  $R_{ku}$ , described in Table 4-7 were calculated for each scanned line.
- Step 6. The average values for  $R_a$ ,  $R_q$ ,  $R_{sk}$  and  $R_{ku}$  were calculated from all twelve (12) lines to represent the total scanned area of the plate. The maximum total height ( $R_t$ ) was calculated as the difference between the deepest valley ( $R_v$ ) and highest peak ( $R_p$ ) for the entire data set.
- Step 7. All data taken from the scans before and after each test was used to generate and plot a bearing area curve (*BAC*). All roughness parameters and bearing area curves from different surface preparation methods were compared to evaluate the surface roughness for each test.

#### 4.7.2. Determination of external stiffness

The average vertical displacement of the plate ( $\rho$ ) obtained from the three DCDT's was used in Equation 4-2, together with the plate diameter ( $D$ ), and Poisson's ratio ( $\nu$ ), taken as 0.35, was used to determine the external stiffness ( $E_{ext}$ ) in MPa. The contact stress ( $q$ ) was taken as the applied load divided by the plate area, which assumed a uniform pressure distribution across the plate. Equation 4-2 was used to calculate the secant stiffness values for different plate settlement.

$$E_{ext} = \frac{\pi \cdot q \cdot D \cdot (1 - \nu^2)}{4 \cdot \rho} \quad (4-2)$$

In order to make a comparison of the secant stiffness which was calculated from Equation 4-2 with the internal stiffness values that were determined with the telescopic probes, the average strain of the soil had to be assessed. This was calculated as the average plate settlement ( $\rho$ ) divided by 1.5 times the plate diameter (675 mm). This was based on the influence depths for circular foundations proposed by Boussinesq's theory, where less than 20% of the applied stress occurs below 1.5 times the plate diameter (Boussinesq, 1885). Figure 4-27 shows the pressure bulbs beneath a uniformly loaded circular area based on Boussinesq's theory.

It was further decided that all secant stiffness data should be plotted against the logarithm of strain, because of the wide range of strain introduces during testing. However, the only disadvantage in plotting secant stiffness values in this method is its sensitivity to the choice of origin. A consistent method was used for the choice of origin in order to minimise variation of stiffness values. Figure 4-28 shows the variation of stiffness values with three different points as their origin. The random noise of the instrumentation has resulted in a scatter of data points at strain levels below 0.001%. Figure 4-28 further shows that the choice of origin does have a significant effect on the calculated stiffness in the region between 0.002% and 0.0002%.

This also demonstrated that the calculated stiffness for the strain levels above 0.005% is not significantly influenced by the choice of origin. If the assumption is made that the instrumentation noise is random, the suitable choice of origin should result in a symmetrical spread of data points about an axis that coincides with a linear plateau.

Taking point C as the origin has resulted in an approximately symmetrical spread of the data points at the strain levels between 0.002% and 0.0002% (Figure 4-28). The value of the stiffness at 0.001% is significantly influenced by the choice of origin; however, the stiffness at 0.005% is only marginally influenced by the choice of origin. A comparison between stiffness values for the origins at points A and C has revealed the following results:

$$\frac{E_{0.001}^C}{E_{0.001}^A} = 0.91 \quad \text{and} \quad \frac{E_{0.005}^C}{E_{0.005}^A} = 0.96$$

In light of this result a uniform method was adopted of selecting the origin at a point that produced a symmetrical spread of the data points at strain levels between 0.002% and 0.0002%.

#### 4.7.3. Determination of internal stiffness

The measured relative displacement of the telescopic probes ( $\partial L$ ) was used in Equation 4-3 together with the distance between the two probe points ( $L = 225$  mm), to determine the axial strain ( $\Delta \epsilon$ ) at any time during testing.

$$\Delta \epsilon = \frac{\partial L}{L} \quad (4-3)$$

Boussinesq's theory was used to calculate the vertical stress at depth  $z$  below the centre of the circular plate with diameter  $D = 2R$ , subject to a uniform pressure ( $q$ ), as shown in Equation 4-4 (After Handy, 2007). Values of the influence factor ( $I_c$ ) are always between zero and unity.

$$\sigma_z = q \left[ 1 - \left\{ \frac{1}{1 + (R/z)^2} \right\}^{3/2} \right] = q I_c \quad (4-4)$$

The radial stress at depth  $z$  below the centre of the circular plate was calculated using Equation 4-5.

$$\sigma_r = \frac{q}{2} \left[ (1+2\nu) - \frac{2(1+\nu)}{\{1+(R/z)^2\}^{1/2}} + \frac{1}{\{1+(R/z)^2\}^{3/2}} \right] \quad (4-5)$$

The internal stiffness ( $E_{Int}$ ) was calculated for every load step using Equation 4-6 which assumes axis symmetrical conditions. The vertical stress increment ( $\Delta\sigma_z$ ) and radial stress increment ( $\Delta\sigma_r$ ) was taken as the average for the two measurement points beneath the plate for the corresponding axial strain increment ( $\Delta\varepsilon$ ).

$$E_{Int} = \frac{\Delta\sigma_z - \nu\Delta\sigma_r}{\Delta\varepsilon} \quad (4-6)$$

In addition, the external and internal stiffness values were also compared with the small strain stiffness values obtained from continuous surface wave tests conducted on the same material. The stiffness degradation envelope developed by Clayton and Heymann (2001) were used to allow comparison of the external and internal stiffness values at various strain levels. Table 4-8 summarise the lower and upper bound of the stiffness degradation envelope proposed by Clayton and Heymann (2001) as illustrated in Figure 4-29.

**Table 4-8: Clayton-Heymann stiffness degradation envelope.**

Axial strain (%)	Lower bound stiffness ( $G/G_0$ )	Upper bound stiffness ( $G/G_0$ )
0.001	1.0	1.0
0.01	0.80	0.95
0.10	0.35	0.55
1.0	0.10	0.20

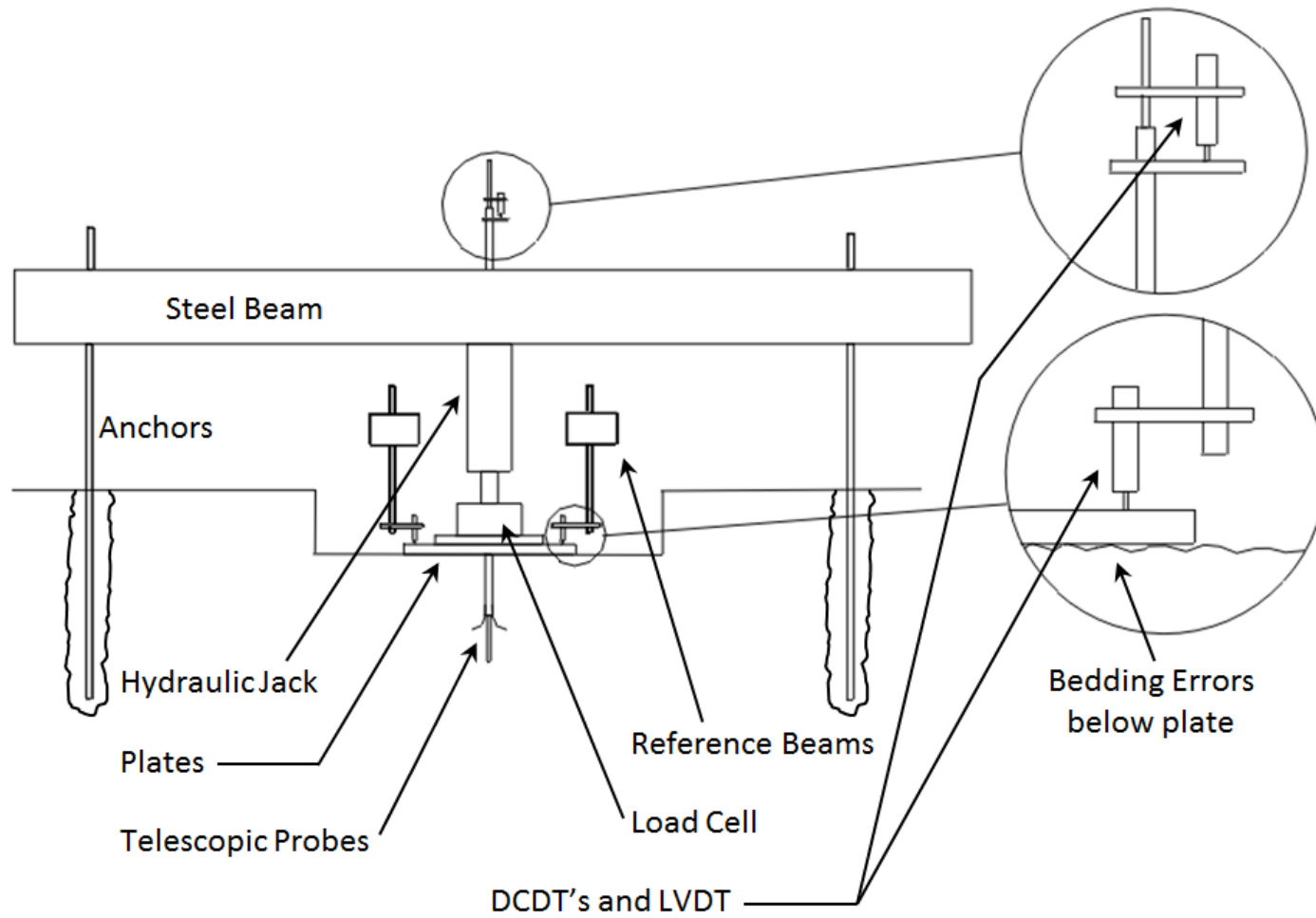


**Figure 4-1: Schematic illustration of the modified plate load test set-up.**



**Figure 4-2: Laser measuring system.**

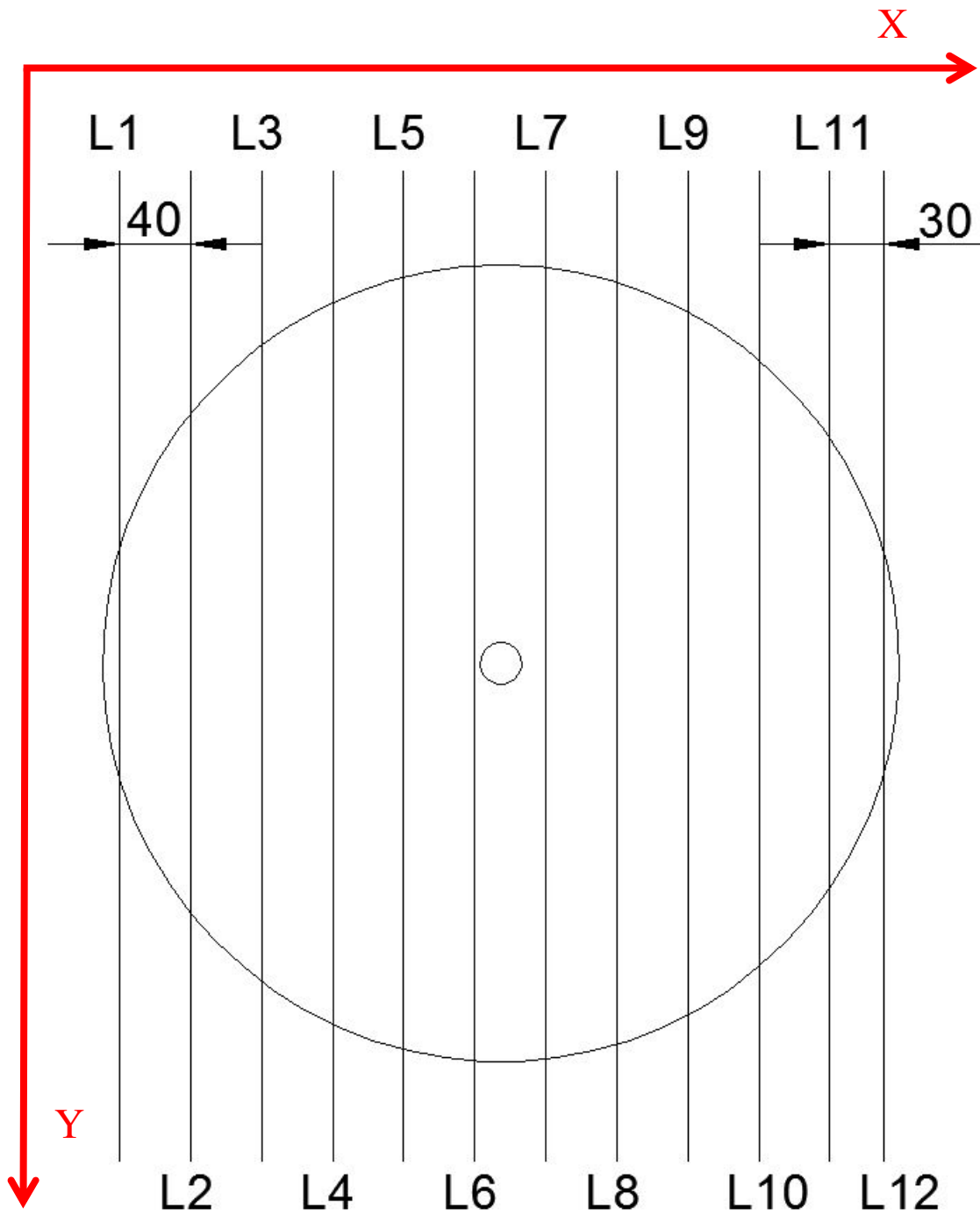


Figure 4-3: Configuration of the 12 consecutive scan lines.



**Figure 4-4: Laser data acquisition system.**



**Figure 4-5: Modified plate load test set-up.**



**Figure 4-6: Anchor installation.**



**Figure 4-7: DCDTs, load cell and hydraulic jack set-up.**



**Figure 4-8: Plate load test data acquisition system.**

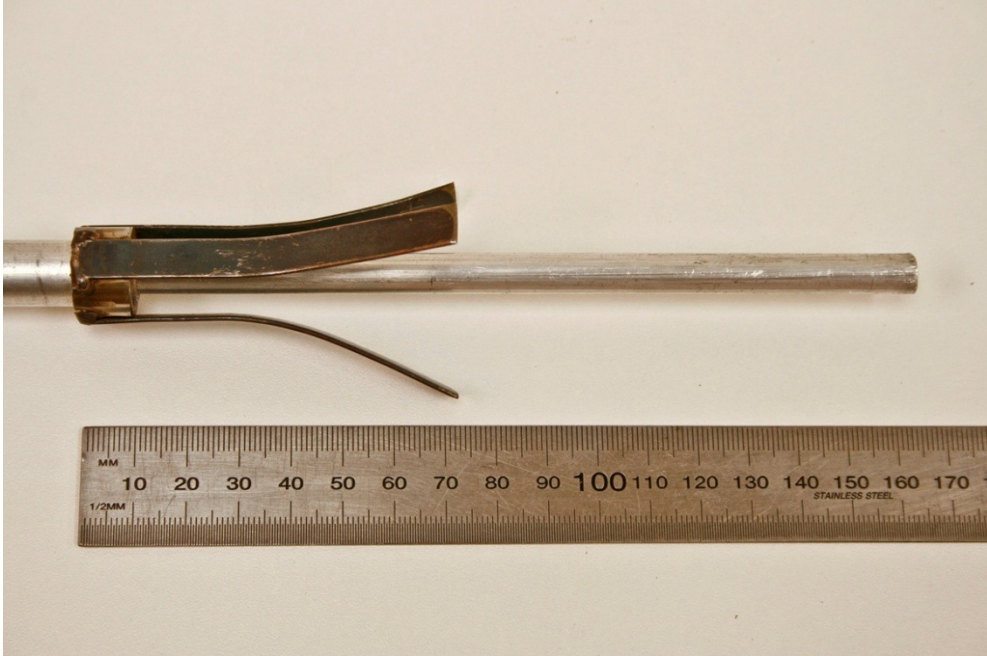


**Figure 4-9: Telescopic probes set-up.**

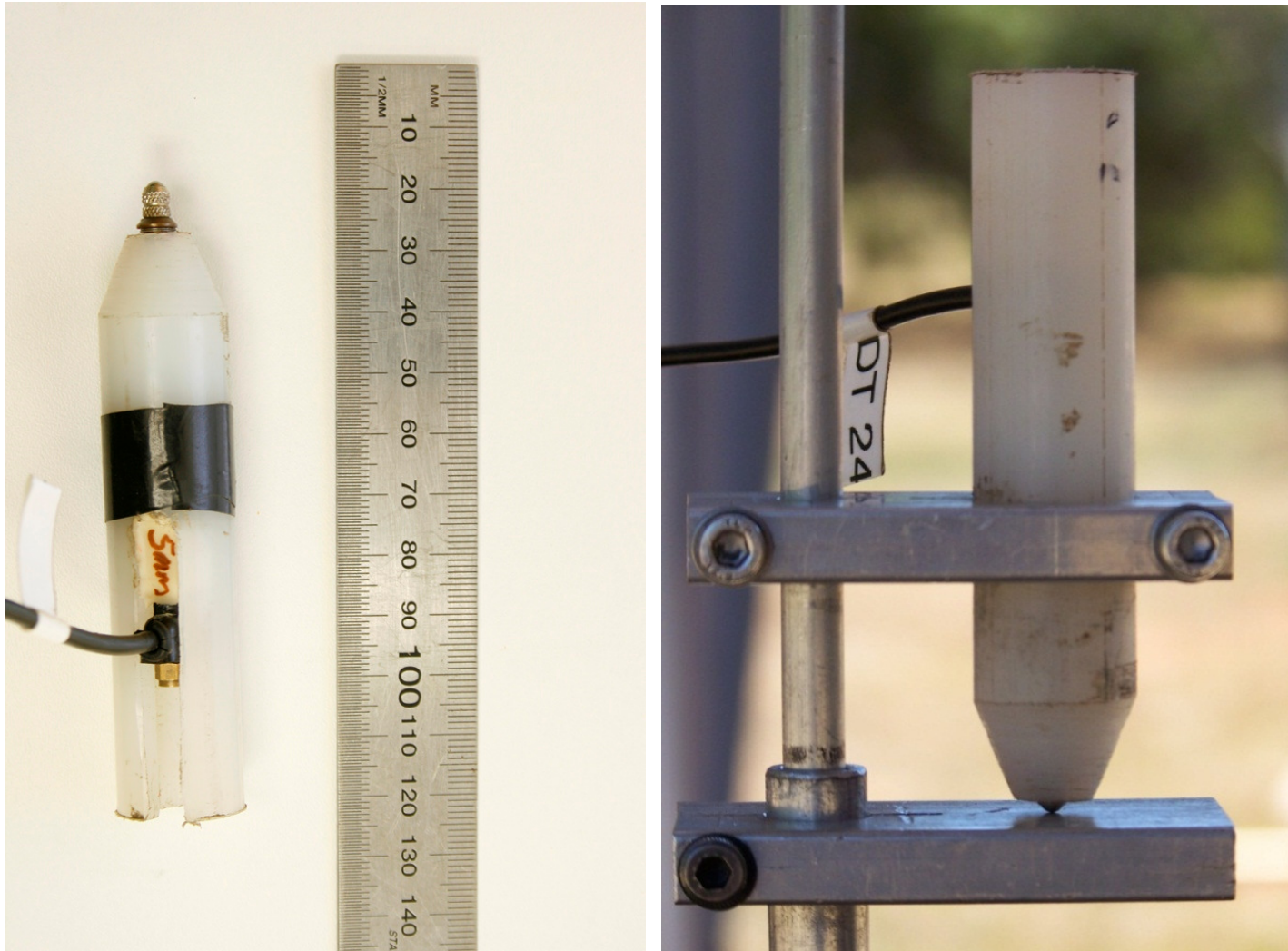


**Figure 4-10: LVDT set-up.**

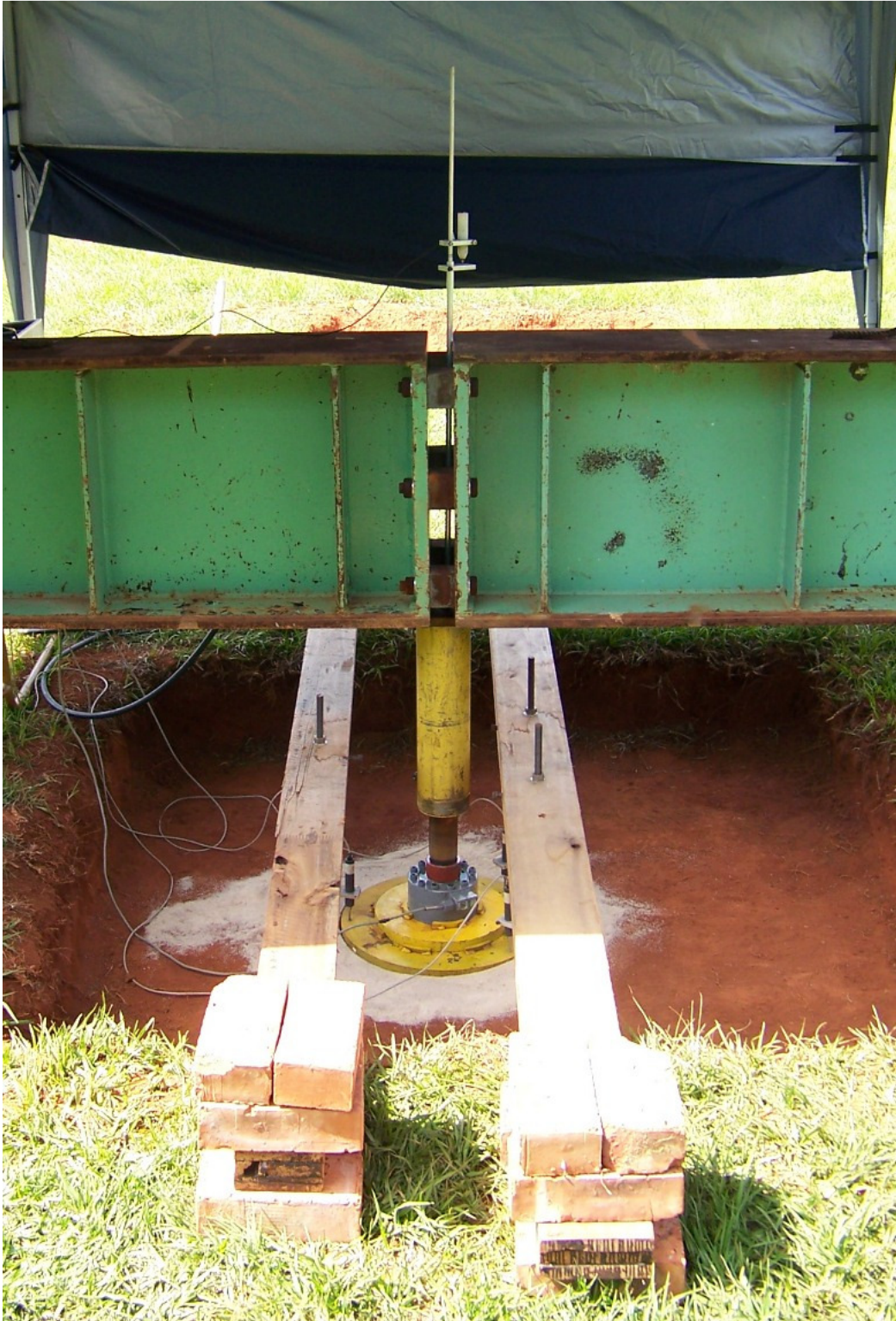


**Figure 4-11: Components of the modified plate load test.**

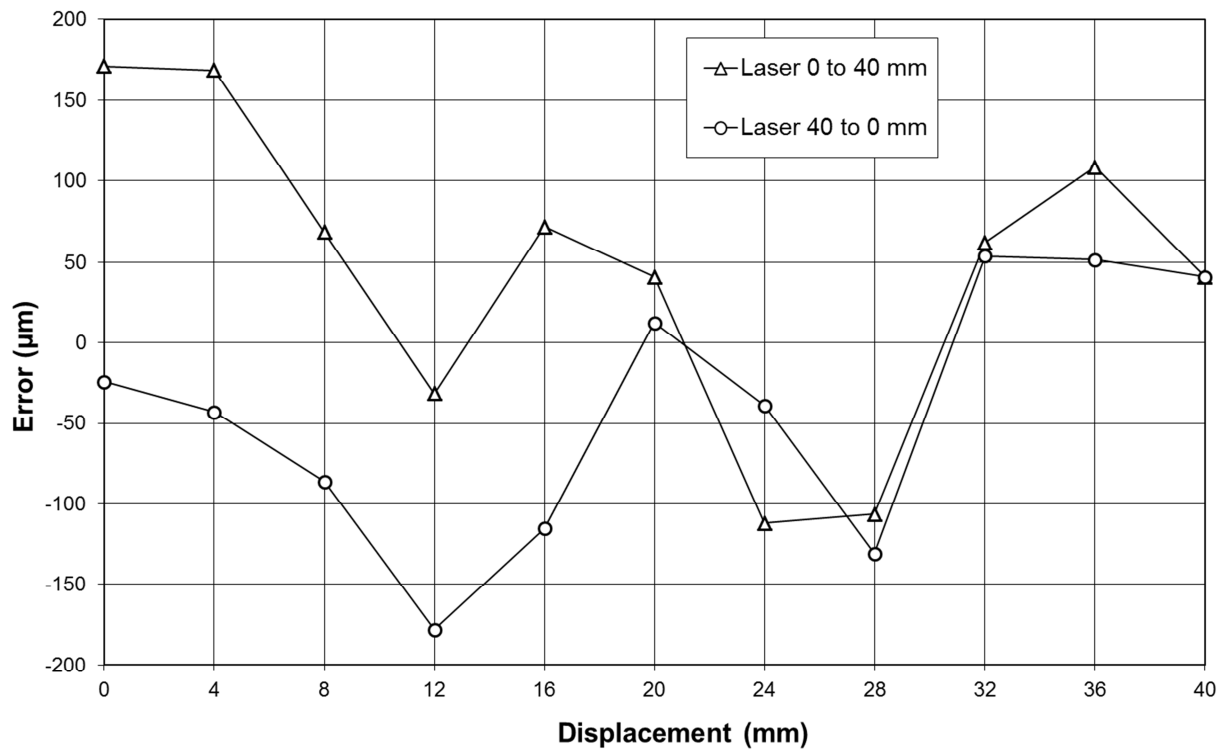
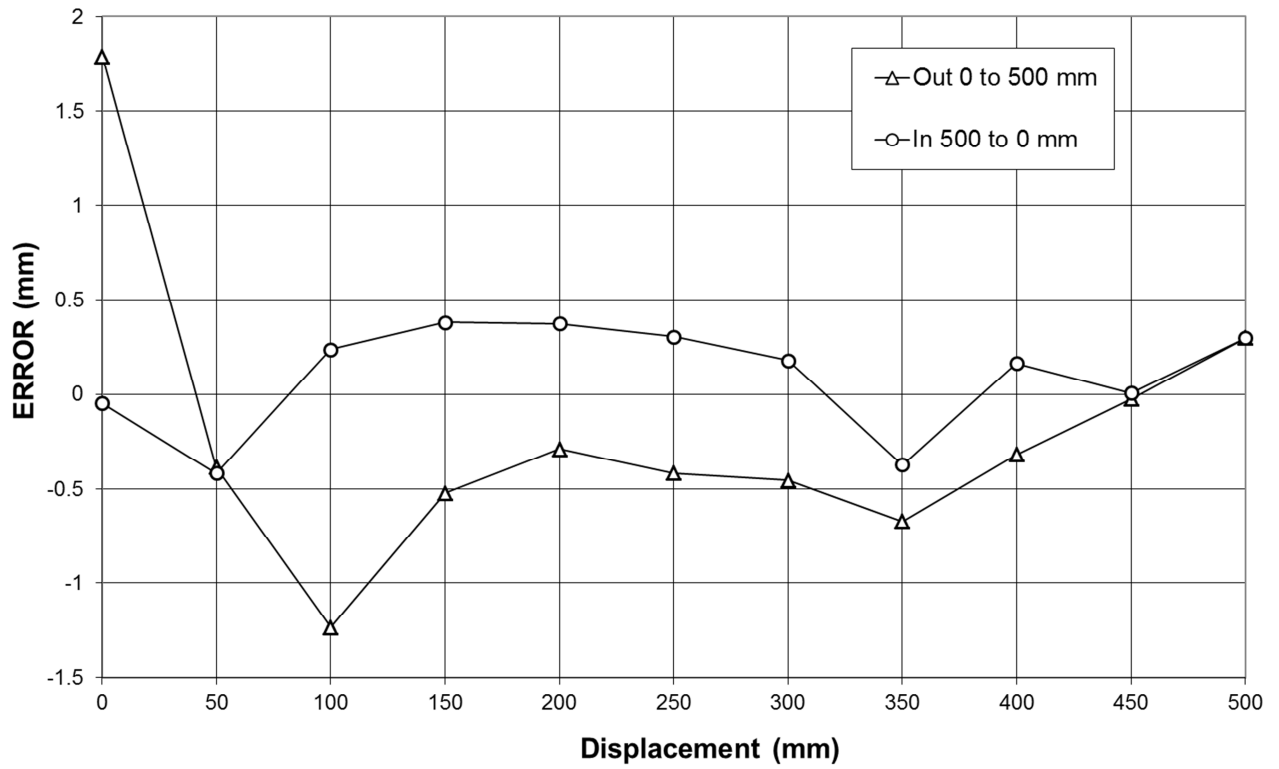
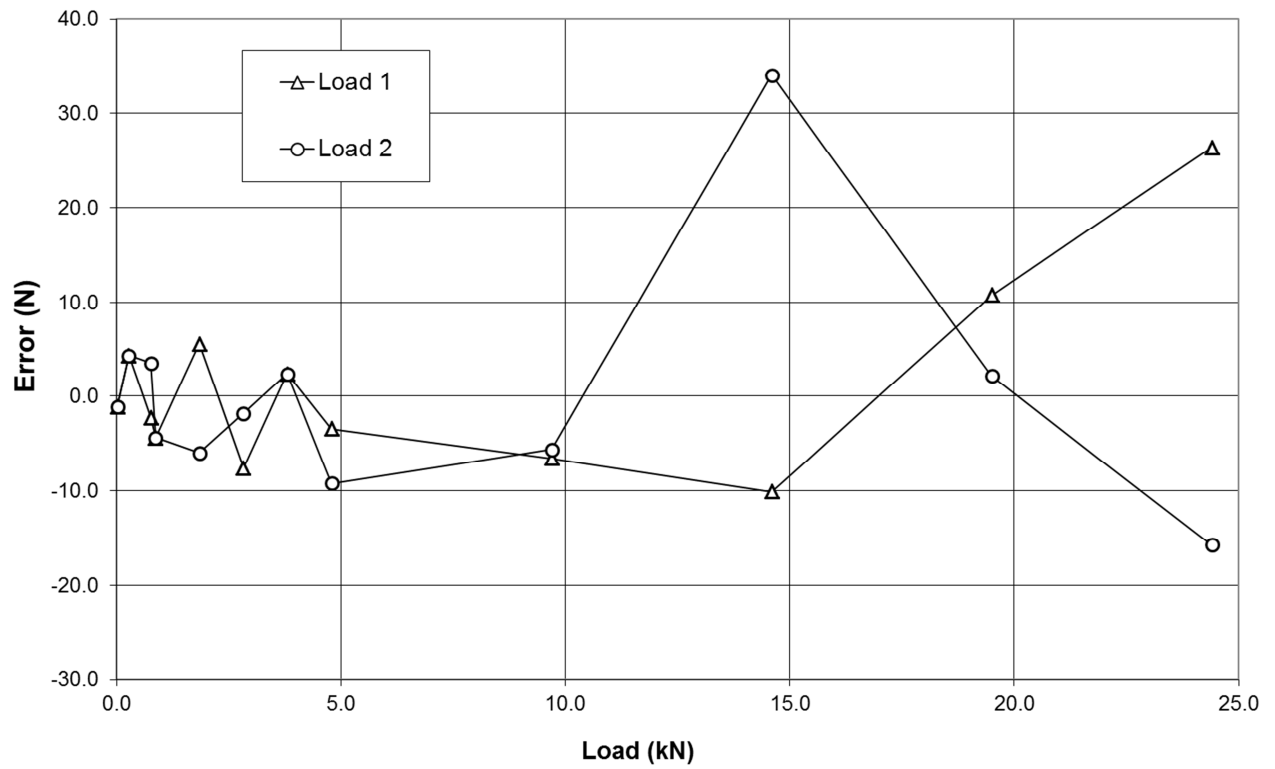


Figure 4-12: Typical laser distance gauge calibration result.



**Figure 4-13: Typical Cable-Extension Position Transducer calibration result.**



**Figure 4-14: Typical load cell calibration result.**



**Figure 4-15: Budenberg 283/500 Series set-up.**



**Figure 4-16: Amsler 2000 kN Compression testing machine.**

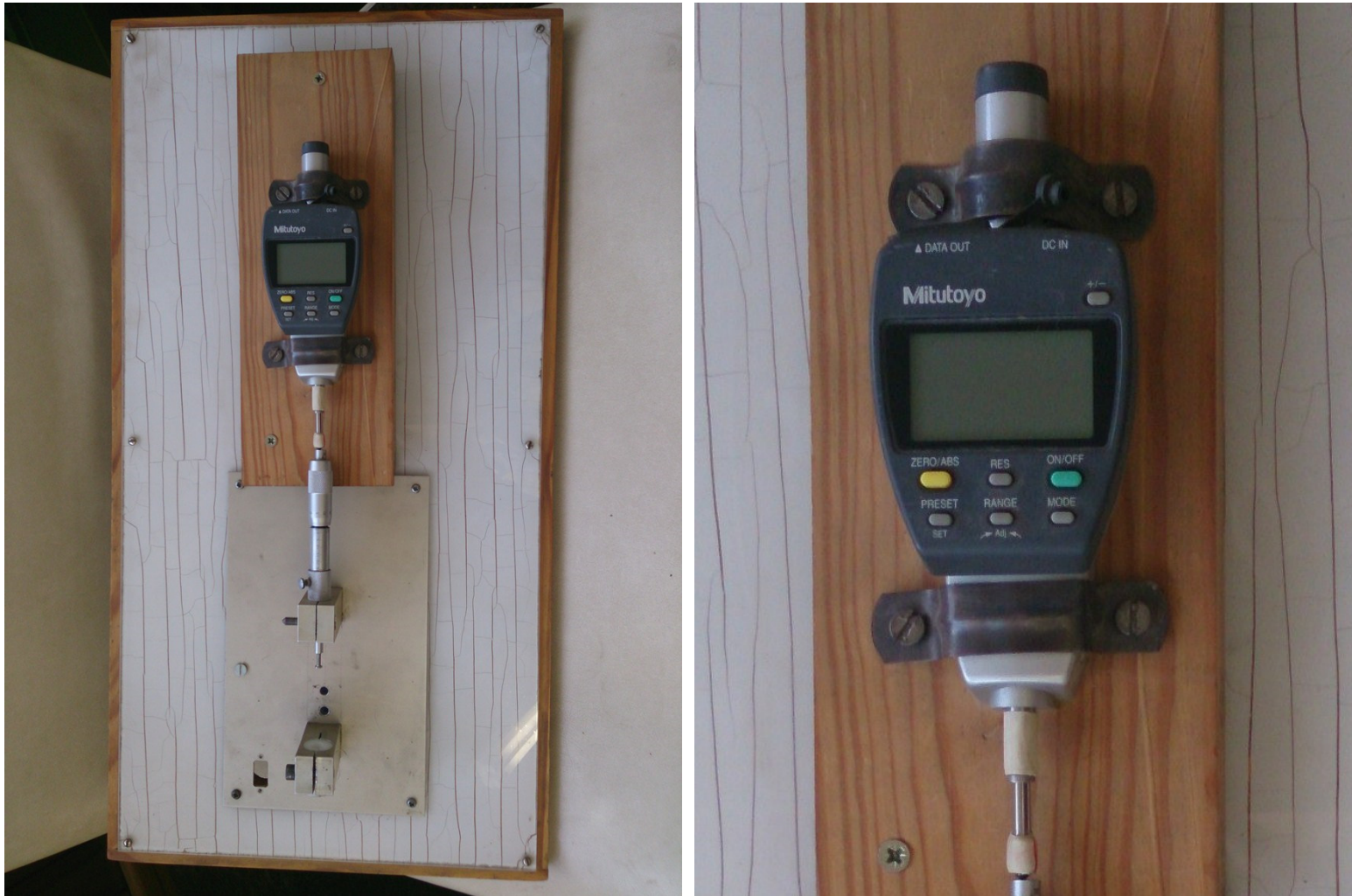


**Figure 4-17: Mitutoyo 543-553-1 Digital Indicator set-up.**

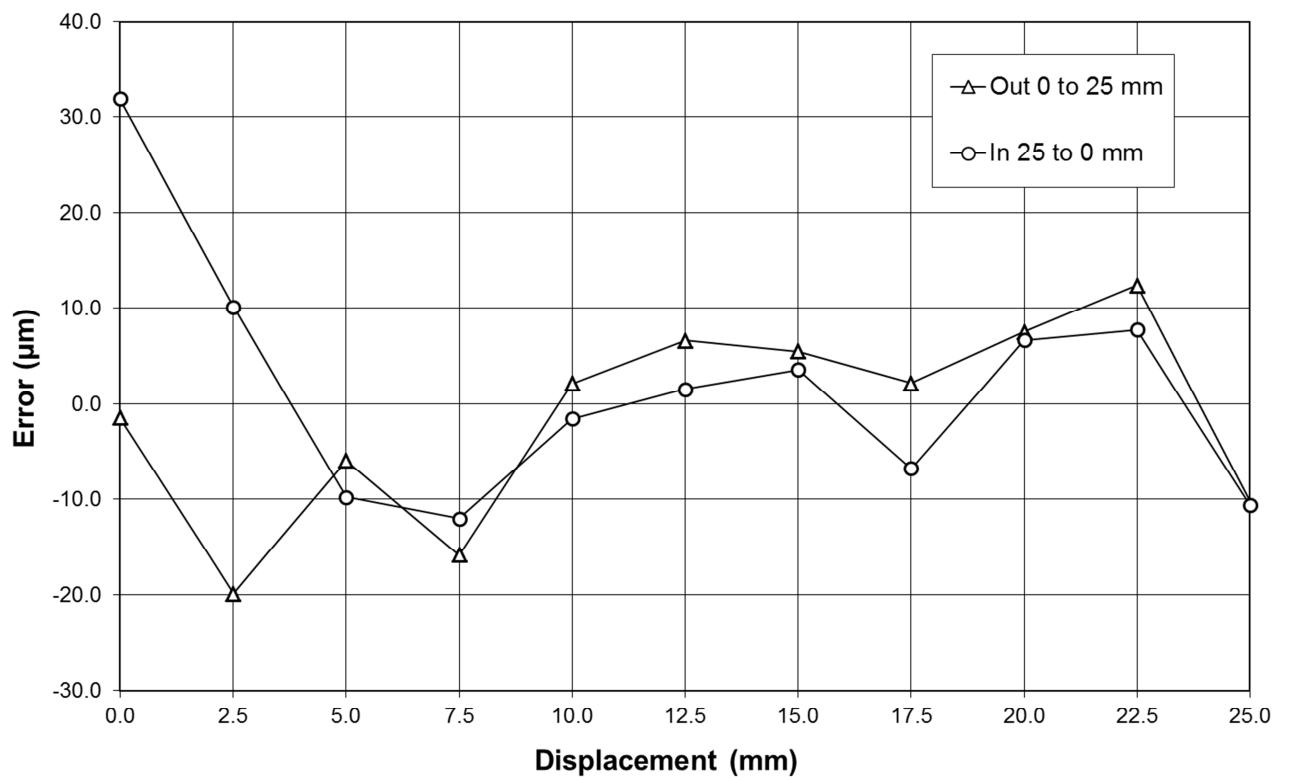


**Figure 4-18: Typical displacement transducer calibration result.**



**Figure 4-19: Plaster of Paris surface preparation.**

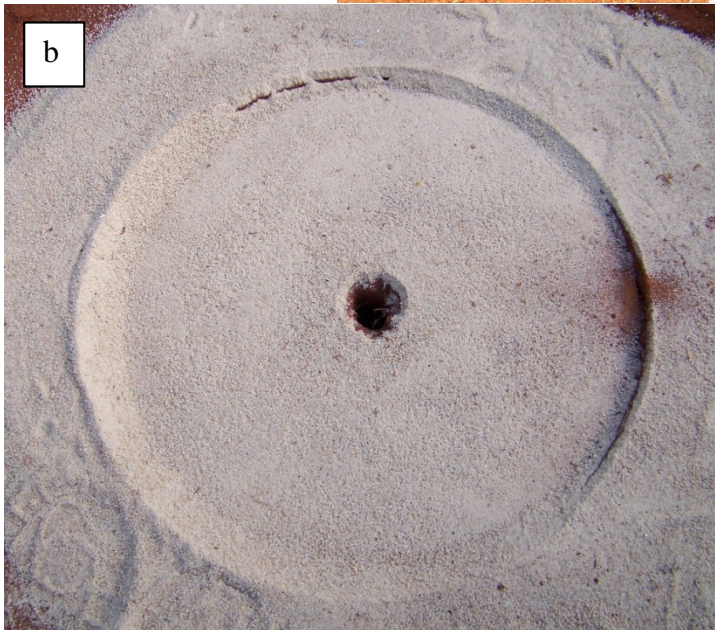
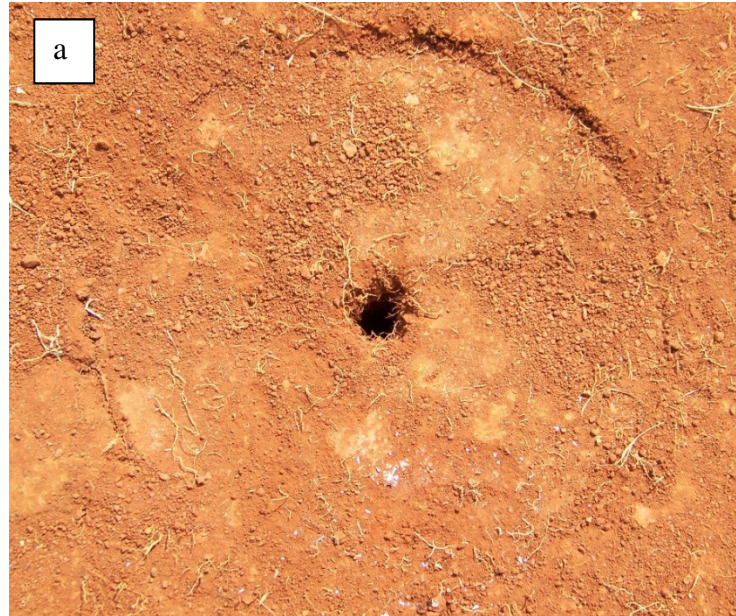


**Figure 4-20: Preparation methods: a) 'No interface material' b) Well-graded Silica sand c) Plaster of Paris.**



**Figure 4-21: Test procedure: Steps 1 to 15.**

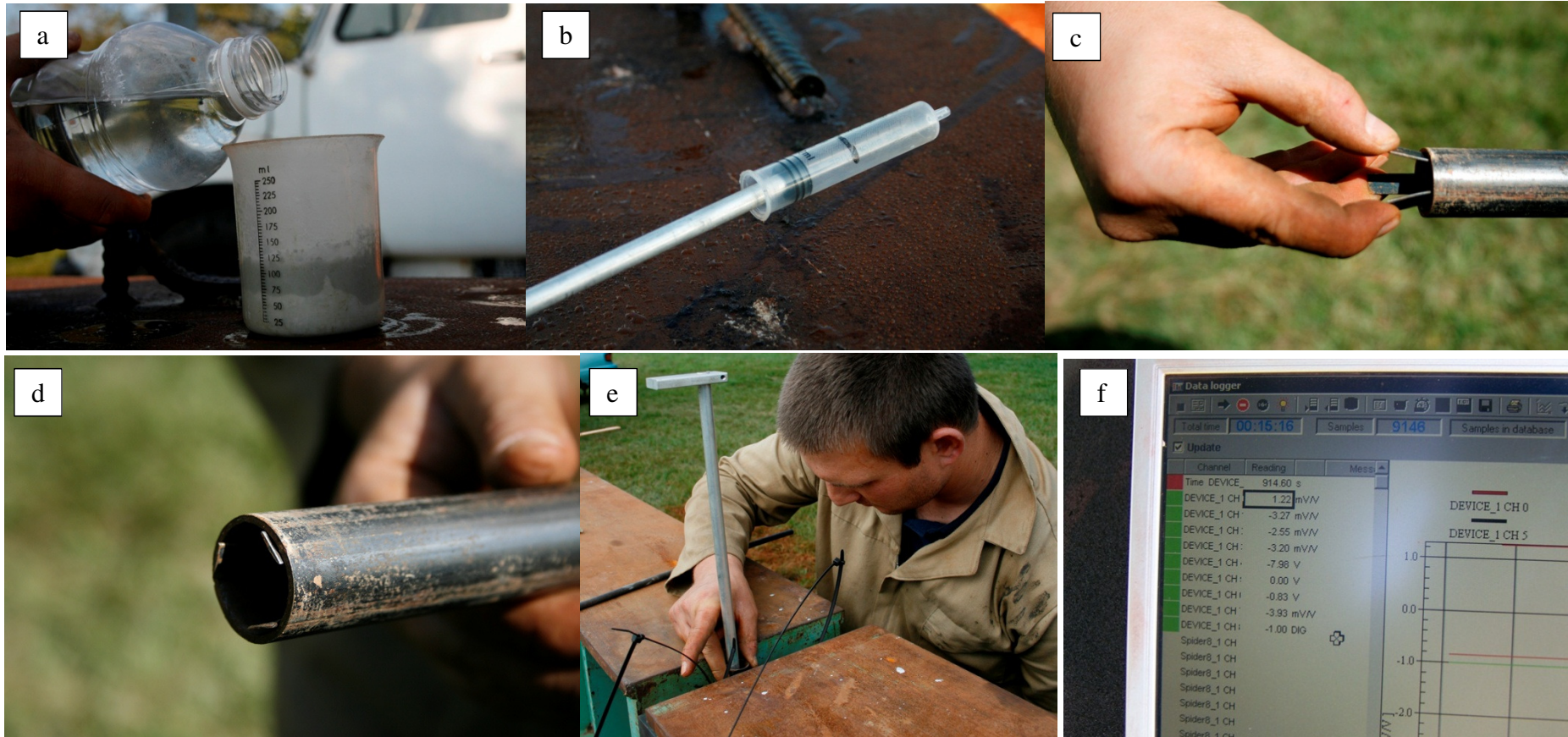


Figure 4-22: Test procedure: Steps 16 to 30.

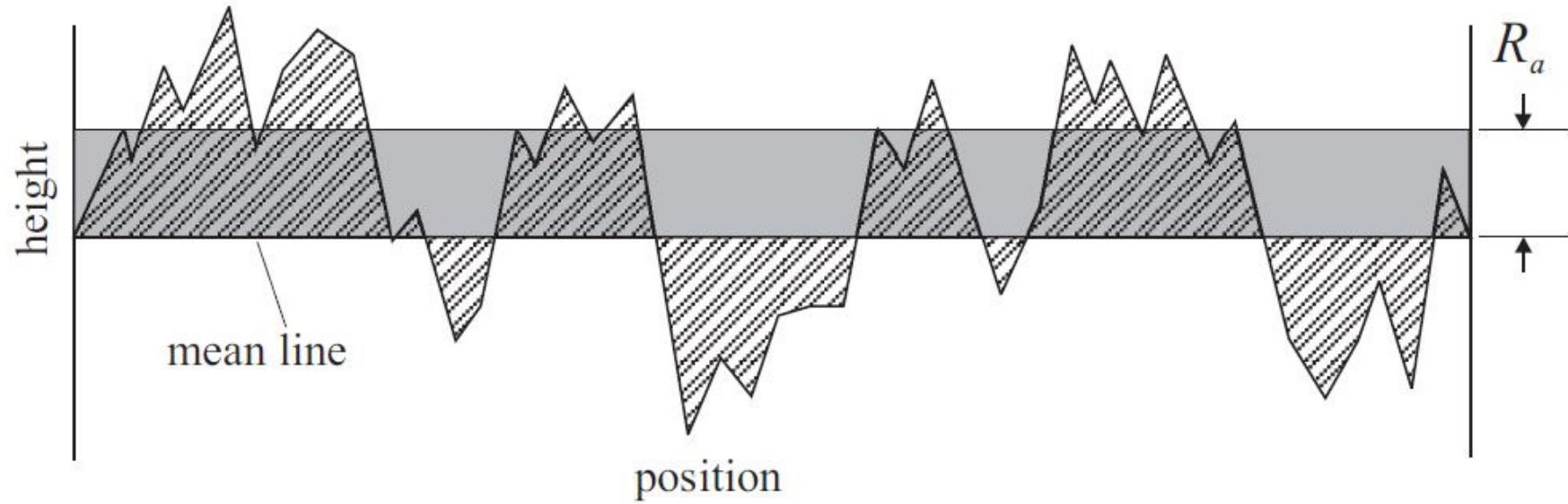
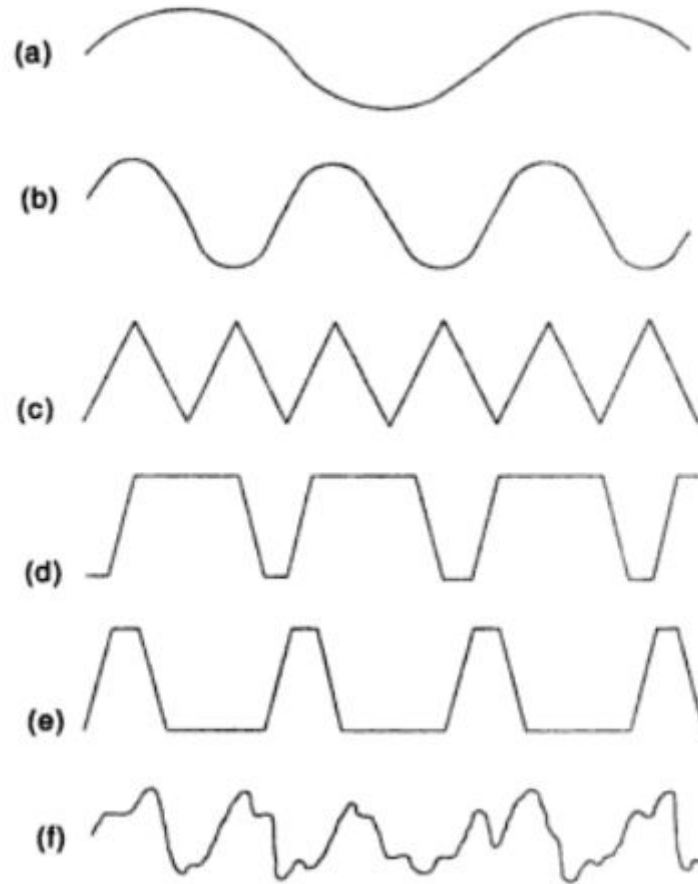


Figure 4-23: Calculation of the average roughness parameter,  $R_a$  (After Schmähling et al., 2006).



**Figure 4-24: Same  $R_a$  values for different profiles (After Sahoo, 2005).**

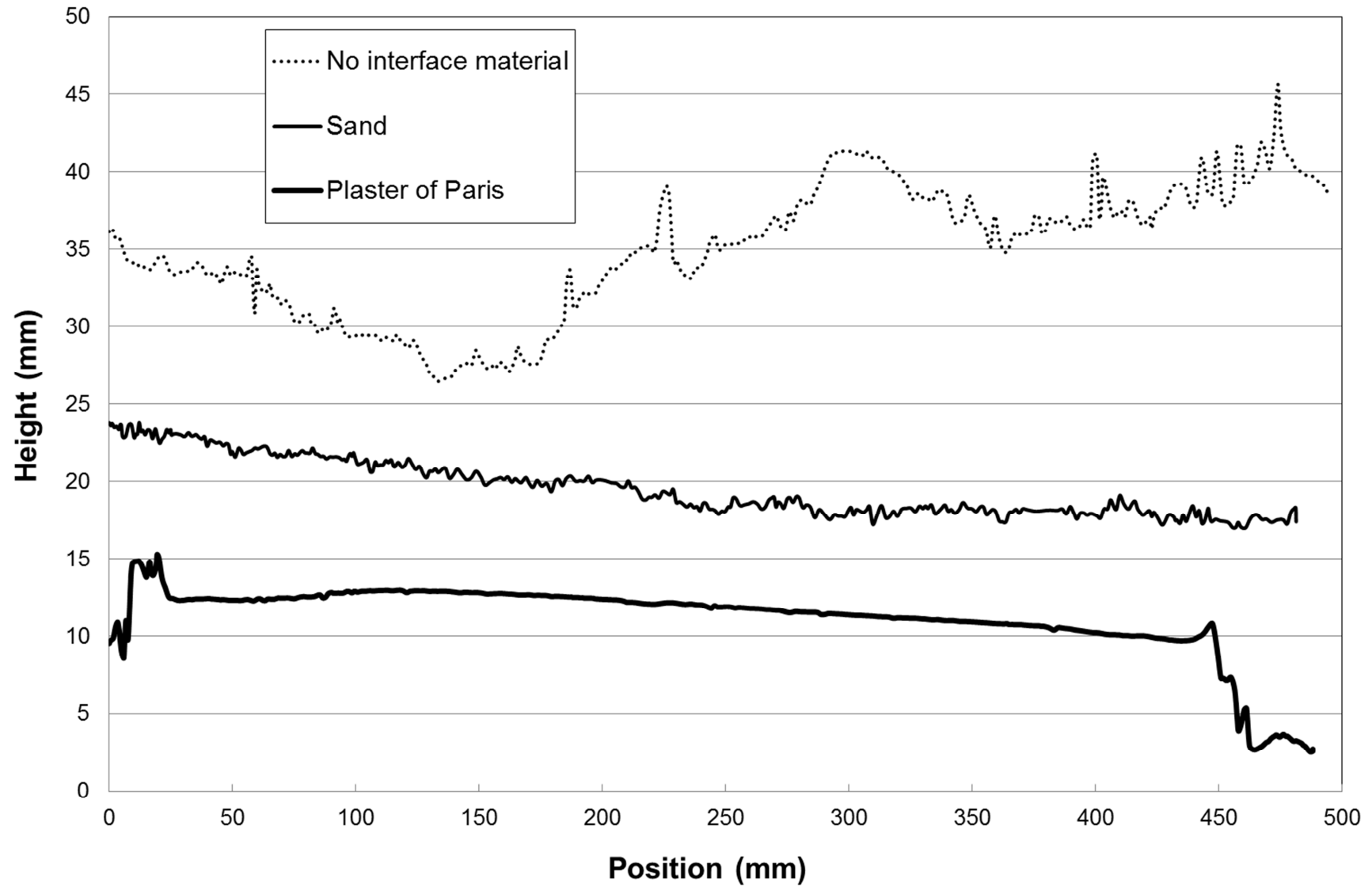


Figure 4-25: Raw data plot for different surface preparation methods.

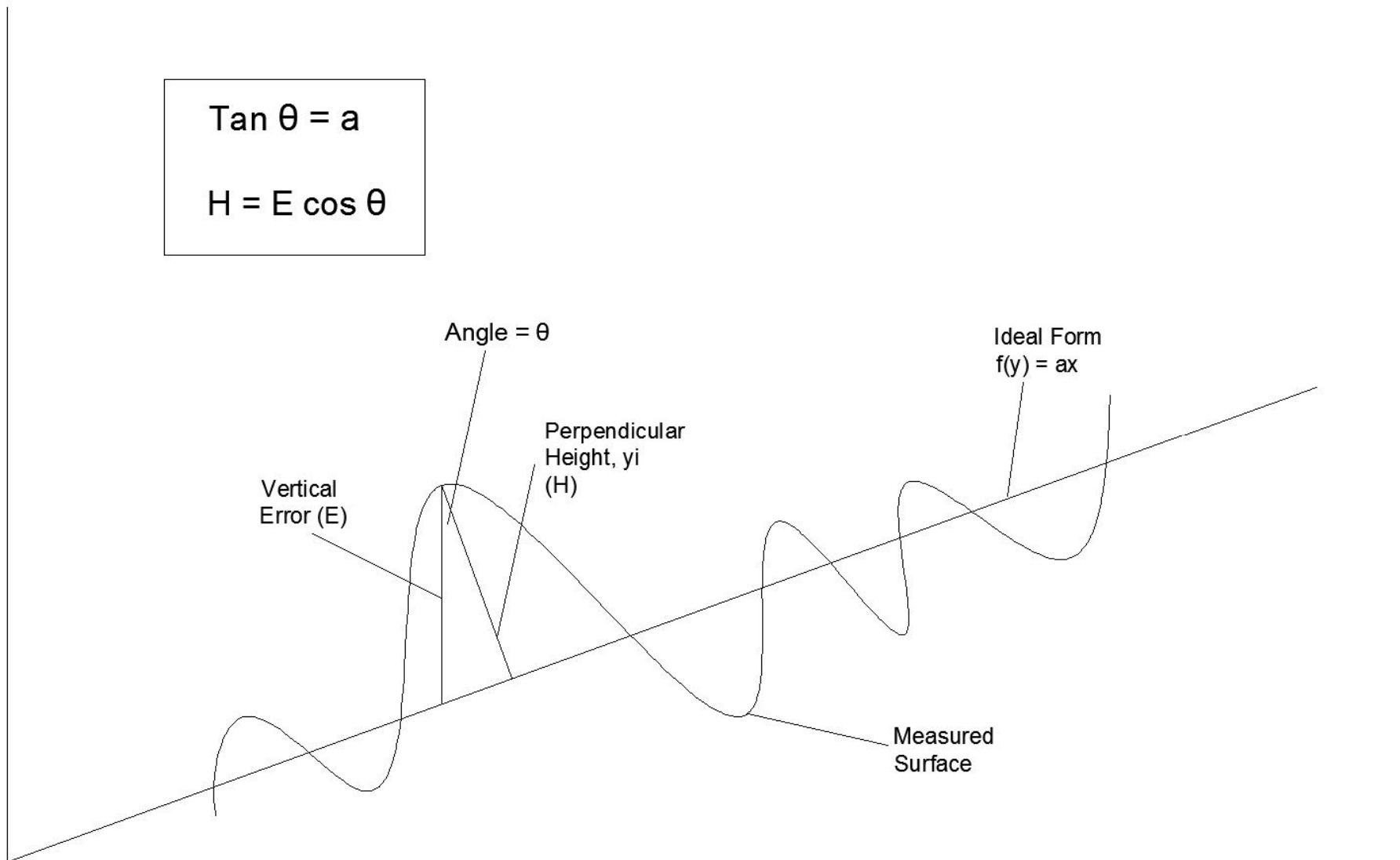


Figure 4-26: Calculation of perpendicular height ( $y_i$ ).

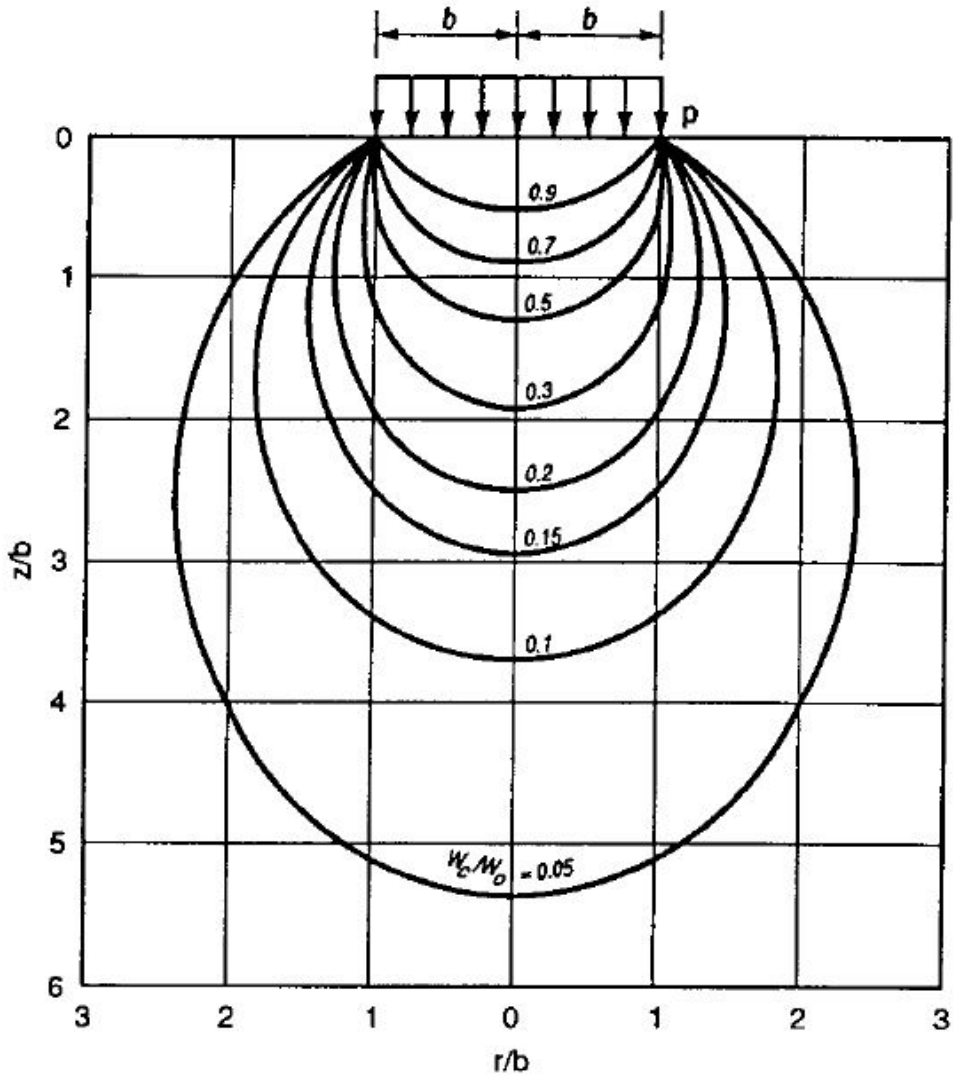


Figure 4-27: Pressure bulbs beneath a uniformly loaded circular area (After Boussinesq 1885).

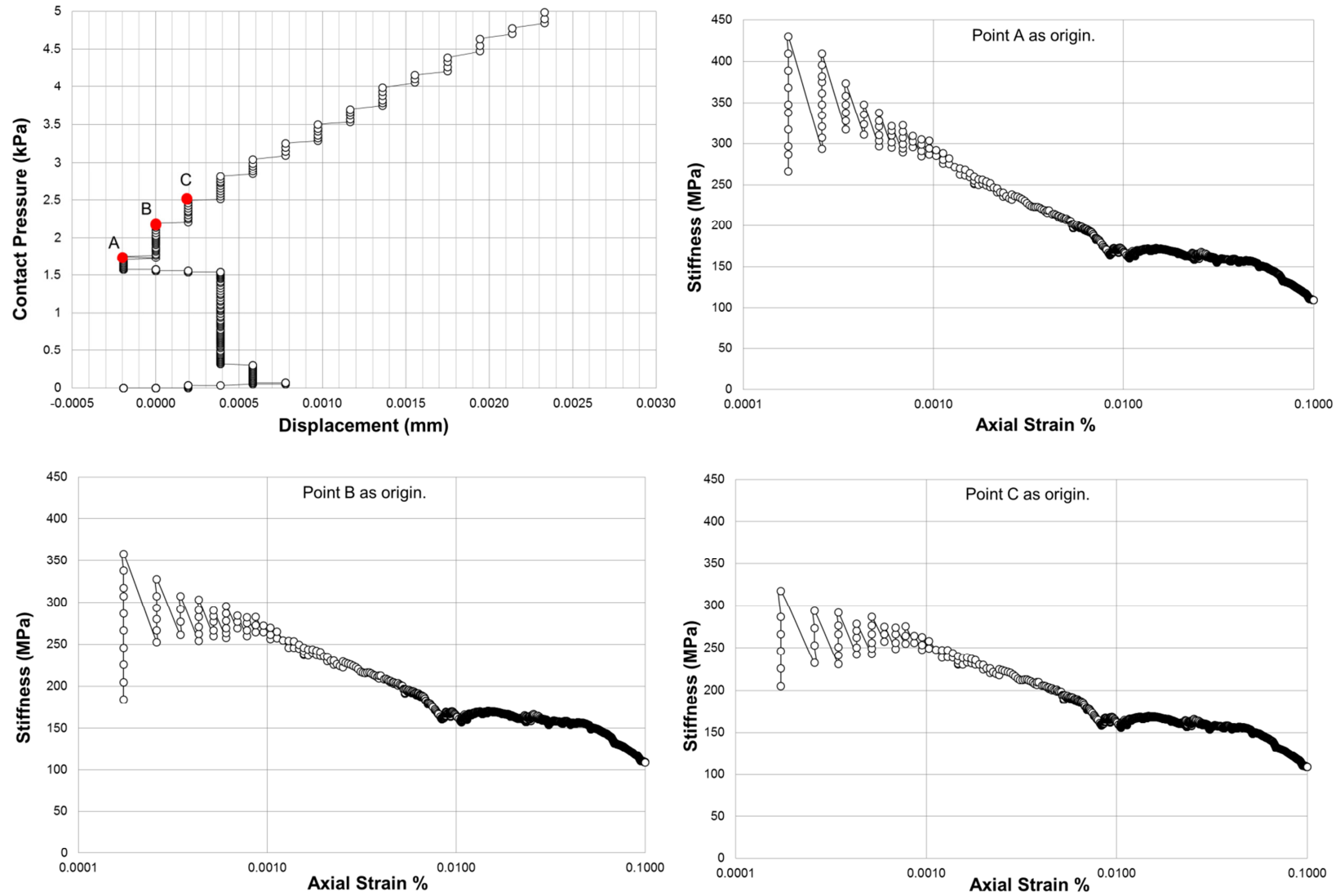
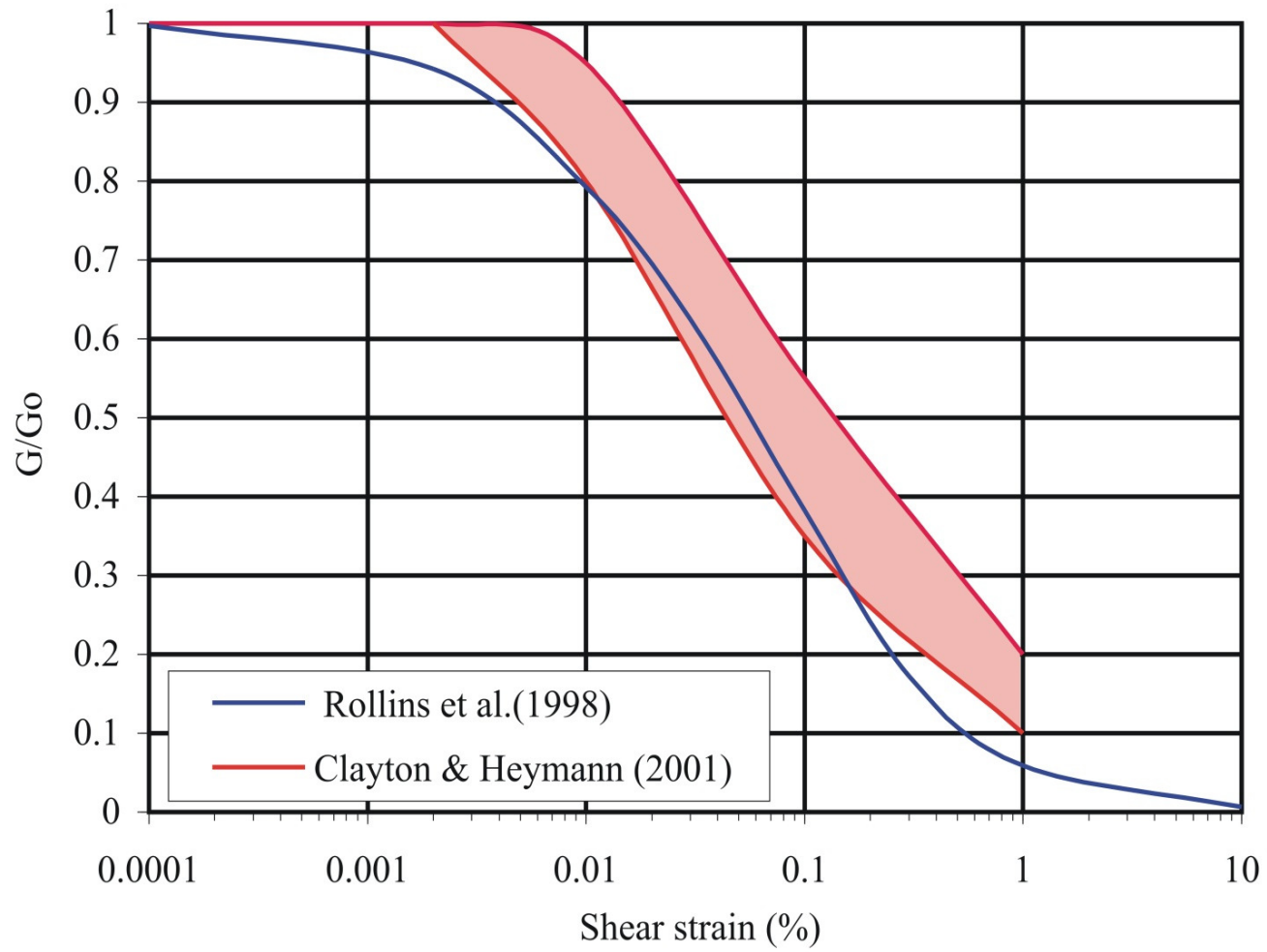


Figure 4-28: Variation of stiffness with choice of origin.



**Figure 4-29: Stiffness degradation curves.**

## CHAPTER 5: DISCUSSION

### 5.1. INTRODUCTION

All data recorded during the six precise plate load tests was analysed as described in the previous chapter of this dissertation. The results from these analyses will be presented in this chapter and will include the following discussions:

- a) The initial surface roughness's that were described for the different surface preparation methods before each test will be compared with each other and this will be followed by a comparison between the initial surface roughness and the surface roughness which was still present after each of the tests;
- b) The pressure-displacement curves generated from all load cycles and  $E_{50}$  stiffness values determined for all tests are discussed;
- c) The external stiffness values determined from the measured data will be compared and then discussed in order to determine the level of accuracy of each surface preparation method that was used for the conventional plate load tests;
- d) The internal stiffness values determined from the measured data will be contrasted and assessed in order to investigate the behaviour of the telescopic probes that were used during the modified plate load tests;
- e) Furthermore, the external and internal stiffness values are compared and discussed to evaluate the accuracy of the conventional plate load test;
- f) In addition, the measured external and internal stiffness values will be evaluated with continuous surface wave (CSW) test results.

As mentioned in the previous chapters, there were three different surface preparation methods evaluated to investigate the effect of bedding errors on the accuracy of plate load tests. For each surface preparation method, two plate load tests were performed as summarised in Table 5-1.

**Table 5-1: Surface preparation methods.**

Test 1	No interface material
Test 2	Sand
Test 3	Plaster of Paris
Test 4	No interface material
Test 5	Plaster of Paris
Test 6	Sand

## 5.2. QUANTIFICATION OF SURFACE ROUGHNESS

The quantification of surface roughness will be discussed in this section. First the initial surface roughness that occurred before each test is discussed followed by a comparison between the initial surface roughness and the surface roughness which was still present after each of the tests.

### 5.2.1. Comparison of initial surface roughness

The seven-step process described in Section 4.7.1 was used to analyse the data scanned and recorded with the laser measuring system. Seven (7) surface roughness parameters were determined for each data set in order to describe the surface roughness.

#### *Initial surface preparation*

The initial surface roughness was first measured and quantified for all six tests prior to any additional treatment with sand or plaster of Paris. The surface roughness parameters determined before all tests are shown in Table 5-2. The results revealed that the maximum average roughness value ( $R_a$ ) calculated for the scans were 2,133 mm and the minimum average roughness value was 0,711 mm. The root mean square roughness values ( $R_q$ ) presented in Table 5-2 represents the standard deviation of the height distribution. The skewness values ( $R_{sk}$ ) for Test 2, 3 and 5 indicate that the height distribution will fit a Gaussian (normal) distribution very well, because of the close-to-zero values.

**Table 5-2: Parameters for surface roughness after hand tool preparation.**

Parameters	Test 1	Test 2	Test 3	Test 4	Test 5	Test 6
$R_a$ (mm)	2.133	2.180	1.523	1.082	0.711	0.845
$R_q$ (mm)	2.655	2.650	1.898	1.315	0.836	1.008
$R_v$ (mm)	-10.844	-8.565	-9.900	-3.814	-3.278	-4.931
$R_p$ (mm)	10.368	11.327	7.334	5.818	3.390	4.380
$R_t$ (mm)	21.212	19.893	17.234	9.632	6.668	9.311
$R_{sk}$ (mm)	0.433	-0.099	0.013	0.424	-0.117	-0.461
$R_{ku}$ (mm)	2.744	2.474	3.441	2.660	2.498	3.079

Table 5-2 also shows a wide range of the maximum valley depth value ( $R_v$ ) that differed between -3.28 mm and -10.84 mm and the maximum peak value ( $R_p$ ) between 3.39 mm and 11.33 mm. These results indicate that for the initial surface preparation, a wide variation in smoothness was recorded, but there appears to be an improvement as the testing programme progressed. Therefore, indicates that the author became more skilled in preparing the surface prior to the tests. The results also indicate the amount of difficulty in levelling the test area consistently by the use of only hand tools.

### *Sand*

The initial surface roughness for the ‘Sand’ case was quantified for Test 2 and Test 6 after a thin layer of well-graded sand was placed on the test surface. These values were measured after the plate was placed and removed. The surface roughness parameters determined before these tests are shown in Table 5-3. The results showed very similar average roughness values ( $R_a$ ) calculated as 0.333 mm and 0.272 mm from the two ‘Sand’ tests. It further shows a very small difference between the maximum valley depth values ( $R_v$ ) and the maximum peak values ( $R_p$ ) from the two ‘Sand’ tests. The results show total height values ( $R_t$ ) of 2.81 mm and 2.99 mm and this indicates a much smoother surface finish than after the initial surface preparation with hand tools only.

The skewness values ( $R_{sk}$ ) for both tests was calculated as almost zero and the calculated average for the kurtosis values is 2.98. This implies that the height distribution will follow a Gaussian (normal) distribution. The results also indicate that the ‘Sand’ preparation method is much more consistent and practical compared to the ‘No interface material’ test.

**Table 5-3: Surface roughness parameters for ‘Sand’ tests.**

Parameters	Test 2	Test 6
$R_a$ (mm)	0.333	0.272
$R_q$ (mm)	0.407	0.339
$R_v$ (mm)	-1,390	-1,564
$R_p$ (mm)	1,418	1,428
$R_t$ (mm)	2,808	2,992
$R_{sk}$ (mm)	0.002	-0.067
$R_{ku}$ (mm)	2.719	3.255

*Plaster of Paris*

The initial surface roughness for the ‘Plaster of Paris’ case was quantified for Test 3 and Test 5. The surface roughness parameters which were determined before these tests are shown in Table 5-4. These values were again measured after the plate had been placed on top of a thin layer plaster of Paris and removed. The results show significant lower average roughness values ( $R_a$ ) calculated as 0.196 mm and 0.146 mm.

The maximum valley depth values ( $R_v$ ) were calculated as -0,89 mm and -1,14 mm and the maximum peak values ( $R_p$ ) as 0,73 mm and 1,0 mm. The skewness value ( $R_{sk}$ ) for both tests showed negative values that indicate that the surface is composed of mainly one plateau with shallow valleys and this is evident on close inspection of Figure 4-20(c). The valleys were probably created by folds of the plastic film used to cover the plate before placing it on the wet plaster of Paris.

**Table 5-4: Surface roughness parameters for ‘Plaster of Paris’ tests.**

Parameters	Test 3	Test 5
$R_a$ (mm)	0.196	0.146
$R_q$ (mm)	0.238	0.192
$R_v$ (mm)	-0.887	-1.138
$R_p$ (mm)	0.731	1.000
$R_t$ (mm)	1.619	2.138
$R_{sk}$ (mm)	-0.620	-0.880
$R_{ku}$ (mm)	3.786	4.998

The kurtosis values of 3.786 mm and 4.998 mm are larger than 3 which indicate a sharper surface height distribution compared with what is considered a normal distribution. These results have also indicated that the ‘Plaster of Paris’ preparation method is more consistent than the method used in the ‘No interface material’ test.

The average values for  $R_a$ ,  $R_v$ ,  $R_p$  and  $R_t$  were calculated and compared for the three surface preparation methods. The results are presented in Table 5-5 and these show that the difference between the average roughness values  $R_a$  is roughly 78% between the ‘No interface material’ tests and ‘Sand’ tests and approximately 88% between the ‘No interface material’ tests and ‘Plaster of Paris’ tests.

**Table 5-5: Initial bedding errors for different surface preparation methods.**

Parameters	NIM*	Sand	PP*	NIM* vs Sand	DN vs PP*	Sand vs PP*
$R_a$ (mm)	1.412	0.303	0.171	78.6%	87.9%	43.4%
$R_v$ (mm)	-6.889	-1.477	-1.013	78.6%	85.3%	31.5%
$R_p$ (mm)	7.103	1.423	0.866	80.0%	87.8%	39.2%
$R_t$ (mm)	13.992	2.900	1.878	79.3%	86.6%	35.2%

Note \* NIM – No interface material; PP - Plaster of Paris

It further shows a difference in  $R_a$  values of about 43% between the ‘Sand’ and ‘Plaster of Paris’ tests. This results indicate that the ‘Plaster of Paris’ tests resulted in the smoothest surface finish for plate load tests. Similar percentages were found by comparing the other parameters for the different surface preparation methods.

Another interesting method of presenting and quantifying the surface roughness is to use bearing area curves for all data sets. As discussed in Section 4.7.1 the bearing area curve is the cumulative distribution of the surface roughness of the complete test surface. A typical bearing area curve for the ‘Plaster of Paris’ tests and ‘Sand’ tests is shown in Figure 5-1, together with a lower and upper boundary generated from the ‘No interface material’ tests. It is evident from the curves that the ‘No interface material’ preparation method resulted in a much rougher surface in comparison to the methods used in the other two preparations.

Furthermore, it shows that the ‘Plaster of Paris’ preparation method have resulted in the smoothest surface with the flattest surface topography.

### 5.2.2. Change in surface roughness

In this section the surface roughness quantified after each test will be compared with the initial surface roughness. This comparison is vital to determine whether any possible change in surface roughness occurred during each test. This will allow a judgement to be made on the bedding errors that occurred during the test. Some engineers believe that an initial load cycle of a few kilo Pascal’s (kPa) can eliminate the effect of bedding errors on the accuracy of plate load tests. This section will aim to answer this important question.

#### *No interface material*

It is important to mention that during Test 4, between cycle 2 and 3, the test had to be temporarily halted due to rain. Approximately one week was allowed for the soil to return to the initial moisture conditions in cycle 2, but it is still believed to have caused the test surface to become smoother under the load of the plate and resulted in reducing the effect of bedding errors. This is evident from the 91,6% improvement in the average roughness value and the 78,3% smaller total height value for Test 4. The results are presented in Table 5-6. The results from Test 1 shows an average roughness value ( $R_a$ ) after the test of 1.054 mm compared with 2.133 mm measured before the test. The improvement in the maximum peak height is a good indication to what degree a change in surface roughness occurred. The maximum peak height improved by only about 20% and the total height value by 32%.

**Table 5-6: Comparison of bedding errors for ‘No interface material’ tests.**

Parameters	Test 1		Improvement Percentage	Test 4		Improvement Percentage	Average Improvement
	Before	After		Before	After		
$R_a$ (mm)	2.133	1.054	50.6%	1.082	0.091	91.6%	71.1%
$R_q$ (mm)	2.655	1.333	49.8%	1.315	0.132	90.0%	69.9%
$R_v$ (mm)	-10.844	-6.169	43.1%	-3.814	-0.528	86.1%	64.6%
$R_p$ (mm)	10.368	8.179	21.1%	5.818	1.559	73.2%	47.2%
$R_t$ (mm)	21.212	14.349	32.4%	9.632	2.088	78.3%	55.3%

Both Test 1 and 4 showed a reduction in average roughness of about 1 mm during the tests. If this is viewed in the context of the typical pressure-displacement curves shown in Figure 5-8, it is clear that a 1 mm error in plate settlement measurements will have a significant effect on the stiffness calculated from this curve.

The bearing area curves for Test 1 are shown in Figure 5-2. The 50.6% improvement in surface roughness is graphically visible as well as the reduction in the  $R_v$ ,  $R_p$  and  $R_t$  values. However, it must be noted here that the average roughness value after Test 1 ( $R_a=1.054$ ) is still approximately 3 times larger when compared with the average  $R_a$  values of 0.303 and 0.171 measured before the ‘sand’ and ‘Plaster of Paris’ tests, respectively. These results supported the conclusion that initial cycle loading will not eliminate bedding errors significantly. Figure 5-3 shows the surface roughness profiles before and after test 1. These graphs present all twelve lines that were scanned for each test surface. It is also evident in Figure 5-3 that an observable amount of bedding errors was still present after the full 628 kPa load cycle was applied to the surface.

### *Sand*

The results from Test 2 shows an average roughness value ( $R_a$ ) after the test of 0.227 mm compared with 0.333 mm measured before the tests. However, the  $R_a$  value for Test 6 actually increased by 4.5%. It is evident that the surface roughness does not change significantly during the test if sand is used as the interface material. The  $R_v$ ,  $R_p$  and  $R_t$  values also did not change in a constant manner with positive and negative changes being evident from Table 5-7.

**Table 5-7: Comparison of bedding errors for ‘Sand’ tests.**

Parameters	Test 2		Improvement Percentage	Test 6		Improvement Percentage	Average Improvement
	Before	After		Before	After		
$R_a$ (mm)	0.333	0.227	31.7%	0.272	0.285	-4.5%	13.6%
$R_q$ (mm)	0.4065	0.2964	27.1%	0.339	0.361	-6.5%	10.3%
$R_v$ (mm)	-1.390	-1.287	7.4%	-1.564	-1.751	-11.9%	-2.2%
$R_p$ (mm)	1.418	1.443	-1.8%	1.428	1.840	-28.8%	-15.3%
$R_t$ (mm)	2.808	2.730	2.8%	2.992	3.591	-20.0%	-8.6%

The bearing area curves for Test 2 are shown in Figure 5-4. This figure exhibits a slight flattening of the surface roughness during the test, but the most striking feature is that the surface was already flat before the test was conducted. Figure 5-5 shows the surface roughness profiles before and after Test 2. The imprint of the 450 mm plate, visible in the sand after the test, creates some concern about the amount of plate settlement that may be due to the compression in the thin sand layer which may lead to unrealistic external stiffness values.

### *Plaster of Paris*

The results from Test 3 shows an average roughness value ( $R_a$ ) of 0.068 mm after the test compared with 0.196 mm measured before the tests and results in a 65% improvement (See Table 5-8). Similarly for Test 5, the  $R_a$  value of 0.146 mm which was calculated before the test improved to 0.109 mm. With an average improvement in  $R_a$  value of about 45%, it is evident that the surface roughness improved for the ‘Plaster of Paris’ tests. The results further show that the maximum peak values ( $R_p$ ) for both tests was reduced significantly.

**Table 5-8: Comparison of bedding errors for ‘Plaster of Paris’ tests.**

Parameters	Test 3		Improvement Percentage	Test 5		Improvement Percentage	Average Improvement
	Before	After		Before	After		
$R_a$ (mm)	0.196	0.068	65.2%	0.146	0.109	25.0%	45.1%
$R_q$ (mm)	0.238	0.088	62.9%	0.192	0.157	18.1%	40.5%
$R_v$ (mm)	-0.887	-0.606	31.7%	-1.138	-1.788	-57.1%	-12.7%
$R_p$ (mm)	0.731	0.276	62.2%	1.000	0.723	27.7%	44.9%
$R_t$ (mm)	1.619	0.883	45.5%	2.138	2.511	-17.5%	14.0%

The bearing area curves for Test 3 are shown in Figure 5-6. The 65.2% improvement in average roughness ( $R_a$ ) is graphically visible as well as the reduction in the  $R_v$ ,  $R_p$  and  $R_t$  values. Figure 5-7 presents the surface roughness profiles before and after Test 3 and it is evident that the surface was very smooth prior to the test. The imprint of the 450 mm plate remains visible in the plaster of Paris before and after the test. The imprint before the test was due to the procedure of the first placing of the plate on the wet plaster of Paris, removing it, scanning the surface and then replacing it. The results further support the conclusion that plaster of Paris is the most effective surface preparation method for creating the smoothest surface for plate load tests.

### 5.3. PRESSURE-DISPLACEMENT RELATIONSHIPS

Three load cycles were applied for all six tests to enable the comparisons between these different tests. The three cycles were comprised of an initial 8 kN load that resulted in about 50 kPa contact pressure; a second cycle of about 25 kN calculated as 150 kPa contact pressure and a last load cycle of roughly 100 kN (628 kPa), or in some cases until ultimate bearing capacity was reached. As has been discussed in previous chapters, these readings from the load cell together with all four displacement measure devices were recorded simultaneously and continuously at 10 Hz (10 readings per second).

#### 5.3.1. External measurements

A typical pressure-displacement curve generated with the conventional plate settlements is shown in Figure 5-8. The permanent displacement after each cycle is evident in the pressure-displacement curve.

The total loads in each cycle were kept constant until the rate of plate displacement was less than 0,030 mm/minute for three consecutive minutes. The creep that occurred during these periods for cycle 2 and 3 is evident in Figure 5-8. This further indicates that the ultimate bearing capacity was possibly reached at 628 kPa in this particular result.

Table 5-9 shows the external displacements that were measured during the three load cycles. The total displacement measured for each load cycle was separated into two portions and this included the displacement measured until the total load was reached and the creep measured while the total load was kept constant.

The results show that the maximum displacements were measured for the 'No interface material' tests (Test 1 and 4). The displacements that have been measured during the two 'Sand' tests (11,432 mm and 12,538 mm) are smaller when compared to the 'No interface material' tests. The results have further demonstrated that the displacements for the 'Plaster of Paris' tests (Test 3 and 5) are the smallest with only about 4,2 mm occurring during Test 5. These results have corresponded well with the findings which were reflected during the quantification of surface roughness in the previous section.

**Table 5-9: External displacement for all tests.**

Description	External displacement measurements (mm)					
	Test 1	Test 2	Test 3	Test 4	Test 5	Test 6
Displacement after cycle 1	0.504	0.337	0.217	0.976	0.442	0.380
Creep after load cycle 1	0.092	0.029	0.034	0.030	0.009	0.041
Displacement after cycle 2	3.657	1.203	0.864	2.950	0.730	1.787
Creep after load cycle 2	0.206	0.078	0.125	0.150	0.070	0.429
Displacement after cycle 3	14.436	10.764	5.562	12.523	3.262	11.432
Creep after load cycle 3	3.114	1.774	1.041	2.016	0.864	0.000
Total displacement	17.550	12.538	6.603	14.539	4.126	11.432

No interface material tests

Sand tests

Plaster of Paris tests

### 5.3.2. Internal measurements

Figure 5-9 shows a typical pressure-displacement curve which is generated with the relative displacement that is measured by the telescopic probes and the contact pressures. The permanent displacement after each cycle is again evident here.

Table 5-10 explains the internal displacements which were measured during the three load cycles as well as the creep measured while the total loads were being kept constant as described above. The results revealed that the total internal displacements ranged between 4,04 mm and 6,55 mm for the ‘No interface material’ and ‘Sand’ tests. However, the ‘Plaster of Paris’ tests again showed smaller displacements compared to the other two surface preparation methods. These results also show that the different surface preparation methods have a lesser effect on the displacements measured with the telescopic probes.

**Table 5-10: Internal displacement for all tests.**

Description	Internal displacement measurements (mm)					
	Test 1	Test 2	Test 3	Test 4	Test 5	Test 6
Displacement after cycle 1	0.143	0.036	0.048	0.053	0.040	0.070
Creep after load cycle 1	0.168	0.004	0.011	0.009	0.003	0.011
Displacement after cycle 2	0.795	0.213	0.231	0.187	0.115	0.438
Creep after load cycle 2	0.910	0.007	0.034	0.030	0.030	0.133
Displacement after cycle 3	6.400	4.412	2.272	3.800	1.155	4.048
Creep after load cycle 3	0.150	0.898	0.520	1.000	0.387	0.000
Total displacement	6.550	5.310	2.792	4.800	1.542	4.048

No interface material tests
  Sand tests
  Plaster of Paris tests

### 5.3.3. $E_{50}$ stiffness values

A common stiffness parameter used to give a quick and first order stiffness value from the pressure-displacement curves is known as the  $E_{50}$  stiffness. The  $E_{50}$  stiffness represents the secant stiffness at 50% of the pressure at failure of the soil. For the tests where soil failure had not been reached, the secant stiffness at 50% of the maximum contact pressure was taken as the estimated  $E_{50}$  values. Figure 5-10 shows a comparison between the pressure-displacement curves which were generated from the external displacement measurements and the estimated  $E_{50}$  stiffness values are also presented graphically here. A comparison between the pressure-displacement curves generated from the internal displacement measurements are shown in Figure 5-11, together with the  $E_{50}$  stiffness values. Table 5-11 shows the  $E_{50}$  external and internal stiffness values for all tests and the corresponding axial strain levels.

**Table 5-11:  $E_{50}$  stiffness values for all tests (Cycle 3).**

Test	$E_{50}$ External (MPa)	Axial Strain (%)	$E_{50}$ Internal (MPa)	Axial Strain (%)	$\frac{E_{50} \text{ External}}{E_{50} \text{ Internal}}$
T1 (No interface material)	26	0.37	36	0.36	71.4%
T2 (Sand)	45	0.32	75	0.27	60.1%
T3 (Plaster of Paris)	61	0.23	92	0.22	67.1%
T4 (No interface material)	48	0.30	104	0.20	46.7%
T5 (Plaster of Paris)	107	0.13	174	0.12	61.4%
T6 (Sand)	42	0.21	69	0.17	61.1%

The results show a similar trend between the external and internal pressure-displacement curves as well as the  $E_{50}$  stiffness values presented in Table 5-11. The axial strain levels are similar for the  $E_{50}$  external and internal stiffness values, except for Test 4 ('No interface material'). Table 5-11 also demonstrates the comparison between the  $E_{50}$  external and the  $E_{50}$  internal stiffness values and illustrates that the  $E_{50}$  internal values were larger with about 60% to 71% in comparison with the  $E_{50}$  external values. In addition, these results support the statement that more accurate stiffness may be determined by using telescopic probes in plate load tests.

#### **5.4. PERFORMANCE OF A CONVENTIONAL PLATE LOAD TEST**

This section will discuss the performance of the conventional plate load test when only the plate settlements have been measured during loading. All stiffness values calculated for this research project were compared with the stiffness degradation curve proposed by Clayton and Heymann (2001). Continuous surface wave (CSW) tests were performed in order to determine the small strain stiffness ( $E_0$ ), required to generate a Clayton-Heymann stiffness degradation curve. The CSW test results showed small strain stiffness ( $E_0$ ) values of 250 MPa.

##### **5.4.1. External stiffness comparison**

In order to compare the results that represent the three surface preparation methods being assessed, it was decided that Test 2, 3 and 4 would be contrasted to highlight these findings. The external stiffness's for the three cycles at different strain levels are shown in Figure 5-12 to Figure 5-14.

Figure 5-12 shows the external stiffness values for all three preparation methods recorded during the first 50 kPa cycle. The results reveal that the 'Plaster of Paris' and 'Sand' tests provide much higher values compared to the values where the surface was levelled by hand ('No interface material' test). Although the 'Plaster of Paris' test shows the highest stiffness values, it was still 50% less when compared to the stiffness degradation curve of the expected results. This presents an important insight into the effectiveness of conventional plate load tests.

Figure 5-13 demonstrates the external stiffness values for the second cycle (150 kPa). These results reveal that the ‘Plaster of Paris’ and ‘Sand’ tests still produce much higher values when compared to the values reported where the surface was only levelled by hand (‘No interface material’ test). Figure 5-14 shows the results where the last cycle (628 kPa) of each tests were plotted and compared. An interesting observation here is that the ‘Sand’ and the ‘No interface material’ tests reveal very similar stiffness values, while the ‘Plaster of Paris’ test still provides evidence for about 20% higher stiffness values in comparison. The results in Figure 5-14 further shows that the ‘Plaster of Paris’ test corresponds well with the lower boundary of the Clayton-Heymann degradation curve above 0.08% axial strain.

All external stiffness values at different axial strain levels are shown in Table 5-12. It is obvious from these results that the ‘Plaster of Paris’ test has significantly higher stiffness values in all three cycles. It is also important to notice that the stiffness values, which were assessed in the last cycle, for all tests are higher compared to the first two cycles.

**Table 5-12: External stiffness values.**

Axial Strain %	External stiffness for 'No interface material' test (MPa)			External stiffness for 'Sand' test (MPa)			External stiffness for 'Plaster of Paris' test (MPa)		
	Cycle 1	Cycle 2	Cycle 3	Cycle 1	Cycle 2	Cycle 3	Cycle 1	Cycle 2	Cycle 3
0.005	39	32	95	86	84	95	105	107	130
0.01	28	25	89	70	82	87	82	100	117
0.05	/	15.3	76	/	63	81	/	74	101
0.1	/	14.9	80	/	49	77	/	59	92
0.5	/	/	36	/	/	36	/	/	46
1.0	/	/	25	/	/	25	/	/	31

## 5.5. PERFORMANCE OF A MODIFIED PLATE LOAD TEST

The performance of the modified plate load test designed for this research project will be discussed in this section. The internal stiffness values determined with the in-situ displacement measurements are compared between the different surface preparation methods. The internal stiffness values are also contrasted with CSW results in order to evaluate the effectiveness of the telescopic probes. Furthermore, the internal stiffness values are compared with the external stiffness values to evaluate the effectiveness of the conventional plate load test.

### 5.5.1. Internal stiffness comparison

It was important to investigate the effect of different surface preparation methods on the internal stiffness values and the expectation was that since bedding errors are avoided with the modified plate load test, the internal stiffness would as a result yield similar values. This effect was investigated by comparing the internal stiffness values that were determined from the three load cycles at different strain levels. The results are presented in Figure 5-15 to Figure 5-17 and all internal stiffness values at different axial strain levels are shown in Table 5-13.

**Table 5-13: Internal stiffness values.**

Axial Strain %	Internal stiffness for 'No interface material' test (%)			Internal stiffness for 'Sand' test (%)			Internal stiffness for 'Plaster of Paris' test (%)		
	Cycle 1	Cycle 2	Cycle 3	Cycle 1	Cycle 2	Cycle 3	Cycle 1	Cycle 2	Cycle 3
0.005	80	153	195	181	172	168	137	146	161
0.01	65	148	158	141	153	147	110	134	144
0.05	/	111	149	/	92	111	/	92	118
0.1	/	85	105	/	71	87	/	65	98
0.5	/	/	39	/	/	37	/	/	43
1.0	/	/	24	/	/	24	/	/	28

Figure 5-15 shows the internal stiffness values for all three surface preparation methods which have been measured during the first load cycle. The results show that the internal stiffness values responded quite differently to each of the three preparation methods and did not produce the expected similar results. The 'Sand' test produced the highest stiffness values as shown in Table 5-13 and this compared fairly well with the Clayton-Heymann degradation curve.

The internal stiffness values for the second load cycle are revealed in Figure 5-16. The results show very similar stiffness values between 0.005% and 0.1% strain for all tests as shown in Table 5-13. However, the internal stiffness values were slightly lower when compared to the stiffness degradation curve.

Figure 5-17 shows that all three tests produced similar internal stiffness values for the entire strain range. This is evident in the results shown in Table 5-13. This also corresponds well

with the Clayton-Heymann stiffness degradation curve for most of the strain levels. The small strain stiffness ( $E_0$ ), determined with the CSW results, compare well with the internal stiffness at 0.001% to 0.002% axial strain in all tests. For the last two cycles, similar internal stiffness values were recorded in all three test results. These results prove that bedding errors were successfully eliminated by means of multi-depth measurements with the telescopic probes. It further proves that telescopic probes can be used to accurately measure the full strain range with plate load tests.

An important factor note here is that the stiffness values determined in the last cycle for all tests were again higher compared to the first two cycles, which was the same result found for the external stiffness values. It is evident that strain hardening of the soil took place during all tests during the last load cycle.

#### 5.5.2. Comparison between external en internal stiffness

The external and internal stiffness at different strain levels calculated from all three cycles was also plotted and compared. In order to understand the soil behaviour during the whole test and to be able to determine whether the bedding errors were reduced, the external stiffness for all three cycles had to be compared with the internal stiffness. Table 5-14 indicates this relationship between external and internal stiffness for the different surface preparation methods.

Figure 5-18 shows the comparison between the measured external and internal stiffness for the 'No interface material' test. It is clear from Figure 5-18 that the stiffness determined with the telescopic probes showed higher values when compared to the external stiffness with up to 1.0% axial strain. This can also be observed in Table 5-14, where the external stiffness is on average 50% of that of the internal stiffness values at up to 0.1% axial strain.

The comparison between the measured external and internal stiffness for the full strain range of the 'Sand' test is shown in Figure 5-19. The stiffness results from the telescopic probes showed between 30 per cent and 40 per cent higher stiffness values from that of the external values up to 0.05% strain. Both these stiffness curves compare well with the lower boundary of the Clayton-Heymann curve above 0.1% axial strain.

**Table 5-14: Comparison between external and internal stiffness values.**

Axial Strain (%)	External vs. Internal stiffness for 'No interface material' test			External vs. Internal stiffness for 'Sand' test			External vs. Internal stiffness for 'Plaster of Paris' test		
	Cycle 1	Cycle 2	Cycle 3	Cycle 1	Cycle 2	Cycle 3	Cycle 1	Cycle 2	Cycle 3
0.005	49%	21%	49%	48%	49%	56%	77%	73%	81%
0.01	43%	17%	56%	50%	54%	59%	75%	74%	81%
0.05	/	14%	51%	/	69%	73%	/	80%	86%
0.1	/	18%	76%	/	70%	89%	/	91%	94%
0.5	/	/	93%	/	/	97%	/	/	107%
1.0	/	/	103%	/	/	103%	/	/	110%

Figure 5-20 shows the comparison between the measured external and internal stiffness for the full strain range of the 'Plaster of Paris' test. This reveals that the stiffness determined with the telescopic probes again showed higher values than those taken from the external measurements, but these values are within 20% of the internal stiffness values. Table 5-14 further reveals that the external stiffness values measured in the 'Plaster of Paris' test are plotted much closer to the internal stiffness values mainly between 0.1% and 1.0% strain. These results show that poor surface preparation for plate load tests does result in low soil stiffness values.

It is evident from Figure 5-12 to Figure 5-14 and Table 5-12 that the external stiffness values for all tests were higher during the last cycle compared with the first two cycles. This raises the question whether this increase in stiffness values can be caused by a decrease in bedding errors. However, this cannot be true for the following reasons:

- i) The same trend was observed with the internal stiffness values (see table 5-13) where the telescopic probes are not influenced by bedding errors; and
- ii) The test surface that was scanned after the tests revealed that after more than 600 kPa pressure was applied to the soil, the significant surface roughness was still present.

## 5.6. LIMITATIONS OF DATA

An important step is to evaluate the results from each test in order to determine any limitations which are evident from the data. During the experimental study it was realised that endurance and perseverance were important factors in making it possible to finish all tests in time. In this section the limitations of data are briefly discussed.

### 5.6.1. Cycle 1

The external and internal stiffness values from the first load cycle of each test are provided in Figure 5-21a and Figure 5-21d, respectively.

#### *External stiffness*

For Test 1 ('No interface material') a steel reference beam was used and this resulted in extensive movements of the DCDTs due to the effect of different temperatures and for this reason the external stiffness readings from Test 1 were only partly useable. It was decided to replace this steel reference beam with two 3,0 m long wooden beams for the remaining five tests. The temperature effects with the wooden reference beams have proved negligibly small and Test 2 to Test 6 produced useful external stiffness measurements, which could be used to compare with various other stiffness readings.

#### *Internal stiffness*

The steel reference beam used in Test 1 had no effect on the internal stiffness readings and produced useful measurements. Test 2, 3 and 4 also produced useful results, which were compared in previous sections. Unfortunately, the telescopic probes did not respond favourably during load cycle 1 of Test 5 and 6. Therefore, it is evident from Figure 5-21d that the results from Test 5 and Test 6 were only partly useable.

### 5.6.2. Cycle 2

The external and internal stiffness values from the second load cycle of each test are shown in Figure 5-21b and Figure 5-21e, respectively.

### *External stiffness*

Unfortunately, the temperature effect of the steel beam in Test 1 was still evident and this limited the results for cycle 2. The two 'Sand' tests had showed almost identical results from 0.01% axial strain. Test 3, 4 and 5 also provided useful results that could be used in the experiment.

### *Internal stiffness*

The results from Test 1 to Test 4 provide useful measurements but Test 2, 3 and 4 also demonstrate similar stiffness values from about 0.004% to roughly 0.01% axial strain. However the telescopic probes were still responding unfavourably during the load cycle 2 of Test 5 and 6. Therefore, it is obvious in Figure 5-21e that the results from Test 5 and Test 6 were only partly useable.

### 5.6.3. Cycle 3

The external and internal stiffness values from the last load cycle of each test are shown in Figure 5-21c and Figure 5-21f, respectively.

### *External stiffness*

The two 'Plaster of Paris' tests carried out provide higher stiffness values in comparison to the 'Sand' and 'No interface material' tests. As already mentioned, during Test 4 between cycle 2 and 3, the test had to be temporarily halted due to rainfall and this rain appears to have minimised the bedding errors. This phenomenon is evident in Figure 5-21c with the higher stiffness values observed for Test 4. Furthermore it is believed that for Test 1 from 0.05% axial strain the measured stiffness values were no longer affected by temperature effects and therefore were used for comparison with the other results.

### *Internal stiffness*

During cycle 3 the telescopic probes in Test 5 and Test 6 had started to respond properly from approximately 0.01% axial strain and has measured usable stiffness values. Figure 5-21f shows similar internal stiffness values in four of the six tests (Test 2, 3, 4 and 5).

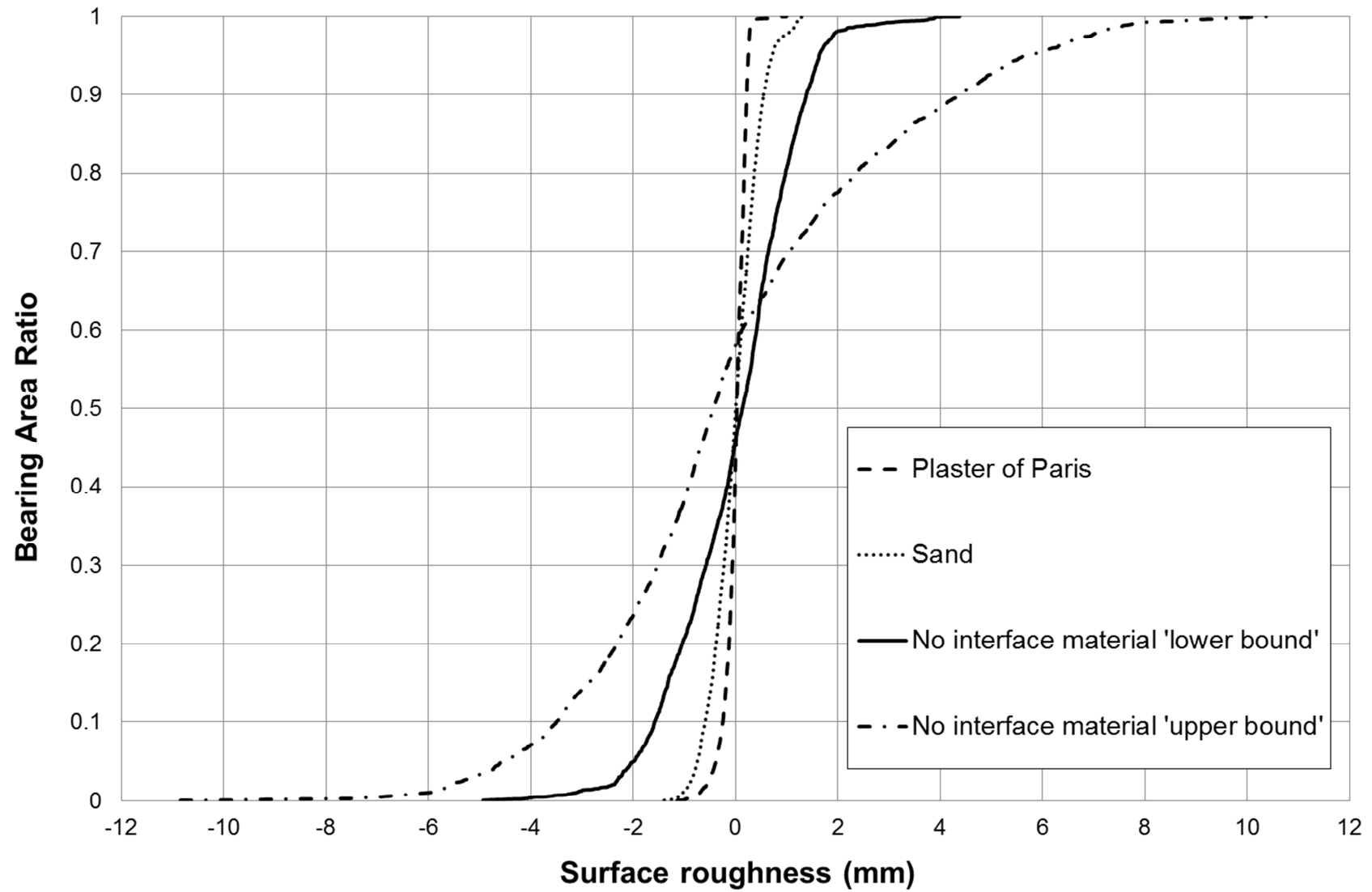


Figure 5-1: Bearing area curves for different surface preparation methods before tests.

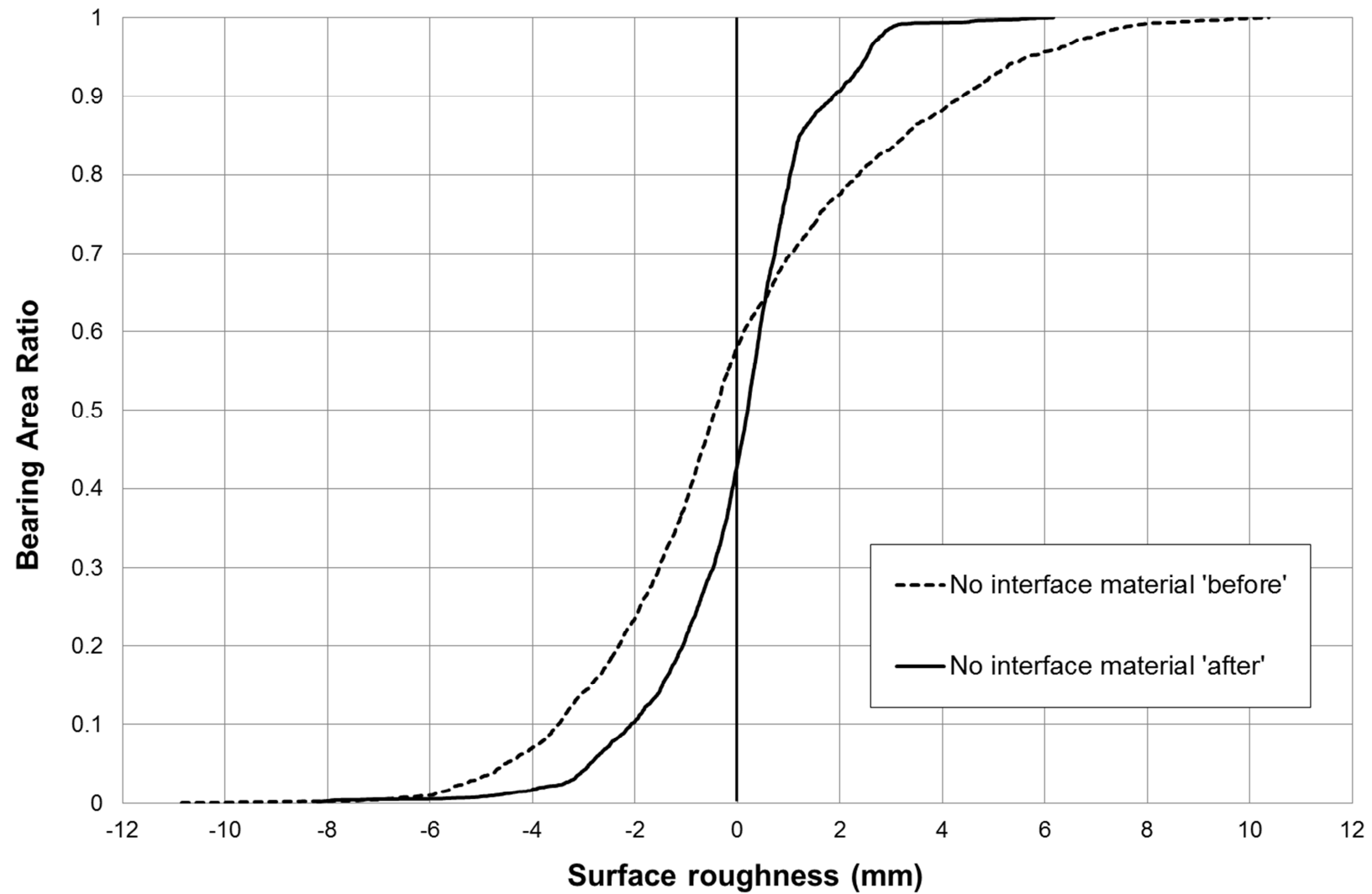


Figure 5-2: Comparison between before and after bearing area curves ('No interface material' test).

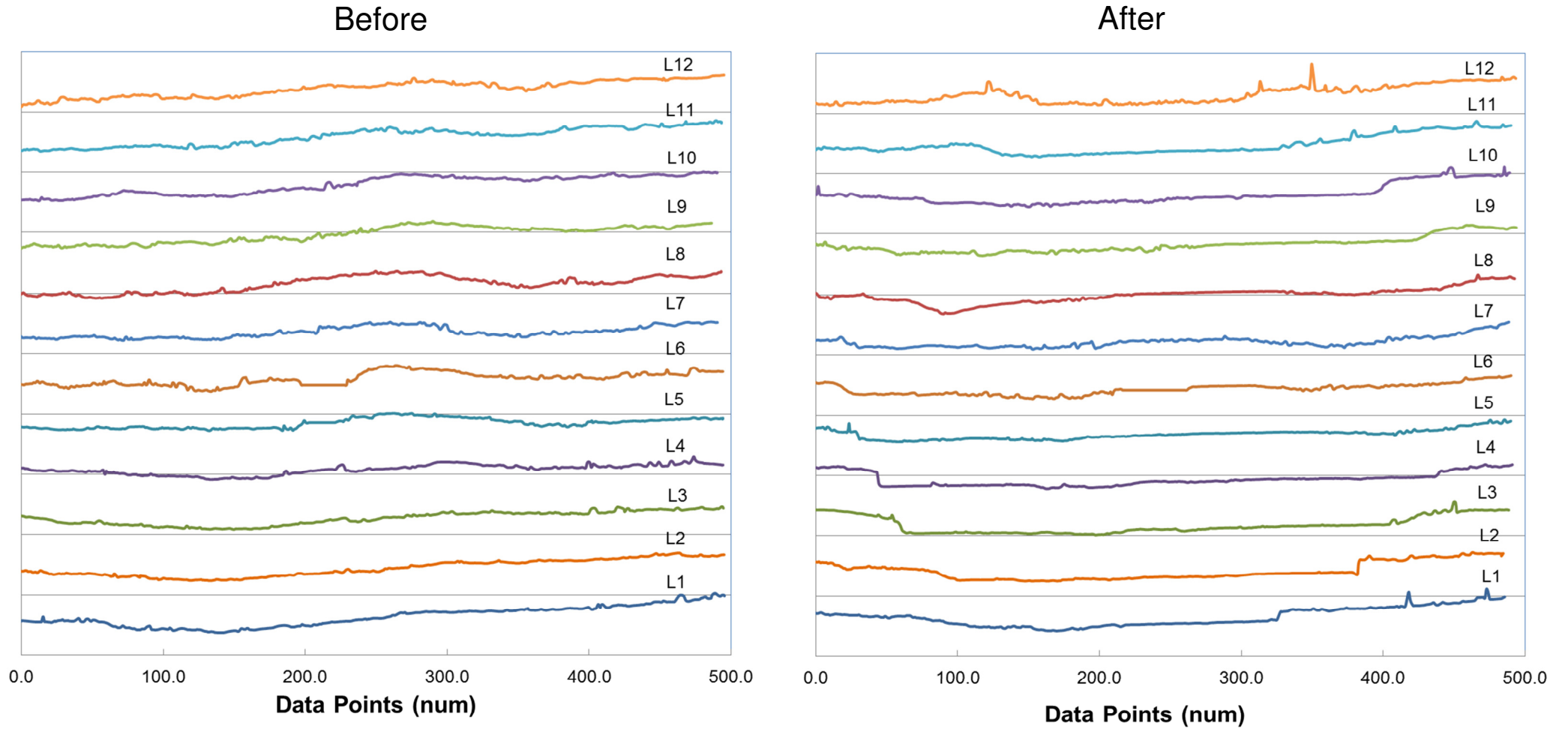


Figure 5-3: Comparison between before and after laser scans for the 'No interface material' test.

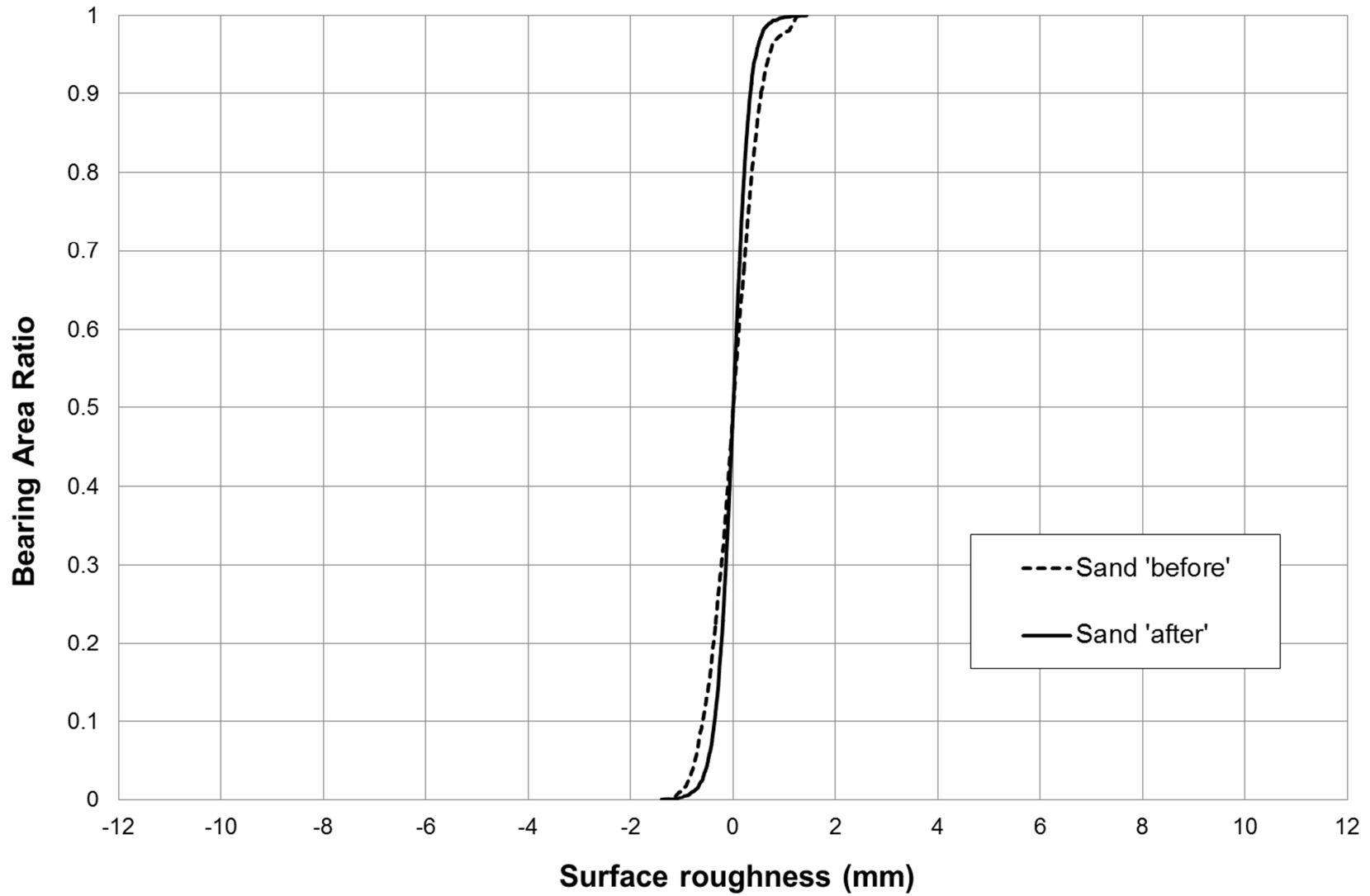


Figure 5-4: Comparison between before and after bearing area curves ('Sand' test).

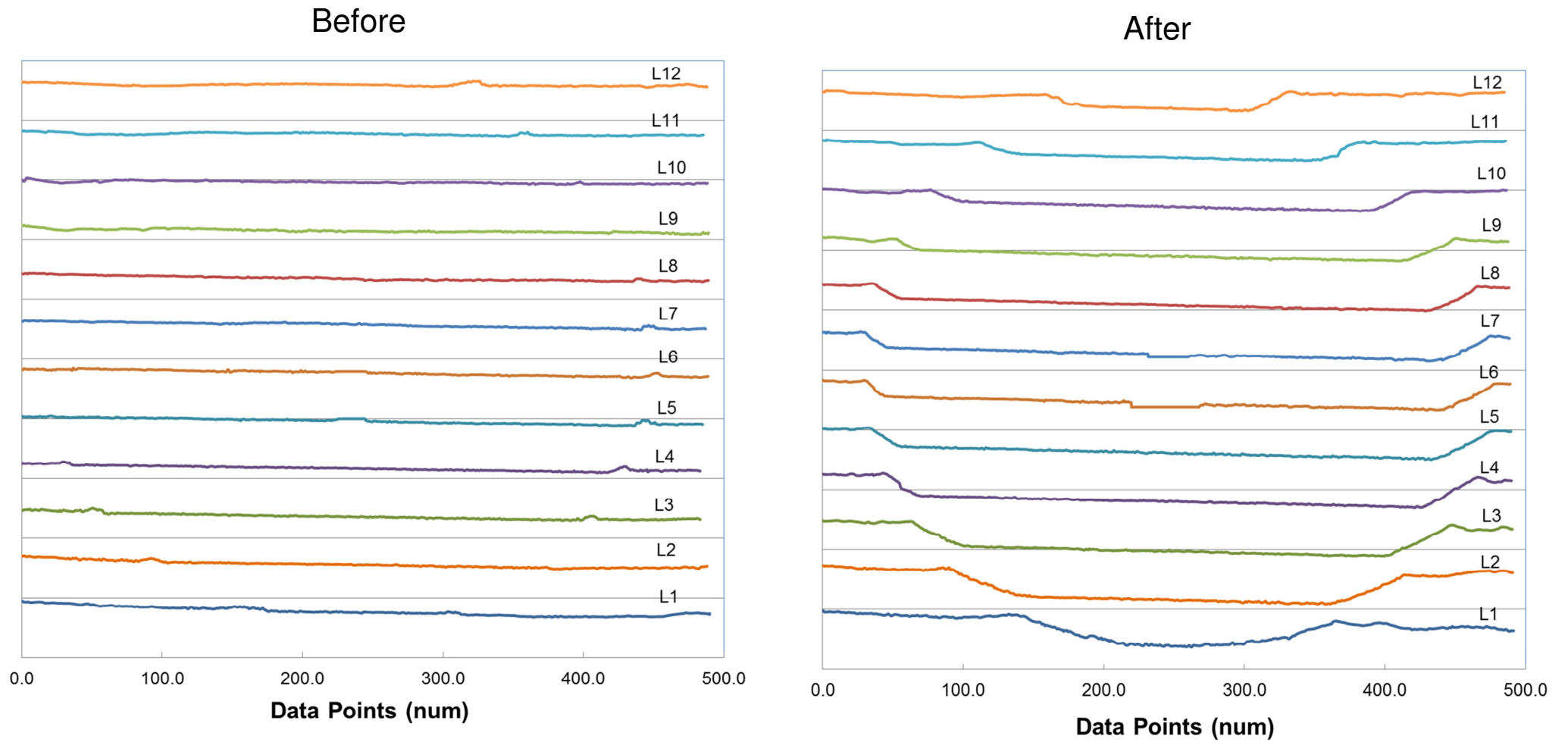


Figure 5-5: Comparison between before and after laser scans for the 'Sand' test.

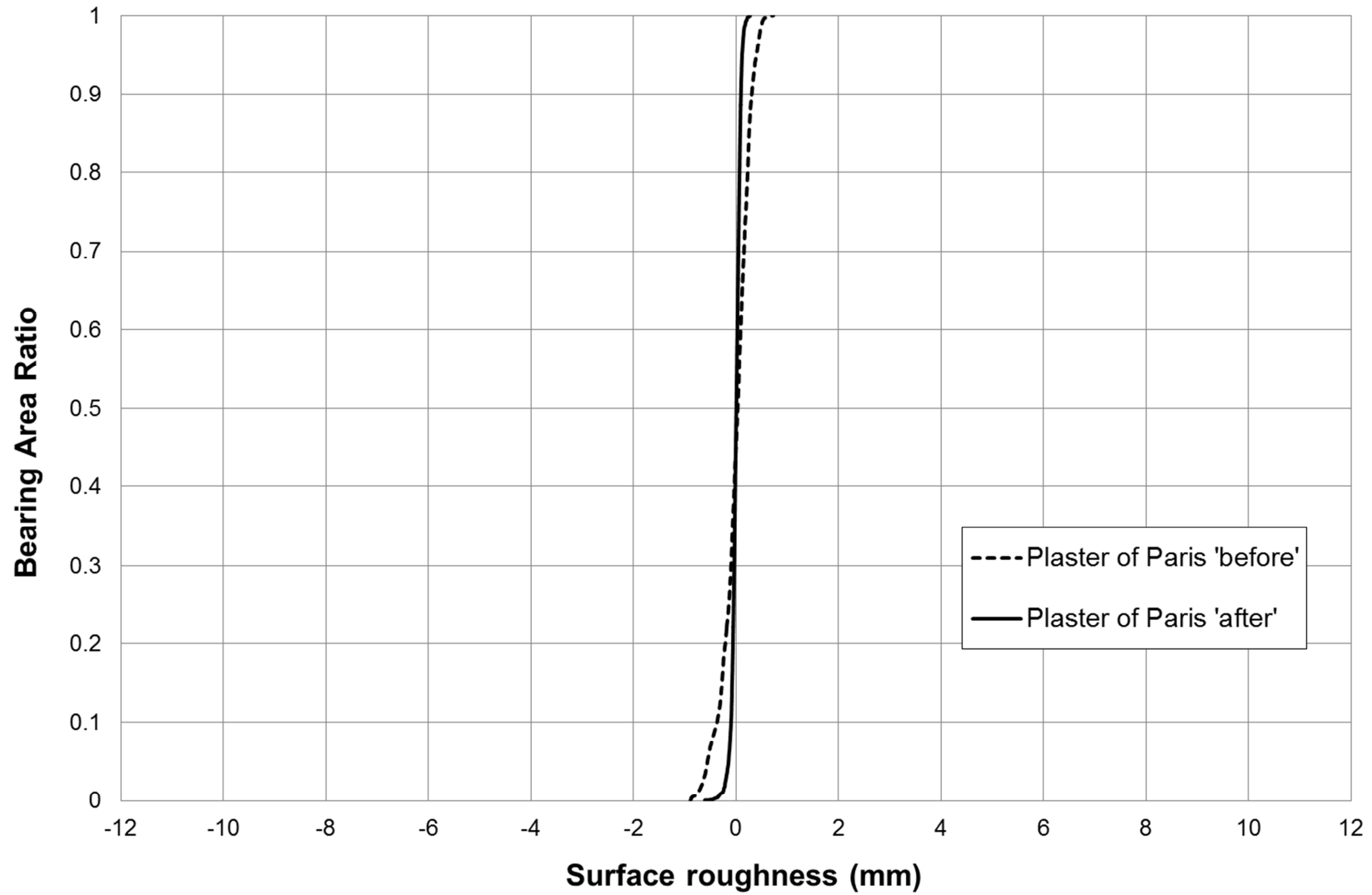


Figure 5-6: Comparison between before and after bearing area curves ('Plaster of Paris' test).

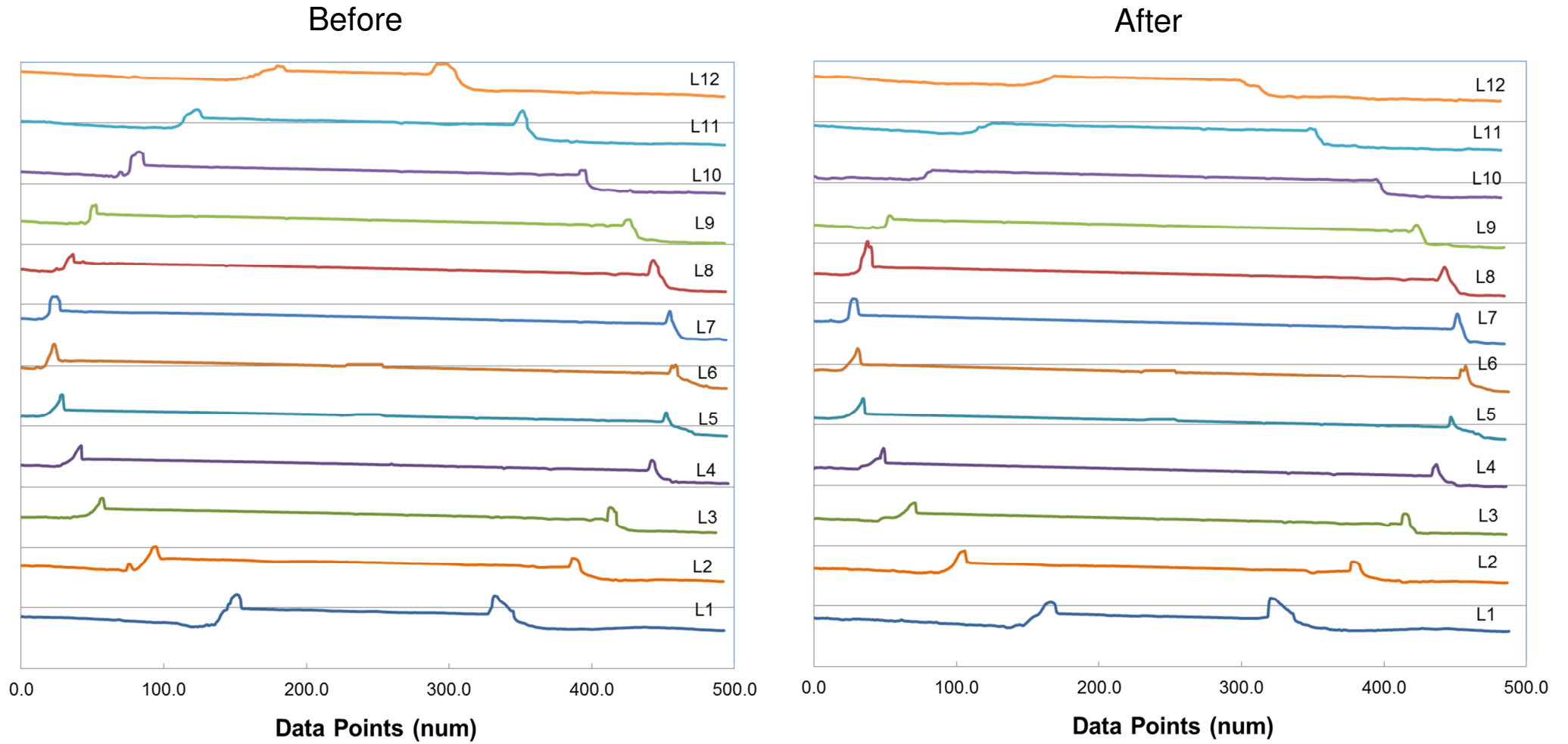


Figure 5-7: Comparison between before and after laser scans for the 'Plaster of Paris' test.

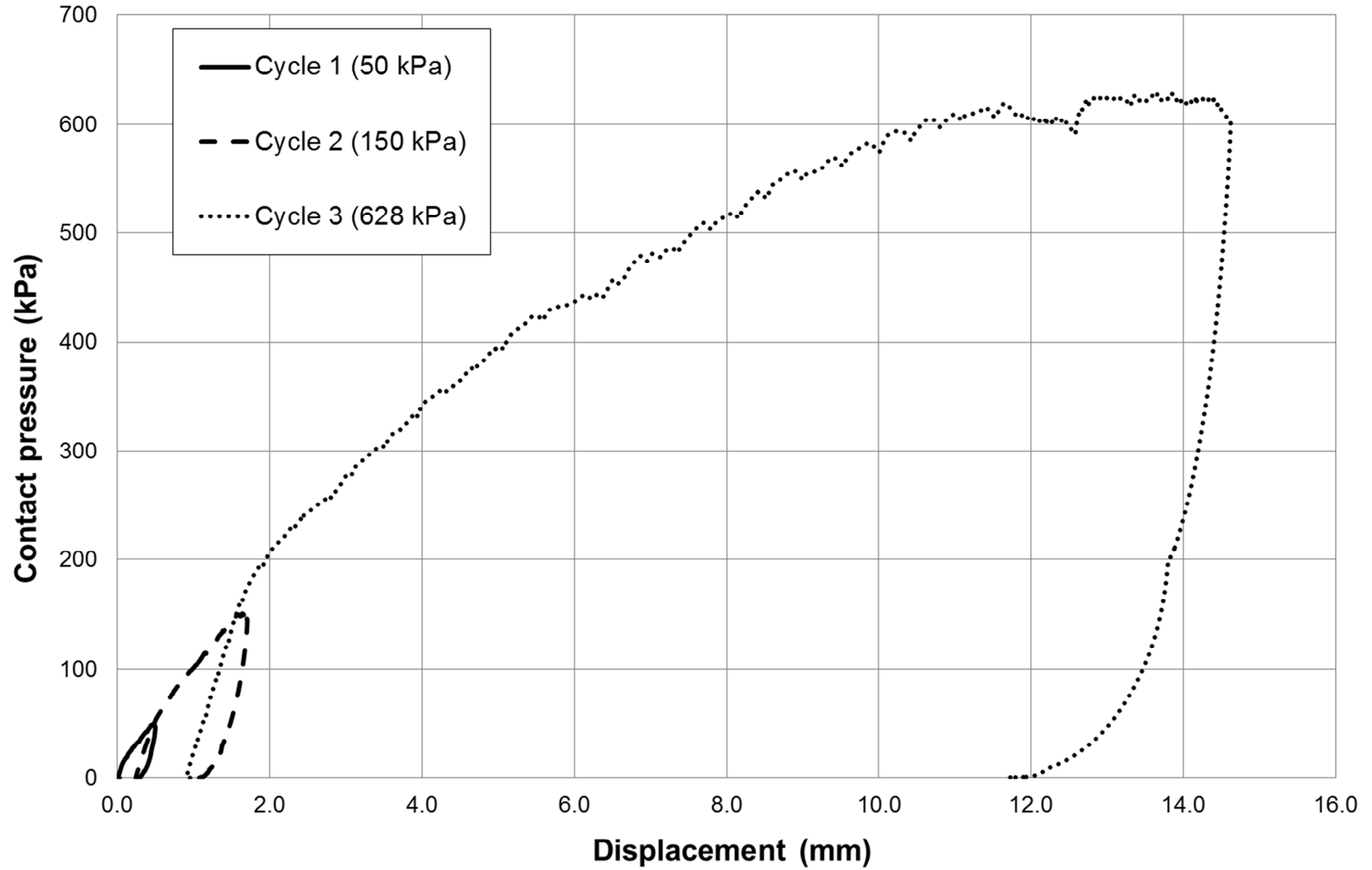


Figure 5-8: Typical external pressure-displacement curve (All cycles).

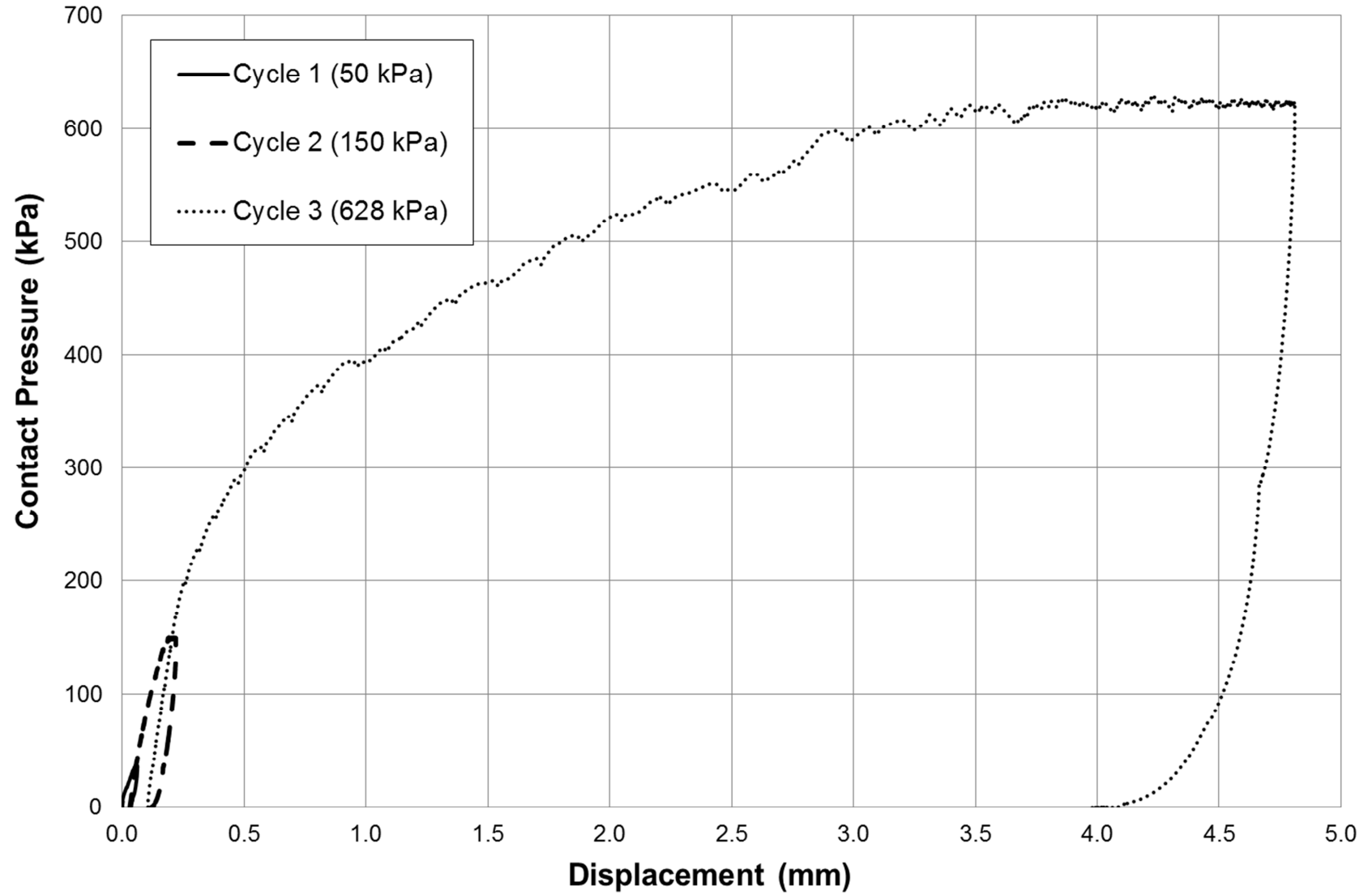


Figure 5-9: Typical internal pressure-displacement curve (All cycles).

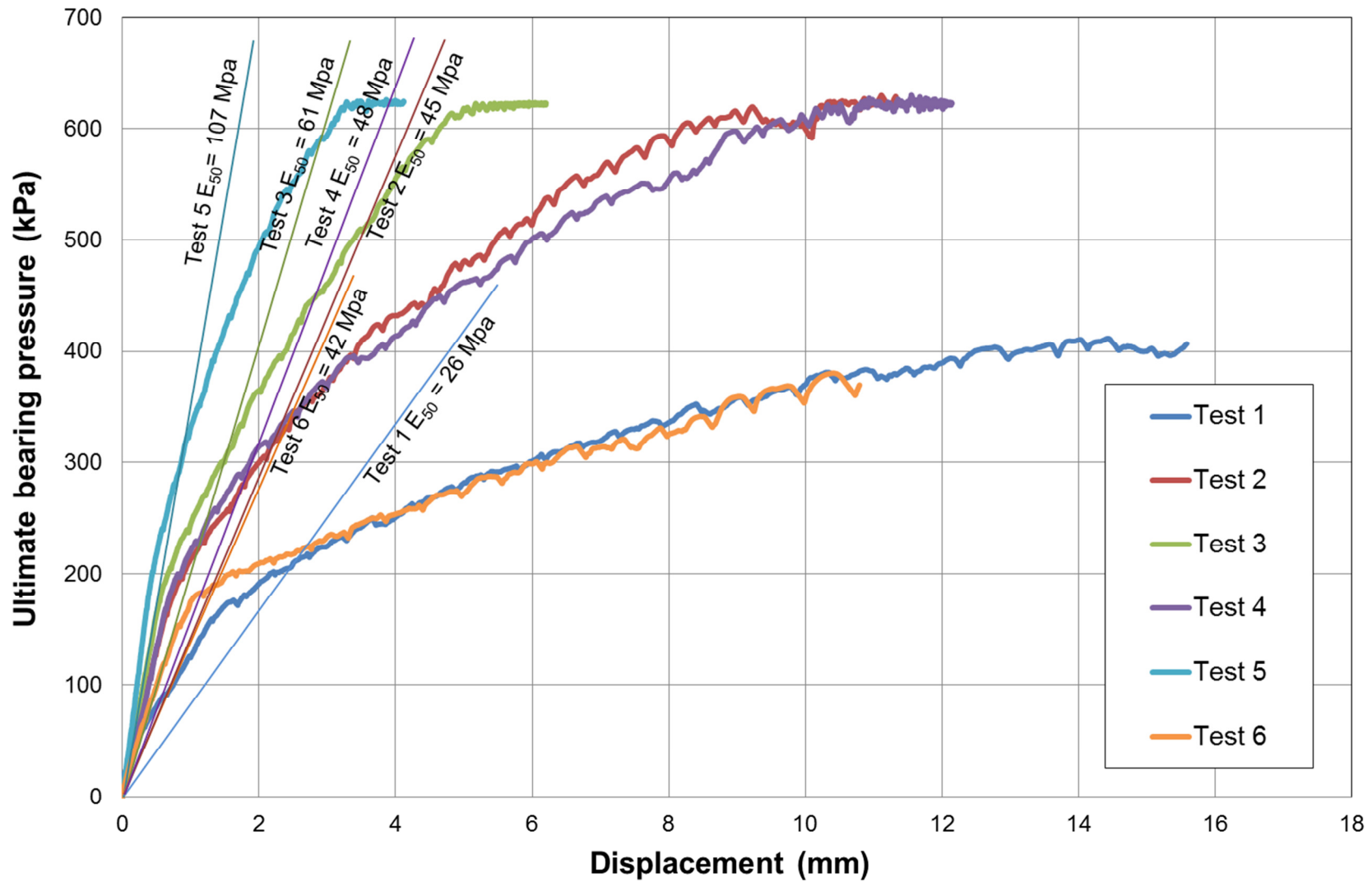


Figure 5-10: Comparison between  $E_{50}$  values from external measurements (Cycle 3).

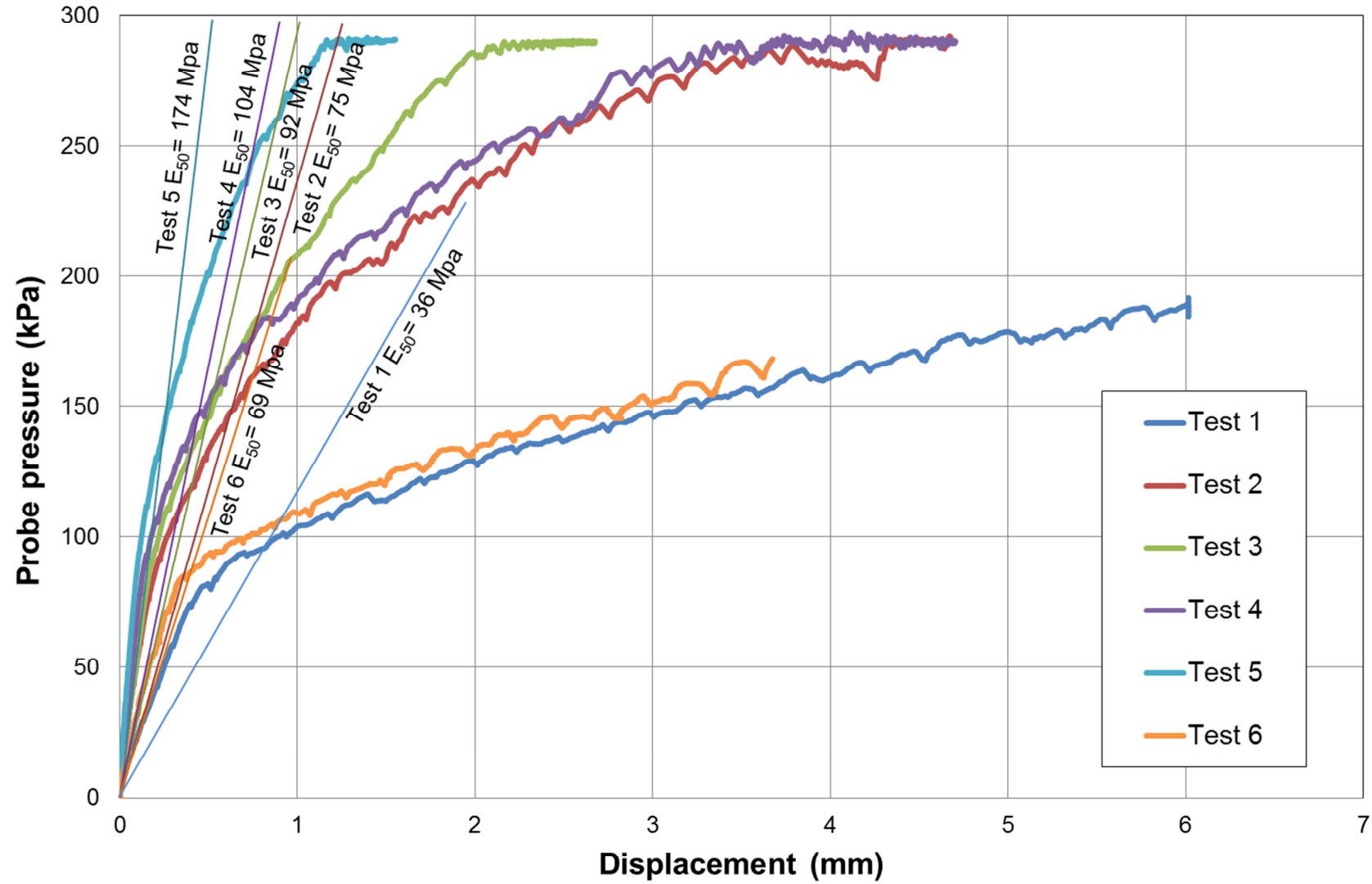


Figure 5-11: Comparison between  $E_{50}$  values from internal measurements (Cycle 3).

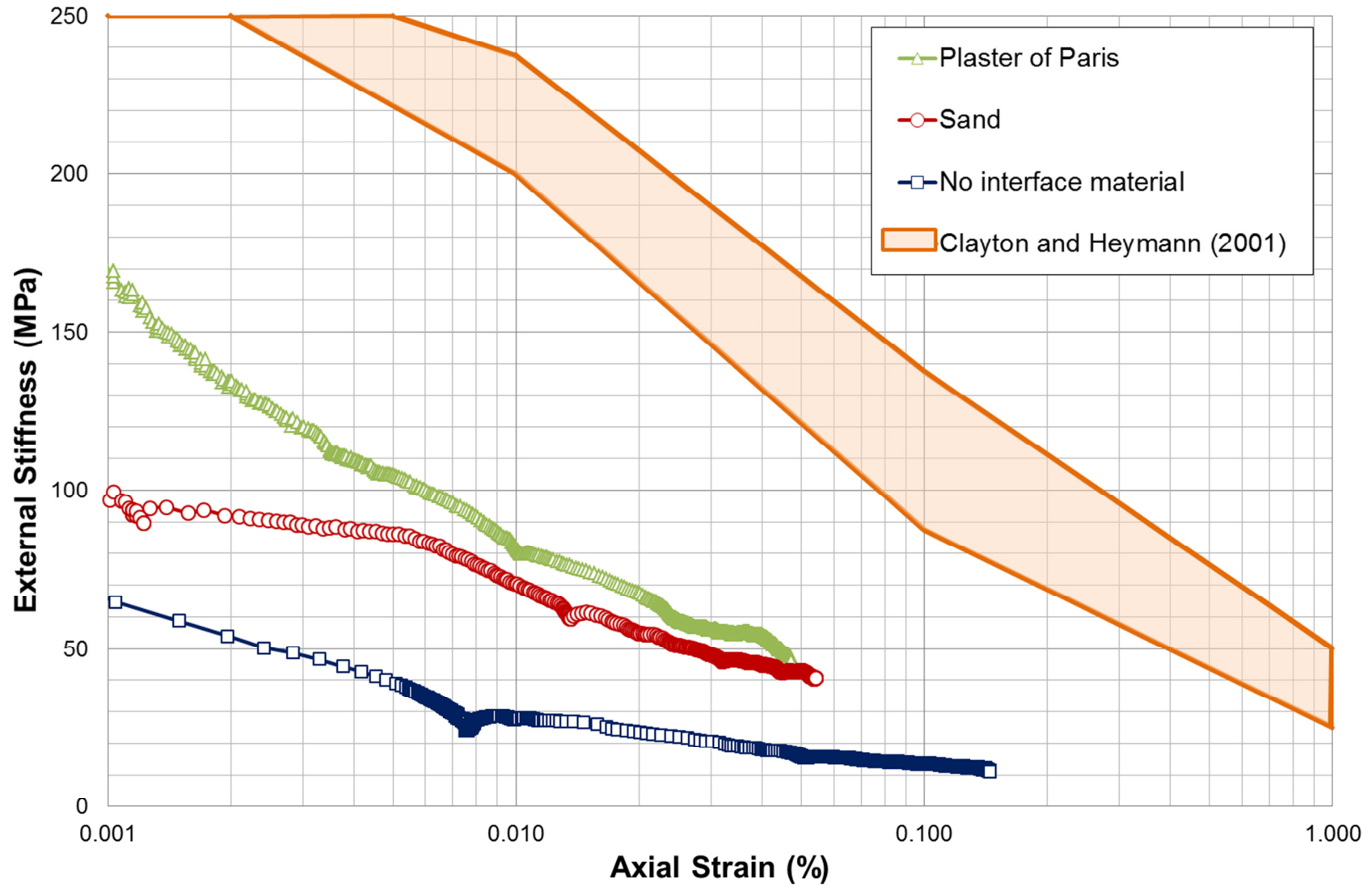


Figure 5-12: Comparison between external stiffness for different preparation methods (Cycle 1).

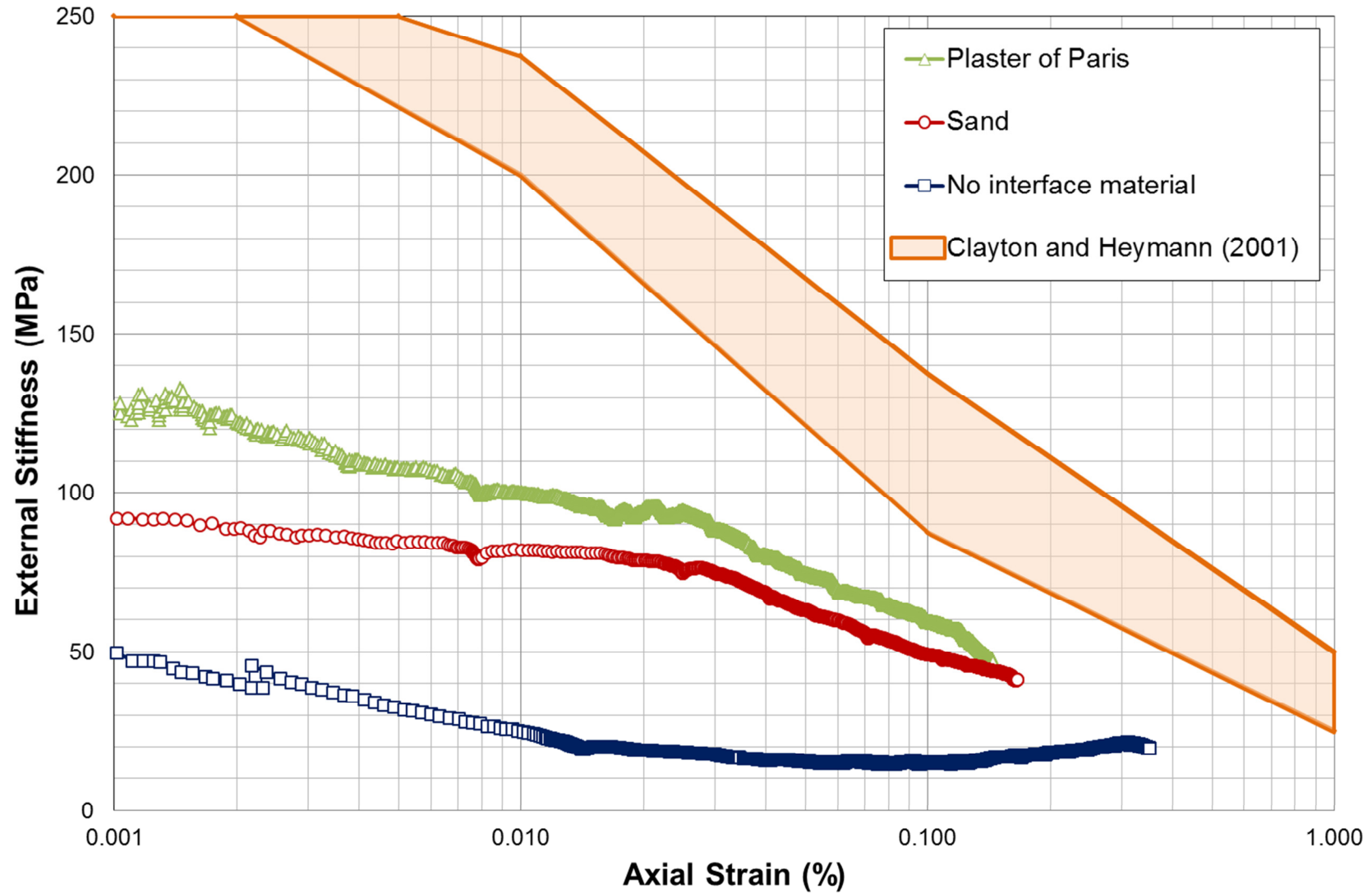


Figure 5-13: Comparison between external stiffness for different preparation methods (Cycle 2).

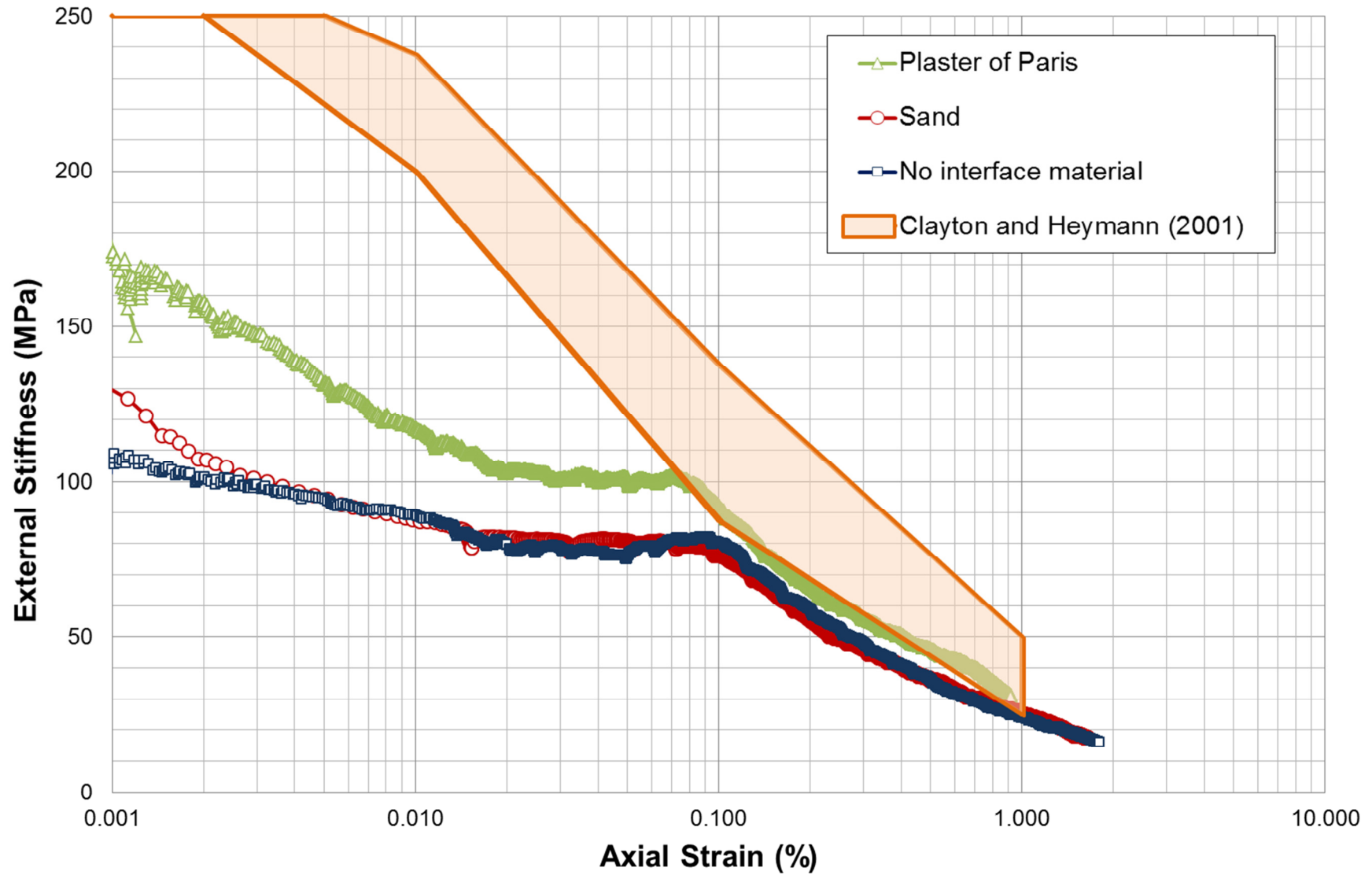


Figure 5-14: Comparison between external stiffness for different preparation methods (Cycle 3).

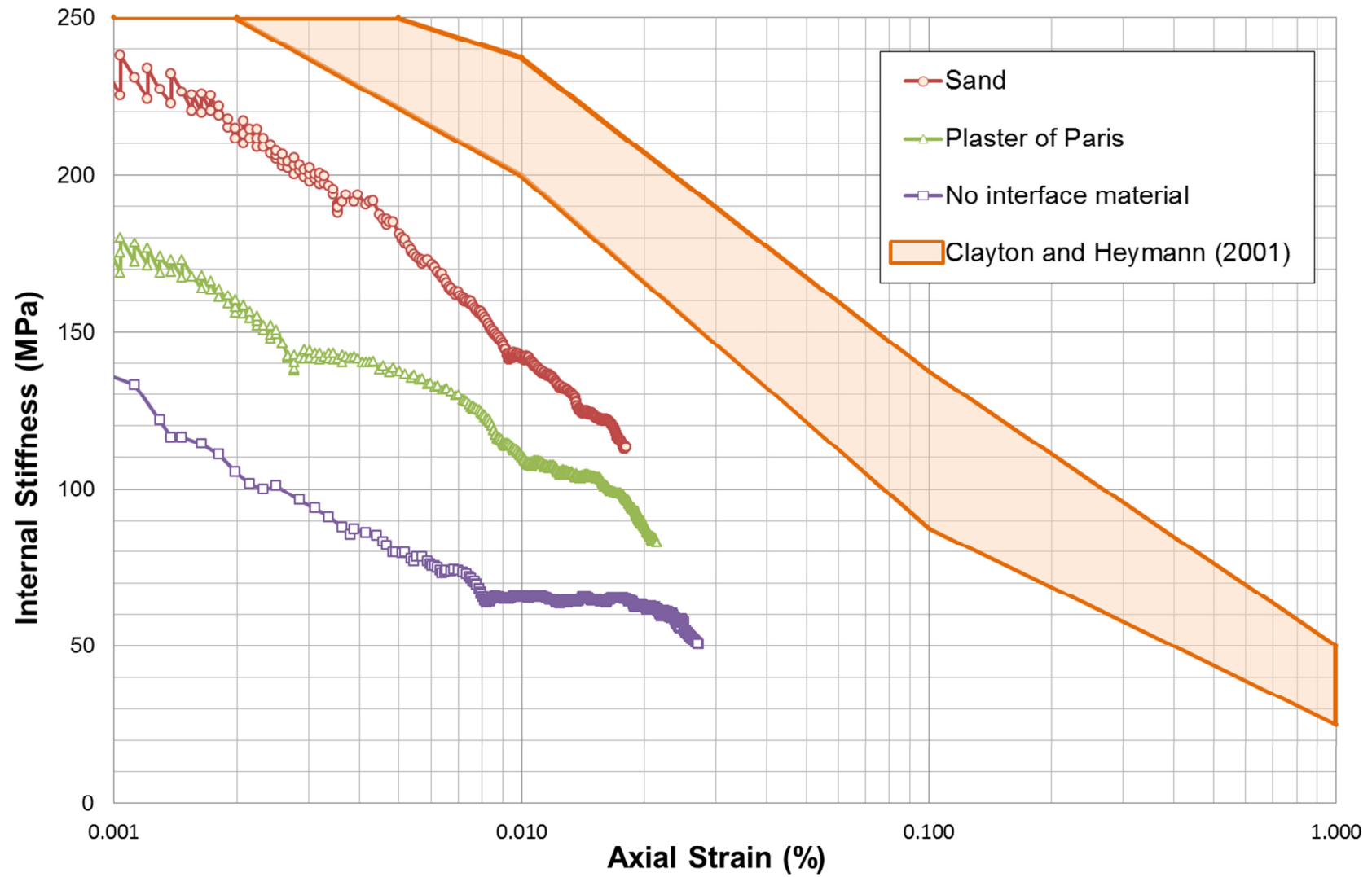


Figure 5-15: Comparison between internal stiffness for different preparation methods (Cycle 1).

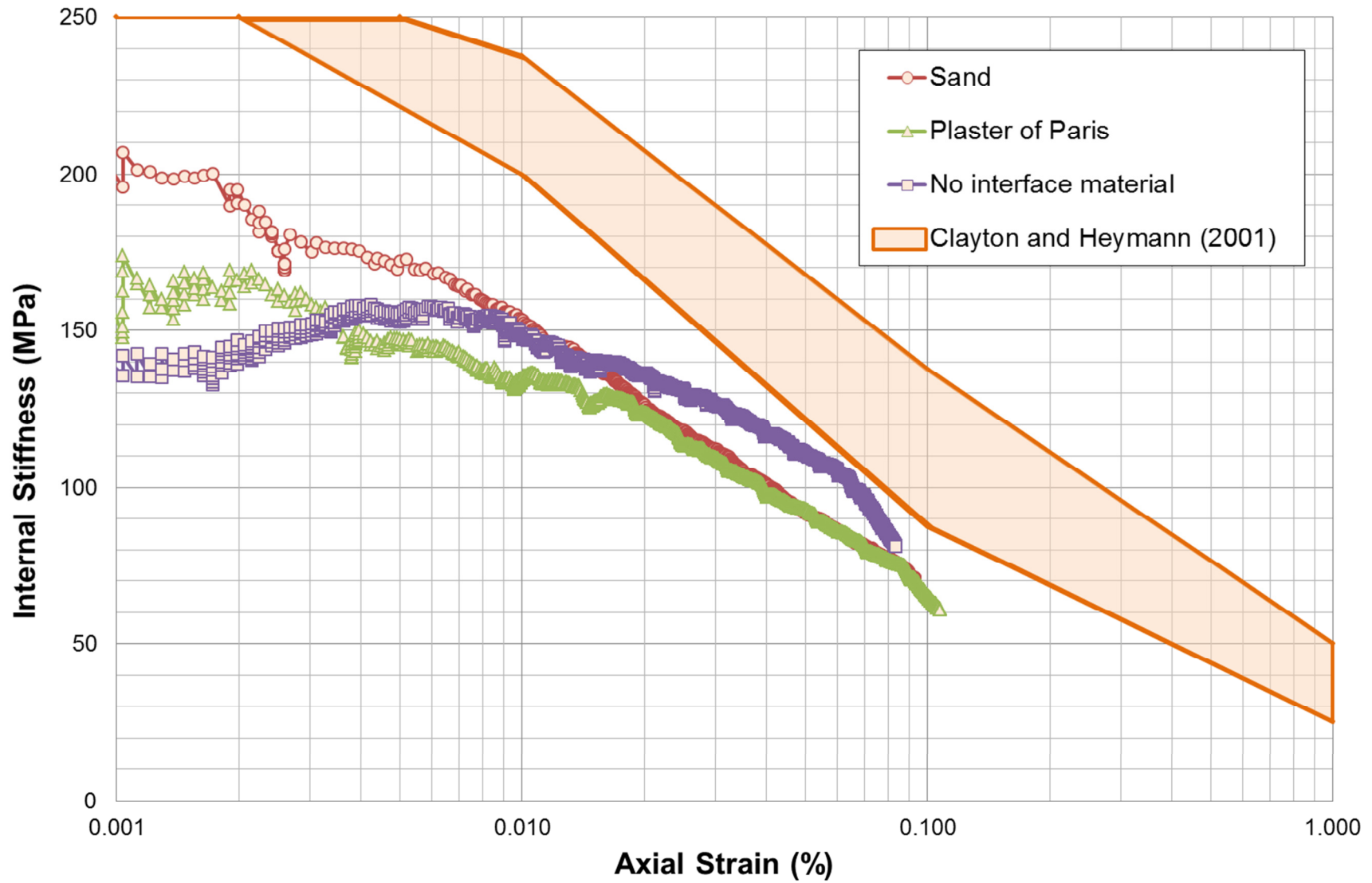


Figure 5-16: Comparison between internal stiffness for different preparation methods (Cycle 2).

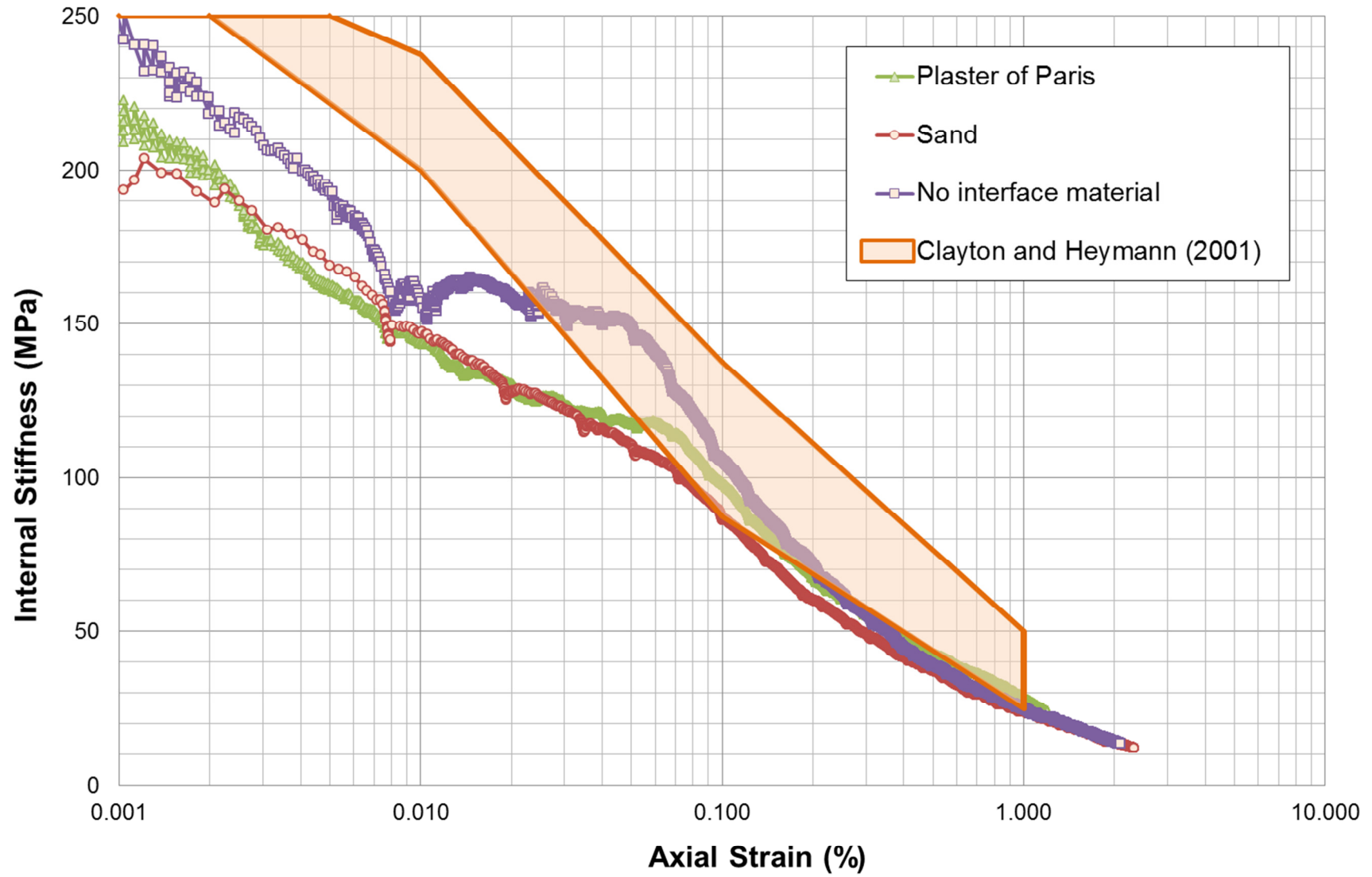


Figure 5-17: Comparison between internal stiffness for different preparation methods (Cycle 3).

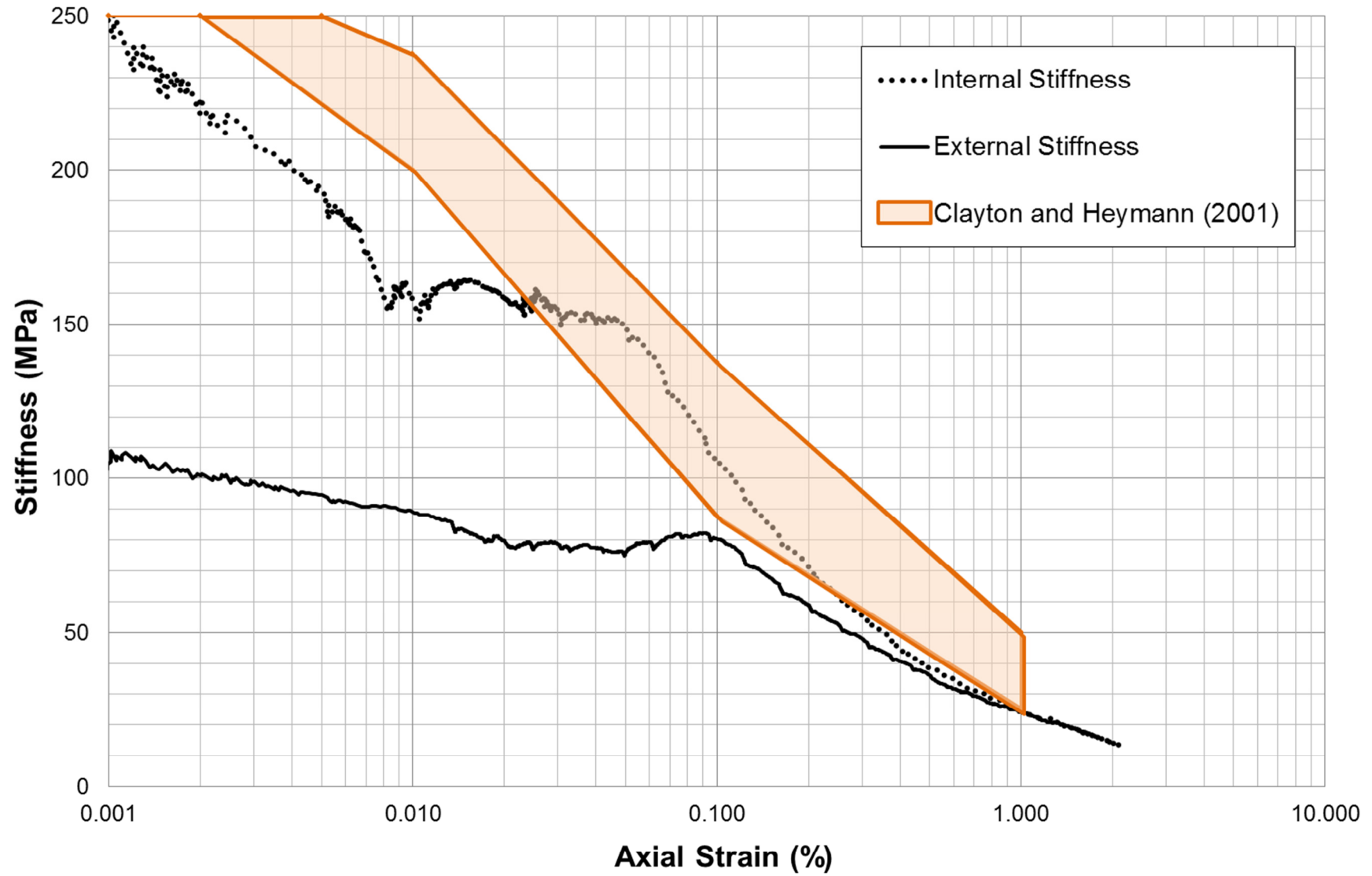


Figure 5-18: Comparison between external stiffness and internal stiffness for ‘No interface material’ test (Cycle 3).

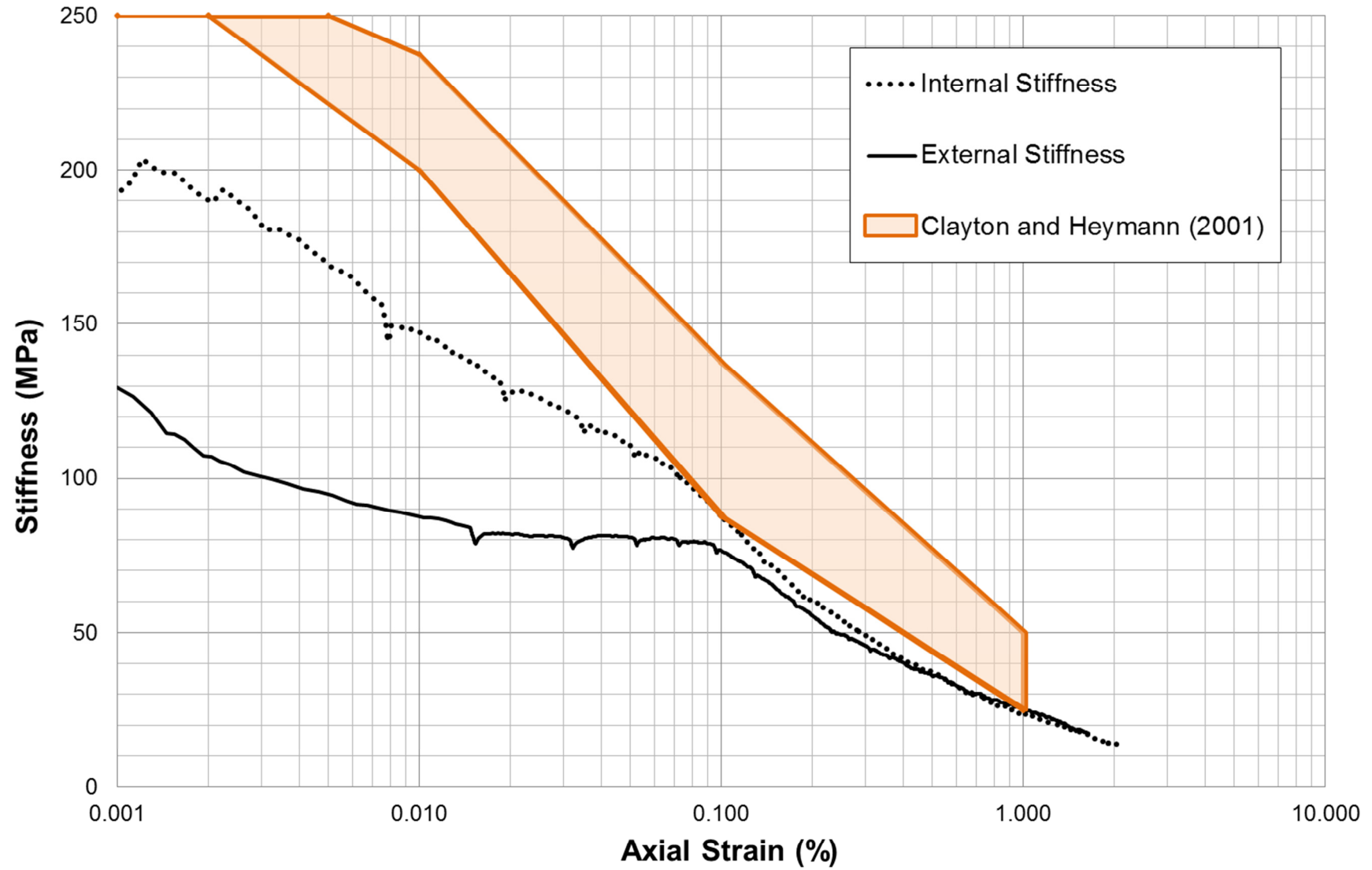


Figure 5-19: Comparison between external stiffness and internal stiffness for 'Sand' test (Cycle 3).

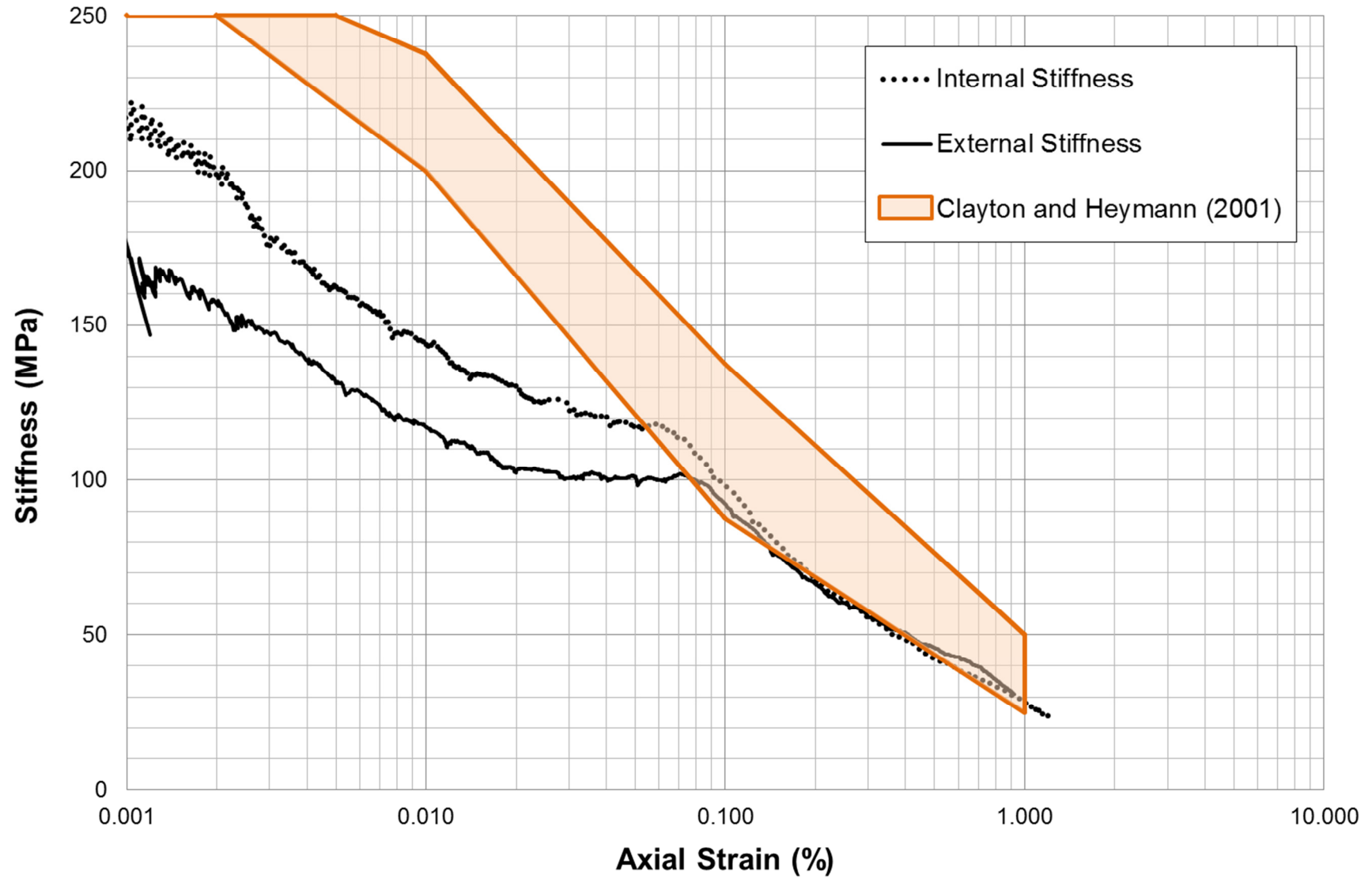
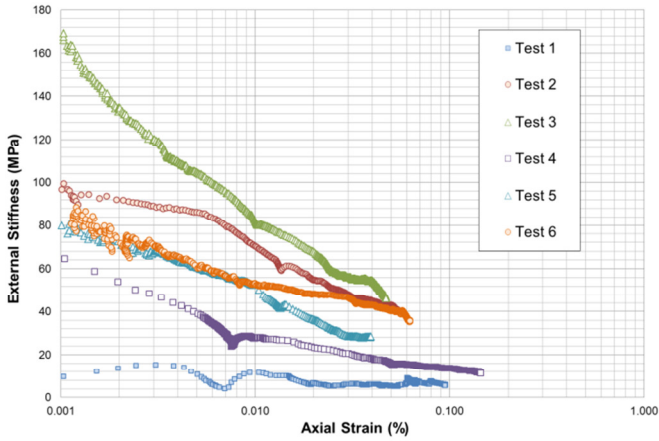
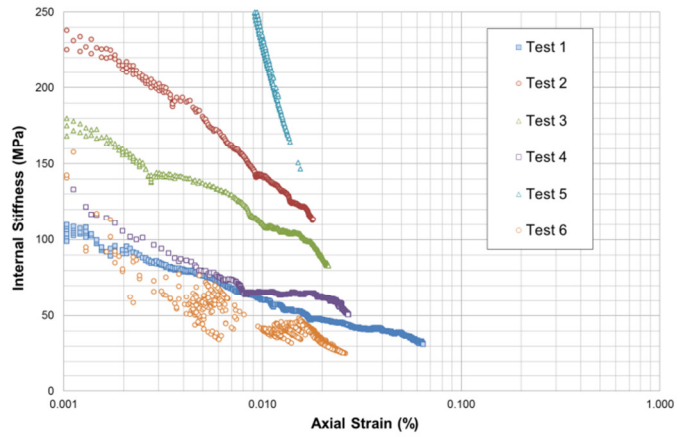


Figure 5-20: Comparison between external stiffness and internal stiffness for 'Plaster of Paris' test (Cycle 3).

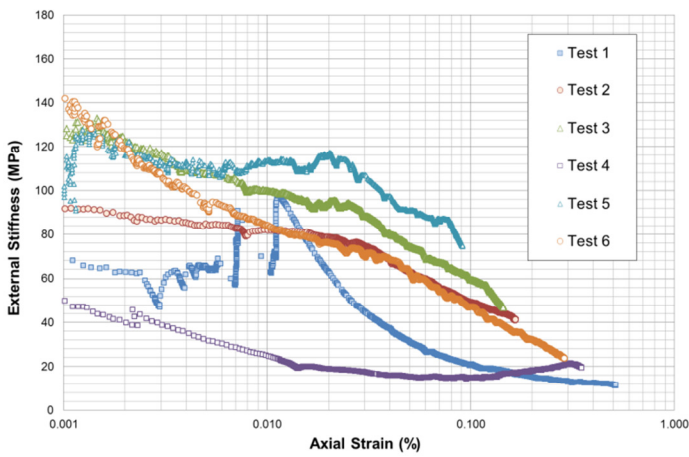
a.) External stiffness (cycle 1)



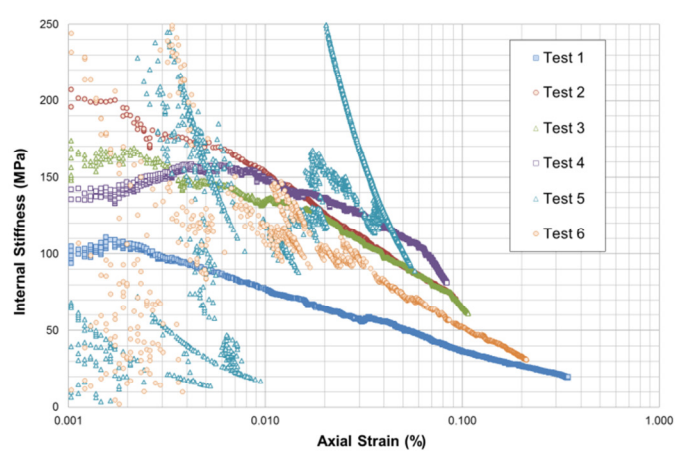
d.) Internal stiffness (cycle 1)



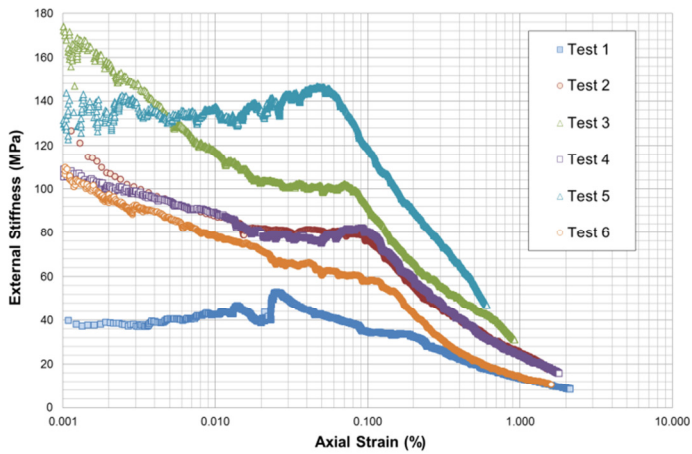
b.) External stiffness (cycle 2)



e.) Internal stiffness (cycle 2)



c.) External stiffness (cycle 3)



f.) Internal stiffness (cycle 3)

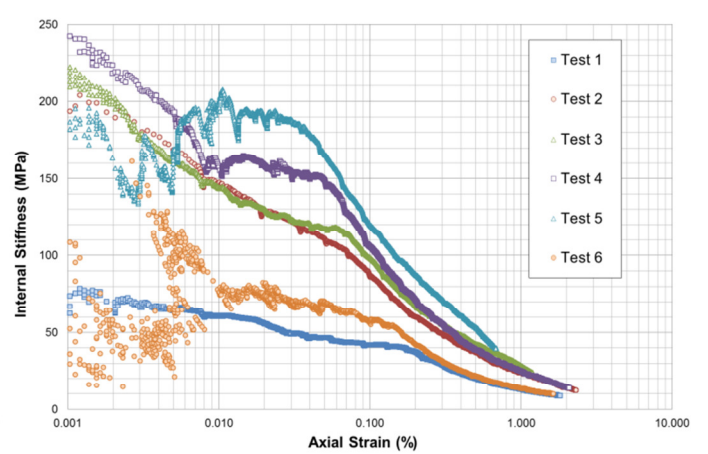


Figure 5-21: Comparison between external stiffness and internal stiffness.

## CHAPTER 6: CONCLUSIONS AND RECOMMENDATIONS

### 6.1. CONCLUSIONS

Plate load tests play an important role in geotechnical engineering in the determination of soil stiffness. The results shown in this research project have demonstrated the following:

- Bedding errors can have a significant effect on soil stiffness values which have been determined by the conventional method of conducting plate load tests where the stiffness has been calculated from the plate settlement;
- Conventional plate load tests can result in stiffness values which are 50% lower than stiffness values inferred from seismic tests;
- Plaster of Paris result in the most accurate stiffness values determined by conventional plate load tests;
- The method which uses well-graded sand may be the most practical material to use as interface material in order to minimise bedding errors; however the accuracy of this method was measured as being approximately 20% less than the plaster of Paris method;
- Telescopic probes are necessary to determine soil stiffness values with a high level of accuracy, especially at small and intermediate strain levels;
- The CSW small strain stiffness ( $E_0$ ) value of 250 MPa has compared very well with the internal stiffness values at 0.001% to 0.002% axial strain, and this suggests that the measurement errors which have been associated with bedding errors can be eliminated by the use of telescopic probes;
- Bedding errors cannot be eliminated on a poorly prepared surface by applying initial load cycles.

## 6.2. RECOMMENDATIONS

The recommendations concluded from the research carried out in this dissertation are that in future, where a high level of accuracy in the stiffness values is required, telescopic probes should be utilized. In addition, the plaster of Paris method is the most effective and should be used for conventional plate load tests. For this research project, Boussinesq's theory was assumed to determine the soil stress below the plate and it is recommended that in future research the stress below the plate should be determined by means of stress cells or other similar instrumentation.

## CHAPTER 7: REFERENCES AND STANDARDS

### 7.1. REFERENCES

- Abbott, E. J. and Firestone, F. A. 1933. Specifying surface quality: a method based on accurate measurement and comparison. *Mechanical Engineering* 55: pp. 569–572
- Acar, Y. B. and El-Tahir, A. 1986. Low strain dynamic properties of artificially cemented sand. *Journal of Geotechnical Engineering, ASCE, Vol. 112, No. 11, pp. 1001-1015.*
- Atkinson, J. H. 1993. An Introduction to the Mechanics of Soils and Foundations: Through Critical State Soil Mechanics. *McGraw-Hill, London, UK, pp. 58-167.*
- Atkinson, J. H. 2000. Non-linear soil stiffness in routine design. *Geotechnique* 50, No. 5, pp. 487-508.
- Atkinson, J. H. and Sallfors, G. 1991. Experimental determination of soil properties. *General Report to Session 1. Proceedings of the 10<sup>th</sup> ECSMFE, Florence 3, pp. 915-956.*
- Bertuzzi, P., and Caussignac, J. M. 1988. Measuring in-situ surface roughness using a Laser profilometer. *Proc. 4th Int. Coll. on Spectral Signatures of Objects in Remote Sensing, Aussois, France, 18-22 January 1988, ESA SP-287, pp. 19-24.*
- Bjerrum, L. 1973. Problems of soil mechanics and construction on soft clays and structurally unstable soils (collapsible, expanding and others). *Proceedings of the 8<sup>th</sup> International Conference of Soil Mechanics and Foundation Engineering, pp. 111-159.*

- Bjerrum, L. and Eggestad, A. 1963. Interpretation of loading test on sand. *Norwegian Geotechnical Institute, Publication No.58, pp.23-27 and Proc., 3<sup>rd</sup> Euro. Conf. on Soil Mech. and Found. Engrg., Wies-baden, Germany., 1, pp. 199-209.*
- Boussinesq, J. 1885. Application des potentiels a la etude de l'equilibre et du mouvement de solides elastiques. *Paris: Gauthier-Villard.*
- Boyle, W. J. 1992. Interpretation of plate load test data. *Int. Journal Rock Mech. Min. Sci. & Geomech. Abst. No. 29(2), pp. 133-141.*
- Bressani, L. A. 1990. *Experimental properties of bonded soils.* PhD thesis. University of London
- Briaud J.-L. 2001. Introduction to Soil Moduli. Geotechnical News, BiTech Publishers Ltd, Richmond, B.C., Canada.
- Burland, J. B. 1989. Ninth Laurits Bjerrum Memorial Lecture: Small is beautiful – the stiffness of soils at small strains. *Canadian Geotechnical Journal 26, pp. 499 - 516.*
- Burland, J. B. and Lord, J. A. 1970. The load deformation behavior of Middle Chalk at Mundford, Norfolk: A comparison between full-scale performance and in situ and laboratory measurements. *Conf. on In Situ investigation in Soils and Rocks, London, British Geotechnical Society, pp. 3-15.*
- Burland, J. B., and Symes, M. J. 1982. A Simple Axial Displacement Gauge for Use in the Triaxial Apparatus. *Geotechnique, Vol. 32, pp. 62-65.*
- Carrier, W. D. and Christian, J. T. 1973. Rigid circular plate resting on a non-homogeneous elastic half space. *Geotechnique 23, No. 30, pp. 67-84*

- Clayton, C. R. I.; Hababa, M. B. and Simons, N. E. 1984. Dynamic penetration resistance and the prediction of the compressibility of a fine-grained sand – a laboratory study. *Geotechnique*, Vol. 35, No. 1, pp. 19-31.
- Clayton, C. R. I. and Heymann, G. 2001. The stiffness of geomaterials at very small strains. *Géotechnique*, Vol. 51 No. 3, pp 245-256.
- Clayton, C. R. I., and Khatrush, S. A. 1986. A New device for Measuring Local Axial Strains on Triaxial Specimens. *Geotechnique*, Vol. 36, pp. 593-597.
- Clayton, C. R. I., Matthews, C. and Simons, N. E. 1995. *Site Investigation*. 2<sup>nd</sup> Edition, Chapter 9. Blackwell Science, Oxford.
- Craig, R. F. 2004. *Craig's soil mechanics*. 7<sup>th</sup> Edition, E & FN Spon., London and New York, pp. 447, ISBN 10:0-415-32702-4 (hbk).
- Cuccovillo, T. and Coop, M. R. 1997a. The measurement of local axial strains in triaxial testing using LVDTs. *Geotechnique*, Vol.47, No. 1, pp. 167-171.
- D'appolonia, D. J., D'appolonia, E. and Brisette, R. F. 1970. Settlement of Spread Footings on Sand. *Proc. ASCE, J. Soil Mech. and Found. Engng. Div.*, 96 (S.12), pp. 754-761.
- Davison, L. 2000. Soil description and classification. *University of the West of England, Bristol in association with Swiss Federal Technical Institute, Zurich*.
- Degarmo, E. P.; Black, J. T. and Kohser, A. 2003. *Materials and Processes in Manufacturing*, 9<sup>th</sup> Edition, Wiley, pp. 223, ISBN 0-471-65653-4.

- Doebelin, E. O. 1990. *Measurement System – Application and design*, 4<sup>th</sup> addition. McGraw-Hill Book Company, New York, 960 pp.
- Ervin, M C; Kurzeme, M. 1992. Evaluation of tertiary age gravel deposits using plate load tests: *Proc 6th Australia-New Zealand Conference on Geomechanics*, Christchurch, 3–7 February, pp. 319–323. Publ New Zealand: New Zealand Geomechanics Society, 1992.
- German Specification 1992. Earthwork and Foundations Working Party, Technical test specifications for soil and rock in road-building, dynamic plate load test using a light falling weight device. *TP BF-StB Part B 8.3, German Federal Ministry of Transport- Road Construction Department*.
- Goto, S., Tatsuoka, F., Shibuya, S., Kim, Y. S., and Sato, T. 1991. A Simple Gauge for Local Small Strain Measurements in the Laboratory. *Soil and Foundations, Vol. 31, No. 1, pp. 169-180*.
- Gibson, R. E. and Anderson, W. F. 1961. In-situ measurement of soil properties with the pressuremeter. *Civil Engineering and Public Works Review, Vol. 56, No. 658, pp. 615-618*.
- Handy, R. L. 2007. *Geotechnical Engineering: Soil and Foundation Principles and Practice*, Fifth Edition, The McGraw-Hill Companies, pp. 385 Eq. 15-17, ISBN: 9780071481205, pp. 882.
- Hardin, B. O. and Drnevich, V. P. 1972. Shear modulus and damping in soils: Design equations and curves. *Journal of the Soil Mechanics and Foundation Division, ASCE, Vol. 98, No. 7, pp. 667-692*.

- Hardin, B. O. and Richart, F. E. Jr. 1963. Elastic wave velocities in granular soils. *Journal of the Soil Mechanics and Foundations Divisions, ASCE, Vol. 89, No. SM1, pp. 33-65.*
- Heymann, G. 1998. *The stiffness of Soils and Weak Rocks at very Small Strains*. PhD Thesis, Department of Civil Engineering, University of Surrey.
- Heymann, G. 2007 Ground stiffness measurement by the continuous surface wave test. *Journal of the South African Institution of Civil Engineering, Vol 49 No1, 2007, pp. 25-31, Paper 631.*
- Hight, D. W. and Higgins, K. G. 1995. An Approach to the Prediction of Ground Movements in Engineering Practice: Background and Application. *International Symposium on Pre-failure Deformation Characteristics of Geomaterials, Sapporo, pp. 909-945.*
- Hobbs, N. B. 1975. Factors affecting the prediction of settlement of structures on rock: with particular reference to the Chalk and Trias: General report and state-of-the-art review for session 4. *Proc. Conf on Settlement of Structures, BGS Cambridge, Pentech Press, London, pp. 579-610.*
- Jardine, R. J. 1995. One perspective of the pre-failure deformation characteristics of some geomaterials. *Proceedings of the First International Conference on Pre-failure Deformation Characteristics of Geomaterials, Vol. 2, pp. 855-885. Balkema, Rotterdam.*
- Jardine, R. J., Potts, D. M., Fourie, A. B. and Burland, J .B. 1986. Studies of the influence of non-linear stress-strain characteristics in soil-structure interaction, *Geotechnique 36, No. 3, pp. 377 -396.*

- Jardine, R. J.; Symes, M. J. and Burland, J. B. 1984. The measurements of soil stiffness in the triaxial apparatus. *Géotechnique*, Vol. 34, No. 3, pp. 323-340.
- Kay, J. N. 1986. Evaluation of Plate load tests. *Proceedings of the 4<sup>th</sup> International Geotechnical Seminar, Field Instrumentation and In-situ Measurements, Singapore*, pp. 103- 110.
- Kokusho, T. 1980. Cyclic Triaxial Test of Dynamic Soil Properties for Wide Strain Range. *Soil and Foundations*, Vol. 20, No. 2, pp. 45-60.
- Kondner, R. L. 1963. Hyperbolic stress-strain response: cohesive soils. *J. Soil Mech. And foundation Engng Div. ASCE* 89, No. 1, pp. 115-143.
- Koning, H. 1960. De Spanningsverdeling in een Homergeen, Anistroop, Elastisch Halfmedium. *LGM Mededelingen, Delft*, Vol. 5, No. 5, pp. 1-19.
- Kummeneji, O. 1956. Foundation of an Oil Tank. *Norwegian Geotechnical Institute Publication No.12, Oslo*.
- Kung, G. T. C. 2007. Equipment and Testing procedures for small strain triaxial tests. *Journal of the Chinese Institute of Engineers*, Vol. 30, No. 4, pp. 579-591.
- Lau, K. C. 1998. A review of down-hole geophysical methods for ground investigation. *Geotechnical Engineering Office, Civil Engineering department, the government of the Hong Kong, special administrative region, Geo report no. 99*.
- Lake, L. M. and Simons, N. E. 1970. Investigations into the engineering properties of chalk at Welford Theale, Berkshire. *Proc. Conf. on In situ Investigations into Soils and Rocks, British Geotechnical Society, London*, pp. 23—29.

- Lawrence, G. J. 1977. Trench Wall Jack: An apparatus to measure the equivalent elastic modulus of soil. *Transport and Road Research Laboratory, Supplementary Report, No. 347.*
- Leonards, G. A. and Ramiah, B. K. 1959. Time effects in the consolidation of clays. *ASTM Special Technical Publication, No. 254, pp. 116-130.*
- Lutenegger, A. J. 1988. Current status of the Marchetti dilatometer test. *Special Lecture, Proc. ISOPT-I, Orlando, Vol. 1: pp.137-155.*
- Lo Presti, D. C. F. 1994. General report: Measurement of shear deformation of geomaterials in the laboratory. *Proceedings of the 1<sup>st</sup> International Symposium on Pre – failure Deformation Characteristics of Geomaterials, IS - Hokkaido-94, Eds. Shibuya et al., Balkema, Rotterdam, Vol. 2, pp. 1067 - 1088.*
- Mair, R. J. 1993. Developments in geotechnical engineering research: Applications to tunnels and deep excavation. *Unwin Memorial Lecture, Proc. Instn. Civ.Engng, 3, pp.27-41.*
- Mair, R. J. and Wood, D. M. 1987. In-Situ Pressuremeter Testing: Methods Testing and Interpretation. *CIRIA Ground Engineering Report, Butterworths, London.*
- Marchetti, S. 1980. In-situ tests by flat dilatometer. *Journal of Geotechnical Engineering, ASCE, Vol. 116, pp. 299-321.*
- Marchetti, S. 1997. The Flat Dilatometer: Design Applications. Keynote Lecture. *Proc. Third Int. Geotechnical Engineering Conference, Cairo University, pp.421-448.*

- Marsland, A. 1971a. Large in-situ tests to measure the properties of stiff fissured clays. *Proceedings 1<sup>st</sup> Australia-New Zealand Conference on Geomechanics, Melbourne, Vol. 1, pp. 180-189.*
- Marsland, A. 1971b. The shear strength of stiff fissured clays. *Proceedings Roscoe Memorial Symposium, University of Cambridge.*
- Marsland, A. 1971c. Laboratory and in-situ measurements of the deformation moduli of London clay. *Proceedings Symposium on the Interaction of Structures and Foundations, The Midland Soil Mechanics and Foundation Engineering Society at the department of Civil Engineering, University of Birmingham, pp. 7-17.*
- Marsland, A. 1972. Clays subjected to in situ plate tests. *Ground Engineering, Vol. 5 (6), pp. 24- 31.*
- Marsland, A. 1974. Comparisons of the results from static penetration tests and large in-situ plate load tests in London clay. *Proceedings European Symposium on Penetration testing, Stockholm, Vol. 2:2, pp. 245-252.*
- Matthews, M. C. and Clayton, C. R. I. 2004. *Large diameter plate tests on weathered in-situ Chalk.* Quarterly Journal of Engineering Geology and Hydrogeology, No. 37, pp. 61-72.
- Meigh, A. C. 1987. Cone penetration testing: methods and interpretation. *CIRIA Ground Engineering Report: In situ testing. Construction Industries Research and Information Association, London.*
- Ménard, L. 1957. Mésures in situ des propriétés physique des soils. *Annales des Ponts et Chaussées, Vol. 127, pp. 357-377.*

- Pantelidis, L. 2008. Determining of the soil strength characteristics through the plate bearing test. *Foundations of civil and environmental engineering, No. 11. Aristotle University of Thessaloniki, Greece.*
- Park, C. B., Miller, R. D., and Xia, J., 1996a, Multi-channel analysis of surface waves using Vibroseis, Presented at the 66th Ann. Mtg. of SEG, Denver, Expanded Abstracts, 68-71.
- Park, C. S. and Tatsuoka, F. 1994. Anisotropic strength and deformation of sands in plane strain compression. Proceedings of the 13th International Conference of Soil Mechanics and Foundation Engineering, Vol. 1, pp. 1-6.
- Pells, P. J. N. 1983. Plate-loading tests on soil and rock. *Proc. Extension Course in situ Testing for Geotech. Investigations*, Sydney, pp. 73-86.
- Poulos, H. G. and Davis, E. H. 1974. Elastic solutions for soil and rock mechanics. *John Wiley, Ch. 3, pp. 43-49 & Ch. 7, pp. 165-180.*
- Ratananikom, W., Likitlersuang, S., and Yimsiri, S. 2007. Development of triaxial system for soil testing at wide strain range: preliminary results. *International Symposium on Geotechnical Engineering, Ground Improvement, and Geosynthetics for Human Security and Environmental Preservation*, Bangkok, Thailand, Ed. Bergado, pp. 395-407.
- Rieke-Zapp D. H., Wegmann H., Santel F., Nearing M. A. 2001. Digital photogrammetry for measuring soil surface roughness. *Proceedings of the American Society of Photogrammetry and Remote Sensing 2001 Conference: Gateway to the New Millenium*, St Louis, Missouri, pp 1–8.

- Reznik, Y. M. 1995. Comparison of results of oedometer and plate load tests performed on collapsible soils. *Engineering Geology* 39, Elsevier, pp. 17-30.
- Rowe, P. W. and Barden, L. 1966. A new consolidation cell. *Géotechnique*, Vol. 16, No. 2, pp. 162-170.
- Sahoo, P. 2005. *Engineering Tribology*. Prentice Hall of India, New Delhi. ISBN: 81-203-2724-1, pp. 336.
- Sanchez-Salineró, I.; Roesset, J. M.; Shao, K. Y.; Stokoe II, K. H. and Rix, G. J. 1987. Analytical evaluation of variables affecting surface wave testing of pavements. *Transportation Research Record No. 1136*, pp. 86-95.
- Schmähling, J.; Hamprecht, F. A. and Hoffmann, D. M. P. 2006. A three-dimensional measure of surface roughness based on mathematical morphology. *Technical Report from Multidimensional Image Processing*, IWR, University of Heidelberg.
- Schmertmann, J. H. 1970. Suggested method for screw-plate load test. Special procedures for testing soils and rocks for engineering purposes. *ASTM STP Vol. 479*, pp. 81-85.
- Schwab, E. F. and Broms, B. B. 1977. Pressure-Settlement-Time relationship by screw-plate tests in situ. *Proceedings 7<sup>th</sup> International conference on soil mechanics and foundation engineering, Vol. 1, Tokyo*, pp. 281-288.
- Shirley, D. J. and Hampton, L. D. 1977. Shear-wave measurements in laboratory sediment. *Journal of Acoustic Society of America, Vol. 63, No. 2*, pp. 607-613.

- Simpson, B. 1993. Development and Application of a New Soil Model for Prediction of Ground Movements. *Predictive Soil Mechanics, Proceedings of Wroth Memorial Symposium, Oxford, G.T. Hously and A.N. Schofield eds, pp. 628- 643. Thomas Telford, London, UK.*
- Steward, M. 1990. A new approach to the use of Bearing Area Curve. *Proceedings of the International Honing Technologies and Applications Conference. Society of Manufacturing Engineers, Novi, Michigan, FC90-229.*
- Stokoe, K. H.; Hwang, S. K.; Lee, J. N. K. and Andrus, R. D. 1995. Effects of various parameters on the stiffness and damping of soils at small to medium strains. *Proceedings of the First International Conference on Pre-failure Deformation Characteristics of Geomaterials, Vol. 2, pp. 785-816. Balkema, Rotterdam.*
- Stroud, M. A. 1989. The standard penetration test – its application and interpretation. *Proceedings of the ICE Conference on Penetration Testing in the UK. Thomas Telford, London.*
- Strout, J. M. and Senneset, K. 1998. International development of the field compressometer. *Geotechnical Site Characterization, Robertson and Mayne (eds), Balkema Rotterdam, ISBN 90 5410 939 4.*
- Tay, C. J., Wang, S. H., Quan, C., Shang, H. M. 2003. In situ surface roughness measurements using a laser scattering method., *Elsevier, Department of Mechanical Engineering, National University of Singapore, Optics Communications No. 218, pp. 1-10.*
- Terzaghi, K. 1925. Erdbaumechanik auf Bodenphysikalischer Grundlage, *Franz Deuticke, Leipzig und Wein, pp. 399.*

- Terzaghi, K. & Peck, R. B. 1948. *Soil Mechanics in Engineering Practice*. 1<sup>st</sup> edition, John Wiley, New York.
- Timoshenko, S. & Goodier, J. N. 1951. *Theory of elasticity*. New York: McGraw-Hill Book Co., Inc, pp. 368-372.
- Tomlinson, M. J. 1980. *Foundation Design and Construction*. Pitman Publishing.
- Totani, G., Marchetti, S., Monaco, P. & Calabrese, M. 2001. Use of the Flat Dilatometer Test (DMT) in geotechnical design. *In situ 2001, Intl. Conf. on In situ Measurement of Soil Properties*, Bali, Indonesia.
- Unal, E. 1997. Determination of in situ Deformation modulus: New Approaches for Plate-loading Tests. *Int. J. Rock Mech. Min. Sci.* Vol. 34, No. 6, pp. 897-915.
- Van Heerden, W. L. & Maschek, R. K. A. 1979. In situ modulus determination: A case study – Elandsberg scheme, South Africa. *Int. Cong. Rock Mech.*, Montreux, Vol. 2, pp. 705-710.
- Vrkljan, I., Kavur, B., Mehingrad, A. and Ghiassi, S. 1995. Rock mass deformability by extra-large flat jacks, plate load and dilatometer testing. *8<sup>th</sup> Int. Cong. Rock Mech.*, ed. T. Fujii, Vol. 2, pp. 185-191.
- Wallace, G. B., Slebir, E. J., and Anderson, F. A. 1969. In-situ methods for determining deformation modulus used by the Bureau of Reclamation. *Symp. On the Determination of the In-situ Modulus and Deformation of Rock*. ASTM Spec. Publication 477.

Ward, W. H., Burland, J. B. and Gallois, R. W. 1968. Geotechnical assessment of a site at Mundford, Norfolk, for a large proton accelerator. *Géotechnique*, Vol. 18, pp. 399-431.

Wong, J.; Hurley, P. and West, G. F. 1983. Cross-hole seismology and seismic imaging in crystalline rocks. *Geophys, Res. Lett.*, No. 10, pp. 686-689.

Wrench, B. P. 1984. Plate Tests for the Measurement of Modulus and Bearing Capacity of gravel. *The Civil Engineer in South Africa*, pp. 429-437.

Wrench, B. P. 1994. Plate Load Test (PLT). *SAICE and University of Pretoria. Department of civil engineering.*

## 7.2. STANDARDS

ASTM D 1194—72 (Re-approved 1987). Standard test method for bearing capacity of soil for static load and spread footings. *American Society for Testing and Materials, Philadelphia, USA.*

ASTM D 1195—64 (Re-approved 1994). Standard test method for repetitive static plate load tests of soil and flexible pavement components, for use in evaluation and design of airport and highway pavements. *American Society for Testing and Materials, Philadelphia, USA.*

ASTM D 1196—64 (Re-approved 1987). Standard test method for non-repetitive static plate load tests of soil and flexible pavement components, for use in evaluation and design of airport and highway pavements. *American Society for Testing and Materials, Philadelphia, USA.*

BS 5930: 1981. Code of Practice for Site Investigations (formerly CP 2001). *British Standards Institution, London.*

BS 1377: Part 9: 1990. British Standard Methods of test for soils for civil engineering purposes. *Part 9: In-situ tests, British Standards Institution, London.*

CP 2001: 1957. Code of Practice for Site Investigations. *British Standards Institution, London.*

ENV 1997-3:1999: Plate load tests. Eurocode 7, Clause 11, pp. 78-84.

JCGM 200:2008: International vocabulary of metrology — Basic and general concepts and associated terms (VIM), *Working Group 2 of the Joint Committee for Guides in Metrology.*

Modified AASHTO T-222-78. 2000. Florida Method of Test for non-repetitive static plate load test of soils and flexible pavement components, FM 5-527, September 2000.

SANS 100099: 2008: International vocabulary of metrology — Basic and general concepts and associated terms (VIM), *South African National Standard, ISBN 978-0-626-21402-9.*

## **APPENDIX A**

### **Plate load test questionnaire**

## **A.1 Introduction**

This appendix contains the nine-question plate load test questionnaire that was sent out to over 90 geotechnical laboratories and companies in South Africa and formed part of the industry research conducted for this research project.

## **A.2 Content**

- I. Plate load test questionnaire

I.) Plate Load Test Questionnaire

**VERTICAL PLATE LOAD TESTS SURVEY  
FOR RESEARCH DONE BY HFT BARNARD FOR HIS MENG (GEOTECHNICAL) ENGINEERING DEGREE**

NAME OF SUPPLIER:

1. WHAT ARE THE TYPICAL PLATE SIZES THAT YOU USE FOR VERTICAL PLATE LOAD TESTS? (300mm; 450mm etc.)

2. WHAT DO YOU TYPICALLY USE TO PROVIDE THE REACTION FORCE FOR VERTICAL PLTs? (Kentledge Blocks, Excavator bucket etc.)

IF OTHER/MORE PLEASE SPECIFY:

3. WHAT DO YOU TYPICALLY USE TO MEASURE THE APPLIED LOAD? (PRESSURE GAUGES; LOAD CELL etc.)

IF OTHER/MORE PLEASE SPECIFY:

4. WHAT DO YOU TYPICALLY USE TO MEASURE THE PLATE SETTLEMENTS? (DIAL GAUGES; LVDTs etc.)

IF OTHER/MORE PLEASE SPECIFY:

5. HOW MANY DISPLACEMENT INSTRUMENTS DO YOU TYPICALLY USE TO MEASURE PLATE SETTLEMENTS?

IF OTHER/MORE PLEASE SPECIFY:

6. WHICH SURFACE PREPARATION METHOD DO YOU TYPICALLY USE TO ACHIEVE A LEVEL AND SMOOTH TEST AREA?

IF OTHER/MORE PLEASE SPECIFY:

7. WHICH REFERENCE BEAM DO YOU USE WHEN PERFORMING PLATE LOAD TESTS?

IF OTHER/MORE PLEASE SPECIFY:

8. WHAT IS THE TOTAL LENGTH OF THE REFERENCE BEAM?

m

9. WHICH TEST METHOD/STANDARD PROCEDURE DO YOU USE WHEN PERFORMING PLATE LOAD TESTS?

IF OTHER/MORE PLEASE SPECIFY:

## **APPENDIX B**

### **Publications by the author**

## **B.1 Introduction**

This appendix contains all publications written during this research project by the author and his supervisor, Professor Gerhard Heymann. The first article was published in the proceedings of the 15<sup>th</sup> African Regional Conference held in Maputo. This article was also presented by Professor Gerhard Heymann in July 2011 (Barnard, H. F. T. & Heymann, G., 2011). The second article was published in the proceedings of the 2011 Young Geotechnical Engineering Conference held in Berg-en-Dal Kruger National Park and was presented by the author in August 2011 (Barnard, H. F. T., 2011).

## **B.2 Content**

- I. 15<sup>TH</sup> ARC CONFERENCE: Maputo Mozambique, July 2011.
- II. 2011 YGE CONFERENCE: Berg-en-Dal Kruger National Park, August 2011.

# Using a Modified Plate Load Test to Eliminate the Effect of Bedding Errors

Hennie BARNARD<sup>a</sup> and Gerhard HEYMANN<sup>b</sup>

<sup>a</sup>*Aurecon, Pretoria, South Africa*

<sup>b</sup>*University of Pretoria, Pretoria, South Africa*

**Abstract.** Plate load tests have been used extensively in the past to determine the bearing capacity and the stiffness of soil. Two of the main advantages of plate load tests are the cost-effectiveness of the test and the relative straight forward test procedure. The plate test can either be performed vertically or horizontally. The test consists of a plate that typically varies in diameter between 150 mm and 600 mm, which are loaded using a hydraulic pump and jack. The displacement of the plate is typically measured with two or more calibrated displacement measuring devices attached to the plate. This paper reports the results of a vertical plate load test designed to eliminate the effect of bedding errors that occurs during plate tests by using telescopic probes to measure the displacement below the centre of the plate. A series of plate tests were performed to determine the effectiveness of installing telescopic probes to eliminate the bedding errors. The measured vertical displacement of the plate was compared with the relative displacement of the telescopic probes and the stiffnesses were compared. The test apparatus, methods and results are discussed in this paper.

**Keywords.** Plate load test, bedding errors, telescopic probes.

## Introduction

Geotechnical engineers are continuously searching for more accurate and cost effective tests to determine the stiffness of soil. Two of the main advantages of plate load tests are the cost-effectiveness and the relative straight forward test procedure. This paper reports on research that was done on vertical plate load tests using a modified apparatus. Bedding errors affect the soil stiffness measurements during plate load tests and therefore it needs to be eliminated or kept to a minimum. Telescopic probes were used to measure the displacement below the center of the plate in order to eliminate effects of bedding errors. The experiment equipment is discussed as well as the test procedure and data interpretation. The results of stiffness measurements for both the external instruments and telescopic probes are compared. Final conclusions are summarised and the way forward for plate load testing is proposed. The conclusions will help practical engineers realize the importance of bedding errors that occurs during plate load tests and argue that engineers should be more critical when interpreting plate load data.

## 1. Experiment Equipment

The conventional plate load test consists of a selection of plates, a hydraulic pump and jack, some means of applying a reaction force and two or three calibrated displacement measuring devices. In the experiments of this project, a steel beam with a weight of 1,3 ton was used for the reaction force, together with grouted anchors. A hydraulic jack and pump system were used to provide the required contact pressure by jacking against the anchored steel beam. The applied load was directly measured with a 10 ton load cell, placed on top of circular plates, and logged with an automatic logging unit. 300 mm and 450 mm steel plates were stacked on top of each other and placed on the prepared surface. The vertical displacement of the bottom plate was measured with three calibrated DCDT's (Direct-Current Displacement Transducers) placed 120° apart and approximately 25 mm from the plate perimeter to accommodate for any tilt that might occur during testing.

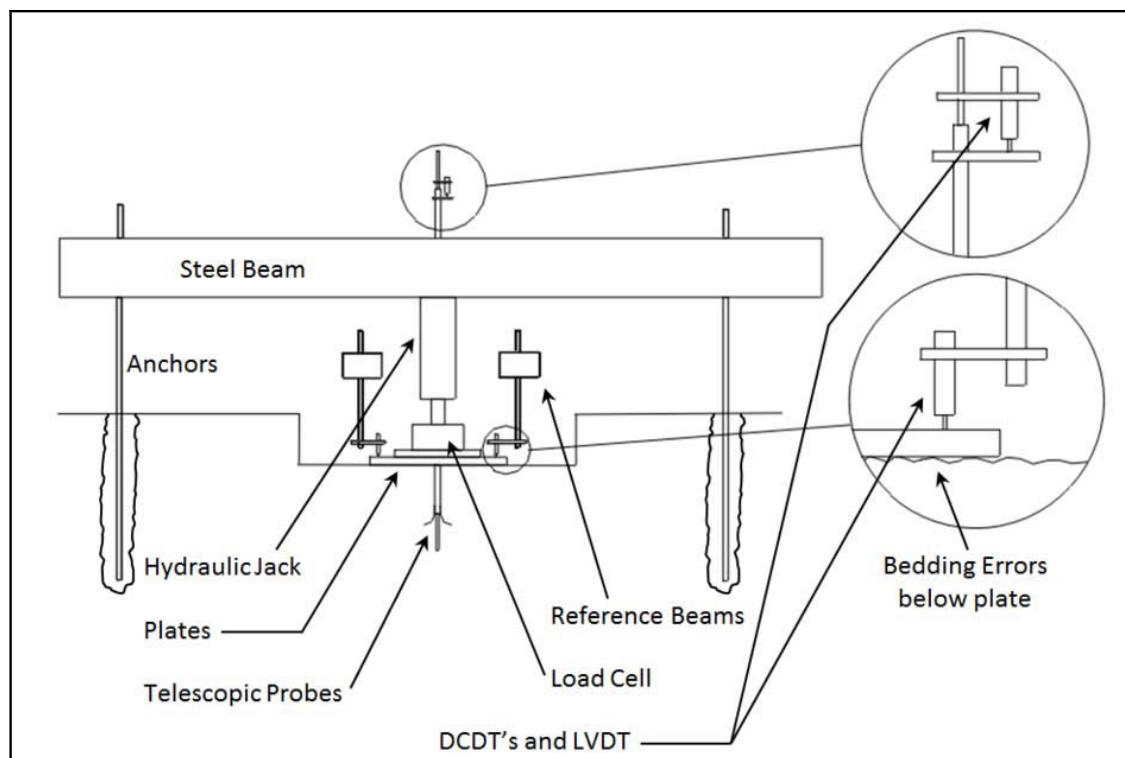


**Figure 1.** Schematic illustration of the modified plate load test set-up

The three external measuring devices were supported by two, 3 m long wooden, reference beams which were placed on both sides of the test area without interfering with any test equipment. Figure 1 illustrates the modified plate load test set-up and the instrument details. The telescopic probe consisted of a solid inner aluminum rod (8 mm), designed to slide freely inside a 13 mm aluminum tube. Three bended spring steel strips were welded onto a bolt and screwed onto the threaded tube. A calibrated LVDT (Linear Variable Differential Transformer) were attached to the probes to measure the relative displacement at two positions below the centre of the plate. Figure 2 shows the telescopic probe set-up.



**Figure 2.** Telescopic probes set-up

## 2. Test Procedure

The plate load tests were performed on a uniform residual andesite (silty clayey sand) at the experimental farm of the University of Pretoria. A steel beam and four anchors, grouted to a depth of 1,5 m, were used to provide the reaction force needed to generate the required contact pressure between the plate and the soil. Tests were conducted in 2 m x 2 m holes and approximately 300 mm deep. The surface was leveled as smooth as possible and cleaned before the test commenced. A 25 mm hole was drilled by means of a hand bore, in the center of the 2 m x 2 m hole, up to a depth of one plate diameter (450 mm) below ground surface. Once the plates, hollow load cell and hollow hydraulic jack were stacked, the external DCDTs were installed on the perimeter of the 450 mm plate. The final step before the test could commence was to install the telescopic probes. The inner aluminum rod was grouted at the bottom of the 25 mm hole using ROCSET<sup>®</sup> grout. The spring steel unit together with the aluminum tube was release at a depth of 225 mm below the plate using a 25 mm steel release pipe. The LVDT with a range of 5 mm was installed at the top of the telescopic probes to record the relative displacement between the two probe points, 225 mm and 450 mm below the plate, respectively. A load sequence was applied which comprised three cycles (8 kN, 24 kN and 100 kN). The applied loads was recorded during the load and unload cycles and logged at 10 reading per second throughout the tests together with the four displacement transducers measurements. A number of tests were performed but only one test is discussed due to limited space.

## 3. Data Interpretation

The average vertical displacement of the plate ( $\rho$ ) obtained from the three DCDT's was used in Eq. (1), together with the plate diameter ( $D$ ); and Poisson's ratio ( $\nu$ ) to determine the external stiffness ( $E_{ext}$ ) in MPa [2]. The contact stress ( $q$ ) was taken as the applied load divided by the plate area, therefore assuming a uniform pressure distribution across the plate.

$$E_{ext} = \frac{\pi \cdot q \cdot D \cdot (1 - \nu^2)}{4 \cdot \rho} \quad (1)$$

The strain level below a loaded plate varies with depth. In order to allow comparison of stiffnesses from Eq. (1) and those calculated from the telescopic probes, the average strain of the soil was taken as the plate settlement divided by 1.5 times the plate diameter. This was taken from the influence depths for circular foundations based on Boussinesq's theory where less than 20% of the applied stress occurs below 1,5 times the plate diameter.

The measured relative displacement of the telescopic probes ( $\partial L$ ) was used in Eq. (2) together with the distance between the two probe points ( $L$ ), to determine the strain levels for the local stiffness ( $E_{Local}$ ). The vertical stress at depth  $z$  below the centre of the circular plate with diameter  $D=2R$ , carrying a uniform pressure ( $q$ ), is calculated using Eq. (3). Values of the influence factor ( $I_c$ ) are always between zero and unity. The local stiffness ( $E_{Local}$ ) was calculated for every load step using Eq. (4) with the average vertical stress ( $\Delta\sigma_z$ ) between the two fixed points, 225 mm apart; and the corresponding strain level calculated with Eq. (2).

$$\Delta\varepsilon = \frac{\partial L}{L} \quad (2)$$

$$\sigma_z = q \left[ 1 - \left\{ \frac{1}{1 + (R/z)^2} \right\}^{3/2} \right] = qI_c \quad (3)$$

$$E_{Local} = \frac{\Delta\sigma_z}{\Delta\varepsilon} \quad (4)$$

#### 4. Results

The main study objective was to investigate the bedding errors that may occur below the plate during plate load testing. The external and local stiffness at different strain levels were plotted and compared. Figure 3 shows the comparison between the measured external and local stiffness for the full strain range.

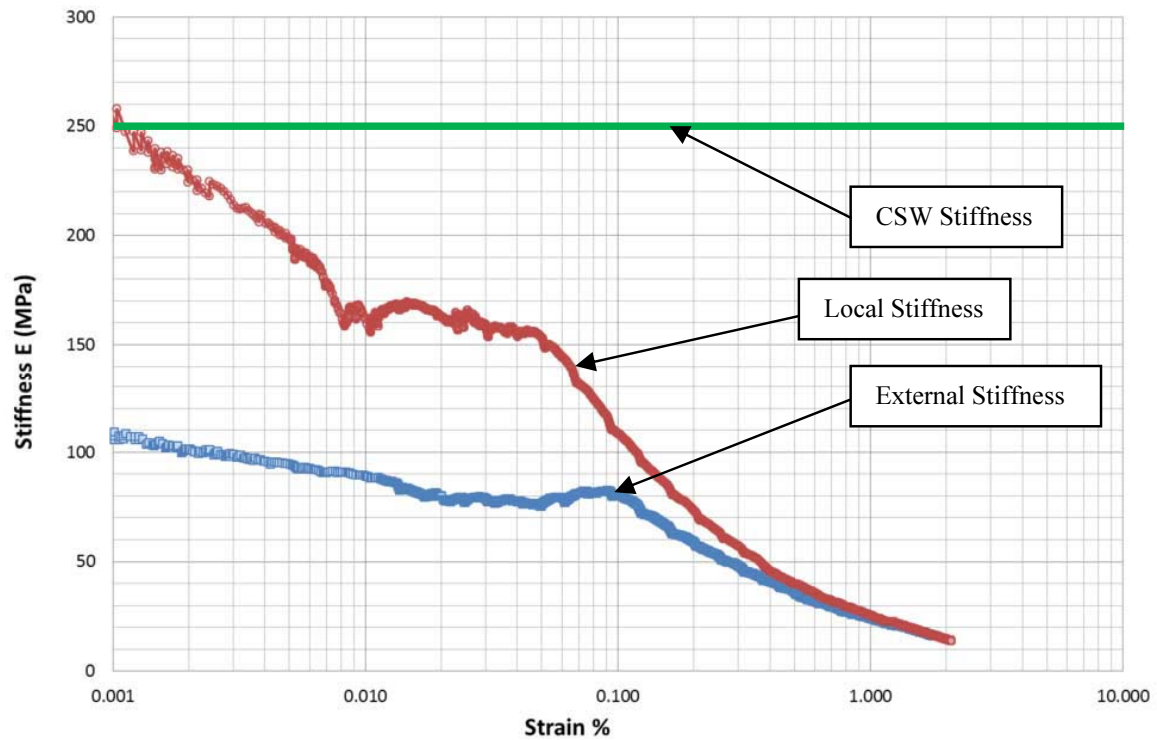


**Figure 3.** Comparison between external stiffness and local stiffness (Cycle 3)

It is clear from Figure 3 that the stiffness determined with the telescopic probes showed significantly higher values than that from the conventional external measurements up to 0.05% strain. Table 1 summarises the local and external stiffness that was determined in all three cycles. It is interesting to notice the higher stiffness measured during the third cycle compared to the first two cycles.

**Table 1.** Comparison between external and local instruments

Strain %	Stiffness E (MPa)					
	Cycle 1		Cycle 2		Cycle 3	
	LS*	ES**	LS*	ES**	LS*	ES**
0.001	137	65	139	50	249	106
0.002	104	54	145	40	225	101
0.01	67	28	152	25	162	89
0.02	64	23	140	19	163	80
0.05	n.a	n.a	114	15.3	153	76

*Note:* \* Telescopic probe stiffness

\*\* External stiffness

Table 2 shows the ratio between the external and local stiffness. In most cases the external stiffness was less than 50% of the local stiffness. Continuous surface wave tests (CSW) on the same site showed small strain stiffness ( $E_0$ ) values of 250 MPa. The local stiffness in cycle 3 at 0.001% to 0.002% compare very well with the CSW value.

**Table 2.** Percentage of external stiffness compared with telescopic probe stiffness

Strain %	Cycle 1 External vs. Local (%)	Cycle 2 External vs. Local (%)	Cycle 3 External vs. Local (%)
0.001	47%	36%	43%
0.002	52%	28%	45%
0.01	42%	16%	55%
0.02	36%	14%	49%
0.05	-	13%	50%

## 5. Conclusions and Way Forward

Plate load tests have an important role in the future of geotechnical engineering and the determination of soil stiffness. The results shown in this paper clearly demonstrate that bedding errors can have a significant effect on stiffnesses determined with the traditional method of measuring plate settlement. This modified plate load test opens new opportunities to be explored and developed. The results of these plate load tests also showed the importance and effectiveness of using telescopic probes to determine the soil stiffness. The authors believe that bedding errors were eliminated by means of telescopic probes and therefore recommend this method for the future use.

## Acknowledgements

The authors would like to thank the following institutes:

- University of Pretoria for the technical support and facilities;
- Aurecon SA, for the financial support during the study period.

## References

- [1] G. Heymann, *The stiffness of soil and weak rocks at very small strains*, University of Surrey, 1998.
- [2] B. Wrench, *Plate load test*, University of Pretoria, 1994.
- [3] B. Wrench, *Plate test for the measurements of modulus and bearing capacity of gravels*, 1984.

# **Investigation of Different Surface Preparation Methods to Minimize Bedding Errors in Plate Load Tests**

**H. F. T. Barnard**

Aurecon SA, Pretoria, Gauteng, hennie.barnard@aurecongroup.com

## **Abstract**

Plate load tests have been used extensively in the past to determine the bearing capacity and the stiffness of soil. Two of the main advantages of plate load tests are the cost-effectiveness of the test and the relative straightforward test procedure. The plate test can either be performed vertically or horizontally. The test consists of a plate that typically varies between 150 mm and 600 mm, which is loaded using a hydraulic pump and jack. The displacement of the plate is typically measured with two or more calibrated displacement measuring devices attached to the plate. This paper reports results of a plate load test, designed to eliminate the effect of bedding errors that occur during plate tests by using telescopic probes to measure the displacement below the centre of the plate. Different surface preparation methods were used to achieve smooth bedding before each test. A series of plate tests was performed to determine the most suitable method. The measured vertical displacement of the plate was compared with the relative displacement of the telescopic probes and the stiffness measured compared both with one another and with Continuous Surface Wave measurements. The test apparatus, methods and results are discussed in this paper.

***Keywords:** Plate load test, bedding errors, surface preparation methods, telescopic probes, soil stiffness.*

## **1 Introduction**

Geotechnical engineers are continuously searching for more accurate and cost effective tests to determine the soil stiffness. Two of the main advantages of plate load tests are the cost-effectiveness and the relative straightforward test procedure. This paper reports on research that was done on vertical plate load tests using a modified apparatus. Bedding errors affect the soil stiffness measurements during plate load tests and therefore they need to be eliminated or kept to a minimum. Telescopic probes were used to measure the displacement below the center of the plate in order to eliminate the effects of bedding errors on the calculation of stiffnesses. Different surface preparation methods were used to achieve smooth bedding before each test. Six plate load tests were performed (two tests on each method) to determine the most suitable method. The experimental equipment is discussed as well as the test procedure and data interpretation. The results of stiffness measurements for both the external instruments and telescopic probes are compared as well as the results for the surface preparation methods. Final conclusions are summarised and recommendations for plate load testing are proposed. The conclusions illustrate the importance of bedding errors that occur during plate load tests and demonstrate that more critical interpretation of plate load data is necessary.

## **2 Experiment Equipment**

The conventional plate load test consists of a selection of plates, a hydraulic pump and jack, some means of applying a reaction force and two or three calibrated displacement measuring devices. In the experiments for this project, a steel beam with a weight of 1,3 ton was used for the reaction force, together with four grouted anchors. A hydraulic jack and pump system were used to provide the required contact pressure by jacking against the anchored steel beam. The applied load was directly measured with a 10 ton load cell, placed on top of circular plates, and logged with an automatic logging unit. Figure 1 illustrates the modified plate load test set-up and the instrument details. Three different methods were used to prepare the surface prior to each test and are being described in the next section. 300 mm and 450 mm steel plates were stacked on top of each other and placed on the prepared surface. The vertical displacement of the bottom plate was measured with three calibrated DCDT's (Direct-Current Displacement Transducers) placed 120° apart and approximately 25 mm from the plate perimeter to accommodate any tilt that might occur during testing.

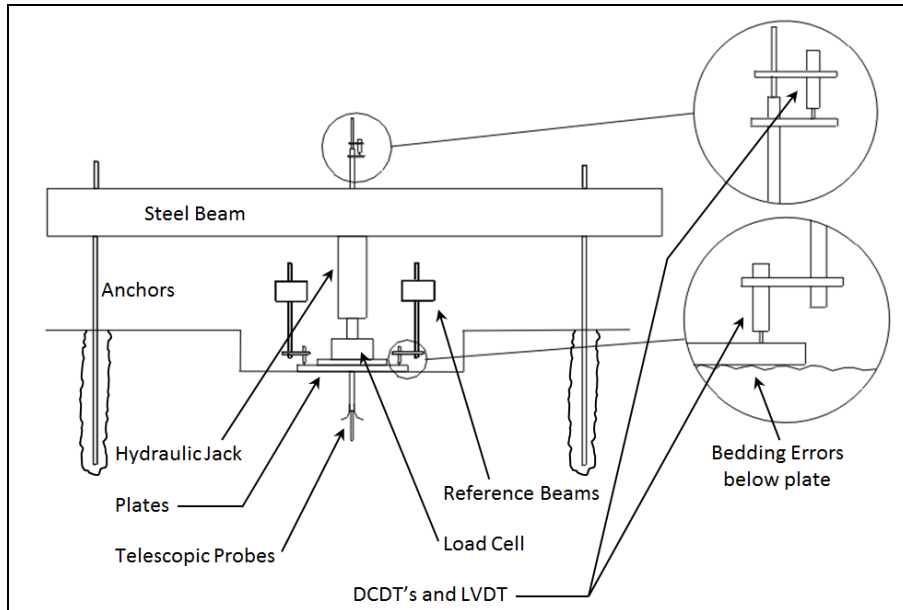


Figure 1. Schematic illustration of the modified plate load test set-up.

The three external measuring devices were supported by two, 3 m long wooden, reference beams which were placed on both sides of the test area without interfering with any test equipment.

The telescopic probe consisted of a solid inner aluminum rod (8 mm), designed to slide freely inside a 13 mm aluminum tube. Three bended spring steel strips were welded onto a bolt and screwed unto the threaded aluminum tube as shown in Figure 2. A calibrated LVDT (Linear Variable Differential Transformer) were attached to the top of the probes, to measure the relative displacement at two positions below the centre of the plate. Figure 3 shows the LVDT set-up.

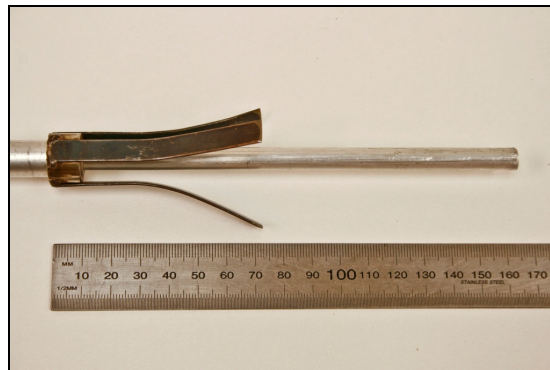


Figure 2. Telescopic probes set-up.

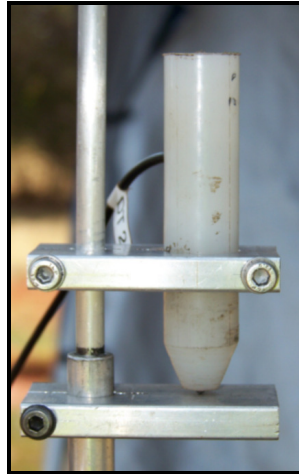


Figure 3. LVDT attached to probes with brackets.

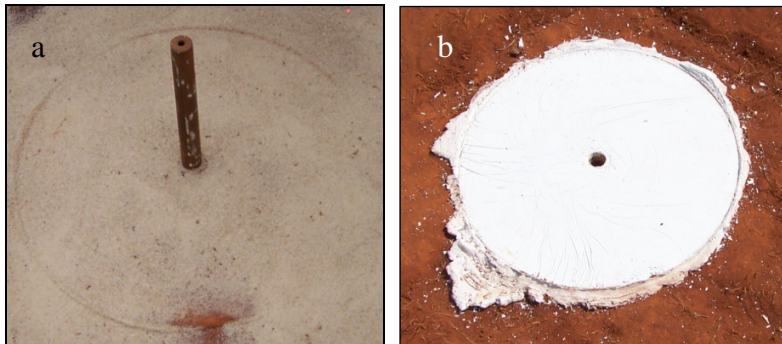
### 3 Surface preparation methods

Three different methods were used to prepare the surface prior to each test. The surface was leveled as smooth as possible and cleaned before each test commenced.

The first method was the conventional method where the surface was only leveled and cleaned as smooth as possible using hand tools. It was very difficult to level the surface because of the sandy nature of the soil and gravels that were also present in some of the holes.

The second method was to use a thin layer of silica sand to level the surface as smooth as possible. This method was the most practical compared to the other methods used.

The third method, also widely used throughout South Africa, was to prepare the surface with Plaster of Paris prior to testing. This method requires skilled technicians due to the fact that the Plaster of Paris sets quickly. A thin plastic sheet was placed over the plate to prevent the Plaster to stick to the plate. Figure 4 shows the preparation for both the sand and Plaster of Paris methods.



.....Figure 4. Preparation methods: a) Silica sand b) Plaster of Paris.

### 4 Test Procedure

The plate load tests were performed on a uniform residual andesite (clayey sandy silt) at the experimental farm of the University of Pretoria. A steel beam and four anchors, grouted to a depth of approximately 1,5 m, were used to provide the reaction force needed to generate the required contact pressure between the plate and the soil. Tests were conducted in 2 m x 2 m holes and approximately 300 mm deep. A 25 mm hole was drilled by means of a hand bore, in the center of the 2 m x 2 m hole, up to a depth of one plate diameter (450 mm) below ground surface. The surface was leveled as smooth as possible with one of the above mentioned preparation methods before the plates, hollow load cell and hollow hydraulic jack were stacked together in order to jack against the steel beam as illustrated in Figure 1. The external DCDTs were installed, on the perimeter of the 450 mm plate, using the wooden reference beams.

The final step before the test could commence was to install the telescopic probes. The inner aluminum rod was grouted at the bottom of the 25 mm hole using ROCSET<sup>®</sup> grout. The ROCSET<sup>®</sup> grout took about 40 minutes to set before the tests

could continue. Once the grout was set, the spring steel unit together with the aluminum tube was released at a depth of 225 mm below the plate using a 25 mm steel release pipe.

The LVDT with a range of 5 mm was installed at the top of the telescopic probes to record the relative displacement between the two probe points, 225 mm and 450 mm below the plate, respectively. A load sequence was applied which comprised three cycles (8 kN, 24 kN and 100 kN) and with the 450 mm plate diameter these loads resulted in 50 kPa, 150 kPa and 628 kPa contact pressures, respectively. The applied loads were recorded during the load and unload cycles and logged at 10 readings per second throughout the tests together with the four displacement transducers measurements.

## 5 Data Interpretation

The average vertical displacement of the plate ( $\rho$ ) obtained from the three DCDT's was used in Eq. (1), together with the plate diameter ( $D$ ); and Poisson's ratio ( $\nu$ ) taken as 0.35, to determine the external stiffness ( $E_{ext}$ ) in MPa as proposed by Wrench (1984). The contact stress ( $q$ ) was taken as the applied load divided by the plate area, assuming a uniform pressure distribution across the plate.

$$E_{ext} = \frac{\pi \cdot q \cdot D \cdot (1 - \nu^2)}{4 \cdot \rho} \quad (1)$$

The strain level below a loaded plate varies with depth. In order to allow comparison of stiffnesses from Eq. (1) and those calculated from the telescopic probes, the average strain of the soil was taken as the plate settlement divided by 1.5 times the plate diameter. This was taken from the influence depths for circular foundations based on Boussinesq's theory where less than 20% of the applied stress occurs below 1.5 times the plate diameter.

The measured relative displacement of the telescopic probes ( $dL$ ) was used in Eq. (2) together with the distance between the two probe points ( $L$ ), to determine the strain levels for the local stiffness ( $E_{local}$ ).

$$\Delta \epsilon = \frac{\partial L}{L} \quad (2)$$

The vertical stress at depth  $z$  below the centre of the circular plate with diameter  $D=2R$ , carrying a uniform pressure ( $q$ ), is calculated using Eq. (3). Values of the influence factor ( $I_c$ ), are always between zero and unity. The local stiffness ( $E_{local}$ ) is calculated for every load step using Eq. (4) with the average vertical stress ( $\Delta \sigma_z$ ) between the two fixed points, 225 mm apart; and the corresponding strain level calculated with Eq. (2).

$$\sigma_z = q \left[ 1 - \left\{ \frac{1}{1 + (R/z)^2} \right\}^{3/2} \right] = q I_c \quad (3)$$

$$E_{Local} = \frac{\Delta \sigma_z}{\Delta \epsilon} \quad (4)$$

## 6 Results and Discussions

The main study objective was to investigate the bedding errors that may occur at the plate/soil interface during plate load testing. The external stiffness at different strain levels from the three preparation methods were plotted and compared. Figure 5 shows the comparison for the first 8 kN cycle of each test. The results reveal that the Plaster of Paris and Sand tests gives much higher values compared to the values where the surface was only leveled by hand ('Do Nothing' test). Figure 6 shows the results where the last cycle (100kN) of each tests were plotted and compared. It is very interesting to observe that at a maximum contact pressure of 628 kPa the Sand and the 'Do Nothing' test give very similar stiffness values, but the Plaster of Paris test still showed about 20% higher stiffness values compared to the other two methods.

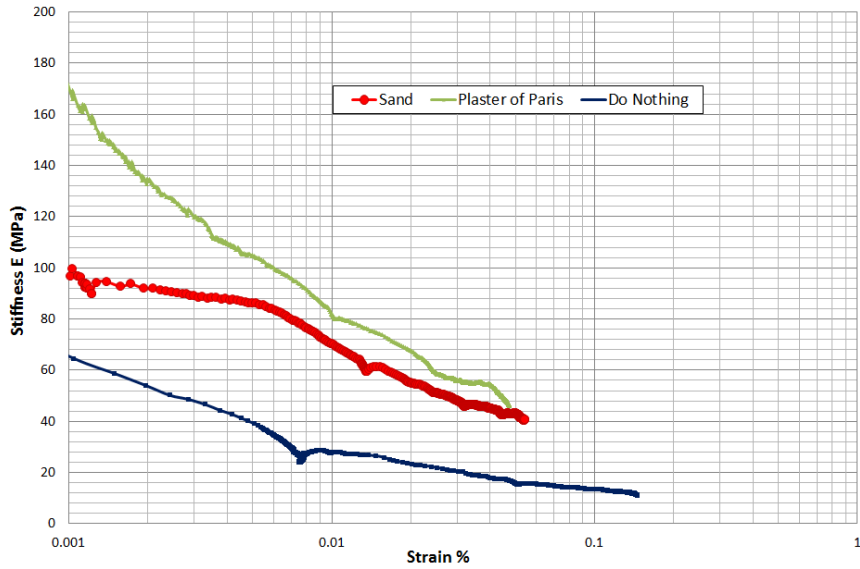


Figure 5. Comparison between external stiffness for different preparation methods (50kPa).

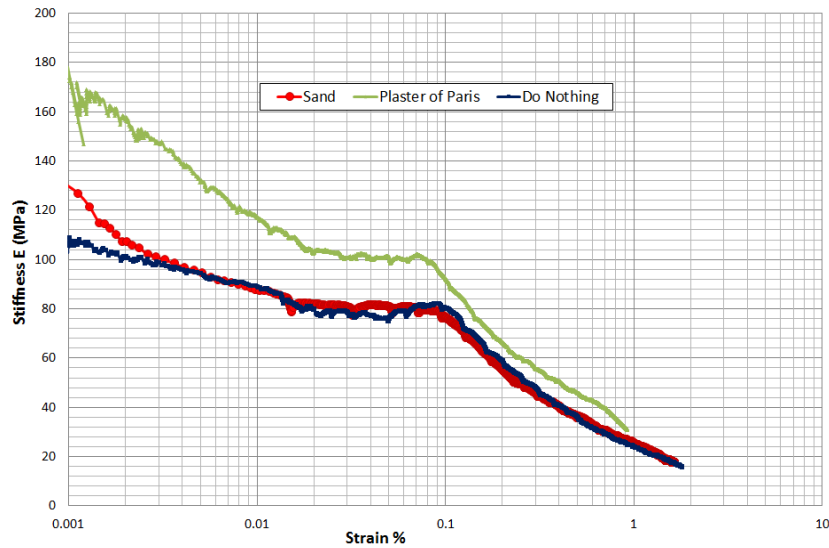


Figure 6. Comparison between external stiffness for different preparation methods (628kPa).

The external and local stiffness calculated from all three cycles, at different strain levels were also plotted and compared. Figure 7 shows the comparison between the measured external and local stiffness for the full strain range in the last cycle of the 'Do Nothing' test. It is clear from Figure 7 that the stiffness determined with the telescopic probes showed significantly higher values than that from the conventional external measurements up to 0.05% strain.

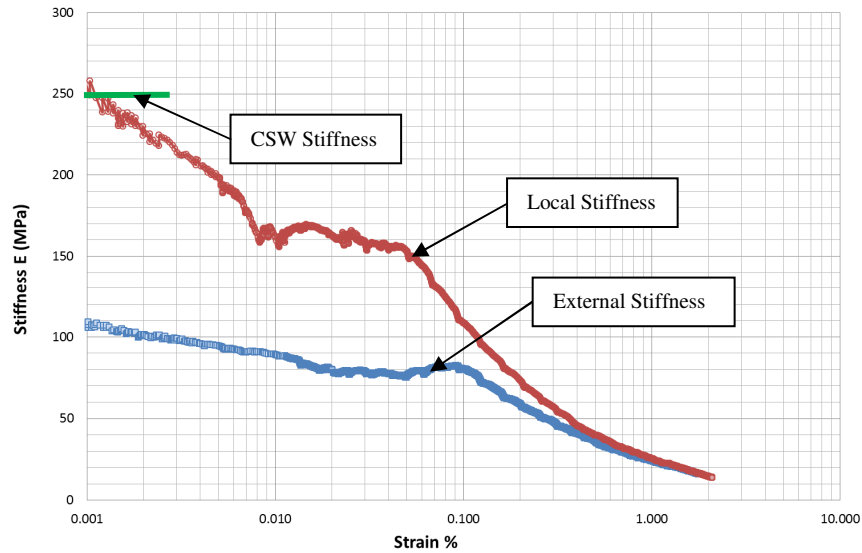


Figure 7. Comparison between external stiffness and local stiffness for 'Do Nothing' test.

The comparison between the measured external and local stiffness for the full strain range of the sand test is shown in Figure 8. The stiffness results from the probe showed about 40% higher values from that of the external values up to 0.05% strain.

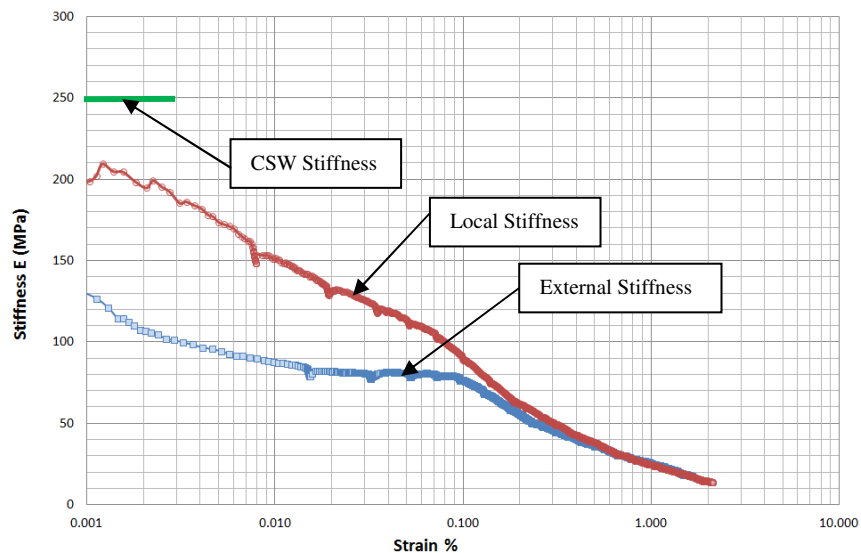


Figure 8. Comparison between external stiffness and local stiffness for sand test (628 kPa).

Figure 9 shows the comparison between the measured external and local stiffness for the full strain range of the Plaster of Paris test, which revealed that the stiffness determined with the telescopic probes again showed higher values than that from the conventional external measurements, but the values are within 20% of the local stiffness values. Continuous surface wave tests (CSW), done by Prof. Heymann from the University of Pretoria, on the same site, showed small strain stiffness ( $E_0$ ) values of 250 MPa, which compare very well with the local stiffness at 0.001% to 0.002% strain in all tests.

Table 1 summarises the local and external stiffness values from the last cycle that was determined in all three tests. The results reveal that the external stiffness values measured in the Plaster test plots much closer to the local stiffness values mainly between 0.01% and 0.1% strain.

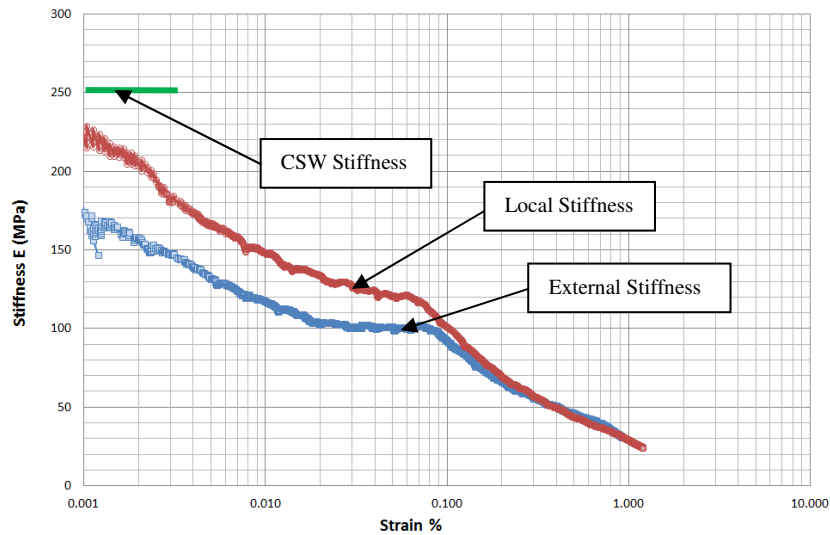


Figure 9. Comparison between external stiffness and local stiffness for Plaster test (628 kPa).

To understand the soil behavior during the whole test and to determine whether the bedding errors were reduced, the external stiffness for all three cycles had to be compared with the local stiffness. Table 2 shows the difference between the external and local stiffness values for all cycles and tests.

Table 1. Comparison of local and external stiffness values for different preparation methods.

Strain %	Stiffness E (MPa)								
	Plaster of Paris		External vs local	Sand		External vs local	Do Nothing		External vs local
	LS*	ES**		LS*	ES**		LS*	ES**	
0.005	166	130	78%	173	95	55%	200	95	48%
0.01	148	117	79%	150	88	59%	162	89	55%
0.05	121	101	83%	115	80	70%	153	76	50%
0.1	101	92	91%	90	77	86%	108	80	74%
0.5	44	46	105%	40	37	93%	40	36	90%
1.0	29	31	107%	25	25	100%	25	24	96%

\* Local telescopic probe stiffness

\*\* External stiffness

The results show that there was a marginal increase of about 10% in the last cycle of both the Plaster and sand tests, compared to the first cycle. The difference between the external and local stiffness values for the "Do Nothing" test were roughly 50% up to the 0.05% strain level.

Table 2. Difference in percentage between external and local stiffness values for all cycles

Strain %	External vs. Local for 'Plaster' test (%)			External vs. Local for 'Sand' test (%)			External vs. Local for 'Do Nothing' test (%)		
	Cycle 1	Cycle 2	Cycle 3	Cycle 1	Cycle 2	Cycle 3	Cycle 1	Cycle 2	Cycle 3
0.005	70%	79%	78%	45%	48%	55%	49%	20%	48%
0.01	73%	72%	79%	48%	51%	59%	41%	16%	55%
0.05		78%	83%		66%	70%		13%	50%
0.1		88%	91%		71%	86%		20%	74%
0.5			105%			93%			90%
1.0			107%			100%			96%

## 7 Conclusions and Recommendations

Plate load tests have an important role in geotechnical engineering in the determination of soil stiffness. The results shown in this paper demonstrates that:

- bedding errors can have a significant effect on stiffnesses determined with the traditional method of conducting plate load tests;
- sand is the most practical method to use in order to level and smooth the test surface;
- Plaster of Paris is the most reliable preparation method to most accurately measure stiffness values in conventional plate load tests;
- using telescopic probes is required to accurately determine soil stiffness and can measure up to 50% more accurate stiffness values compared to the external measurements;
- the CSW small strain stiffness ( $E_0$ ) values of 250 MPa, compared very well with the local stiffness at 0.001% to 0.002% strain.

The study shows that calculations associated with bedding errors can be eliminated by means of telescopic probes and therefore recommends this method for the future use where accurate stiffness values are required.

## 8 Acknowledgements

The author would like to thank the following institutes and persons:

- University of Pretoria for the technical support and facilities;
- Aurecon SA, for the financial support during the study period;
- Prof. G. Heymann for all his support and guidance.

## References

- Heymann, G. 1998. The stiffness of soil and weak rocks at very small strains. PhD Thesis. University of Surrey.
- Marsland, A. and Eason, B.J. 1973. Measurements of displacements in the ground below loaded plates in deep boreholes. Proc. British Geotech. Soc. Symposium on Field Instrumentation. Part 1, pp. 304-317.
- Wrench, B. 1994. Plate load test, University of Pretoria.
- Wrench, B. 1984. Plate test for the measurements of modulus and bearing capacity of gravels. University of Pretoria.